# Bioremediation of wastewaters utilising iron oxide-bearing wastes

## Safaa Abdalrasool Al-Obaidi

### B.Sc./ M.Sc.

**A thesis submitted in fulfilment of the requirement for the degree of**

**Doctor of Philosophy**

**School of Engineering - Cardiff University**

**UK**

**February 2021**

# ABSTRACT

Iron oxides bearing sludge, including mine water treatment sludge (MWT), a mix of mine water treatment and wastewater treatment sludge, herein termed mixed sludge (MX), and water treatment sludge (WT) were investigated as microbial substrates to remediate recalcitrant aromatic hydrocarbons in textile and BTEX bearing wastewaters. Also, these sludges were used to treat municipal wastewater. The concept of the experimental work is based on using iron oxide bearing sludges, which are abundance waste materials generated from mining activity and water treatment processes, to remediate industrial and municipal wastewaters using a practical and simple application.

The textile wastewater experiments included three phases of work based on different influent recipe compounds and the types of iron oxides bearing sludge used as a column's substrate. Dye decolourisation during textile wastewater experiments varied between 60 - 99 % during these phases. A maximum MWT adsorption capacity was 3.50 mg/g and the highest normalised methyl orange (MO) removal rate was 178 $g/m^3/day$ by MWT sludge. It was shown that the dye removal during these experiments was mostly due to biodegradation rather than adsorption. Furthermore, iron-reducing microorganisms and the affiliated bacteria in MWT sludge mineralised 3000 $g/m^3/day$ and 216 $g/m^3/day$ of the total influent carbon (TC) and total nitrogen (TN) during phase two as a maximum normalised removal rate. The indigenous MWT consortia degraded MO as a sole carbon source by reduction of the azo dye double bond as a first step then oxidation of the aromatic hydrocarbon ring. Furthermore, it was found that adding additional organic carbon as glycerol accelerated the MO decolourisation during textile wastewater experiment. In municipal wastewater experiment, iron oxides bearing sludge microbial community included iron-reducing bacteria and the affiliated genera efficiently degraded carbon and transform nitrogen contaminants. The highest normalised TC removal rate was 301 $g/m^3/day$ by MWT, and the highest normalised TN removal rate was 159 $g/m^3/day$ by MX columns. Anaerobic ammonium oxidation under iron-reducing condition (Feammox) in addition to anaerobic ammonium oxidation (Anammox), might be the main mechanisms for nitrogen transformation during municipal and textile wastewater treatments. In the BTEX bearing wastewater experiments, initial anoxic and

aerobic microcosms conditions were undertaken to degrade benzene, toluene, ethylbenzene, and xylene (BTEX) using iron oxides bearing sludge as substrates. The indigenous microbial community, including iron-reducing microorganisms, degraded BTEX as a sole carbon source more efficiently for the initial anoxic condition.

The next-generation sequencing confirmed that iron-reducing bacteria, e.g., *Geothrix, Geobacter Gallionella*, *Prevotella, Rhodoferax*, and *Clostridium* were detected in most of the post-test sludge which were used in all wastewater experiments. Iron-reducing bacterial genera were affiliated with other bacterial species as a consortium. This consortium degraded azo dye by cleavage of the azo bond and the aromatic hydrocarbon ring without generating aromatic amines, and it mineralised the BTEX. It also degraded carbon and transform nitrogen contaminants during wastewater treatments. The microbial consortia that flourished in post-test sludge degraded recalcitrant wastewater contaminants as a sole carbon source to simplest compounds without pre-acclimatisation.

The experimental work demonstrated that the iron oxide bearing sludge and their indigenous microbial consortia are feasible substrates to degrade recalcitrant wastewater contaminants to simplest compounds as a sole carbon source without pre-acclimatisation. It can be concluded that iron oxides bearing sludge can be used as reactive bioremediation media in a simple flow-through system to treat wastewater and groundwater pollutants with effective contaminant removal.

# DEDICATION

*This thesis work is dedicated to my little angel Zahraa (Gege)*

*(25/5/2015-26/12/2017).*

# ACKNOWLEDGEMENTS

**Safaa Al-Obaidi**

**August  2020**

# Table Of Contents

# LIST OF FIGURES

X

XII

XIII

XIV

# LIST OF TABLES

# Chapter 1   Introduction

Increasing global population and expanding industrialisation are leading to a rise in municipal and industrial wastewaters contamination in rivers and oceans (Jern 2006). In developing countries, conventional wastewater treatment techniques are unable to degrade aromatic contaminants such as dyes and BTEX. Feasible and effective wastewater treatment processes are a fundamental global need to maintain natural water resources (Gijzen 2002; Hernández Leal et al. 2007).

Textile and fabric industries are discharging massive quantities of wastewater during various dyeing processes. The discharge water is rich in colours and chemicals, many of which are considered hazardous to the environment. In China, about 70 billion tons of textile wastewater is generated annually (Wang et al. 2010). Dyes in water cause several diseases to humankind, also they block or reduce the sunlight penetration through water which is essential for photosynthesis (Ghaly et al. 2014). BTEX bearing wastewater is another source of recalcitrant aromatic pollutants. The tremendous global demands for raw and manufactured petroleum compounds expands the environment hydrocarbon contamination footprint. Benzene, toluene, ethylbenzene, and xylene (BTEX) comprise about 20 % of the fossil fuel. These monoaromatic hydrocarbons are common pollutants in aquifers (Farhadian et al. 2008a). Municipal wastewater also has negatively affected the aquatic ecosystem when treatment is inefficient (Jern 2006). Biological wastewater treatments are highly recommended to remediate organic contaminants (Ahn and Logan 2010). Anaerobic biodegradation could be an appropriate alternative to degrade wastewater contaminants (Sponza and Uluköy 2005). Developing new techniques to remediate municipal and industrial wastewaters can help in the maintenance the natural water resources (Chan et al. 2009).

Iron is the fourth abundance element in the Earth (Nealson 1982). Iron oxides bearing wastes are often generated during mining activities and drinking water treatment processes. Literature suggests that iron reduction mechanism can be utilised as an innovative technique to mineralise wastewater contaminants (Xu et al. 2007; Guo et al. 2010). Harder (1919) noticed that some microorganism reduced iron oxides which become known as iron-reducing bacteria (IRB). These microorganisms can be found in sediments and aquifers where Fe (III) is the main electron acceptor (Shelobolina et

1

al. 2004). IRB simultaneously degrades aromatic organic pollutants as an electron donor and it reduces Fe (III) as an electron acceptor to Fe (II) (Lovley 1987; Lovley and Philips 1988). IRB was recently shown to play an essential role in removing pollutants from a freshwater lake (Fan et al. 2018). Aburto-Medina and Ball (2015) noted that IRB metabolised aromatic compounds as a carbon source. It also mineralised BTEX in contaminated aquifers, where Fe (III) is the electron acceptor, and BTEX is the electron donor (Müller et al. 2017). This mechanism was demonstrated as an effective mechanism in Bemidji, Minnesota (USA) when the aquifer was polluted by oil leakage (Lovley et al. 1989). Other studies have shown the importance of coupling iron-reducing mechanism with nitrogen contaminants transformation in wastewater. For example, ammonium oxidation under iron-reducing condition (Feammox) was reported as an innovative mechanism to transform nitrogen contaminants under the iron-reducing condition in municipal wastewater (Li et al. 2018). Yang et al. (2019) highlighted the relation between Feammox and Fe (III) reduction mechanism during nitrogen removal. Utilising IRB as a single bacterial species to remediate wastewater contaminants is a complicated process; because it requires restricted growth conditions as nutrients and autoclaving (Zhang et al. 2013c). Provide these conditions is one of the barriers to set up a practical and simple wastewater process. Alternatively, IRB can be found in iron oxides bearing sludge affiliated with other microorganisms as a microbial consortium. A recent study highlighted that MWT sludge is a natural habitat for IRB which are synergetic with other microorganisms. It is also rich with iron oxides (Roberts 2018). Based on the mentioned evidence, iron oxides bearing sludge generated from mining and water treatment processes were investigated as substrates to remediate textile, BTEX and municipal wastewater using simple and practical flow-through process; furthermore, it is the first attempt to mineralise the recalcitrant azo dye to simplest compounds without generating aromatic amines using mine water treatment sludge.

## 1.1 Aims of the thesis

The main aim of the thesis is to investigate the potential for bioremediation of textile, municipal and BTEX bearing wastewaters using iron oxide-bearing sludge via indigenous microbial communities. Within this main aim, there are several highlighted objectives:

- To determine the amount of contaminant (dye and BTEX) removal by adsorption as a physical process, compared to contaminant removal by biodegradation, in order to distinguish the dominant removal mechanism.
- To determine whether iron oxide-bearing wastes and their indigenous microorganisms can degrade textile, municipal, and BTEX bearing contaminants without pre-acclimatisation.
- To determine the contaminants removal and/or degradation rates over a long experiment operation time.
- To determine the ability of iron oxide-bearing wastes and their indigenous microbial community to degrade the methyl orange (MO) and BTEX as sole carbon sources and the impact of adding glycerol as an additional carbon source on MO biodegradation compared with unamended columns.
- To chemically characterise the azo dye degradation products during textile wastewater treatments to determine any aromatic amines generated.
- To determine the microbial community changes at a genus level for post-test sludge compared with pre-test sludge for all wastewater experiments.

## 1.2    The thesis organisation

Chapter one: Is the thesis introduction.

Chapter two: A literature review for textile, municipal, and BTEX bearing wastewater biodegradation highlighting the contribution of iron-reducing bacteria and the related degradation mechanisms.

Chapter three: This chapter included the experiments research strategy for textile, municipal, and BTEX bearing wastewater, described iron oxides bearing wastes collection, wastewater experiments setup and operation conditions, methods used to measure experiment parameters, analytical techniques, and the biological analysis.

Chapter four: The preliminary dye experiments to study the MO adsorption capacity and equilibrium curve.

Chapter five: Discussions for phase one textile wastewater experimental results, demonstrating MO decolourisation, degradation products, and MO removal rate over 170 days. The biological analysis for pre-test and post-test column substrates at genus level was conducted to study the iron-reducing bacteria that flourished and the synergetic species. A conceptual model describes the mechanism involved.

Chapter six: Phase two textile wastewater experiment results and discussions included MO decolourisation efficiency by anaerobic and sequential reactors, MO removal by adsorption, MO degradation products to identify any aromatic amines generated, and the biological analysis for pre-test and post-test column substrates at phylum and genus level for comparison. A conceptual model demonstrated the mechanism involved.

Chapter seven: Phase three textile wastewater experiment discussions. The appropriate wavelength was investigated to calculate the real dye decolourisation, to study the dye removal by adsorption using iron oxides bearing wastes in a batch experiment, and to monitor aromatic amines generated by spectrophotometric method and LC-MS technique. The flourished bacterial genera in post-test column substrates were studied compared with pre-test sludge to identify the abundant bacterial genera. The conceptual model was used to explain the mechanism occurred during textile wastewater treatment.

Chapter eight: Highlighted results and discussions for municipal wastewater experiment included, nitrogen and organic carbon removal rate, other experiment parameters, pre-test and post-test column substrates were determined by gene sequencing to identify the flourished iron-reducing bacteria and other species at the genus level. A conceptual model explained the mechanism.

Chapter nine: BTEX bearing wastewater treatment results and discussions including a batch experiment to study the BTEX adsorption by iron oxides bearing sludge, and BTEX mineralisation at initial aerobic and anoxic microcosms conditions. Gene sequencing was used to analysis microcosm substrates to identify the prosperous bacterial species after treatment compared with pre-test sludge to identify the flourished genera. A conceptual model is developed to describe the BTEX mechanism.

Chapter ten: a cross-chapter general discussion.

Chapter eleven: Conclusions of the study and recommendations arising for future work.

# Chapter 2   : Literature review

## 2.1 Iron-reducing environments

Fe (III) oxides are widely abundant materials in the Earth's crust (Nealson 1982). Abiotic (chemical) and biotic (biological) iron reduction-oxidation cycles occur in the environment. Oxygen is one of the control parameters in abiotic iron reactions, while microorganisms are the key parameter for the biotic cycle (Ionescu et al. 2015). Iron oxidation-reduction is a dynamic reaction at the oxic-anoxic interface, where iron is discontinuously exposed to oxygen (Lin et al., 2004). During this cycle, Fe (III) reduces to Fe (II) and it re-oxidises to Fe (III) at the oxic-anoxic interface (Lovley et al. 1990; Thamdrup 2000). Mining residues can contain massive amounts of iron oxides, and by exposure to the ambient air, Fe (II) oxidises to poorly crystalline ferric oxyhydroxide (Lundgren 1980; Mccarty et al. 1998). Under anoxic conditions, Fe (III) acts as an electron acceptor, reducing to Fe (II) for microbial processes which oxidised organic contaminants (Kappler and Brune 2002).

## 2.2 Iron-reducing bacteria and electron mobility

Iron reducing bacteria (IRB) reduce Fe (III) to Fe (II). These bacteria are found in various anaerobic sediments (Lovley 1987). Diverse iron-reducing microorganisms include bacteria and archaea are shown in Figure 2-1 (Lovley et al. 2002). Insoluble Fe (III) is the most available form of iron oxide in sediments, and IRB can reduce it by direct contact. Alternatively, electrons are transferred from these microorganisms to Fe (III) by another mechanism, such as electron shuttles in case of indirect contact (Nevin and Lovley 2002b; Van der Zee and Cervantes 2009).
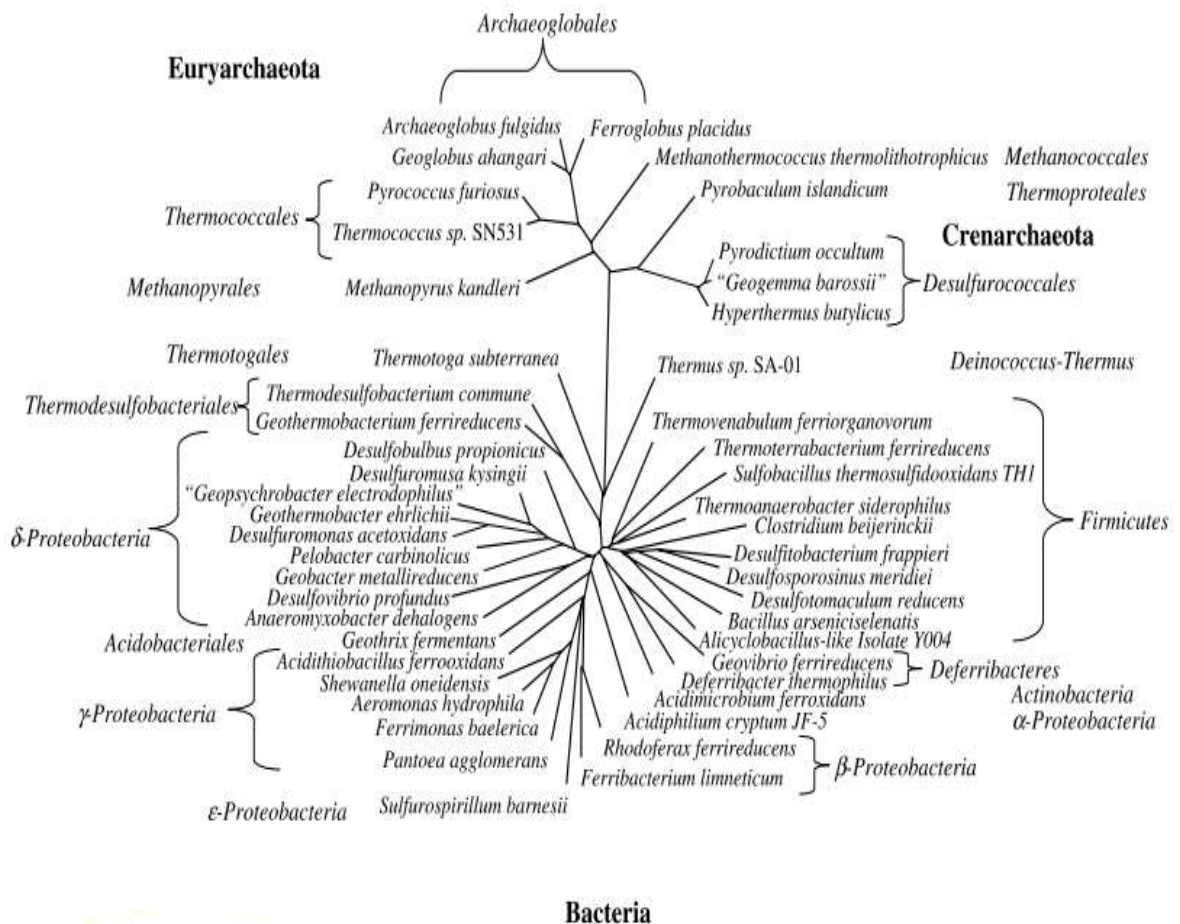
**Figure 2-1 Iron-reducing microorganisms (Lovley et al. 2002).**

Understanding whether the indirect iron reduction was possible has evolved considerably over time, with the first studies incorrectly concluding that only direct reduction was possible. Early studies such as Munch and Ottow (1980) assumed that Fe (III) was reduced by the direct contact between iron-reducing bacteria and iron oxides. A semi-permeable membrane was used to segregate the microorganism from iron oxide to enable only electron shuttles to penetrate through the semi-permeable membrane; however, the microorganism was unable to reduce Fe (III) by indirect contact. Other experiments confirmed the same conclusion by using different iron-reducing bacteria (Lovley and Philips 1988; Caccavo et al. 1992). These results highlighted the fact that iron chelators did not penetrate through the semi-permeable membrane to transfer electrons from iron-reducing microorganism to Fe (III) surface even when the size of the pores in the semi-permeable membrane was greater than the chelator's molecule. However, the validity of these studies was criticised because of the lack of rigorous controls. Subsequent research highlighted that some iron-reducing

8

bacteria could reduce Fe (III) by indirect contact, for example with electron shuttles being shown to be able to reduce Fe (III) inside alginate beads. These beads allowed molecules up to 12 KDa to penetrate to the trapped Fe (III) without direct contact between the bacteria and Fe (III). Unlike the above-described semi-permeable membrane experiments, the alginate beads allow bacterial chelators to transfer electrons to reduce Fe (III) (Nevin and Lovley 2000a; Nevin and Lovley 2002b). Iron-reducing microorganisms use chelators to solubilise crystalline Fe (III) (Munch and Ottow 1980; Nevin and Lovley 2002b; Shelobolina et al. 2004). Electron shuttles were discovered by Cohen in 1931 (Cohen 1931). An electron shuttle is an organic compound which can be re-generated by oxidation-reduction reaction and its lower reaction energy (Van der Zee and Cervantes 2009). Humic substances can be used as redox mediators (RM) which is a type of electron shuttle. It supports organic contaminants anaerobic oxidation (Field and Cervantes 2005). It was one of the reasons for using wastewater sludge as an additive in MX sludge in the textile, BTEX bearing, and municipal wastewater experiments (see Chapters 7, 8 and 9) because wastewater sludge contains humic substrates. Aquatic sediments usually contain electron shuttles (Nevin and Lovley 2002b). Iron-reducing bacteria use electron shuttles, either those found in the environment or otherwise, they can be generated by the microbes themselves. Electron shuttles eliminate the need for direct contact between iron-reducing bacteria and Fe (III) molecules (Myers and Myers 1992; Seeliger et al. 1998; Newman and Kolter 2000). Figure 2-2 summarises the proposed mechanisms for solubilised crystalline Fe (III) oxides (Nevin and Lovley 2002b).
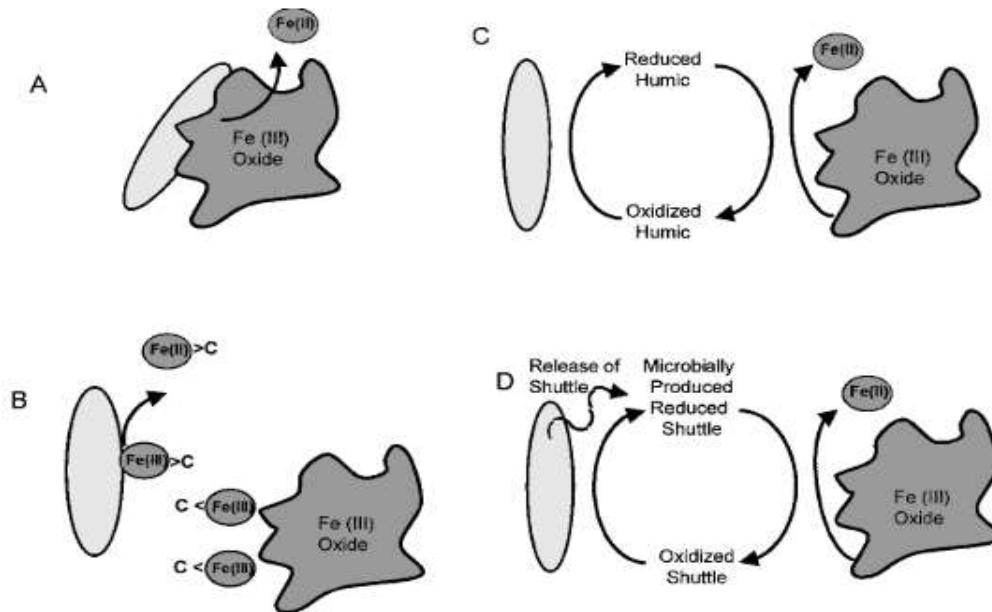
**Figure 2-2 The reduction of Fe (III) oxide, (A) direct contact between iron-reducing organism and Fe (III) oxide, (B) in the presence of soluble Fe(III), (C) by electron shuttling with soluble humic substances, (D) by bacterial electron shuttle (Nevin and Lovley 2002b).**

*Shewanella* is a widespread *Proteobacteria* subclass iron-reducing bacteria. It is a facultative species, and it can be found in diverse environments (Heidelberg et al. 2002). It was isolated from aquatic sediments, where favourable conditions existed for iron reduction (Caccavo et al. 1992). Electron shuttles were highlighted in *Shewanella* species to reduce Fe (III). It transfers electrons through the gap between the cell membrane and Fe (III) surface. Without electron shuttles, *Shewanella* reduces the attached Fe (III) only with the outer cell membrane (Caccavo et al. 1997; Newman and Kolter 2000; Northwest et al. 2003). Nevertheless, *Shewanella* makes direct contact with iron oxides using filaments as nanowires see Figure 2-3 (Gorby et al. 2006; El-Naggar et al. 2010).

*Geobacter* is another widespread iron-reducing bacteria. It is found in aquatic sludge and sediments where iron oxides are available (Stein et al. 2001). It reduces crystalline Fe (III) by direct contact. However, it cannot generates electron shuttles (Nevin and Lovley 2000). Instead, it uses flagella and pili to reduce Fe (III) oxides which are not in direct contact with bacteria outer membrane (Childers et al. 2002). *Geobacter* uses direct extracellular electron transfer (DEET) using pili as nanowires to transfer electrons to electron acceptors without direct binding (Reguera et al. 2005; Gorby et

al. 2006). Some iron-reducing bacteria use DEET as a direct electrical connection with other microorganisms or insoluble Fe (III) oxides, as *Geobacter* does (see Figure 2-4). It generates a highly conductive network of filaments which transfer electrons to Fe (III) as an electron acceptor. It also supports the generation of biofilm as a substrate to remediate various contaminants in water. Microorganisms with DEET technique contribute effectively to environmental bioremediation (Lovley 2011a). DEET microbial respiration transfers electrons outside the cell to electron acceptors. It is different from the electron shuttle which is used to transfer electrons from bacteria to Fe (III), e.g. *Shewanella* (Newman and Kolter 2000; Canstein et al. 2008). However, both mechanisms are functional in environmental bioremediation (Lovley 2011a).
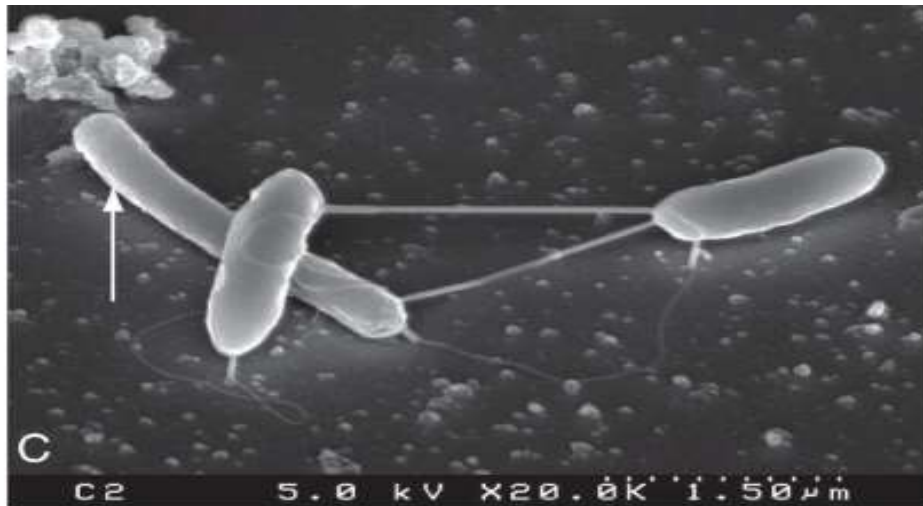


**Figure 2-3 *Shewanella* nanowires, as shown by an electron microscope (Gorby et al. 2006).**
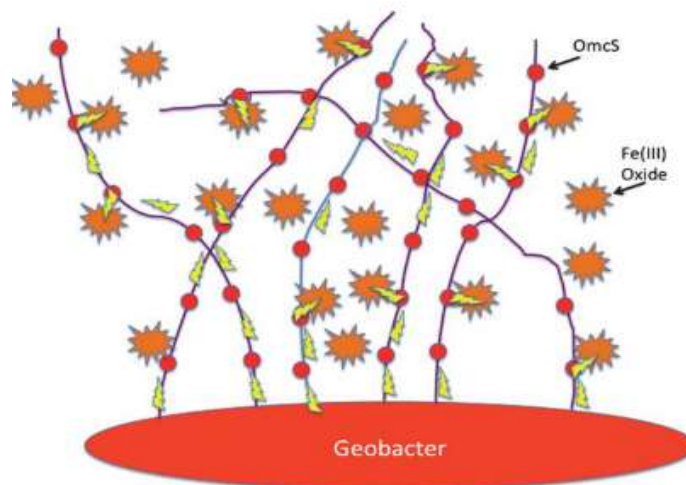


**Figure 2-4 Direct electron transfer (DEET) by *Geobacter* pili, OmcS is a c-type cytochrome mediate electron from pili to Fe (III) oxide** (Lovley 2011a)**.**

## 2.3 Iron-reducing bacteria and organic carbon biodegradation

The iron oxidation-reduction cycle has been exploited in many bioremediation techniques (Tay et al. 2008; Ivanov et al. 2014). Iron-reducing condition boosts aromatic hydrocarbon removal (Johnson and McGinness 1991; Küsel et al. 2002; Zhang et al. 2013a; Li et al. 2017a). Coates et al. (1996) noticed iron-reducing microorganisms mineralise mono-aromatic hydrocarbons as a source of electrons to reduces Fe (III) to Fe (II). Lovley (2000) found that about 30 bacterial species can simultaneously reduce Fe (III) coupled with organic material oxidation. Iron-reducing bacteria (IRB) mobile electrons generated from aromatic compounds biodegradation by direct contact using cytochrome via Fe (III) reductases to reduce Fe (III) (Lovley et al. 1989; Gorby and Lovley 1991). Cytochrome is a bacterial complex protein which is used for transport electrons across the bacteria cell membrane to electron acceptors (White et al. 2013; Li et al. 2017a). It consists of two subunit proteins, MtrC and MtrA. It is the link across iron oxides and the bacterial outer membrane to transport electrons (White et al. 2013). Iron-reducing bacteria, e.g. *Geobacter*, *Shewanella* and *Rhodoferax* use direct contact to transfer electrons from an electron donor (organic compound) to an electron acceptor Fe (III) while other species as *Pseudomonas aeruginosa* uses electron shuttle as indirect technique (Rabaey and Boon 2005; Van der Zee and Cervantes 2009). Chelates and humic substances act as electron shuttles to accelerate pollutants degradation in both landfill and groundwater aquifers (Lovley et al. 1989). Anderson et al. (1998) found that electron shuttles boost recalcitrant contaminants biodegradation.

## 2.4 Recalcitrant wastewater and groundwater contaminants

In wastewater treatment, dyes were not considered a crucial issue until the industrial sector began to use synthetic dyes instead of natural dyes (Pearce et al. 2003). Mauveine was the pioneer commercial dye; it was synthesised in 1856 by William Henry Perkin (Chequer et al. 2011). Dyes are used in fabric manufacturing facilities and medicine. They are also used in a wide range of technological applications, e.g. optical data storage, inks, and solar cells (Singh and Arora 2011). The vast majority of industrial products consume dyes since they have the broadest range of colours and

are fast fixed when used in fabrics (Ferdous Rumky et al. 2013). Fabrics and textiles, with their infixation dyes, have a significant contaminant influence upon release to the aquatic environment (Pearce et al. 2003). Van der Zee and Cervantes (2009) demonstrated, about 10% of the used colour does not fix during fabric dyeing, but it discharged to the aquatic system. Table 2-1 highlights a list of conventional dyes used in industries (Bardi and Marzona 2010).

Table 2-1 The standard dye classification and their applications.

| Class | Substrates | Application |
|---|---|---|
| Acid | Nylon, wool, silk, paper, inks and leather | Usually, forms neutral to acidic dye baths |
| Azoic dyes | Cotton, rayon, cellulose acetate, polyester paper and inks | Fibre impregnated with a coupling component and treated with a solution of stabilised di-diazonium salt |
| Basic | Acrylic, modified nylon and polyester paper and inks | Applied from an acidic dye bath |
| Direct | Cotton, cloth, paper, leather and nylon | Applied from neutral or slightly alkaline baths containing additional electrolytes |
| Dispersed | Polyester polyamide, Cellulose acetate, acrylic and plastics | Fine, aqueous dispersions often applied by higher temperature, pressure, or lower temperature carrier dye may be padded on cloth, baked-on or thermo-fixed |
| Optical brighteners | Soap and detergents, oils, paints and plastics | From solution dispersion or suspension in a mass |
| Reactive | Cotton, rayon, wool, silk and nylon | The responsive site on dye reacts with a functional group in the fibre to bind dye covalently under the influence of heat and the proper pH |
| Sulphur | Cotton and rayon Aromatic | Aromatic substrate valued with sodium sulfide and re-oxidised to insoluble sulphur containing products in the fibre |
| Vat | Cotton, rayon and wool | Water-insoluble dye solubilised by reducing with hydro sodium sulphate then exhausted in the fibre and re-oxidised |
| Solubilised vat | Cotton, wool, cellulose, fibres and silk | Impregnated fibre, treated with an oxidised agent, usually sulfuric acid and sodium nitrite for cotton dichromate wool and silk; therefore, no alkali is involved. This class applies to cellulose and protein fibre |

13

Dyes are distinguished according to chromophores chemical structure. The chromophore is the chemical structure responsible for dye colour. The azo dye (N=N) is the most abundant group of chromophores; it is followed by carboxyl (C=O), ethylene (C=C) and carbon-nitrogen (C=NH). The auxochrome is the attached electron-withdrawing or donating group to the aromatic benzene ring (see Figure 2-5). It includes amines (NH$_2$), carboxyl (COOH), sulphate (SO$_3$Na) as in MO, and hydroxyl (OH) (Hunger 2009). Cleavage of the azo dye chromophores eliminates the dye colour, and it usually generates aromatic amines (Liu et al. 2017a; Liu et al. 2018). Dye colours are varying according to the visible wavelength range, as shown in Table 2-2 (Bardi and Marzona 2010).

**Table 2-2 The dye wavelength range according to colour.**

| Wavelength (nm) | Colour |
| --- | --- |
| 400–440 | Green-yellow |
| 440–480 | Yellow |
| 480-510 | Orange |
| 510-540 | Red |
| 540–570 | Purple |
| 570-580 | Blue |
| 580–610 | Greenish-blue |
| 610–670 | Blue-green |

Dyes are xenobiotic chemicals (Barragán et al. 2007; Hsueh et al. 2009). The azo bond (N=N) and the electron-withdrawing group (R group) make the dye structure recalcitrant for biodegradation (Barragán et al. 2007; Hsueh et al. 2009). About 50% of the dyes used in fabric industries are azo dyes (Baiocchi et al. 2002), and 60% of the global dye production is consumed by this industry (Singh and Arora 2011). MO (Sodium p-dimethyl-aminoazobenzene sulphonate) is an anionic mono azo dye. It is soluble in water (Zhu et al. 2010; Yao et al. 2011a). It was selected as a case study to represent the azo dye contamination in textile wastewater (Figure 2-5). MO is a widely used dye in various industrial applications. It has a characteristic and chemical structure similar to wastewater contaminants (Yao et al. 2011b).
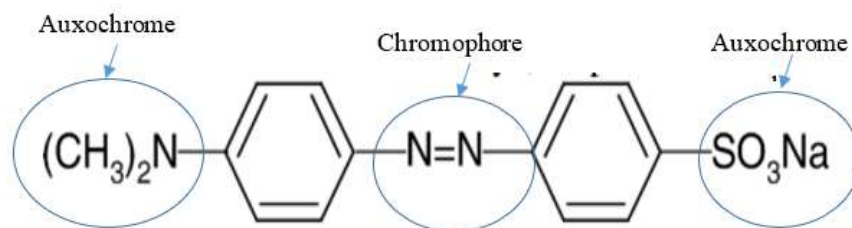
**Figure 2-5 MO chemical structure. Blue circles highlight the molecule's auxochromes and chromophore.**

Petroleum refinery industries consume massive water quantities during processing crude oil products (Bagajewicz, 2000). The quantity of wastewater discharges is equal to about 0.4 to 1.6 times the refined products (Coelho et al. 2006). The generated wastewater has an adverse effect on living habitats as it contains toxic wastes as benzene, toluene, ethylbenzene and xylene (BTEX) (Irwin et al. 1997). Soil and water pollution by BTEX is an environmental burden. It could be caused by accidents of oil spills and storage tank leakage (Jo et al. 2008; USEPA 2011). BTEX has become a common environmental contaminant which affects water quality, especially in aquifers (Reusser and Istok 2002; Farhadian et al. 2008a; Simantiraki et al. 2013). As a consequence, there is a continuing requirement for developing new and efficient BTEX removal methods (Mazzeo et al. 2010). BTEX are substantial constituents of crude oil (Weelink et al. 2010). BTEX is widely using as a raw material in industries (El-Naas et al. 2014) where it is used in adhesives, coatings, degreasers, detergents, explosives, fuels, inks, lacquers, paints, polishes, resins, rubbers and solvents (Sack and Steele 1992; Kwon et al. 2007; Bolden et al. 2015). Additional BTEX is added sometimes added to enhance the performance of gasoline (Potter and Simmons 1998; Bolden et al. 2015). BTEX has low adsorption in soil but high solubility in water (Nakhla 2003). BTEX are mono-aromatic hydrocarbons that are carcinogenic and poisonous (Mazzeo et al. 2010; Seifi et al. 2011). Benzene is a carcinogenic chemical and the most toxic material among the BTEX hydrocarbons (Badham and LM Winn 2007). Table 2-3 illustrates the main BTEX properties (Mitra and Roy 2011).

**Table 2-3 The general BTEX properties.**

| Parameters | Benzene | Toluene | Ethylbenzene | Xylene |
|---|---|---|---|---|
| Formula | $C_6H_6$ | $C_6H_5CH_3$ | $C_6H_5CH_2CH_3$ | $C_6H_4(CH_3)_2$ |
| Molecular weight | 78.12 | 92.15 | 106.18 | 106.18 |
| Density g/mL | 0.87 | 0.86 | 0.86 | 0.86 |
| Polarity | Nonpolar | Nonpolar | Nonpolar | Nonpolar |
| Solubility mg/L | 1780 | 500 | 150 | 150 |

### 2.4.1 Textile wastewater treatment techniques

The demand is increasing all over the world to find convenient and efficient methods to remediate textile wastewater. Efficient textile wastewater treatment aims to degrade dyes to less toxic chemicals to keep the aquatic system within a minimal range of pollution. However, conventional municipal wastewater treatment cannot tackle many textile wastewaters components. Various techniques that have been used to treat dyeing wastewater include chemical, physical and biological methods, as shown in Figure 2-6 (Chang et al. 2011).
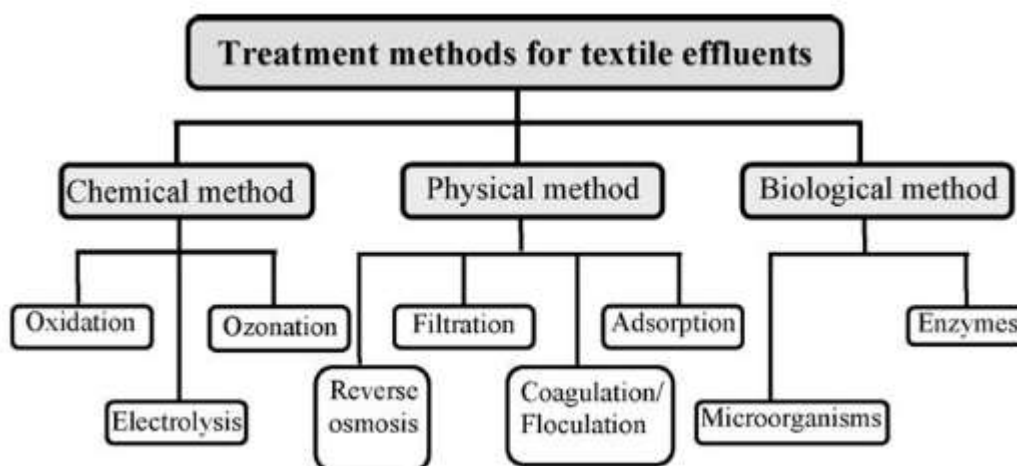


Figure 2-6 Textile wastewater treatment techniques (Chang et al. 2011).

Biological treatments tend to be relatively low-cost, green, and efficient methods for dye wastewater treatment (Chang et al. 2011). Microorganisms can be used to breakdown azo dye to its simplest form and reduce pollutants hazardous (Bennett 1993). Biodegradation is a biological oxidation-reduction reaction, governed by the availability of electron acceptors (Popli and Patel 2015). Adams and Holmes were the pioneer researchers who removed dye by biological methods in 1935 (Volesky and

Holan 1995). Joshi et al. (2008) noted that the dye degradation rate is linked to dye molecular weight: that is, a high rate of decolourisation was observed when dye had low molecular weight, while a high azo dye molecular weight was more resistant to biodegradation and exaggerated toxicity (Khan et al. 2013). Similarly, mono-azo dyes degrade faster than di-azo and tri-azo dyes (Hu 2001). Furthermore, azo dyes with attached hydroxyl or amino group degraded more quickly than methyl groups (Claus et al. 2002). The azo dye structure can affect colour biodegradation due to the toxicity on the microorganisms used for treatment (Pasti-Grigsby et al. 1992). Therefore, adaptation should be considered by continuous exposure to the dye. Sufficient adaptation can induce microbial enzymes activity and enhance biodegradation (Tauber et al. 2008; Kumar et al. 2009). Under anaerobic conditions, the azo bond can be cleaved, and aromatic amines generated. These aromatic amines can be further degraded under aerobic conditions (Tomei et al. 2016b; Jayapal et al. 2018).

Bacteria are usually selected for azo dye biodegradation due to their positive features, e.g. convenient regeneration, diverse oxygen tolerance and acclimatisation with harsh environments (Solís et al. 2012a). Other microorganisms (algal and fungal) have several drawbacks, e.g. a critical pH range, long generation time, and high generation time (Ozer and Turabik 2006). The azo dye can be anaerobically degraded by single bacterial species (Boothman et al. 2006; Khalid et al. 2008; Zhang and Tang 2014; Liu et al. 2017b) or by microbial consortia (Khehra et al. 2005b). Nevertheless, the main drawback for using single microorganism is the generation of aromatic amines, which are often more toxic and recalcitrant than the original azo dye molecules. Furthermore, a single strain is usually selective to a specific azo dye; it also needs particular nutrients, supplements, and strict growth conditions (Solís et al. 2012a). Alternatively, the use of microbial consortia is a practical approach to remediate textile wastewater. The main advantage of using biological consortia are the symbiotic metabolism and diverse degradation mechanisms by the variety of microorganisms in the consortium. Such microbial consortia can degrade the generated aromatic amines (He et al. 2004; Littlejohns and Daugulis 2008; Tony et al. 2009; Phugare et al. 2011; Abiri et al. 2017; Oon et al. 2018; Zhu et al. 2018a). Microbial consortia degrade azo dye more efficiently than single bacterial species because they are functionally acclimatised to the environmental changes (Khehra et al. 2005b; Moosvi et al. 2007). Additionally, the synergetic performance of microorganism within a consortium can boost dye

decolourisation rates and thereby reduce the required residence time. For example, azo dye decolourisation increased from 70 % in 60 min to 100 % in 30 min if a consortium was used instead of single bacterial species as *Enterococcus casseliflavus* (Liu et al. 2011b).

Sophisticated analytical techniques, such as liquid chromatography-mass spectrometry (LC-MS) and/or gas chromatography-mass spectrometry (GC–MS) are used to reveal azo dye degradation products including amines during textile wastewater experiments (Dhanve et al. 2008; Meetani and Rauf 2013). Furthermore, spectrophotometric methods can also be used to distinguish dye decolourisation and highlighted any aromatic amines generated during azo dye biodegradation (Dafale et al. 2008; Murali et al. 2013a). Cai et al. (2012) reported that dye decolourisation was monitored by spectrophotometric scan (200-700 nm). Table 2-4 illustrates a review for textile wastewater using MO as a case study, and Table 2-5 highlights real textile biodegradation experiments. According to Table 2-4, the main drawback for biological textile wastewater treatment was the toxic aromatic amines generated from azo dye biodegradation and the needs to use additional organic carbon sources. Furthermore, some experiments parameters such as retention time and adsorption capacity were reported for comparison with the wastewater experiment parameters in the next chapters.

**Table 2-4 Review of textile wastewater treatments using MO as an azo dye case study.**

| Process and micro-organism used | MO decolourisation | Parameters | Additional carbon | Aromatic Amines generation | Analytical method | Reference |
|---|---|---|---|---|---|---|
| Anaerobic sequencing batch reactors | Partial decolourisation | MO 20 mg/l, sludge adsorption capacity 36 mg/g, adsorption contact time 10min, pre acclimatising for 89 days, HRT 8-12 hrs, T 30$^0$C | + | + | HPLC, GC | Yu et al. 2011 |
| Anaerobic sludge substrate from wastewater | 90-96 % | MO 50 to 150 mg/l, ORP-158 to -200 mV, pre- acclimatising 28 days, RT 24 hrs, at room temperature | + | + | spectrophotometer analysis | Murali et al. 2013b |
| Integrated anaerobic-aerobic biofilm by activated wastewater sludge | 95 % | MO 50 - 300 mg/l, coconut fibre adsorption capacity 1.20 mg/g, ORP -100 to -169, pre-acclimatisation 72 days, HRT 24 hrs | + | + | GC-MS spectrophotometer | Murali et al. 2013a |
| Anaerobic *Shewanella oneidensis* | 80 % | MO 100 mg/l, RT 16 hrs, T 30 $^0$C adsorption capacity neglected | + | + | HPLC, spectrophotometer | Cai et al. 2012 |
| *Anaerobic Kocuria rosea MTCC 1532* | 100 % | MO 10- 70 mg/l, T 10-50 $^0$C, RT 60 hrs | + | + | FTIR and GC-MS | Parshetti et al. 2010 |
| *Anaerobic Aeromonas sp. strain DH-6* | 100 % | MO 100 mg/l, pH 3-7, T 5 - 45 $^0$C | + | + | GC-MS HPLC | Du et al. 2015a |
| Anaerobic *Pseudomonas putida mt2* using a batch system | 100 % | MO 500 mg/l, T 35 $^0$C, pH 7 - 9, dye removal 7.50 mg/g, RT 60 hrs | + | Not reported | spectrophotometer | Thao et al. 2013 |

| | | | | | | |
|---|---|---|---|---|---|---|
| *Anaerobic Klebsiella oxytoca* using a batch system | 100 % | MO 32 mg/, hematite, goethite Fe (III) was added as an electron acceptor, RT 24 hrs, T 25 °C | + | - | spectrophotometer | Yu et al. 2016 |
| **Aerobic mixed-bacteria** (***E.coli and Enterobacter***) batch system | 92 % | MO 20 mg/L, pH 8.0, T 37 $^0$C, RT 1 hr | + | Not reported | spectrophotometer | Ferdous Rumky et al. 2013 |
| Anaerobic baffled membrane bioreactor anaerobic wastewater sludge | 100 % | MO 50 mg/l, RT 23 hrs, pH 6-7 | + | - | LC-MS | Liu et al. 2018 |
| Aerobic removal by bacterial consortium *Sphingomonas paucimobilis, Bacillus cereus* | 92 % | MO 750 mg/l, RT 48 hrs, pH 7, T 30 $^0$C | + | - | Fourier transform infrared (FTIR), (NMR) | Ayed et al.2010a |
| Anaerobic sludge | 100 % | MO 70 - 300 mg/l, RT 12hrs, T 30 $^0$C | + | - | HPLC GC | Yemashova et al. 2009 |

**Table 2-5 Lists of real textile biodegradation experiments showing the decolourisation efficiency, a technique used and parameters.**

| Technique | Decolourisation % | Parameters | Notes | Reference |
|---|---|---|---|---|
| Microbial fuel cell using activated carbon | 70 % | HRT 48 hrs, T30 °C, pH 12.20 | No sophisticated analysis of degradation products | Kalathil et al. 2012 |
| Biodegradation (fungi) | 70 % | HRT 25 hrs, T 25 °C, pH 3, Influent concentration 200 mg/l | Additional carbon was not used, but no sophisticated analysis of degradation products | Nilsson et al. 2006 |
| Anaerobic fluidised bed | 59 %-82 % | HRT 24 hrs, T 35 °C, pH 9.9 | Additional carbon did not influence decolourisation, no sophisticated analysis of degradation products, acclimatisation for 24 days | Şen and Demirer 2003 |
| Anaerobic sludge bioreactor | 67-71 % | HRT 12 hrs, T 29 °C, pH 9.5 Influent concentration 0-500 mg/l | Acclimatised bacterial for about 5 years, additional carbon source added, no sophisticated analysis of degradation products | Chinwetkitvanih et al. 2000 |
| UB and semi-continuous activated sludge reactor | 98-95 % | HRT 1 - 2 days, T33 °C, pH 5.5 | No sophisticated analysis of degradation products | Kuai et al. 1998 |
| Anaerobic system | 57 % | HRT 12 - 24 hrs, T 27 °C, pH 7-8 | No sophisticated analysis of degradation products, acclimatised for 30 days | Igor et al. 2010 |
| Aerobic sludge bioreactor | 70 % | HRT 3 - 4 days, pH 7.5 | No sophisticated analysis of degradation products acclimatised for 70 days; additional carbon source added | Patel et al. 2018 |
| Aerobic sludge bioreactor | 92 % | HRT 24 hrs, T35 °C, pH 9.2 | No sophisticated analysis of degradation products, no acclimatising, additional carbon source added | Somasiri et al. 2008 |
| UB-submerged aerated biofilter | 30-89 % | HRT 14-21 hrs, T 30 °C | No sophisticated analysis of degradation products | Amaral et al. 2014 |
| Electro- and bio-oxidation | 90 % | HRT 100 min, T 25 °C, pH 2,4, 8 | FT-IR and GC–MS analysis for organic compounds, acclimatisation for 144 hrs, | Aravind et al. 2016 |

| | | | | |
|---|---|---|---|---|
| Constructed wetland | 70 % | HRT 1-24 hrs, T 10 - 20 °C pH 9.4 - 12 | No sophisticated analysis of degradation products | Bulc and Ojstršek 2008 |
| Anaerobic biofilm-Ozonation | 99 % | HRT 3 days, pH 7.5 - 8 | No sophisticated analysis of degradation products reduced toxicity by 20 times | Punzi et al. 2015 |
| Aerobic Biodegradation | 70 % | HRT 3 days, T 25 °C, pH 3,6,9 | The mass analysis used to determine degradation products, efficient mineralisation by fungi consortium | Tegli et al. 2014 |
| Upflow anaerobic fixed bed reactor | 90 % | HRT 23 hrs, T 30 °C, pH 7 | No sophisticated analysis for degradation products, acclimatisation used, rich nutrients used, additional carbon source added | Sandhya and Swaminathan 2006 |
| Aerobic granular | 100 % | HRT 12 - 24 hrs, T 27 °C, pH 8.8 | No sophisticated analysis for degradation products, acclimatisation was used, additional carbon source added | Bashiri et al. 2018 |
| Aerobic activated sludge | 85 - 93 % | HRT 38 hrs, T 25 °C, pH 7 | No sophisticated analysis of degradation products | Arsalan et al. 2018 |
| Fluidised bed (aerobic) | | HRT 1 - 3 days, T 30-40 °C, pH 10 - 11 | No sophisticated analysis of degradation products | Francis and Sosamony 2016 |
| Sequential treatment | 90 % | HRT 2 days, pH 7 - 8 | No sophisticated analysis for degradation products, 16S rDNA approach for microorganism involved | Dafale et al. 2010 |
| Upflow Column Bioreactor | 92 % | HRT 12 hrs, T 30 °C, pH 7.5 | No sophisticated analysis of degradation products, Microbial consortia | Lade et al. 2015 |
| Aerobic, anaerobic, sequential | 65 %, 80 % | HRT 24 hrs, T 27 °C | No sophisticated analysis for degradation products, no additional carbon added 30day for acclimatisation | Tomei et al. 2016a |

### 2.4.1.1    Azo dye biodegradation mechanism

Azo dye biodegradation as a sole carbon and nitrogen source has been noted after a period of gradual adaptation to acclimatise bacteria with the new condition (Ayed et al. 2011; Solís et al. 2012a). 4-aminobenzene sulfonic acid (4-ABA) and N,N-dimethyl-p-phenylenediamine (DPD) are the typical aromatic amines generated during MO anaerobic biodegradation, as shown in Figure 2-7 (Liu et al. 2017b; Sarvajith et al. 2018). The generated aromatic amines can subsequently be degraded aerobically (Chang et al. 2004; Pandey et al. 2007a). Perei et al. (2001) highlighted that some bacterial species, e.g. *Pseudomonas paucimobilis* mineralised 4-ABA as a sole carbon and nitrogen substrate during azo dye biodegradation as highlighted in Figure 2-8 (Perei et al. 2001).
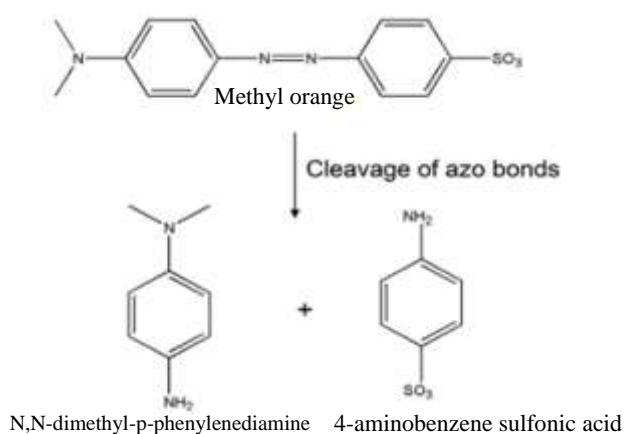


**Figure 2-7. Typical MO degradation products (Liu et al. 2017b; Sarvajith et al. 2018).**
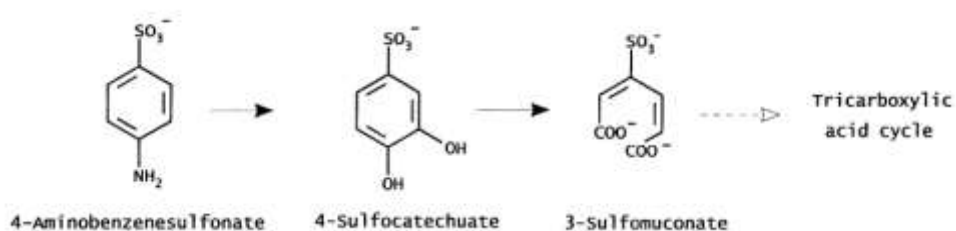


**Figure 2-8 The suggested 4-aminobenzene sulfonic acid (4-ABA) degradation mechanism (Perei et al. 2001).**

Organic carbon, e.g. glucose, is frequently added to boost the azo dye degradation process (Ogugbue et al. 2012; Shah et al. 2013). Additional to that, when starch which is used as an additive during the dyeing process, microorganisms utilised it as a substrate to enhance azo dye decolourisation (O'Neill et al. 2000b). Organic carbon compounds raise azo dye decolourisation rates directly as electron donors or indirectly by stimulating microorganism growth as a metabolism substrate (Van der Zee and Cervantes 2009). It was reported that the presence of additional carbon, as an energy source, initiated microbial growth rate and boosted azo dye degradation as an electron donor (Pandey et al. 2007a; Popli and Patel 2015). These findings agreed with Solís et al. (2012), who noticed that the abundance of nitrogen and carbon sources affect azo dye biodegradation significantly. However, additional carbon source could become a more favourable substrate for microorganisms than the azo dye molecules, which might reduce azo dye decolourisation efficiency (Kumar et al. 2009). It was reported that the azo dye biodegradation could be enhanced by added iron oxides to provide convenient, reducing condition for microorganisms by lowering the redox potential (Chang et al. 2001; Yu et al. 2012; Khan et al. 2015). Iron oxides also enhanced electron transfer and improved azo dye removal (Zhao et al. 2017b). Iron-reducing bacteria oxidise aromatic compounds anaerobically as an electron donor (Lovley et al. 1989; Lovley and Lonergan 1990). Iron-reducing bacteria, e.g. *Shewanella* degrades azo dye such as MO, the respiratory transmembrane electron transport chains (MtrA, MtrB and MtrC) releases electrons from cytochrome via the respiratory chain to be shuttled to the azo bond (Cai et al. 2012). Furthermore, *Shewanella* decolourised MO by nanowires mechanism. Nanowires are cross-linked between *Shewanella* and azo dye to transfer electrons from the bacterial outer membrane to dye molecule to breakdown the azo bond (Ng et al. 2014). The azo dye can be anaerobically degraded directly by enzymes or indirectly by redox mediators (electron shuttles) as elucidated in Figure 2-9 (Pandey et al. 2007b). Redox mediator shuttles electron between dye molecules and iron-reducing bacteria to accelerate azo dye biodegradation (Rau et al. 2002; Pereira et al. 2010). During azo dye biodegradation, the generated intermediate compounds could act as a redox mediator (Xu et al. 2014; Li et al. 2017a). Russ et al. (2000) mentioned that redox mediators can be generated during microbial metabolism or can be added artificially. It can be regenerated by cell nicotinamide adenine dinucleotide ($NAD^+$) or nicotinamide adenine dinucleotide phosphate ($NADP^+$) via

azo reductase see Figure 2-10 (Keck et al. 1997; Robinson et al. 2001; Santos et al. 2007; Van der Zee and Cervantes 2009). Yu et al. (2016) noticed that the added electron shuttles enhanced MO degradation under iron-reducing condition. Enzymes, e.g. azo reductase, which was first reported in 1990 (Rafii et al. 1990). Azo reductase is an essential enzyme for azo dye biodegradation because dye molecules are unlikely to penetrate through cell membranes due to their high molecular weight. The redox mediator is the key between dye molecules and azo reductase depending on the NADH (nicotinamide adenine dinucleotide) that is localised in the cell outer membrane (Gingell and Walker 1971; Myers and Myers 1992). The azo reductase-redox mediator may be the first step in dye biodegradation (Kudlich et al. 1997; Stolz 2001).
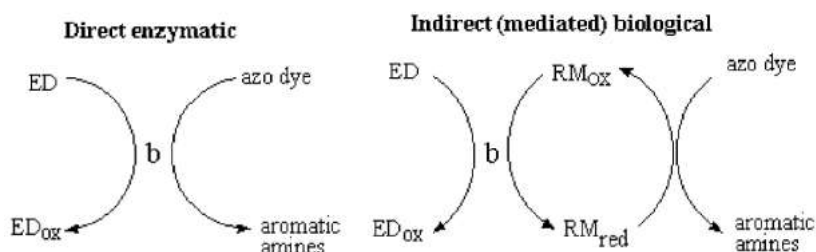


**Figure 2-9 Azo dye anaerobic mechanism, by (A) Directly by bacterial enzyme, (B) redox mediation (RM) (Pandey et al. 2007b).**
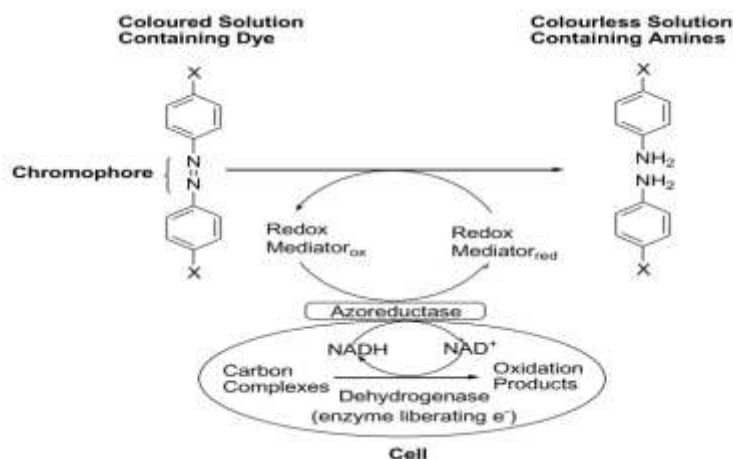


**Figure 2-10 Azo dye proposed mechanism by azoreductase (Keck et al. 1997).**

Iron-reducing bacteria, *Klebsiella oxytoca* (GS-4-08) was used to degraded MO, see Figure 2-11, this bacteria degraded MO at a low efficiency without electron shuttle as shown in mechanism Ⅰ. Humic acid anthraquinone-2-disulfonate (AQS) was added as an electron shuttle and glucose was added as an electron donor to raise the MO

degradation, during MO biodegradation, humic acid was regenerated by an oxidation-reduction mechanism, and it increased MO degradation and Fe (III) reduction which was represented as in a mechanism II. The iron oxidation-reduction reaction can also act as an electron shuttle to raised MO decolourisation, as highlighted in mechanism III (Yu et al. 2016). Iron reducing bacteria uses another technique to transfer electrons additionally to electron shuttles. It uses pili as nanowires to transfer electrons to another bacterial species; this mechanism is known by direct Interspecies electron transfer (DIET) (Rotaru et al. 2014). This mechanism was highlighted between iron-reducing bacteria, *Geobacter* and other species as *Methanosaeta* in rice paddy soil (Holmes et al. 2017). The DIET could enhance the removal of the organic contaminants (He et al. 2017). This mechanism could be found in the utilised iron oxide bearing sludge in the latter wastewater treatment chapters, as it is probably rich in iron-reducing bacterial species.
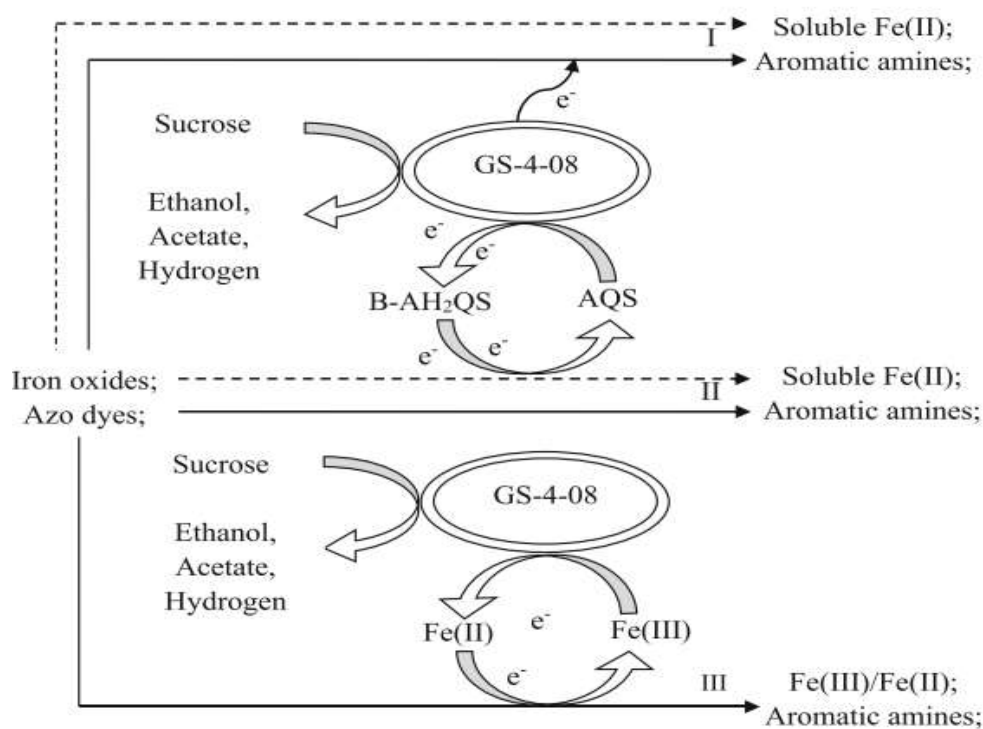


**Figure 2-11 Hypothetical mechanism for azo dye degradation by *Kebsiella oxytoca* (GS-4-08) using glucose as a substrate, (I) without electron shuttle, (III) with electron shuttling (quinone AQS), and (III) with electron shuttle (iron oxidation-reduction)**(Yu et al. 2016)**.**

### 2.4.1.2    Dye removed by adsorption

During biological textile wastewater treatment, adsorption and biodegradation are the two dye removal mechanisms involved. It is important to determine the amount of dye remove by each mechanism. Adsorption starts when dye molecules diffuse from a high concentration to a low concentration (the adsorbent surface). The dye molecules diffuse through to the substrate surface and bind with the surface-active site (Vadivelan and Vasanth Kumar 2005). Dye removal by adsorption has a limited capacity (Doğan et al. 2004). During textile wastewater experiments (in chapters 5, 6 and 7), batch experiments were conducted to determine the sludge adsorption capacity to calculate the amount of dye removed by adsorption during the experiments according to adsorption capacity equation (see section 3.11).

### 2.4.1.3    Adsorption Models

An adsorption isotherm is a function of adsorbed concentration at constant temperature (Tchobanoglous et al. 2003). It also defined as "An adsorption isotherm represents the equilibrium relationship between the adsorbate concentration in the liquid phase and that on the adsorbent surface at a given condition" (Das et al. 2014). Langmuir's isotherm model is one of the adsorption theories, and it fits many contaminants. It assumes that there is no competitive interaction between the adsorbate molecule (dye in this case) and the active site in a monolayer and homogeny adsorbent surface (Das et al. 2014). The monolayer is referred to the adsorption surface, which is equal to the thickness of one molecule of the adsorbent (Nasuha et al. 2010). This theory depends on the following assumptions:

1. The adsorption has occurred in an adsorbent monolayer.
2. The number of active adsorbent sites which are ready to bind with the adsorbate is specified, and it has the same affinity.
3. The adsorption phenomenon is a reversible process; this means that the adsorbate can be disassembled in certain conditions.

Equation 1 represents, the Langmuir isotherm equation, $q_{max}$ and Langmuir's constant can be obtained by plotting I/qe vs 1/Ce. This theory fits the performance of monolayer adsorption on an adsorbent surface (Tchobanoglous et al. 2003).

27

$$\frac{1}{q_e} = \frac{1}{K_L q_{max}}\left(\frac{1}{C_e}\right) + \frac{1}{q_{max}}$$ (Equation 1)

Where $q_e$, is the adsorption capacity of adsorbate in mg on the specific weight of adsorbent in g, and $q_{max}$ refers to the maximum adsorption capacity for adsorbate mg/g adsorbent. $K_L$: Langmuir constant l/mg. Ce is the equilibrium adsorbate concentration mg/l referring to the degree of interaction between the adsorbate and the adsorbent.

Freundlich's isotherm theory (1906) is another adsorption theory. This theory rests on the assumption that the dominant site of the adsorbent is binding first with the adsorbate particles at multi-layer (Li et al. 2013). At first, it was used to describe activated carbon adsorption performance in water and wastewater processes (Tchobanoglous et al. 2003). Equation 2 represents the Freundlich's isotherm theory, the value of n and k indicate the affinity of the adsorbent and how to extend the sorption process deviates from the linear trend (Shahwan and Erten 2004). It ranges between 0 and 1, with zero as the maximum heterogeneous value (Haghseresht and Lu 1998).

$$\mathbf{Log q_e = Log K_f + \frac{1}{n}Log C_e}$$ (Equation 2)

where ($q_e$) is the adsorption capacity which represents the amount of adsorbate in mg in a specific amount of adsorbent in g at equilibrium, $K_f$ is the Freundlich constant mg.l/g. n is the driving force which represents by slope, whereas 1/n refers to the heterogeneity of the surface. Ce is the concentration of adsorbate that is adsorbed on the adsorbent surface matrix in equilibrium conditions.

### 2.4.2 BTEX removal techniques

BTEX are recalcitrant monoaromatic compounds (Aihara 1992). BTEX can be removed by chemical or physical methods (Aleghafouri et al. 2015). These methods have several drawbacks, such as the high cost of surfactants and adsorbent materials used, and the generation of toxic by-products as the adsorbent's material required further treatment to remove the BTEX (El-Naas et al. 2014). Alternatively, biological treatment is a functional and low-cost method to remediate BTEX (Alexander et al. 2002; Massalha et al. 2007; Farhadian et al. 2008b; Weelink et al. 2010; Akmirza et al. 2017; Müller et al. 2017).

The pioneering study for BTEX biodegradation was undertaken in 1928 by Gray and Thornton. In this experiment *Bacillus hexabovorum* isolated from soil was used to metabolise toluene and xylene (Bushnell and Haas 1940). Until 1980, studies focused on aerobic BTEX biodegradation; but since then, researchers have studied anaerobic BTEX biodegradation (Weelink et al. 2010). BTEX can be completely mineralised by microbial consortium due to the complementary metabolic mechanism. Experimental study confirms that mixed bacterial culture degraded BTEX more efficiently than a single bacterial strain (Oh and Bartha 1997). This finding agreed with Venosa and Zhu (2003) who also noticed that microbial consortia degraded BTEX more efficiently than single bacterial species by using various metabolism pathway. Mixing two or more bacterial cultures degrade benzene more efficient than using a single bacterial species (Liu et al. 2010). Efficient BTEX biodegradation using a microbial consortium can be attributed to the varied metabolic mechanisms or interspecies interaction (Deeb and Alvarez-cohen 2000). Additionally, the bacterial consortium may use syntrophic associations to overcome the BTEX toxicity and any unfavourable environmental conditions as pH and temperature (Morlett-Chávez et al. 2010). Furthermore, Mazzeo et al. (2010) highlight that biodegradation using an indigenous consortium is a convenient methodology for BTEX bioremediation.

El-Naas et al. (2014) noted that some microorganisms metabolise BTEX to $CO_2$ without generating toxic by-products. Furthermore, some bacterial species metabolise BTEX as a sole carbon source (Kelly et al. 1996; Berlendis et al. 2010). For example, *Pseudomonas* degrades BTEX aerobically as a sole carbon source. This aerobic bacteria degraded benzene by breakdown the aromatic ring to generate catechol (Gibson 1984). Benzene tends to demonstrate lower removal rates than toluene, ethylbenzene, and xylene because it is a thermodynamically stable and benzene aromatic ring has a symmetrical electron distribution which makes it difficult to degrade by anaerobic bacterial enzymes (Foght 2008; Weelink et al. 2010). Toluene could be more easily biodegradable than other BTEX compounds due to the position of the subsequent group on the aromatic ring (Andreoni and Gianfreda 2007).

### 2.4.2.1 BTEX biodegradation at the iron-reducing condition

In the last decade, more attention has been devoted to removing mono aromatic hydrocarbons such as BTEX using anaerobic biodegradation since these contaminants can be found in anoxic aquifers (Weelink et al. 2010). BTEX bioremediation often occurs in iron-reducing environments (Botton and Parsons 2006). Fe (III) oxide is the most abundant electron acceptor in the earth (Lovley 1993). Kunapuli et al. (2008) highlighted that benzene mineralised to $CO_2$ under iron-reducing conditions. Iron-reducing culture solubilises Fe (III) as an electron acceptor during benzene anaerobic oxidation (as electron donor) (Lovley et al. 1994). Chelators and a humic substrate can be found in soil at a high ratio (Lovley et al. 1996). It accelerates the rate at which Fe (III) reduces to Fe (II) and eliminates the need for direct contact between microorganisms and Fe (III) oxides as illustrated in Figure 2-12 (Lovley 1997). The stoichiometry of BTEX oxidation by various electron acceptors is represented by benzene, as demonstrated in Table 2-6 (McCarty 1971).
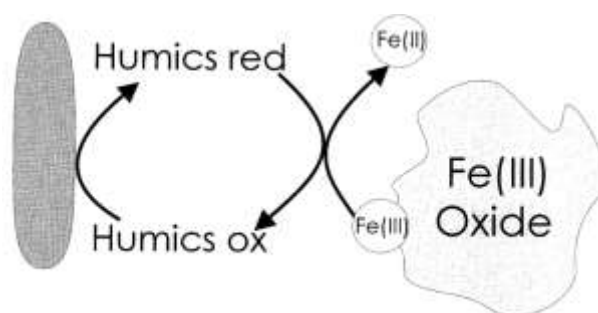


**Figure 2-12 The role of electron shuttle (humic substances)** (Lovley 1997)**.**

**Table 2-6 The stoichiometric reaction for benzene oxidation by various electron acceptors.**

| Electron acceptors (ox/red) | Stoichiometric equation |
|---|---|
| $ClO_3^-/Cl^-$ | $C_6H_6 + 5ClO_3^- + 3H_2O \rightarrow 6HCO_3^- + 5Cl^- + 6H^+$ |
| $O_2/H_2$ | $C_6H_6 + 7.5O_2 + 3H_2O \rightarrow 6HCO_3^- + 6H^+$ |
| $NO_3^-/N_2$ | $C_6H_6 + 6NO_3^- \rightarrow 6HCO_3^- + 3N_2$ |
| $NO_3^-/NO_2^-$ | $C_6H_6 + 15NO_3^- + 3H_2O \rightarrow 6HCO_3^- + 15NO_2^- + 6H^+$ |
| $Fe^{3+}/Fe^{2+}$ | $C_6H_6 + 30Fe^{3+} + 18H_2O \rightarrow 6HCO_3^- + 30Fe^{2+} + 36H^+$ |
| $SO_4^{2-}/H_2S$ | $C_6H_6 + 3.75SO_4^{2-} + 3H_2O \rightarrow 6HCO_3^- + 1.875H_2S + 1.875HS^- + 0.375H^+$ |

The coupling of organic carbon oxidation with Fe (III) reduction to Fe (II) by iron-reducing bacteria is an efficient mechanism to mineralise BTEX in groundwater pollutants (Lovley 1997). *Firmicutes* Bacteria and affiliated phyla degrade benzene

into small molecules to generate acetic acid and hydrogen gas while the synergistic *proteobacteria* phylum mineralises acetic acid to $CO_2$ (Zaan et al. 2012). *Firmicutes Clostridia* uses Fe (III) as a terminal electron acceptor while it anaerobically degraded benzene (Aburto-Medina and Ball 2015). *Geobacter* iron-reducing bacteria can mineralise BTEX (Müller et al. 2017). Silva and Alvarez (2002) reported that *Clostridium* and *Geobacter* were the dominant bacterial genera during BTEX biodegradation. Figure 2-13 shows the general common forms of organic carbon biodegradation by iron reduction microorganisms (Lovley 1997).
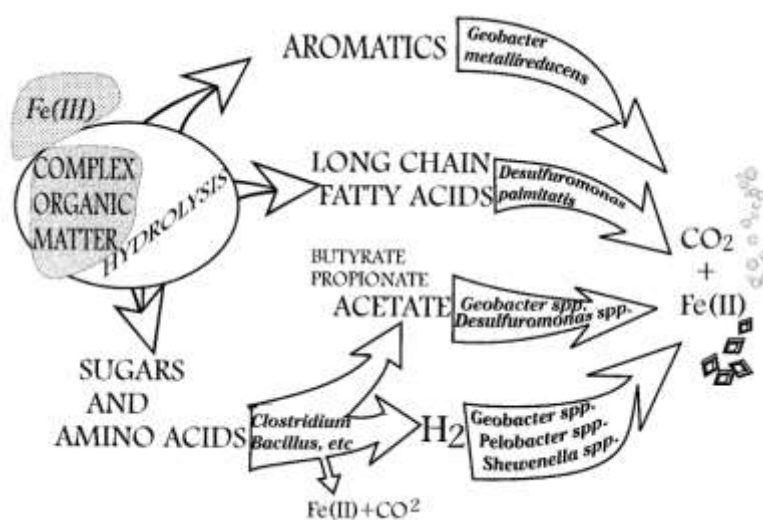


**Figure 2-13 Oxidation of organic compounds coupling with iron reduction microorganisms**
(Lovley 1997)**.**

*Geothrix* and *Geobacter* simultaneously reduced Fe (III) as a terminal electron acceptor process (TEAM) by using BTEX as a carbon source. They cleaved the mono aromatic hydrocarbons to $CO_2$. Grbic-Galic and Vogel (1987) highlighted, methanogenic bacterial species mineralised benzene to carbon monoxide and methane, the pathway of this mechanism is illustrated in Figure 2-14. This mechanism was also reported in other literature (Aburto-Medina and Ball 2015; Firmino et al. 2015b). Other bacterial species as *Pseudomonas cluster (putida* and *fluorescen)* degraded BTEX as a sole carbon source (Shim and Yang 1999). Table 2-7 reported a review for BTEX biodegradation highlighted several iron-reducing bacteria which degrade BTEX. The majority of the reported studies degraded the BTEX using additional carbon source, and the microorganism involved was pre-acclimatised.
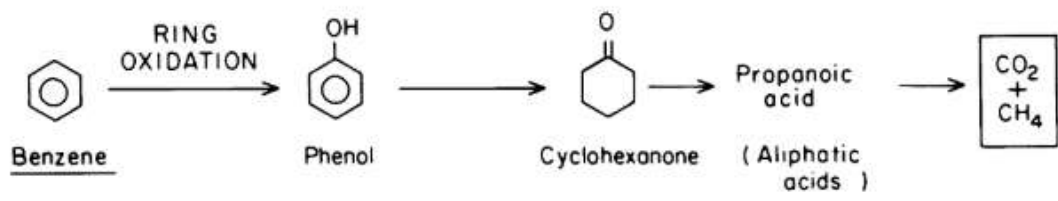
**Figure 2-14  Anaerobic benzene degradation by methanogenic bacteria (Grbic-Galic and Vogel 1987).**

<p align="center">**Table 2-7 Review for BTEX biodegradation literature.**</p>

| Microorganism involved | Comments | Sole carbon source | Pre-acclimatisation | Reference |
|---|---|---|---|---|
| A bacterial consortium from hydrocarbon-contaminated soil | Aerobic BTEX removal 80 – 100 % within incubation time 48-72 hrs | No | yes | Singh and Celin 2010 |
| *Janibacter* isolated from a crude oil-contaminated tidal flat sediment sample | Aerobic BTEX removal  7.4 – 60 % over 11 days incubation time | No | Yes | Jin et al. 2013 |
| Pure bacterial consortia included *Pseudomonas*, *Yarroia, Acinetobacter, Corynebacterium and Sphingomonas* | BTEX removal 90 -  98 %, 50 hrs incubation | NO | yes | Jo et al. 2008a |
| Bacterial consortium. *Pseudomonas, Shewanella, Burkholderia, Alcanivorax, Rhodococcus and Bacillus.* | Aerobic BTEX removal 95 %, Influent 50 mg/l, pH 7.2, T 36 $^{\circ}$C, incubation for 60 hrs | Yes | yes | Morlett-chávez et al. 2010 |
| Immobilized *Mycobacterium sp. CHXY119 Pseudomonas sp. YATO41* | Aerobic BTEX removal 84.7- 97.8 %, 25 $^{\circ}$C at 150 rpm, influent 100 mg/l, RT 400 hrs<br><br>$C_6H_6 + 7.5O_2 \rightarrow 6CO_2 + 3H_2O$  Benzene<br>$C_7H_8 + 9O_2 \rightarrow 7CO_2 + 4H_2O$  Toluene<br>$C_8H_{10} + 10.5O_2 \rightarrow 8CO_2 + 5H_2O$  Ethylbenzene<br>$C_8H_{10} + 10.5O_2 \rightarrow 8CO_2 + 5H_2O$  Xylene | Yes | yes | Xin et al. 2013 |

| | | | | |
|---|---|---|---|---|
| *Geobacter metallireducens* (single strain iron-reducing bacteria) | Anaerobic benzene mineralisation (82 – 100 %) to $CO_2$. Fe (III) is the electron acceptor. Influent concentration 0.25 mM, incubation for 8 days | yes | yes | Zhang et al. 2013c |
| *Mycobacterium cosmeticum* (single strain) | Aerobic BTEX partially mineralised to $CO_2$, 30 °C, 160 rpm in the dark, incubation for 40 hrs. | yes | yes | Zhang et al. 2013b |
| *Pseudomonas putida F1* (single strain) | Aerobic BTEX mineralised to $CO_2$ influent 15-90 mg/l. T 30 °C, pH 7, incubation for 14 hrs | yes | No | Robledo-Ortíz et al. 2011 |
| *Mycobacterium* and *Pseudomonas* | Aerobic BTEX degradation (67 – 90 %), pH 7-8, T 28 - 30 °C, HRT 0.872 day. | No | Yes | Lin et al. 2012 |
| A bacterial consortium included: *Geobacter, Geothrix, Shewanella* (Iron-reducing condition) | Anaerobic benzene and toluene mineralisation to $CO_2$ using Fe (III) as electron acceptor over 80 days | yes | yes | Anderson et al. 1998 |
| The bacterial consortium included: *Geobacter, Geothrix, Variovorax paradoxus* (Iron-reducing condition) | Anaerobic benzene oxidation to $CO_2$ using Fe (III) as electron acceptor | yes | yes | Rooney-Varga et al. 1999 |
| Contaminated soil sediments by (Iron reducing consortium) | Anaerobic benzene oxidation 90 % using Fe (III) as an electron acceptor. Incubation 140 days, 238 °C in the dark. | yes | yes | Caldwell et al. 1999 |
| Geobacteraceae Geobacter (Iron-reducing conditions) | Anaerobically, Benzene, toluene and xylene were only degraded Microcosms 20 - 60 µM, incubation 230 days Fe (III) as electron acceptor<br><br>$C_6H_6 + 30Fe^{3+} + 12H_2O \rightarrow 6CO_2 + 30H^+ + 30Fe^{2+}$ Benzene<br>$C_7H_8 + 36Fe^{3+} + 21H_2O \rightarrow 6HCO_3 + 43H^+ + 36Fe^{2+}$ Toluene<br>$C_8H_{10} + 42Fe^{3+} + 16H_2O \rightarrow 8CO_2 + 32H^+ + 42Fe^{2+}$ xylene | yes | yes | Botton and Parsons 2006 Botton et al. 2007 |
| The bacterial consortium included: *Geobacter* and *Rhodoferax.* (iron-reducing conditions) | Anaerobic BTEX degradation using Fe (III) and nitrogen were used as electron acceptors | | yes | Farkas et al. 2017 |

| | | | | |
|---|---|---|---|---|
| Iron-reducing bacteria and methanogenic bacteria | BTEX to $CO_2$, Fe (III) as an electron acceptor to generated $CH_4$ and Fe (II). Iron Fe (II) and methane oxidised: <br><br> $Fe^{2+} + 0.25O_2 + HCO_3 + 0.5H_2O \rightarrow Fe(OH)_3 + 2CO_2$ <br><br> $CH_4 + 2O_2 \rightarrow 2H_2O + CO_2$ | yes | yes | Hideo and Kiang 2019 |
| *Peptococcaceae, Rhodocyclacea and Burkholderiaceae* (Denitrifying bacterium consortia) | Anaerobic benzene degradation, nitrate used as electron acceptor <br><br> $C_6H_6 + 6NO_3^- + 6H^+ \rightarrow 6CO_2 + 3N_2 + 6H_2O$ | yes | yes | Zaan et al. 2012 |
| Azoarcus denitrification bacteria | Anaerobic benzene degradation <br><br> $C_6H_6 + 6NO_3^- \rightarrow 6HCO_3^- + 3N_2$ | yes | Not reported | Takahata et al. 2007 |
| Bacterial consortia under Mn(IV) and Fe (III) reducing conditions | Anaerobic benzene as the sole carbon to $CO_2$. Mn (IV) or Fe (III) as electron acceptors <br><br> $C_6H_6 + 30Fe^{3+} + 12H_2O \rightarrow 6CO_2 + 30H^+ + 30Fe^{2+}$ <br><br> $C_6H_6 + 15Mn^{4+} + 12H_2O \rightarrow 6CO_2 + 30H^+ + 15Mn^{2+}$ | yes | No | Morales-Ibarria et al. 2008 |
| *Ferroglobus placidus* (Iron-reducing bacteria) | Anaerobic benzene degradation to $CO_2$. Fe (III) as electron acceptor <br><br> $C_6H_6 + 30Fe^{3+} + 12H_2O \rightarrow 6CO_2 + 30H^+ + 30Fe^{2+}$ | yes | Not reported | Holmes et al. 2011 |

## 2.5 Municipal wastewater

Efficient municipal wastewater treatment can make an intrinsic contribution to water recycling as it maintains the natural water resources. Nitrogen compounds are considered as pollutants due to the toxicity of free ammonia to aquatic life (Cleverson Vitorio Andreoli and Fernandes 2007; Sperling 2007). In municipal wastewater, urea (a form of organic nitrogen) comprises about 60 % of the total nitrogen in sewage. Ammonium generated from urea and other organic nitrogen compounds contaminate aqueous systems (Von Sperling and Chernicharo 2005). Even though nitrogen is an essential nutrient for aquatic life at low concentration (Sedlak 1991; Sperling 2007; Kadlec and Wallace 2009).

### 2.5.1 Nitrogen removal mechanisms

In municipal wastewater experiment, nitrogen removal took more attention because researches recently focused on nitrogen removal at iron-reducing condition (Zhou et al. 2016a; Li et al. 2018). Nitrogen removal at iron-reducing condition could be the expected mechanism for nitrogen transformation during wastewater experiments in the latter chapter.

### 2.5.2 Nitrification-denitrification and partial nitrification

Nitrification is the first steps in conventional nitrogen removal, under aerobic conditions ammonium first converts into nitrite as intermediate ammonium oxidation compound, which is then further oxidised to nitrate (Henze et al. 2002; Maltais-Landry et al. 2009). It is a limiting step in nitrogen removal unless sufficient dissolved oxygen is available, and an appropriate temperature is maintained (Tanner and Kadlec 2003). Denitrification is the reaction responsible for the production of nitrogen gas in an anoxic environment (Hallin et al. 2005). The sequence of nitrification followed by denitrification and anaerobic ammonium oxidation is the main classical techniques for microbial nitrogen removal (Chen et al. 2012; Ali and Okabe 2015; Wang et al. 2015; Zhao et al. 2017a). Carbon should be available to achieved efficient nitrogen removal, the ratio of carbon/ nitrogen should be more than 3.50 when it less than that

nitrification stage (aerobic) should be increased, and denitrification stage should be decreased (anaerobic) (Wang et al. 2015).

Nitrifying bacteria as *Nitrosomonas* and *Nitrobacter* are chemotrophic microorganisms. They utilise inorganic nitrogen as a source of energy. The nitrification reaction requires oxygen to oxidise ammonium to nitrate by ammonia-oxidising bacteria (see Equations 3 and 4). The process can be continued under anaerobic conditions by denitrification (when sufficient carbon is available as an energy source to reduce nitrate to nitrogen (Sedlak 1991; Sperling 2007; Zhu et al. 2008; Margot et al. 2016). Denitrification is the complementary step for nitrification under anaerobic or anoxic conditions, as shown in Equation 5 (Kosolapov et al. 2004). Partial nitrification involves microbial oxidation of ammonium at anoxic condition (see Equation 6) (Juni 1972; Paredes et al. 2007).

$$2NH_4^+ + 3O_2 \xrightarrow{\text{Nitrosomonas}} 2NO_2^- + 2H_2O + 4H^+ + \text{New cell} \quad \text{(Nitrification) (Equation 3)}$$

$$2NO_2^- + O_2 \xrightarrow{\text{Nitrobacter}} 2NO_3^- + \text{New cell} \quad\quad\quad \text{(Nitrification) (Equation 4)}$$

$$\text{Nitrate} \xrightarrow{\text{Organic carbon} - \text{anaerobic condition}} \text{Nitrogen} \quad\quad\quad \text{(Denitrification) (Equation 5)}$$

$$NH_4^{++} + 0.75O_2 + HCO_3^- \rightarrow 0.5NO_2^- + 0.5NH_4 + CO_2 + +1.5H_2O \quad\quad \text{(Equation 6)}$$
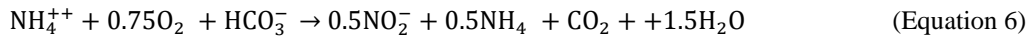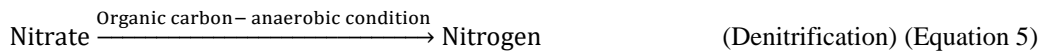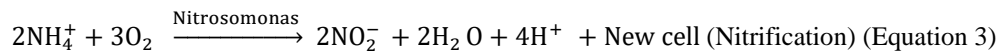
### 2.5.3 Anaerobic ammonium oxidation (Anammox)

Ammonia can also be oxidised to dinitrogen when nitrite is available as an electron acceptor at an anoxic environment; this reaction is known as Anammox. This mechanism is more favourable than nitrification-denitrification (Ali and Okabe 2015; Ma et al. 2016). Anammox was first reported by Strous and his group in 1998 when they observed ammonia oxidation under anaerobic conditions. Anaerobic bacteria oxidise ammonia (the electron donor) with nitrite (the electron acceptor) to generate dinitrogen gas with a small amount of nitrate (Strous et al. 1998). This mechanism was recognised to make an important contribution to the nitrogen cycle (Li et al. 2017b). Usually, in wastewater, both ammonium and nitrate ($NO_3^-$) co-exist. Nevertheless, nitrate cannot be used as an electron acceptor for Anammox. Alternatively, organic carbon may be the electron donor for nitrite reduction (Winkler et al. 2015; Du et al.

2016). During Anammox, some organic compounds can be degraded (Kartal et al. 2007).

### 2.5.4 Ammonium oxidation coupled with Fe (III) reduction (Feammox)

Anaerobic ammonium oxidation, coupled with Fe (III) reduction is known as Feammox (Ding et al. 2017; Li et al. 2018). This mechanism was recently discovered as part of the natural nitrogen cycle at iron oxide-rich habitats (Ding et al. 2014). Feammox can be distinguished in natural habitats where iron and nitrogen are abundant such as paddy soil, lake sediments and wetlands. In such environments, the dominant reaction is the generation of nitrogen gas by Feammox microorganisms (Wijsman et al. 2001; Cl'ement et al. 2005; Shrestha et al. 2009; Yang et al. 2012; Ding et al. 2014). Appropriate pH conditions for Feammox bacteria varied between 6.5 and 8 (Jetten et al. 1999). Feammox is a biotic process whereby ammonium is oxidised to nitrite, and Fe (III) is reduced to Fe (II) (Shrestha et al. 2009; Yang et al. 2012; Li et al. 2017b). In situ, this mechanism can be demonstrated when iron oxide is added to Anammox sludge: this stimulates the Feammox mechanism (Li et al. 2017b). Equations 7 - 9 show the Feammox reactions, including the energy yield. In the first reaction, Fe (III) is reduced, and ammonium is oxidised to nitrogen while in the second and third reaction nitrite and nitrate is generated (Zhou et al. 2016b; Yang et al. 2019).

$$3Fe(OH)_3 + 5H^+ + NH_4^+ \rightarrow 3Fe^{2+} + 9H_2O + 0.5N_2 \qquad \Delta_r G_m = -245 \text{ Kjmol}^{-1} \quad \text{(Equation 7)}$$

$$6Fe(OH)_3 + 10H^+ + NH_4^+ \rightarrow 6Fe^{2+} + 16H_2O + NO_2^- \qquad \Delta_r G_m = -164 \text{ Kjmol}^{-1} \quad \text{(Equation 8)}$$

$$8Fe(OH)_3 + 14H^+ + NH_4^+ \rightarrow 8Fe^{2+} + 21H_2O + NO_3^- \qquad \Delta_r G_m = -207 \text{ Kjmol}^{-1} \quad \text{(Equation 9)}$$
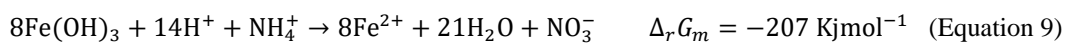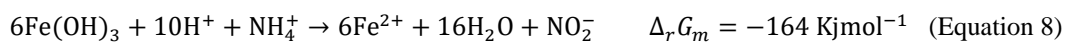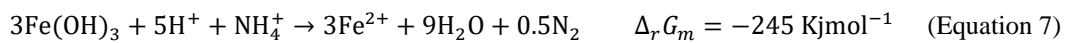
The generated nitrate and nitrite can be reduced by nitrate-dependent iron oxidation (NDFO) to regenerate Fe (III) as highlighted in Equations 10 and 11(Li et al. 2018)

$$2NO_2^- + 6Fe^{2+} + 8H^+ \rightarrow 6Fe^{3+} + N_2 + 4H_2O \qquad \text{(Equation10)}$$

$$2NO_3^- + 10Fe^{2+} + 12H^+ \rightarrow 10Fe^{3+} + N_2 + 6H_2O \qquad \text{(Equation 11)}$$
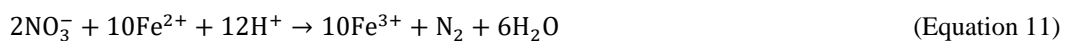
Shrestha et al. (2009) reported, in wetlands, iron-reducing bacteria converted ammonium to nitrite, nitrate and nitrogen gas as the end products by anaerobic oxidation using Feammox mechanism. Yang et al. (2012) highlighted, there is a shortage of studies have tackled the use of indigenous iron-reducing microorganisms

in wastewater treatment. Table 2-8 summarises a review for the biological nitrogen removal rate for municipal wastewater treatments. It also included the nitrogen removal rates for chapter six, seven and eight, which was normalised to be valid for comparison see Appendix 2.

**Table 2-8 Review for municipal wastewater nitrogen removal compared with the current study.**

| Paper title | Removal rate | Reference |
|---|---|---|
| **Kinetics of nitrogen removal in high rate Anammox up-flow filter** | 1.24-6.11 g/l/day | Jin and Zheng 2009 |
| **The annual cycle of nitrogen removal by a pilot-scale subsurface horizontal flow in a constructed wetland under moderate climate** | 0.15-0.70 $g/m^2$/day | Kuschk et al. 2003 |
| **Simultaneous Fe (III) reduction and ammonia oxidation process in Anammox sludge** | 28.30 $kg/m^3$/day | Li et al. 2017b |
| **Anaerobic ammonium oxidation (ANAMMOX) sludge immobilised by waterborne polyurethane and its nitrogen removal performance-a lab-scale study** | 1.53 $kg/m^3$/day | Chen et al. 2015 |
| **Combination of upflow anaerobic sludge blanket UB) reactor and partial nitrification/Anammox moving bed biofilm reactor MBBR) for municipal wastewater treatment** | 1.60 $g/m^2$/day | Malovanyy et al. 2015 |
| **Removal of nutrients in various types of constructed wetlands** | 250-630 $g/m^2$/year | Vymazal 2007 |
| **CANON and Anammox in a gas-lift reactor** | 8.90 $kg/m^3$/day | Sliekers et al. 2003 |
| **Microbial nitrogen removal pathways in integrated vertical flow constructed wetland systems** | 18.90 nmol/g/hr | Hu et al. 2016 |
| **Enhancement of total nitrogen removal through effluent recirculation and fate of PPCPs in a hybrid constructed wetland system treating urban wastewater** | 6.60 ±1.40 $g/m^2$/day | Ávila et al. 2017 |
| **Effect of by-pass and effluent recirculation on nitrogen removal in hybrid constructed wetlands for domestic and industrial wastewater treatment** | 8.40 $g/m^2$/day | Torrijos et al. 2016 |
| **The use of hybrid constructed wetlands for wastewater treatment with special attention to nitrogen removal: A review of a recent development** | 1.72-2.84 $g/m^2$/day | Vymazal 2013 |
| **Pilot-scale evaluation of Anammox-based mainstream nitrogen removal from municipal wastewater** | 30-240 mg/l/day | Lotti et al. 2015 |
| **Anammox-based technologies for nitrogen removal: Advances in process start-up and remaining issues** | 0.40 g/l/day | Ali and Okabe 2015 |
| **Anammox sludge immobilised in polyvinyl alcohol PVA) cryogel carriers** | 0.50 $kg/m^3$/day | Magrí et al. 2012 |
| **Nitrogen Loss through Anaerobic Ammonium Oxidation Coupled to Iron Reduction from Paddy Soils in a Chronosequence (Feammox)** | 0.17-0.59 mg/kg/day | Ding et al. 2014 |
| **Phase two textile wastewater (chapter six)** | 216 $g/m^3$/day or 12 $g/m^2$/day or 0.21 g/kg/day | |
| **Phase three textile wastewater (chapter seven)** | 39 $g/m^3$/day or 1.10 $g/m^2$/day or 0.03 g/kg/day | |
| **Municipal wastewater experiment (chapter eight)** | **159** $g/m^3$/day or 8 $g/m^2$/day or 0.15 g/kg/day | |

## 2.6    Literature review conclusion

According to the reported literature in this chapter, iron-reducing bacteria (IRB) was used to remediate recalcitrant wastewater contaminants as a single species or as part of a consortium. These microorganisms can oxidise aromatic organic carbons (azo dye and BTEX) as an electron donor simultaneously with reduction Fe (III) to Fe (II) as an electron acceptor. IRB reduce Fe (III), which is in contact with the bacterial outer membrane to Fe (II), while it uses electron shuttles to reduce remote Fe (III). Furthermore, IRB has developed a mechanism to transmit electrons between similar species using pili as nanowires. This mechanism is known as direct extracellular electron transfer (DEET). In addition, its transfer electrons to other species by direct interspecies electron transfer (DIET). It was reported that at iron-reducing condition, anaerobic ammonium oxidation coupled with iron-reduction mechanism was highlighted, which was recently known as Feammox. In this mechanism, ammonium becomes the electron donor, and Fe (III) is the electron acceptor (Ruiz-urigüen et al. 2018). Feammox is described as a potential alternative for conventional nitrogen removal where electron shuttles contribute to shuttle electron to Fe (III) electron acceptor (Yang et al. 2019). Iron oxides bearing sludge could be promising substrates to treat wastewater contaminants, and this hypothesis will be investigated in this study, as shown in the following chapters. Usually, in previous studies, either iron oxides or iron-reducing bacteria was added. In contrast, in this study, iron oxides bearing wastes probably contained both iron-reducing microorganisms and iron oxides, which can be used as a substrate to remediate recalcitrant wastewater contaminants.

# Chapter 3   : Materials and methods

## 3.1     Introduction

This chapter presents the research strategy, experimental setups and operational conditions followed by a description of the physical, chemical, and biological parameters measured during wastewater experiments.

## 3.2     Experiments research strategy

The research plan is illustrated as a flowchart as shown in Figure 3-1. In the beginning, preliminary experiments were undertaken to determine the MO calibration curve and the mine water treatment (MWT) sludge adsorption capacity, which is used in the later column experiments to estimate the amount of dye removed by adsorption. The textile wastewater treatment experiments included three phases. Phase one investigated the ability of MWT (live and autoclaved sludge) which was used as column substrates to degrade a simple textile wastewater contained 15 mg/l MO dissolved in deionised water over 170 days of continuous treatment. The effect of adding additional carbon source as glycerol to the influent wastewater was studied. MO concentration at 15 mg/l was used in previous studies to prepare textile wastewater (Zhu et al. 2012; Ghaedi et al. 2015). In phase two, live MWT was also used as column substrates to degrade simulated textile wastewater over 100 days at 25 °C. In this phase, the textile wastewater recipe was more complicated compared with phase one as it contained chemicals similar to real textile wastewater even though the MO concentration was remained at 15 mg/l. In this phase, the aerobic reactor was added after the anaerobic column as an attempt to enhance the azo dye degradation as recommended in previous studies (García-martínez et al. 2015; Patel 2015). The term sequential was used in to describe the consecutive anaerobic-aerobic treatment as the anaerobic column effluent was used as an influent for the aerobic reactor. The amount of sludge media was decreased compared with phase one, and the flow rate was increased. This was done mainly for practical reasons: to establish biodegradation as the predominant removal mechanism, the feasible limit of removal by adsorption has to be exceeded. To achieve this within the timeframe of the Ph.D. work, it was necessary to increase the loading rate of the columns. This was done by keeping the same reactor size as phase 1 and increased the flow rate at the same as a decreased the amount of column media. This

also provided an insight into how far the system could be challenged in terms of treatment efficiency.

After phase one and phase two textile wastewater experiments and because the promising results for these phases, the research strategy was developed by introduced water treatment sludge (WT) as a column substrate. This sludge is another abundant waste which might contain iron-reducing microorganisms. The aim was establishing whether another common iron oxide sludge waste would have the same effects during textile wastewater treatment. Additionally, Mixed sludge (MX) which contained 90 % w/w MWT sludge and 10 % w/w of the autoclaved wastewater treatment sludge (WW) was also used as column substrate. The reason of adding wastewater sludge as an amendment was because it could contain an additional organic carbon and nutrient also it possibly containing substrates that could act as electron shuttles. These three wastes (MWT, MX and WT) were used in this phase, municipal wastewater and BTEX bearing wastewater experiments. Phase three was the last phase in textile wastewater experiments. In this phase, real textile wastewater was supplied by Blackburn Yarn Dyers Ltd, and it was used as influent wastewater. MWT, WT and MX were used as column substrates to treat real textile wastewater for 120 days. In textile wastewater experiments, the treated effluents were characterised by LC-MS and GC-MS to determine the dye biodegradation products included aromatic amines. The bacterial genera in the pre-test and post-test column substrates were determined by biological analysis using next-generation sequencing to highlight the flourished genera in post-test column media. Different experiment parameters were monitors during textile wastewater experiments as pH, DO, ORP and temperature. Furthermore, a spectrophotometric method was used to highlight the colour intensity change and to detect any aromatic amines might be generated during textile wastewater treatment.

After the achievements in textile wastewater experiments, iron oxides bearing sludge were investigated as substrates to remediate municipal carbon and nitrogen contaminants and to study the mechanisms involved. In this experiment MWT, WT and MX were used as column media to treat synthetic municipal wastewater over 140 days. In this experiment, the role of iron-reducing bacteria and the synergetic microorganism were highlighted by determining the bacterial genera in pre-test and

post-test column substrate using next-generation sequencing. Nitrogen and carbon removal rates were calculated, and experiment parameters were highlighted.

The BTEX bearing wastewater experiment was conducted to test the ability of iron oxides bearing sludge to remediate mono aromatic hydrocarbons using 20 ml batch microcosm reactor. A sealed batch experiment was chosen to overcome the problems of BTEX volatilisation. MWT, MX and WT were used as microcosm substrates to mineralise BTEX at 45 mg/l of each. The experiments were conducted with either initial aerobic or anoxic conditions for 160 days. GC-MS was used to measure the BTEX concentration during the experiment. The biological analysis was conducted to highlight the influence the prospered species in post-test sludge compared with pre-test samples.

It should be noted that in the columns wastewater experiments (textile and municipal), the strict anaerobic condition was not imposed. However, the subsequent ORP data gathered during the experiments (see Figure 5-15 and 6.12) demonstrated that the column anaerobic conditions prevailed in the columns (as anticipated). They are therefore referred to in the remainder of the thesis as anaerobic columns. The bacterial analysis of column substrates also indicates that the prevailing condition was anaerobic, although this does not exclude the possible occurrence of a range of aerobic and sub-aerobic conditions at a microscale. During phase three textile wastewater, municipal and BTEX-bearing wastewater experiments, the temperature was low due to cold external temperatures affecting the uninsulated metal-roofed laboratory (which also had open windows).
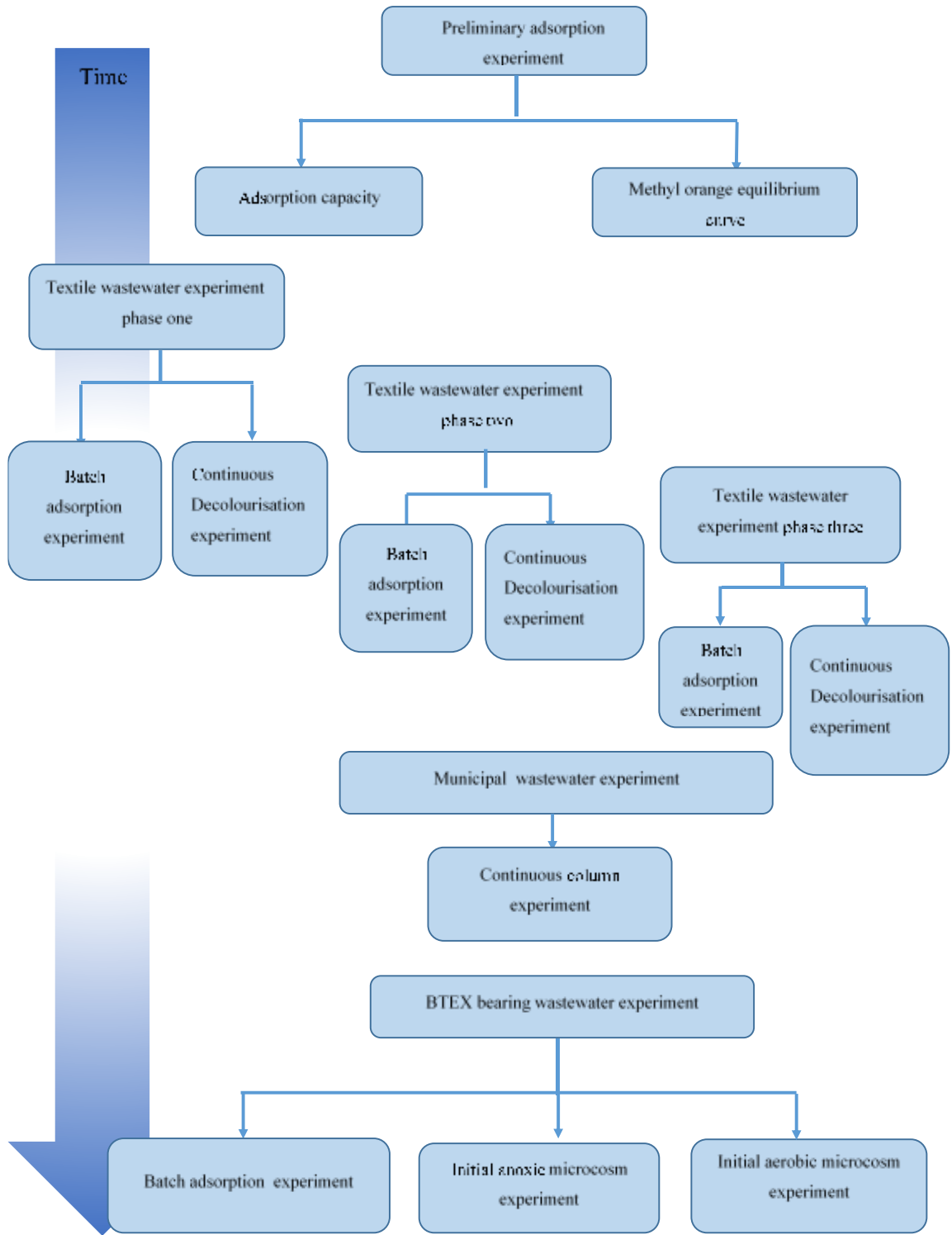
**Figure 3-1 the research plan progress with time.**

## 3.3    Iron oxides bearing wastes

Mine water treatment sludge (MWT) was collected from Lindsay in Capel Hendre, Carmarthenshire, South Wales. It is a remediation pond where discharged water from an abandoned mining site is treated. It is a so-called "passive" remediation site, and the pond is surrounded by a settling channel to precipitate the sludge where the sample has been collected. The high iron concentration detected, and the colour variation noticed in the sludge cross-section layer was probably due to the indigenous microbial activity within it, as shown in Figure 3-2.



**Figure 3-2 Cross-section of pre-test mine water treatment sludge (MWT).**

Water treatment sludge was collected from a Dwr Cymru Welsh Water (DCWW) treatment plant in Hirwaun. It was collected from the settling tank after adding ferric oxide. Wastewater sludge (WW) was collected from the digester unit at the wastewater treatment plant in Cardiff, which was used to prepare the mixed sludge (MX). The MX was contained 90 % (w/w) MWT sludge plus 10 % (w/w) autoclaved WW sludge (at 121 °C for 30 min). Polypropylene buckets (20 l) were used to collect sludge samples. The containers of sludge samples were mixed for about 10 min to homogenise the contents of the buckets and then kept for 48 hrs, and the excess water was decanted. The sludge wastes were then ready for packing in the columns. Sludge samples were collected according to research strategy progress. It started with MWT sludge which was used in all experiments, WT and WW sludge were collected before phase three textile wastewater was conducted, and they were used in the later experiments. All sludge samples were stored in a refrigerator at 4 °C.

The physical properties of sludge, dry content, porosity and void ratio were calculated according to civil engineering methods (Karl Terzaghi et al. 1996) as shown in Table 3-1 by using Equations 12-15. Sludge calculation was based on used iron oxide density (5.25 g/cm$^3$). Samples were gently dried by oven at (40°C for 48 hrs) as reported by Schwertmann and Cornell (2000). It was spread over a drying tray which was covered with a sheet of brown paper to prevent contamination. An agate mortar was used to grind any aggregated particles (Schwertmann and Cornell 2000).

$$\text{Bulk density of wet sludge (g/cm}^3\text{)} = \frac{\text{weight}}{\text{Volume}} \qquad \text{Equation 12}$$

$$V_{total} = V_{solid} + V_{void} \quad \text{and} \qquad V_{solid} = \text{dry mass/ iron oxide density} \quad \text{Equation 13}$$

$$\text{Void ratio } e = \frac{v_{void}}{v_{solid}} \qquad \text{Equation 14}$$

$$\text{Porosity } n = \frac{v_{void}}{v_{total}} \qquad \text{Equation 15}$$

Table 3-1 Physical properties for mine water treatment sludge (MWT), water treatment sludge (WT) and mixed sludge (MX).

| Parameters | MWT | WT | MX |
|---|---|---|---|
| Wet volume | 50 cm$^3$ | 50 cm$^3$ | 50 cm$^3$ |
| Dried volume | 38 cm$^3$ | 19 cm$^3$ | 22 cm$^3$ |
| Wet weight | 63 g | 58 g | 51 g |
| Dry weight | 16 g | 14 g | 10 g |
| Bulk density for wet sludge | 1.27 g/cm$^3$ | 1.17 g/cm$^3$ | 1.03 g/cm$^3$ |
| Volume of void | 46 cm$^3$ | 47 cm$^3$ | 48 cm$^3$ |
| Void ratio e | 15 | 18 | 25 |
| Porosity n | 0.93 | 0.94 | 0.96 |

## 3.4  Preliminary MO adsorption experiment setup

Batch adsorption experiments were conducted using 100 ml plastic containers fitted with screw-on lids. Mine water treatment sludge (MWT) was used as adsorbent material to determine the adsorption capacity compared with other abundant iron oxides, e.g., goethite, magnetite, and hematite. Methyl orange solution at a specific concentration was prepared using deionised water as the adsorbate. MWT was autoclaved (at 121 °C for 30 min), and then it was gently dried at 40 °C for 48 hrs before use to exclude the biological influence as reported by Schwertmann and Cornell (2000); the other adsorbents were already in dry powder form. A specific amount of

adsorbent was suspended with 100 ml MO solutions under shaking conditions (150 rpm) at room temperature. Samples were withdrawn periodically and filtered by 0.45 µm syringe filter before measuring the absorbance at 464 nm (peak absorbance for the MO chromophore) using a spectrophotometer as recommended by literature (Cui et al. 2012).

## 3.5      Textile wastewater experiments

### 3.5.1   Phase one textile wastewater experiment setup

In this phase, the influent was simply prepared by using 15 mg MO in one-litre deionised water. Two feeding tanks were used one with glycerol (0.46 g/l) as an additional organic carbon. Glycerol was used as an additional organic carbon source, as recommended in a previous study (Roberts, 2018). The eight acrylic columns (2.6 cm ×20 cm) were loaded with 128 g wet MWT sludge in each column. Four of them contained autoclaved sludge while the other contained live sludge. The autoclaved sample was prepared by decanting 500 g MWT sludge in Pyrex glassware (2 l), and it was covered with aluminium foil before being autoclaved (for a 30 min cycle at 121 °C) using a Prestige Medical 2100 series autoclave (Prestige Medical Blackburn UK). An autoclave indicator was used to ensure that the requisite temperature had been achieved. A glass wool was used to support the sludge and rubber stoppers with a quick fit adapter was used to seal both columns ends and to connect inlet and outlet tubes see Figure 3-3. Columns were labelled as live (L) and autoclaved (D) according to the MWT column substrates used, where L refers to live MWT sludge and D refers to autoclaved MWT sludge. Furthermore, column treated MO with glycerol were labelled by (G). According to that, the column contains live MWT sludge and it treats MO with glycerol was labelled as L+G. Similar to that, D+G referred to the column with autoclaved MWT, which treats MO with glycerol. Samples were withdrawn daily from the collection tanks, and these tanks were washed and cleaned daily to avoid sample accumulation and contamination. An eight-cassette peristaltic pump was used to feed each column with 100 ml/day for 170 days. This flowrate generates nominal hydraulic retention equal to 28.70 hrs based on the volume of voids in Table 3-1. A practical preliminary experiment was carried to determine the appropriate peristaltic

flowrate using a column loaded with the same amount of MWT sludge (128 g). The observation concluded that 100 ml/day was an achievable flow rate according to the permeability of the sludge.
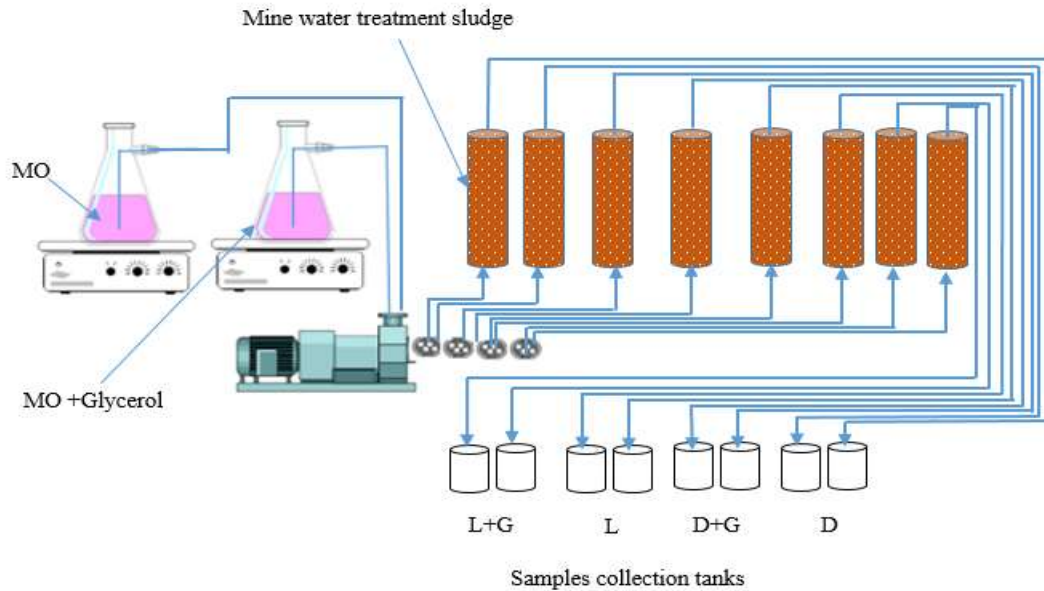


**Figure 3-3 Phase one textile wastewater experiment schematic diagram.**

### 3.5.2 Phase two textile wastewater experiment setup

In phase two textile wastewater experiment and after the positive feedback from phase one, only the live MWT sludge was used as column substrates. However, the amount of loaded wet sludge in each column was reduced from 128 g in phase one to be only 28 g in this phase. This modification was made for a practical reason (as explained in Section 3.2). According to that, the columns substrate will reach a maximum MO sorption (with respect to MO concentration under column conditions) after a short time, and the dye removed by biodegradation can be identified and continued for longer than it was in phase one. Acrylic cylinders (2.5×10 cm) were used as aerobic columns, and glass wool was used to support the sludge. These columns were fitted with lids made from the same column's material. These lids were fitted with a quick fit tube adapter to connect the inlet and outlet tubes. The aerobic columns were also made from acrylic cylinders (20×50 cm). It contains a sand layer (3 cm thikness and 600 µm particles diameter) to support K1 micro filter media (was purchased from Swell UK K1). This media was added to increase the surface area in the aerobic

column. The sand used was autoclaved (121 °C for 30 min) and washed with acid and rinsed repetitively with deionized water. A spiral tube with uniform holes (1cm each in diameter) was fitted on the top of the aerobic reactor. This tube was connected with the anaerobic effluent to drip into the aerobic reactor (see Figure 3-4). The peristaltic pump was feeding each anaerobic column with 300 ml/day to generate a nominal hydraulic retention time (HRT) equal to 2 hrs based on the volume of voids in Table 3-1. Valves were fitted on the anaerobic and sequential effluent tubes to regulate samples collection between different containers. Sequential valves were closed, and anaerobic valves were opened only when anaerobic samples required. The samples of the treated water were collected every ten days, and these containers were decanted and cleaned daily. The recipe used for the synthetic dye wastewater was as follows: One litre of deionised water contained 2.8 g modified starch, 530 mg acetic acid, 15 mg modified MO, 0.15 g NaCl, 0.23 g $NH_4Cl$, 0.28 g $(NH_4)_2SO_4$, 0.12 g $Na_3PO_4.12H_2O$, 0.03 g $Na_2HPO_4$, 2 g $NaHCO_3$ (O'Neill et al. 2000a). According to the mentioned reference, starch and MO should be hydrolysis before adding to the recipe to simulate the real textile wastewater properties as following: 2.8 g starch was hydrolysed with 1.19 g NaOH in one litre deionised water under mixing for 24 hrs, and MO was hydrolysed by prepared 50 g/l MO stock solution and raising the pH to 12 using NaOH at 80 °C for 1.5 hr. 1 ml of a trace elements solution was added for each one-litre recipe. It contained 5 g $FeSO_4.7H_2O$, 0.01 g $ZnSO_4.7H_2O$, 0.10 g $MnCl_2.4H_2O$, 0.39 g $CuSO_4.5H_2O$, 0.24 g $Co(NO_3)_2.6H_2O$, 0.01 g $NaB_4O_7.10H_2O$ and 0.02 g $NiCl_2$ were dissolved in one litre deionised water (O'Neill et al. 2000a). The influent feeding tank was under a gentle mixing by a magnetic stirrer, and the experiment was run with duplicate columns over 100 days inside an incubator at 25 °C.
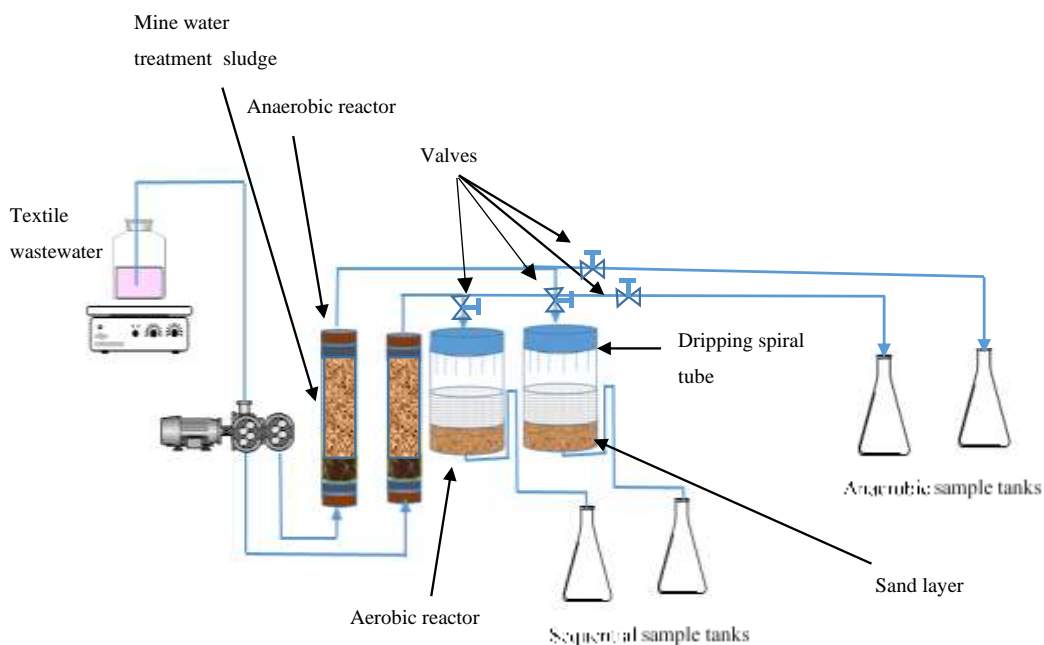
**Figure 3-4 Phase two textile wastewater experiment schematic diagram.**

### 3.5.3 Phase three textile wastewater experiment setup

In this experiment, three types of iron oxides, MWT, WT and MX sludge containing 90 % (w/w) MWT sludge and 10 % (w/w) autoclaved WW sludge (121˚C for 30 min) were used as column substrates to degrade real textile wastewater. Further details for sludge collection can be found in section 3.3. Acrylic columnar (2.5×10 cm) similar to those used in phase two, each column was loaded with 28 g of wet sludge. A glass wool was used to support the sludge. Experiments were run in duplicate, as shown in Figure 3-5. A peristaltic pump was feeding each column with 100 ml/day for 120 days. This flow rate generated a nominal hydraulic retention time equal to 5.5 hrs in the WT columns and about 6.3 hrs in MWT and MX columns based on the volume of voids in Table 3-1. The column's retention time varies according to the column's substrate used because each material has a specific volume of voids and different porosity. The flow rate used was similar to phase one because the influent is a harsh material and the substrate microorganisms could require more time to degrade the dye and other contaminants (Talarposhti et al. 2001; Saratale et al. 2011). Real textile wastewater

(120 l) was supplied by Blackburn Yarn Dyers Ltd, which is a cotton dyeing company. The wastewater was collected from the accumulation waste tank, which is received the dyeing wastewater from many processes, as such the textile wastewater contained a combination of various types of dyes and chemical compounds (see Appendix 1). It was stored at < 4 °C until further use. Table 3-2 illustrates the textile wastewater properties. The tank contains homogenised by mixing before decanting two litres into the experiment feeding tank every 48 hrs. The column effluents were collected in closed containers, and these containers were discharged and cleaned daily to avoid samples accumulation. Samples were withdrawn every ten days for further analysis.

**Table 3-2 the textile wastewater properties.**

| Parameters | Concentration | Parameters | Concentration mg/l |
|---|---|---|---|
| pH | $9.5 \pm 0.2$ | K | 312 |
| COD | $1397 \pm 10$ mg/l | Na | 316 |
| Salinity | 5 ppt | Mg | 6.45 |
| DO | 10.17 mg/l | Ca | 4.51 |
| TSS | 7 mg/l | Ba | 0.41 |
| TDS | 4104 mg/l | Fe | 0.12 |
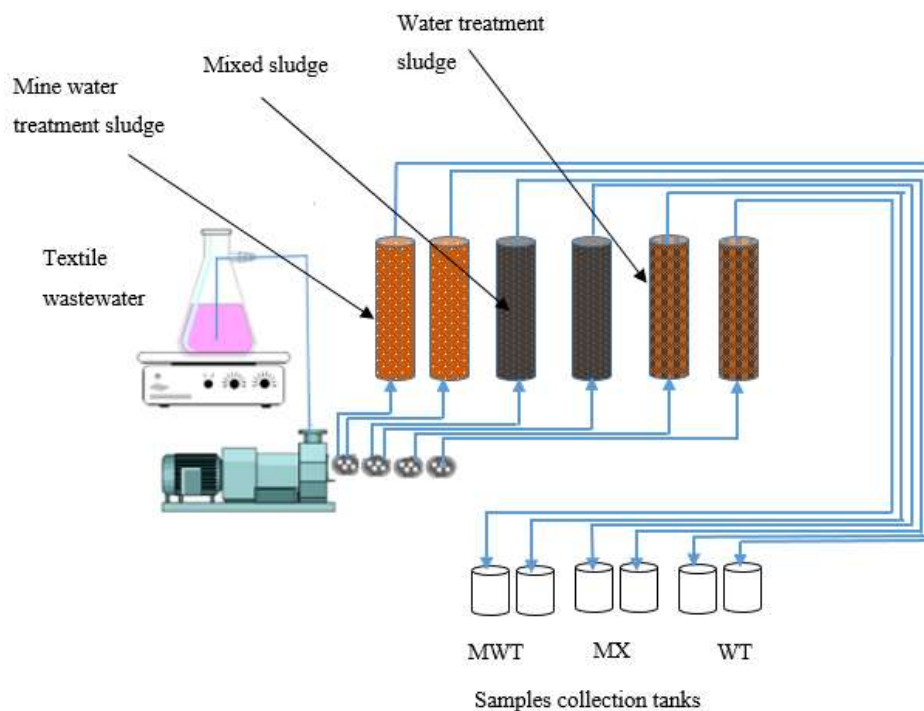


**Figure 3-5 Phase three textile wastewater experiment schematic diagram.**

## 3.6　　　Municipal wastewater experiment setup

In this experiment, MWT, WT and MX sludge (containing 90% (w/w) MWT sludge and 10 % (w/w) autoclaved WW sludge at 121 ˚C for 30 min were used as column substrates to treat municipal wastewater. The experiment was run in duplicate columns for 140 days. Each acrylic column (2.5 × 10 cm) contained 28 g of wet sludge. Municipal wastewater has variable parameters with time, place, and source (Elmitwalli et al. 2001; Gomec 2010) according to that, a synthetic recipe was used as described in Table 3-3 (Valladares Linares et al. 2013). Synthetic wastewater was freshly prepared every three days to ensure steady influent parameters. A magnetic stirrer vortex was used to homogenise the feeding tank. A peristaltic pump with ten cassettes equipped with silicone tubing was used to generate a flow rate equal to 100 ml/day. This flow rate generated a nominal hydraulic retention time equal to 5.5 hrs for WT columns and  6.3 hrs for MWT and MX columns based on the volume of voids for each substrate, as shown in Table 3-1. The effluent treated water was collected in plastic containers. Samples were withdrawn every ten days from the column collection tanks for analysis. These containers were discharged and cleaned daily to avoid sample accumulation, see Figure 3-6 for system schematic diagram.

Table 3-3 The synthetic municipal wastewater ingredients.

| Chemical compounds | mg/l | Trace metals | mg/l |
|:---:|:---:|:---:|:---:|
| Urea | 91 | $Cr(NO_3)_3$ | 0.77 |
| $NH_4Cl$ | 63 | $CuCl_2 .2H_2O$ | 0.53 |
| Sodium acetate | 79 | $MnSO_4 .H_2O$ | 0.10 |
| Peptone | 17 | $NiSO_4 .6H_2O$ | 0.33 |
| $MgHPO_4 .3H_2O$ | 29 | $PbCl_2$ | 0.10 |
| $KH_2PO4$ | 23 | $ZnCl_2$ | 0.20 |
| $FeSO_4 .7H_2O$ | 5 | | |
| Starch | 122 | | |
| Skimmed milk powder | 116 | | |
| Yeast extract | 52 | | |
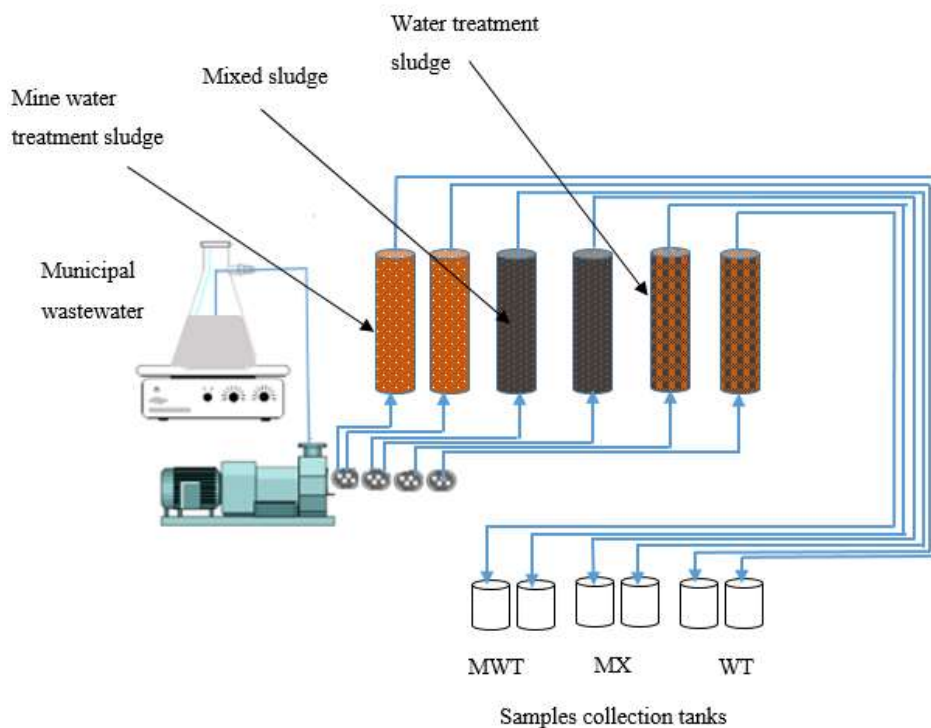
**Figure 3-6 Municipal wastewater experiment schematic diagram.**

## 3.7     BTEX bearing wastewater experiment setup

BTEX bearing wastewater was treated by using MWT, WT and MX as a biological substrate to degrade benzene, toluene, ethylbenzene, and xylene (BTEX) using a microcosm condition. GC-MS 20 ml sealed glass vials with PTFE gas-tight aluminium silicone crimp lids were used as microcosm batch reactors. In this experiment, the use of real refinery wastewater was avoided as it contains a wide range of soluble and insoluble organic compounds alternatively, artificial BTEX bearing wastewater was prepared according to the following (mg/l): benzene (45), toluene (45), ethylbenzene (45), xylene (45), $NH_4Cl$ (46), $KH_2PO_4$ (10), $NaHCO_3$ (200), $CaCl_2.2H_2O$ (0.01), $MgSO_4.7H_2O$ (0.05), $FeCl_3.6H_2O$ (0.07) (Shariati et al. 2011). BTEX biodegradation was tested using initially aerobic and anoxic conditions over 160 days. Each microcosm was filled with 15 g wet sludge and 10.4 ml BTEX bearing wastewater. In the initially aerobic experiments, the wastewater was aerated for 30 min by an air pump fitted with a 0.2 µm filter to avoid contamination before adding the BTEX to the recipe (Chen et al. 2003).  Microcosms vials were sealed with no headspace immediately after decanting the BTEX bearing wastewater to reduce the effect of BTEX volatility, and

it was labelled as aerobic mine water treatment sludge (AMWT), aerobic water treatment sludge (AWT), aerobic mixed sludge (AMX). For the initially anoxic condition, all the components include the microcosms and wastewater were put in anaerobic isolation chamber. The chamber was flushed several times with nitrogen. Nitrogen gas was pumping for 30 min into the prepared wastewater before adding the BTEX to decrease the oxygen concentration. (Lovley and Lonergan 1990; Yu et al. 2011). The microcosms vials were sealed with no headspace immediately after decanting the BTEX bearing wastewater inside the chamber. Samples were labelled as anoxic mine water treatment sludge (UMWT), anoxic water treatment sludge (UWT) and anoxic mixed sludge (UMX). Samples were arranged in a dark cardboard box to avoid the influence of sunlight under shaking at 150 rpm. They were arranged vertically with enough space for rolling to homogenise the contents.

## 3.8     General physiochemical characterisations

Iron concentration in the aqueous samples was quantified by Inductively Coupled Plasma Optical Emission Spectrometer (ICP-OES) (Perkin Elmer Optima 2100DV in conjunction with an AS90plus Auto-sampler), and the results were analysed using Winlab 32 software. The ICP-OES was calibrated for each element by a three-point process set used commercial standards covering the expected concentration of elements. In addition, deionised water containing 2 % (v/v) nitric acid was analysed periodically to detect any alteration greater than 10 % in the concentration of the standards. Experimental duplicate samples were acidified by 0.1 ml 20 % (v/v) nitric acid. It was kept in a fridge (4 °C) waiting to be analysed. Solid samples were digested to detect the concentration of the element using a 6 ml aqua regia mixture of 70 % (w/w) nitric acid and 30 % (w/w) hydrochloric acid in a 50: 50 ratios. A 100 ml PTFE lined ceramic vessel with a vented PTFE cap was used in a Multiwave 3000 microwave where the wattage increased gradually to 900 W for 12 min then held at this wattage for 30 min reaching a maximum temperature of 200 °C, after which the samples were left to cool for 25 min. The ICP-OES was used to analyse the solution element according to the following equation:

Element concentration $= \frac{A \times V}{W}$       (Equation 16)

where A: analytical value, V: volume of the aqua reqia and W: the weight of the sample

The dye decolourisation was measured by a Spectrophotometer (H-1900 HITACHI) at a wavelength of 464 nm for MO. The water sample was filtered by a 0.45 µm syringe filter before taking the wavelength measurement to discard the sludge particles which might interfere with the absorbance.

A Mettler Toledo Seven Excellence™ Multi-parameter system was used to measure the pH, conductivity, and dissolved oxygen. For pH probe, calibration was conducted using a three-point process (pH 4, 7 and 10). Conductivity (EC) was measured by a Mettler Toledo LE703 probe, which was calibrated with a 1413 µS/cm standard solution. The EC measurement was ± 0.5 % accurate. Dissolved oxygen (DO) was measured by a Mettler Toledo 605-ISM probe and calibrated with two points, zero and the ambient oxygen concentration. The zero-oxygen solution was prepared by a dissolved Mettler Toledo tablet in 30 ml deionised water. During wastewater column experiments in the next chapters, the DO concentrations were taken as soon as enough samples were collected. However, exposure to the atmosphere might skew the results because the flowrate used was quite low, and it took a long time to collect sufficient effluents volume. The redox potential (ORP) was measured by a Mettler Toledo Inlab™ Redox ORP probe and a reference solution (220 mV) was used as the standard solution for the ORP probe.

The ferrous content was measured by a HACH DR900 colourimeter using phenanthroline powder and pillows for 25 ml samples. It followed the HACH DR900 handbook procedure outlined for water analysis. The maximum detection limit for ferrous content was 3 mg/l. Samples with concentration exceeding the method limit range were diluted using deionised water, and the appropriate correction factor was applied to calculate the final reading. In case the alteration in reading due to the influence of oxygen might have skewed the data acquired, the ferrous ion reading was taken as soon as a sufficient volume was available to minimise the impact of oxidation. Nitrite and nitrate were measured by an ICS-2000 Ion chromatography system (IC) using an AS18 detection column, with 5 ml containers with filter caps for loading the samples. A calibration curve was applied, and the detection was conducted according to the retention time for each compound. The applied current was 57 mA, injection volume was 20 µL, a storage solution used was 100 mM sodium tetraborate, the

temperature was 30 °C, and the flow rate was 1 ml/min. Ammonia-nitrogen was detected using the HACH 900 Salicylate method at a detection range between 0 and 50 mg/l. Sulphate ($SO_4^-$) concentration was determined by the HACH DR900 using SulfaVer reagent pillows for the 10 ml samples following the procedure in the DR900 water analysis handbook. Dilution with deionised water to a range of 2-70 mg/l was used when the sulphate concentration exceeded the range, and the subsequent correction factor was applied to the determined concentration. COD was measured by the HACH 3900 using an LC1400 COD cuvette test kit. The kit range was from zero up to 1000 mg/l. The analytical procedure followed the instructions accompanying the kit, which include digestion for the filtered samples (0.45 µm) at 148 °C for 120 min before taking the measurement; dilution by deionised water followed when the data went beyond the kit range, and a subsequent correction factor was applied for concentration. This kit used mercury as mercury sulphate.

A HANNA temperature data logger was located inside the lab, was used to continually monitoring, and recording the lab temperature. A Total Organic Carbon Analyzer (TOC-V CSH (Shimadzu) was used to detect the total amount of carbon (TC and TOC) in the liquid samples and the total carbon in the pre-test and post-test column substrates. Analysis with this instrument yields a repeatability range of ± 1 %. The liquid samples were filtered before analysis by a 0.45 µm filter. Glucose (40 % carbon) was used to prepare the calibration curve to secure an accurate reading. For total carbon ratio in solid sludge samples, the composition chamber was heated to 400 °C to convert the carbon in the solid column substrates to carbon monoxide, which can be detected by a specific instrument. Duplicate withdrawal tests were conducted for the samples, and the average reading was recorded.

### 3.9     Chemicals and reagents

Chemicals and reagents, including GC-MS standards and MO, were purchased from Sigma Aldrich and Fisher Scientific. They were stored according to the safety instructions provided. A high purity deionized water was used (18 MΩ) in all the experiments. Grade A glassware were used for preparing the reagents and chemicals to ensure accurate measurements, while grade B glassware were used when accuracy was less important.

## 3.10     Removal rate

The removal rate was calculated using Equation 17 for several parameters, e.g., dye, nitrogen, and carbon removal to compare them with the literature. The removal rate was calculated based on the concentration at time t according to experiment, and it was normalised from mg/cm$^3$/day to g/m$^3$/day to determine the removal capacity of the sludge used. The removal rate can also be calculated as g/m$^2$/day or as g/kg/day by determined the column cross-sectional area and the weight of the sludge used which was normalised from cm$^3$ to m$^3$ and from g to kg (see Appendix 2 for details).

$$\text{Removal rate (g/m}^3\text{/day)} = q(C_o - C_t)/V \qquad \text{(Equation 17)}$$

where q is the flow rate (l/day), $C_0$ is the initial concentration (g/l), $C_t$ is the concentration at time t in g/l and v is the substrate volume (m$^3$)

## 3.11     Dye adsorption capacity

The dye adsorption capacity was used to determine the amount of dye adsorbed in one gram of adsorbent, which represents the sludge used. A mass balance equation 18 was used to calculate the adsorption capacity. Samples were filtered by an 0.45 µm syringe filter to detect the absorbance of dye water at 464 nm for MO by a spectrophotometer.

$$q_t \;\; = \frac{(C_o - C_t) \times V}{W} \qquad\qquad \text{(Equation 18)}$$

where qt= adsorbent capacity (mg adsorbate/g adsorbent). $C_0$: MO initial concentration (mg/l). $C_t$: MO concentration at time t (mg/l). V: volume of the solution (l). W: the dry adsorbent weight (g).

## 3.12     LC-MS

Liquid chromatography-mass spectrometry (LC-MS) was used to identify the organic compounds in the influent and the degradation products in the effluent according to the retention time. Liquid samples were injected directly after filtered it by a 0.45 µm filter, while the solid sludge samples were prepared as the following: One gram of the dried sludge was mixed with 10 ml deionised water, and the suspension was filtered (0.45 µm) before injected it in the LC-MS to highlight any organic compounds as the LC-MS technician recommended. It was a preliminary test to determine the presence of any soluble organic compounds in the pre-test sludge, with the intention that more

efficient extraction method will be used if the LC-MS spectrum highlights any organic compounds peaks. This step did not influence the other LC-MS analyses because it was carried out on water extracts from the solid phase, while other analyses involved the column effluents. The LC-MS analysis for the first dye experiments was conducted by Cardiff University School of Chemistry. The operating instrument's condition was reported in Table 3-4. ChemDraw software was used to analyse LC-MS data based on the m/z ratio which obtained from LC-MS spectrum to predict the chemical structure.

**Table 3-4 LC-MS Acquisition Parameter by Cardiff University School of Chemistry.**

| Ion Source Type | ESI | Ion Polarity | Positive | Alternating Ion Polarity | off |
|---|---|---|---|---|---|
| Mass Range Mode | Ultra Scan | Scan Beginning | 100 m/z | Scan End | 400 m/z |
| Accumulation Time | 7869 µs | RF Level | 96 % | Trap Drive | 74 |
| SPS Target Mass | n/a | Averages | 5 Spectra | Auto MS/MS | off |

For the real textile wastewater experiment, the samples were analysed by the EPSRC National Facility in Swansea University. A positive and negative mode analysis was used due to the lack of information about the type of dye used (see Table 3-5 for the experimental conditions). Remote analyser software was used to elucidate the LC-MS Data. The programme was used to calculate the theoretical m/z values to all the possible compositions of carbon, hydrogen, oxygen, nitrogen, sulphur, and sodium in the chemical structure.

**Table 3-5 Parameters set for positive and negative LC-MS analysis by the EPSRC National Facility Swansea.**

| LC Parameter | | |
|---|---|---|
| Column | Fortis C18, 3um, 150 x 2.1mm | |
| Mobile phase A | 0.10 % Formic Acid in water (positive) 100 % Water (negative) | |
| Mobile phase B | 100 % Acetonitrile | |
| Gradient | 0-40 min: 5-95 % mobile phase B, 40-50 min: 95 % mobile phase B, 50-55 min: 95-5 % mobile phase B, 55-60 min: 5 % mobile phase B | |
| Flow rate | 200 uL/min | |
| Column temperature | Room temperature | |
| Injection volume (ul) | 10 | |
| Total Run time (min) | 60 | |
| Wash solvent | Acetonitrile: Water 50:50 | |
| **MS Parameter** | | |
| Ionization mode | ESI Positive | ESI Negative |
| Sheath gas flow (arb) | 15 | 10 |
| Aux gas flow rate(arb) | 15 | 3 |
| Spray voltage (kV) | 4.00 | 3.60 |
| Capillary temp (°C) | 300 | 275 |
| Capillary voltage (V) | 3.00 | 29 |
| Tube lens (V) | 150 | 100 |

## 3.13    GC-MS

Gas chromatography (GC-MS) by Clarus 500 GC-MS was equipped with an HS Turbo matrix 40 from Perkin-Elmer (RTX-5 Amine Crossband 5 % diphenyl 95 % dimethyl polysiloxane from RESTEK). This is a specific column to detect amines. The GC-MS operating conditions were as follows: (Oven: Initial temp 50 °C for 1.5 min, ramp 15 °C/min to 240 °C, Injection auto 250 °C, Volume 5.000 μl, Split 50:1, Carrier Gas He, Solvent Delay 2.00 min, Transfer Temp 200 °C, Source Temp 180 °C, Scan: 50 to 300 Da, Column 30.0 m x 250 μm). GC-MS was also used to detect the BTEX concentration by headspace analysis during the BTEX bearing wastewater treatment (Chapter nine). The BTEX calibration curve was conducted using a standard  BTEX for GC- MS from Sigma to determine an accurate quantitative analysis. All the glassware was pre-washed with ethanol to remove any organic contamination. For textile wastewater phase one, a liquid-liquid extraction was applied using method 3520C. In this method, 50 ml methylene chloride was added to a distilling flask of the extractor, and 100 ml of the sample was added to the extractor and extracted for 18-24 hours. After cooling, the extract was dried using a Kuderna-Danish apparatus(Agency 1986).

## 3.14    Biological analysis

### 3.14.1 DNA **extraction**

For biological analysis, 100 g of pre-test iron oxides bearing sludge were preserved in a deep freeze at –80 °C for the biological analysis. The post-test iron oxides bearing wastes which represent the column substrates were collected from columns after the experiments were ended. They were poured in sample pages and preserved in the deep freeze. Sludge samples were mixed by stirrer before the DNA was extracted from the preserved sludge by a fast DNA spin kit for soil (MP Biomedicals, Solen, OH, USA). The kit procedure was followed but with some adjustment (Webster et al. 2003). A Bioline Hyper ladder 1Kb was used in gel electrophoresis to confirm the kit results. Then the second step for verification was involved using a Qubit fluorimeter 3.0 to

determine the DNA concentration in ng/µl employing a Qubit dsDNA assay kit (Invitrogen, Carlsbad, CA, USA).

### 3.14.2 **Next-generation sequencing of bacteria and archaea 16S rRNA genes**

A next-generation 16S rRNA gene sequencing was performed for pre-test and post-test column media in all the conducted wastewater experiments. After DNA was extracted by fast DNA spin kit for soil (MP Biomedicals, Solen, OH, USA. Polymerase chain reaction (PCR) was used to amplified 1/100 DNA dilution in a 96 well PCR plate to create a bacterial 16S rRNA for gene library sequence. Primers were used to target the V4 variable region of the 16S rRNA. The forward and reverse primers were quoted from Kozich et al. (2013) as highlighted in Table 3-6.

**Table 3-6 The primer constructed data.**

| Illumina adapter sequence | F:5'-AATGATACGGCGACCACCGACATCTACAC-3'<br>R; 5'-CAAGCAGAAGACGCATACGAGAT-3' |
|---|---|
| **Index or barcode sequence**<br>**(8-base pair i5 and i7) a pad sequence to**<br>**boost the primer melting temperature** | F: 5'-TATGGTAATT-3'<br>R: 5'-AGTCAGTCAG-3' |
| **Link sequence 2 base pair as anti-**<br>**complementary to the known sequence** | F: 5'-GT-3'<br>R: 5'-CC-3' |
| **The 16S rRNA gene sequence V4** | F: 5'-GTGCCAGCMGCCGCGGTAA-3'<br>R:5'-GGACTACHVGGGTWTCTAAT-3' |

According to the previous table, the PCR primer sequence:

Forward:AATGATACGGCGACCACCGAGATCTACAC\<i5\>\<pad\>\<link\>\<16SF\>

Reverse: CAAGCAGAAGACGGCATACGAGAT\<i7\>\<pad\>\<link\>\<16SR\>

In the PCR plate, each well contained 17 µl of Accuprime PFX Supermix, 1 µl DNA template, and 2 µl of each paired set of index primers. Negative control included 1 µl of nuclease-free PCR grade water was used, and Mock Community (BEI Resources, Virginia, USA) at 1 µl was a positive control. A programme thermocycler was used as followed: 2 mins at 95 °C; 30 cycles of 95 °C for 20 sec, 55 °C for 15 sec and 72 °C for 5 mins; followed by a final step of 72 °C for 10 mins before maintaining a constant 4 °C until removed from the thermocycler. After PCR amplification, each sample was tested by Qubit fluorometric assay, Agilent Genomic DNA ScreenTape–HSD-1000 and Genomic DNA Reagents, Agilent, Santa Clara CA, USA to check mass and

sequence length. The samples were cleaned and normalised by SequalPrep™ 96 well normalisation plate (Invitrogen, Carlsbad, CA, USA) (Kozich et al., 2013). Another step to check mass and sequence length was conducted by Qubit and Tape Station. According to Qubit data, manual normalisation was performed to calculate the sample required to be added to the pooled library to give a sample concentration of 0.5 nM in each pool. At this point, a Tape Station analysis showed that the adapter dimer still present. According to that, SPRI select magnetic bead clean-up (Beckman Coulter, Brea, CA, USA) was prepared using 0.8 volume of SPRI select beads, chosen using the left-hand selection method as reported in the manufacturer. The pooled library was concentrated by reducing the volume of elution buffer used for clean-up. Qubit and Tape Station was used as a final step to check that the adapter dimer was removed, an average of 2.2 Nm was adequate concentration to generate reliable data. Samples were analysed by Illumina MiSeq sequencer (Illumina, San Diego, CA, USA) to generate next-generation sequencing. Sequencing was performed 2 bp $\times$ 250 bp paired-end flow cells and reagent cartridges. Sequencing was conducted by the Institute of Medical Genetics at the Cardiff University Heath Campus. The data generated by Illumina sequencing was analysed by Qiime v.1.8 (Caporaso et al. 2010). Forward and reverse paired were merged, removed any sequence that contained errors. Low-quality sequences which are shorter than 200 bp were removed by filtration. Taxonomy was then generated for the filtered sequences using BLAST and the SILVA 128 database with a 97% similarity (Altschul et al. 1990).

# Chapter 4 : Preliminary dye adsorption experiments

## 4.1     Introduction

In this chapter, the adsorption capacity of mine water treatment sludge (MWT) was determined, and it was compared with other iron oxides, e.g., magnetite, hematite, and goethite using dye water contains methyl orange. The MWT adsorption data was analysed using Langmuir and Freundlich isotherm theories. Furthermore, a MO calibration curve was determined, and the effect of pH and time on MWT adsorption capacity were studied.

## 4.2     Methyl Orange calibration curve and the influence of pH solution

The MO calibration curve was distinguished at various concentrations using a spectrophotometer at 464 nm wavelength. In Figure 4-1, the data recorded was out of the spectrophotometer range as the tested MO concentration range was 0.25-1000 mg/l. In Figure 4-2, the MO concentration range was reduced to 0-20 mg/l, and the calibration curve equation (Equation19) was used to calculate MO concentration at any time.

$$y = 0.086x \qquad (R^2 = 0.99) \tag{equation 19}$$

The influence of changing the pH solution on MO calibration curve was also studied. Three different pH solution were selected (4, 8, and 10). One litre of MO stock solution was prepared for each pH samples. The pH of the solution was adjusted by pH meter using NaOH and HCL under gently mixing by a magnetic stirrer. Figure 4-3 shows that changing the pH can affect the MO calibration curve equation.
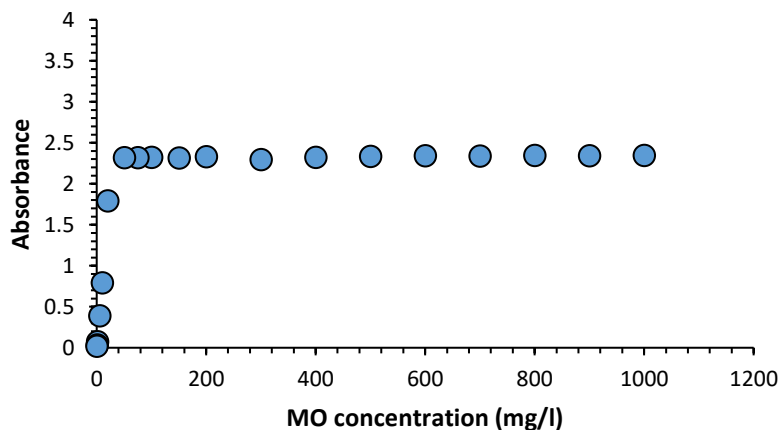


**Figure 4-1 MO calibration curve (0.25-1000) mg/l at 464 nm.**
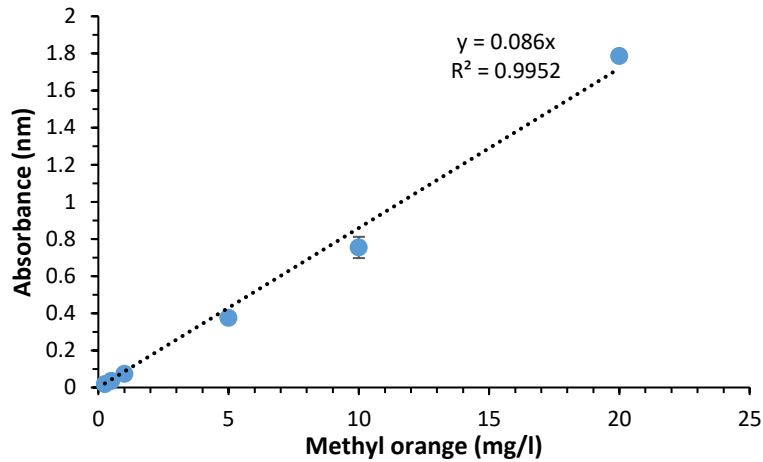
**Figure 4-2 MO calibration curve (0-20) mg/l at 464 nm wavelength.**
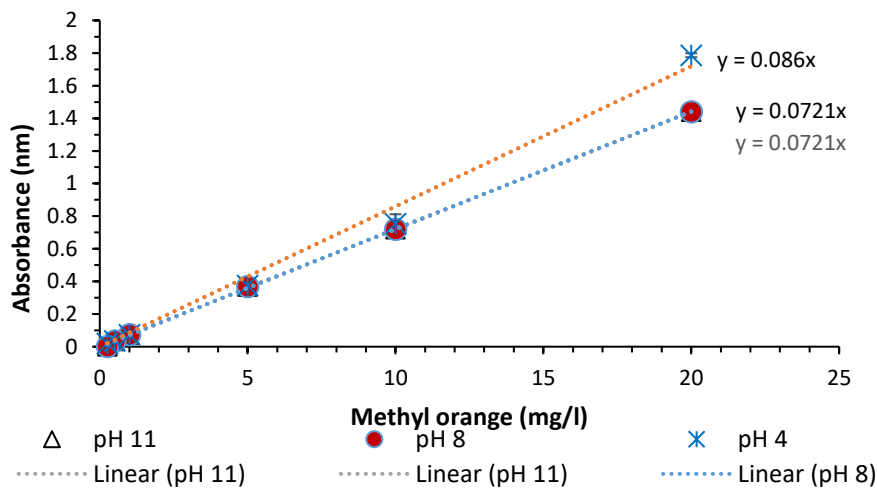


**Figure 4-3 Methyl orang calibration curve at different pH ranges (4, 8, and 11).**

## 4.3 The adsorption capacity for mine water treatment sludge

### 4.3.1 Effect of adsorbent doses

Studying the impact of changing the adsorbent dose is one of the parameters studied by conducted a batch experiment. 100 ml plastic containers with screw lids were used for this purpose. Mine water sludge sample (MWT) (500 g) was poured in a Pyrex glassware (2 l) and it was covered with aluminium foil before autoclaved by Prestige Medical 2100 series (Prestige Medical Blackburn UK). The autoclave was run for a 30 min cycle at 121 °C. An autoclave indicator was used to ensure that the requisite temperature had been achieved. After autoclaved the sludge sample, it was dried in the oven at 40 °C for 48 hrs as reported

by Schwertmann and Cornell (2000). Three different doses of the dried MWT sludge were selected (1, 5 and 20 g) and it was mixed with MO concentration ranges 5, 10, 15 and 20 mg/l to measure the sludge adsorption capacity using Equation 18. After 24 hrs, 5 ml was withdrawn from each sample container, and it was filtered using 0.45 µm syringe filter before measuring the absorbance at 464 nm using a spectrophotometer analysis.

$$q_t = \frac{(C_o - C_t) \times V}{W}$$  (Equation 18)

where qt= adsorbent capacity (mg adsorbate/g adsorbent). $C_0$: MO initial concentration (mg/l). $C_t$: MO concentration at time t (mg/l). V: volume of the solution (l). W: the dry adsorbent weight (g).

Figure 4-4 shows that MWT sludge adsorption capacity had a comparable value for different weights. For example, at 15 mg/l MO solution, the adsorption was 3.25 mg/g using 1g MWT as a substrate, and it was 3.50 mg/g using 20 g MWT according to that, and since no significant change on adsorption capacity between the two different weights, 1 g/l of MWT as adsorbents will be considered for the following batch experiments. Figure 4-4 was also used to calculate MWT sludge adsorption capacity by column substrates in textile wastewater experiments in chapter five because MO concentration in phase one textile wastewater was 15 mg/l which is within the range of this figure. According to that, 3.50 mg/g is used to estimate the adsorption capacity of MWT sludge in chapter five (see sections 5.2).
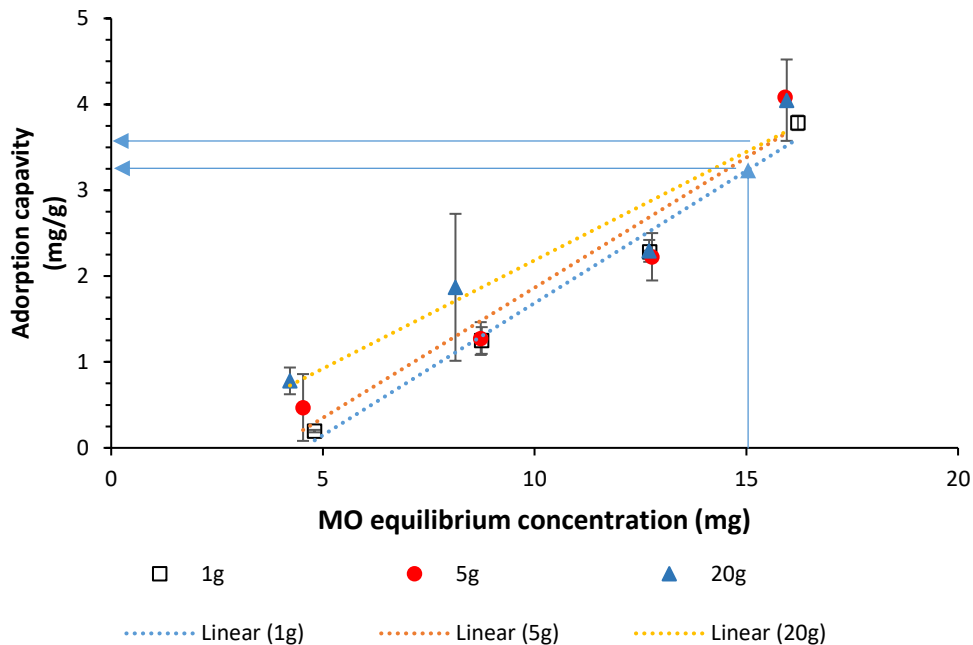


Figure 4-4 Mine water treatment sludge adsorption capacity at different weights after 24 hrs.

### 4.3.2 **Effect of contact time**

In this batch experiment, MWT sludge adsorption capacity was compared with other abundant iron oxides as goethite, magnetite, and hematite. Two different time intervals (3 and 24 hr) were tested to study the influence of time on iron oxides adsorption capacity. 1 g of adsorbents (MWT, goethite, magnetite, and hematite) were mixed with 100 ml of (1, 5, 10, 15 and 20 mg/l) MO under shaking (150 rpm) using appropriate plastic containers with screw lids. Samples were analysed after 3 and 24 hrs by withdrawn a 5 ml from each container which was filtered using 0.45 µm syringe filter before measuring the absorbance at 464 nm using a spectrophotometer. The presented data in Figure 4-5 showed that 3 hrs was adequate to determine the substrate adsorption capacity and extended the experiment to 24 hrs had a margin influence on the adsorption capacity. MWT sludge adsorption capacity was about 3.50 mg/g while magnate, hematite and goethite adsorption capacity were about 5 to 5.80 mg/g. Different materials, including agricultural wastes and sludge, were used to adsorbed MO. Alzaydien (2015) noticed wheat bran adsorbed 12.33 mg/g of MO at room temperature. In comparison, hog plum peel was used to adsorb 20 mg/g of MO (Ferdous Rumky et al. 2013). Wastewater sludge adsorbed 3 mg/g of MO (Yu et al. 2011). The MWT adsorption capacity was low than the majority of the literature review studies in Table 2-4, in this table the adsorption capacity for MO was varied between 7.50 to 36 mg/g based on the substrate used. Contact time between the adsorbent material and the adsorbate (dye) might influence the adsorption capacity. Alzaydien (2015) mentioned, the wheat bran adsorption capacity was quickly increased in the first hour, and then the adsorption trendline levelled off after 3 hrs due to saturation. Similarly,  Rumky et al. (2013) found that 70 min was the time required for hog plum peel to saturation using MO due to the limited free active site on the adsorbent surface area. In another study, it was noticed that 10 min was a sufficient contact time to remove 80% of methylene blue by sludge ash (Weng and Pan 2006). However, Santos and Boaventura (2016) argued that contact time for efficient dye removal varied between 8 to 24 hrs, according to the dye used. In this experiment, contact time for three hrs was sufficient to determine the MWT and other iron oxides adsorption capacity.
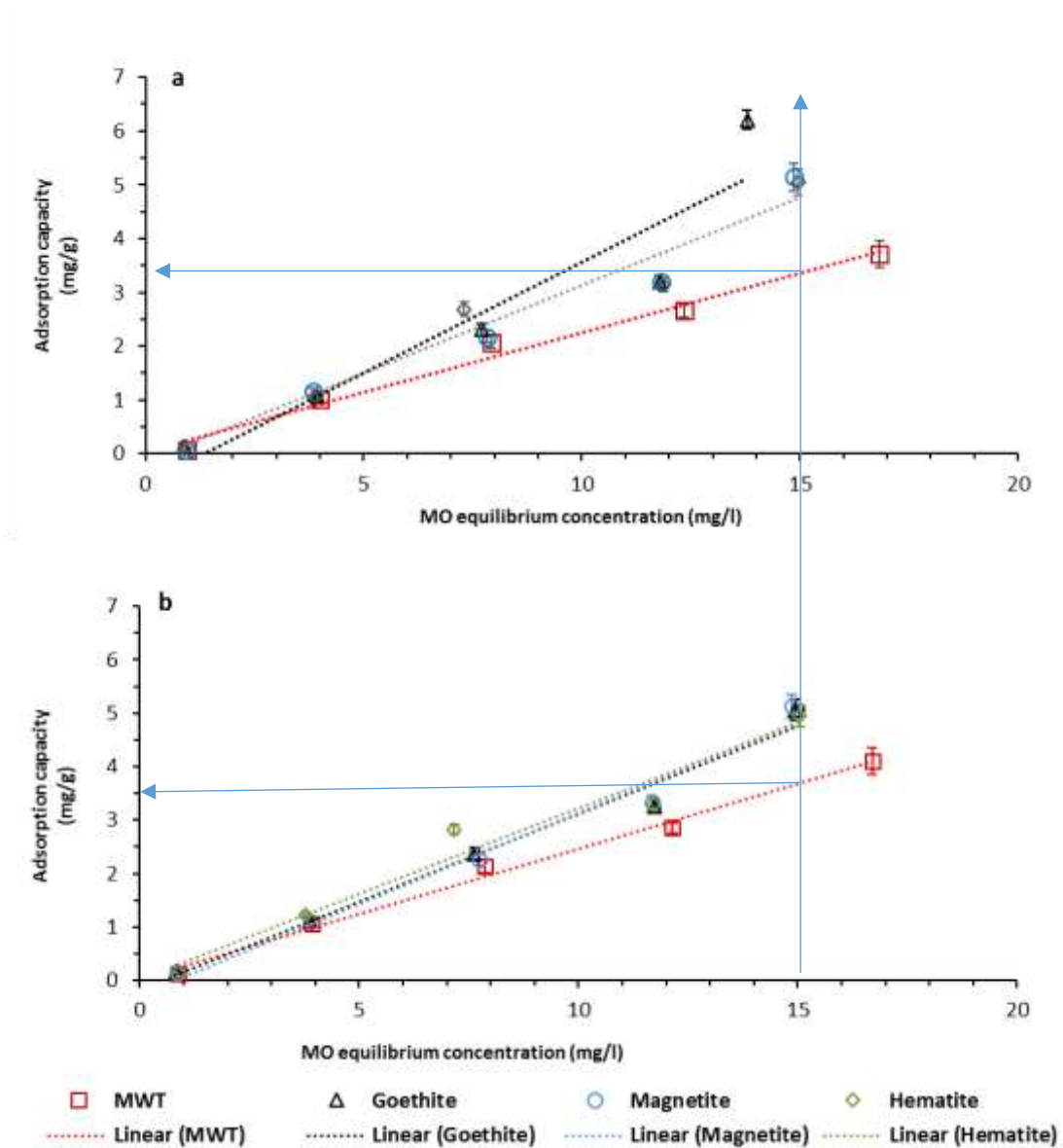
**Figure 4-5 The adsorption capacity for mine water treatment sludge, goethite, magnetite, and hematite after (a) 3 hrs and (b) 24 hrs.**

## 4.4 Adsorption Isotherm for MWT sludge using batch experiments

'Langmuir and Freundlich isotherm theories were used to investigate which theory best fitted with the performance of MO adsorption by MWT sludge (see section 2.4.1.3). A batch experiment was used to plot Langmuir and Freundlich isotherm. 1g MWT was mixed with 100 ml MO different concentrations. In Langmuir, $1/q_e$ was plotted vs $1/C_e$ (Equation 1),

while log qe was plotted vs log Ce to represent the Freundlich isotherm (Equation 2). According to the data from plots in Figures 4-6, Langmuir and Freundlich could both represent mine water treatment sludge adsorption behaviour.
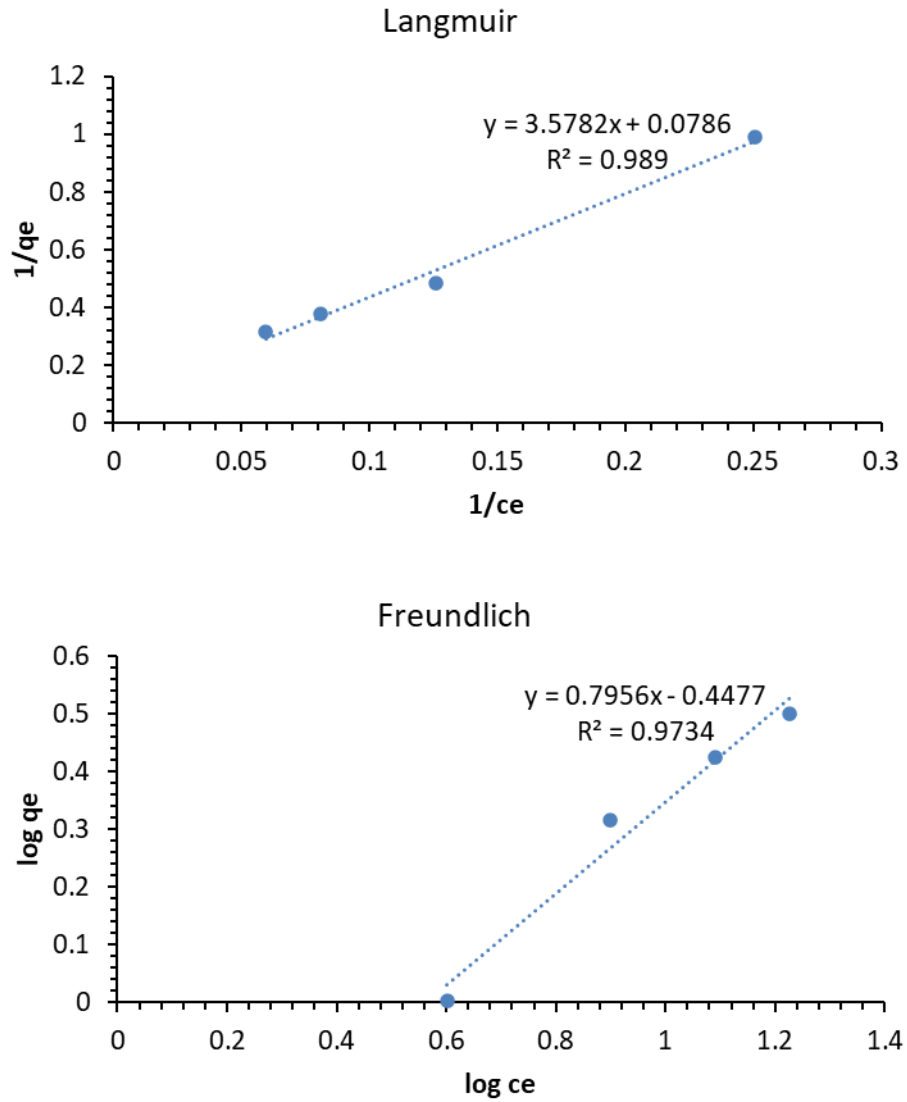


**Figures 4-6  Langmuir and Freundlich isotherms for mine water treatment sludge.**

# Chapter 5   : Phase one textile wastewater experiment results and discussions

## 5.1    Introduction

This chapter presents and discusses phase one textile wastewater experiment results. It includes the MO decolourisation by adsorption and biodegradation and estimated the MO removal rate. The MO degradation products as aromatic amines were investigated using a spectrophotometer scan. Liquid chromatography (LC-MS) and gas chromatography (GC-MS) were also used to characterise the MO degradation products. ChemDraw software was used to draw the biodegradation products structures. Gene sequencing was used to characterise the column substrate microbial community before and after treatment to distinguish the changes after 170 days of MO treatment.

## 5.2    Methyl orange decolourisation and colour removal rate

 The experiment setup was reported in section 3.5.1. During phase one textile wastewater experiment, two sample collection techniques were followed: the "instant" technique, where dye colour intensity was measured as soon as an adequate amount had been collected (Figure 5-1A) and the "composite"  where samples were collected from the sample tanks after 24 hrs (Figure 5-1b). The plotted data shown that the dye removal trend line was similar in both sampling techniques. It can be highlighted that the live columns fed by MO with glycerol (L+G) had the highest decolourisation. After two weeks, the L+G columns removed 99 % of the influent methyl orange. While the live columns (L) which did not contain any glycerol decolourised 60 % of MO during the first month. Though, after the second month, MO decolourisation increased up to about 95%, and then it regressed to 66 % by the end of week 21. Columns contained the autoclaved mine water treatment sludge fed with glycerol which labelled as (D+G) and the autoclaved columns (D) which treated only MO dye water without additional carbon as influent were decolourised about 65 % of the dye over the first six weeks. After this point, a substantial change was noticed in the (D+G) column, the dye decolourisation efficiency rose to more than 85 % for two months, and finally, it declined to under 70 %. The dye decolourisation in the D columns was about 65% during the experiment, and it dropped to under 40 % by the end of the experiment. Figure 5-2 shows the decolourised treated water samples with time. In this experiment, the influent flowrate generated a hydraulic retention time equal to 28.7 hrs which was comparable to other reported studies in Table 2-4 and Table 2-5.

The MO removal rate was also monitored during phase one textile wastewater treatment, as shown in Figure 5-3, see Appendix 2 for clarification. According to that, the highest MO removal rate was 29.71 $g/m^3/day$ by L+G columns, it was followed by L (29.17 $g/m^3/day$), D+G (26.72 $g/m^3/day$), and D (22.19 $g/m^3/day$).

Calculate the amount of the azo dye removed by adsorption is a fundamental step during dye biodegradation. According to section 4.3.1, the maximum MWT adsorption capacity at 15 mg/l MO is 3.50 mg/g (see Figure 4 4). The calculated adsorption capacity was used to determine the amount of MO adsorbed in each column after 170 days of continuous treatment. Table 3-1 was used to determine the amount of dried MWT sludge which was about 32.90 g. Equation 20 was used to calculate the amount of MO adsorbed in each column which was about 115 mg. According to Equation 21, the amount of MO treated by each column over 170 days was 280 mg, and by excluded the dye removal by adsorption from the total dye removal, the minimum net dye removed by other mechanisms (including mineralisation) was approximately 165 mg MO.

$$\textbf{Dye adsorbed in each column (mg)} = \textbf{DW} \times \textbf{q} \qquad \text{(Equation 20)}$$

$$\textbf{Amount of dye treated in 170days} = \textbf{C}_0 \times \textbf{q} \times \Delta\textbf{t} \qquad \text{(Equation 21)}$$

Where: DW is column substrate dye weight ( 32.9 g), q is the MWT adsorption capacity (3.50 mg/g), $C_0$ is the influent Mo concentration (15mg/l), q is the flow rate (100 ml/day), $\Delta t$ is the experiment time (170 days).

From the above calculations, it can be concluded that the amount of MO removed by biodegradation was more than the amount of dye removed by adsorption. This information was the motivation for reducing the amount of column's substrate in phase two textile wastewater experiment (in chapter six) to raise the amount of MO demonstrably removed by biodegradation clearly over and above the MO removal by adsorption. Murali et al. (2013b) noted that the substrate used in azo dye biodegradation reached saturation after a particular time; they concluded that biodegradation was the main mechanism for the azo dye removal. Yu et al. (2011) reported that during MO decolourisation, two mechanisms were distinguished, adsorption, which is saturated after a short time (10 min) and anaerobic mineralisation. Efficient and long term azo dye removal is related to biodegradation, and any dye that adsorbed during could also be degraded by microorganisms (Shen et al. 2005).

The data collected from this experiment demonstrate that the additional carbon source (glycerol) decreased the time needed for complete MO decolourisation as noticed in the L+G

columns, these columns took about 20 days to achieve efficient dye removal compared with two months for the L columns (see Figure 5-1). Glycerol probably decreased the time for microbial acclimatisation in L+G columns compared with the starved L columns. Murali et al. (2013b) reported that the acclimatised microorganism could boost the MO decolourisation. It was noticed that three weeks was sufficient for microbial acclimatisation to mineralise the azo dye (Zhang et al. 2012a). Igor et al. (2010) demonstrated that the acclimatised consortia ( for 30 days) could mineralise 97% of the influent azo dye. In the starved columns, microorganisms probably utilised MO as a sole carbon source. Even though D column's substrate was autoclaved, but some bacterial species might be regenerated by spores which did not affect by the autoclaving. Stolz (2001) who reported that some microorganisms degraded azo dyes as a sole carbon source. Nevertheless, the majority of microorganisms need an additional carbon source to degrade azo dye wastewater. Telke et al. (2009) concluded that azo dye could be insufficient to be the main substrate for microbial growth. Therefore, the additional organic substrate could produce a dynamic microbial growth as well as efficient dye degradation. Moreover, it supports the microorganisms to tackle and adapt with textile wastewater harsh environment (Jin et al. 2007; Franciscon et al. 2015). In phase one textile wastewater, the collected data highlighted that the indigenous MWT consortia degraded MO as a sole carbon source while the majority of the MO review studies in Table 2-4 utilised additional organic carbon during MO decolourisation.
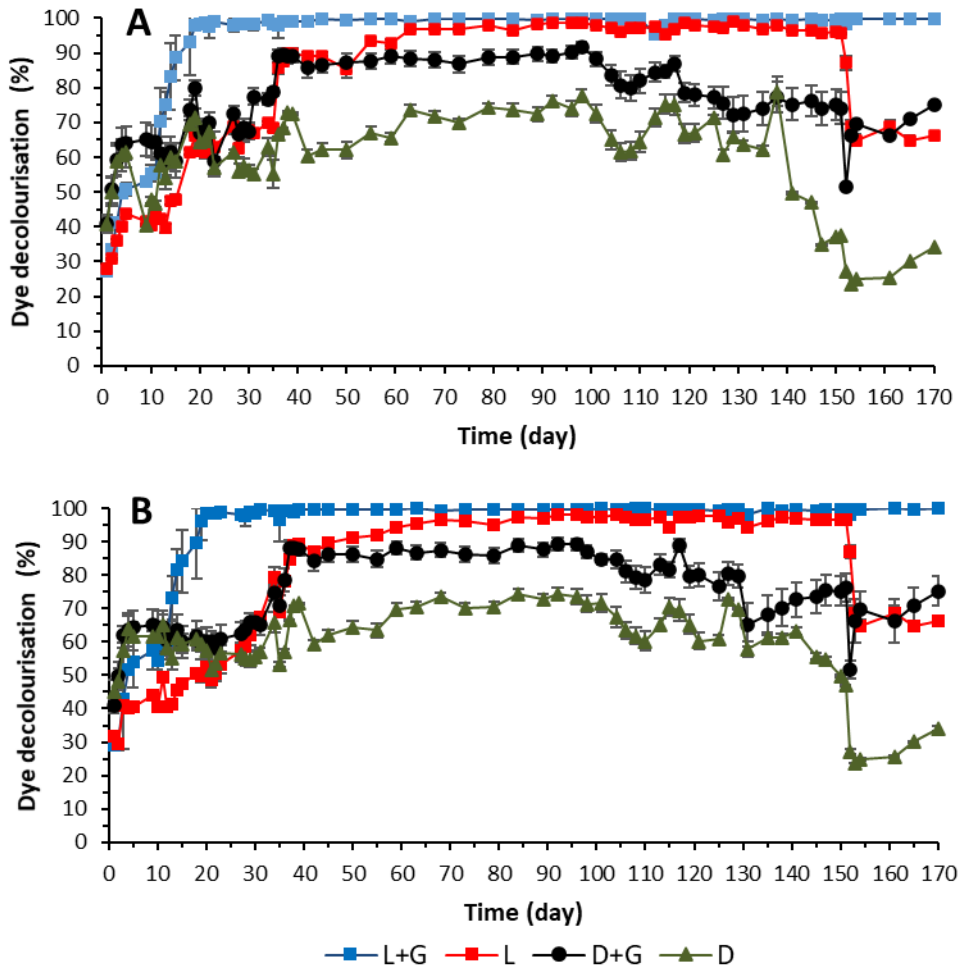
**Figure 5-1  MO decolourisation during phase one textile wastewater experiment where: (A) is the instant data, and (B) is the composite data.**



**Figure 5-2 Comparison of influent and effluents during phase one textile wastewater experiments.**
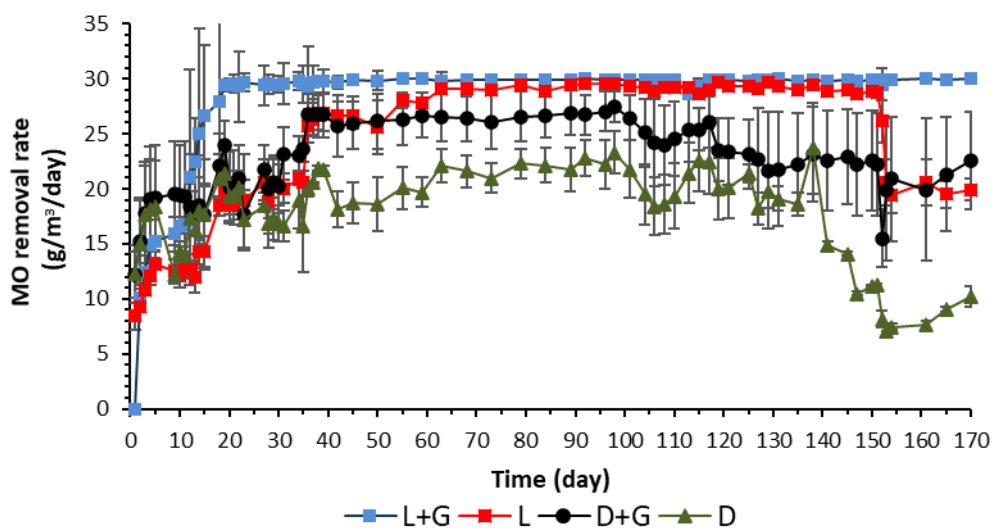
**Figure 5-3 MO removal rate (normalised) during phase one textile wastewater experiment.**

## 5.3 Aromatic amine detection by spectrophotometer

Aromatic amines are highlighted as azo dye intermediate biodegradation products under anaerobic conditions. These chemicals are generated by cleavage the dye azo double bond. It was first described by Milich and his group in 1936 as azo dye biodegradation products (Milch et al. 1936). It can be distinguished using a spectrophotometric method at the ultraviolet range (Boothman et al. 2006). 4-aminobenzene sulfonic acid (4-ABA) and N, N-dimethyl-p-phenylenediamine (DPD) were the reported aromatic amines which generated during MO biodegradation (O'Neill et al. 2000a; Kalyuzhnyi 2000; Yu et al. 2011).

In this experiment, the effluents and influents of phase one textile wastewater after 170 days were analysed by spectrophotometer at the wavelength range 200 to 700 nm; also, both 4-ABA and DPD were also plotted at 15 mg/l concentration. The ultraviolet range of 200-400 nm was used to detect aromatic amines generated in the column effluents (Abiri et al. 2017), while the visible range (400-700 nm) was used to show dye decolourisation compared with the influent. Figure 5-4 shows that in the influent wastewater, there were two peaks were highlighted at 464 nm and 290 nm. The 464 nm peak was for MO. In this peak, the colour intensity was dramatically reduced from about 1 to 0.04 in L+G effluents and to 0.14 in L effluents, while it declined to about 0.40, and 0.62 in D+G and D effluents. The peak at 290 nm did not change significantly during the experiment.

During anaerobic MO biodegradation, aromatic amines generated at a 249 nm wavelength as a newly formed peak (Murali et al. 2013b). Highlighted aromatic amines during azo dye biodegradation is an indication for incomplete mineralisation process (Manu and Chaudhari 2002a; Işik and Sponza 2005). Also, the experimental work revealed that N, N-dimethyl-p-phenylenediamine was not a colourless compound; it was a violet at 15 mg/l while 4-aminobenzene sulfonic acid was a colourless compound, as shown in Figure 5-5. According to the effluents plotted data in Figure 5 4, it can consider that the MWT indigenous microbial consortia degraded MO without detected aromatic amines. This finding confirmed the importance of the diversity of the indigenous microorganisms in the utilised sludge, which could include iron-reducing bacteria. Mineralisation of MO without detected aromatic amines is an uncommon mechanism as the majority of the reported studies in Table 2-4 detected aromatic amines as a part of MO degradation products.
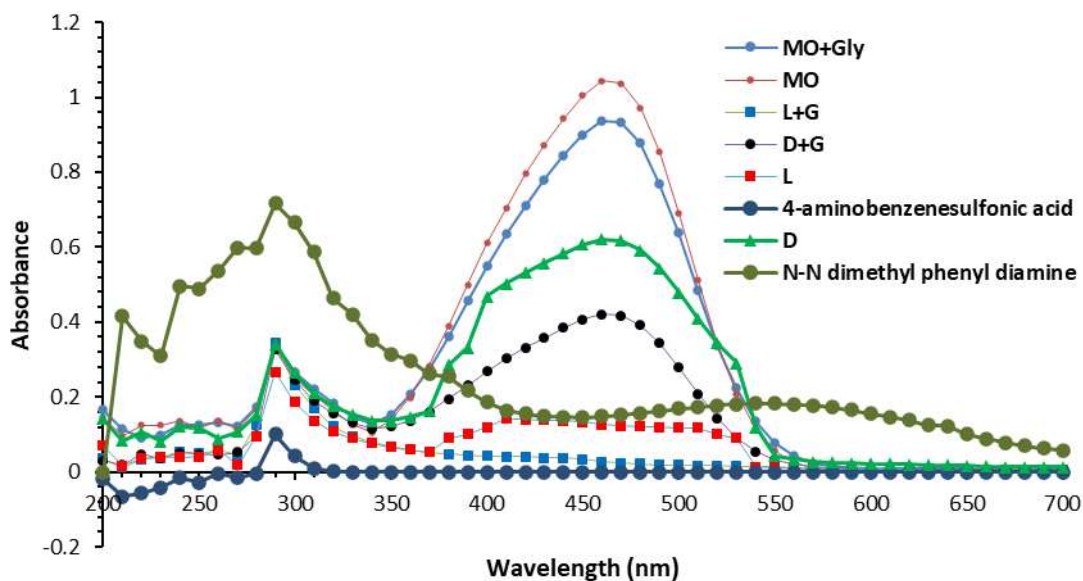


**Figure 5-4 Spectrophotometer analysis for phase one textile wastewater effluent columns after 170 days compared with both the influent N, N-dimethyl-p-phenylenediamine, and 4-aminobenzene sulfonic acid.**
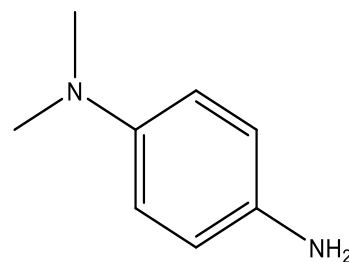
**Figure 5-5 N,N-di- methyl-p-phenylenediamine at 15 mg/l concentration.**

## 5.4      Total organic carbon (TOC) and total carbon

The total organic carbon (TOC) was measured phase one textile wastewater experiment influents and effluents as elucidated in section 3.8. TOC was $200 \pm 3$ mg/l in the influent MO with glycerol while it was $7.90 \pm 0.1$ mg/l in the influent without glycerol. In the L+G and D+G effluents, the TOC concentration fluctuated between the influent value and 165 mg/l until days 100. After this point, the TOC general trendline was gradually declined to approximately 140 mg/l while in L and D columns the TOC dropped to 2.60 mg/l and 3.70 mg/l respectively (see Figure 5-6).

The total carbon (TC) was distinguished in columns sludge as a solid sample using TOC-Shimadzu (see section 3.8). In the pre-test MWT, the TC was 1.51 %, and after 170 days, TC in post-test MWT in all columns was marginally changed as highlighted in Figure 5-7. This finding is an indication that the adsorbed MO during the experiment was probably mineralised by MWT indigenous consortia and the MO adsorption during dye mineralised could be ignored. The decline of TOC in the L confirmed that MWT indigenous consortia mineralised MO as a sole carbon source; furthermore, the additional organic carbon helped these microorganisms to degraded MO in L+G columns. It was reported that azo dyes and their degraded compounds are toxic to microorganisms (Manu and Chaudhari 2002b; Chang et al. 2011). Du et al. (2015a) noticed organic carbon improved azo dye degradation process. It was found that added glucose (20 mg/l) as an additional organic carbon source enhances the cleavage of the azo bond during dyeing wastewater treatment (Yu et al. 2011).

Some microorganisms decolourised azo dye and their degradation products as a single carbon source (Knappi et al. 2000). Coughlin et al. (2002) demonstrated that some microorganism species, e.g. *Sphingomonas sp strain 1CX* degrade azo dye as a sole carbon source. Moreover, It was reported that *pseudomonas species* isolated from soil could mineralise MO as the sole carbon source (Bheemaraddi et al. 2014; Khan and Srivastava 2014). The reported data in Figure 5-6 show that the microbial community in MWT sludge was able to mineralised MO as a sole carbon source whereas all the reported literature in Table 2-4 degraded MO as an additional carbon source.
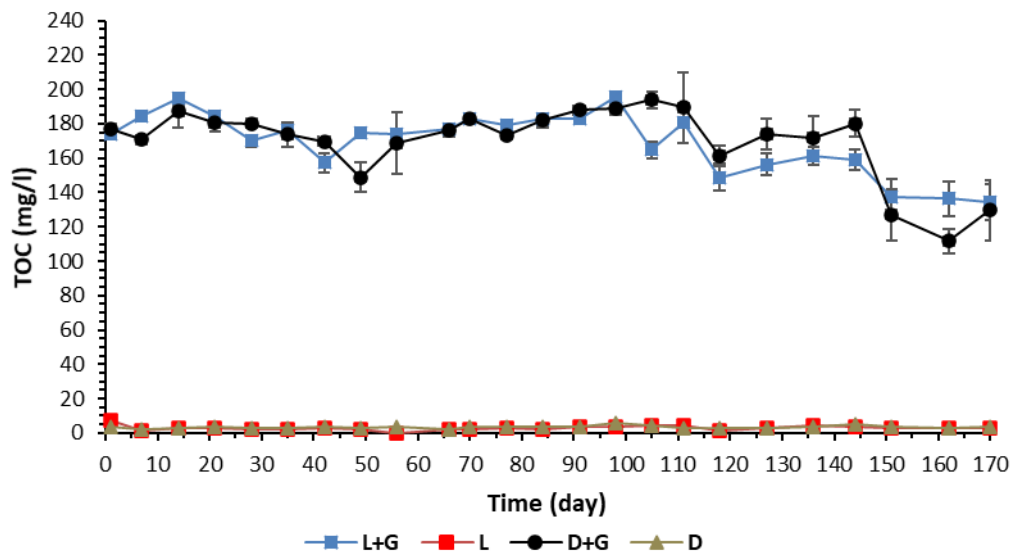


**Figure 5-6 Total organic carbon (TOC) during phase one textile wastewater experiment.**
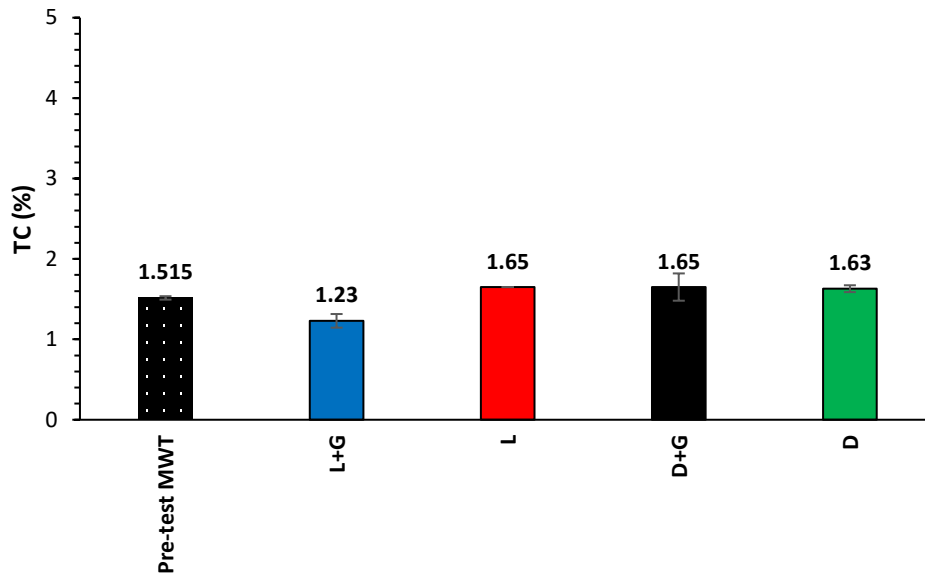
**Figure 5-7 Total carbon concentration in the pre-test MWT sludge and post-test MWT sludge (L+G, L, D+G, and D) after 170 days.**

## 5.5 Total iron and ferrous iron concentrations

Total iron concentration was monitored in column effluents during phase one textile wastewater, as reported in section 3.8. Figure 5-8 referred that efficient MO decolourisation was associated with iron releasing, especially in the L+G effluents. In the first two weeks, the total iron rose from zero to about 110 mg/l and in the remaining time; it was fluctuated between 44 to 125 mg/l. Meanwhile, iron concentrations in the other columns (L, D+G, and D) was below 1 mg/l. Ferrous concentration was also monitored during the experiment, and the highest concentration was 11 mg/l in the discharged water from the L+G columns, while it was below 1mg/l in the L effluents. Ferrous concentration in both D+G and D effluents were lower than the detection range as reported in Figure 5-9. Detection of iron and ferrous in columns effluent was probably referred to the presence of iron-reducing bacteria in MWT sludge, and this could be confirmed by gene sequencing detection in section 5.10. Iron is one of the enzyme's micronutrients (Liu et al. 2012). Iron oxides provided an electron acceptor which enhanced the biodegradation of azo dye (Albuquerque et al. 2005; Zhang et al. 2011; Zhang et al. 2012a).
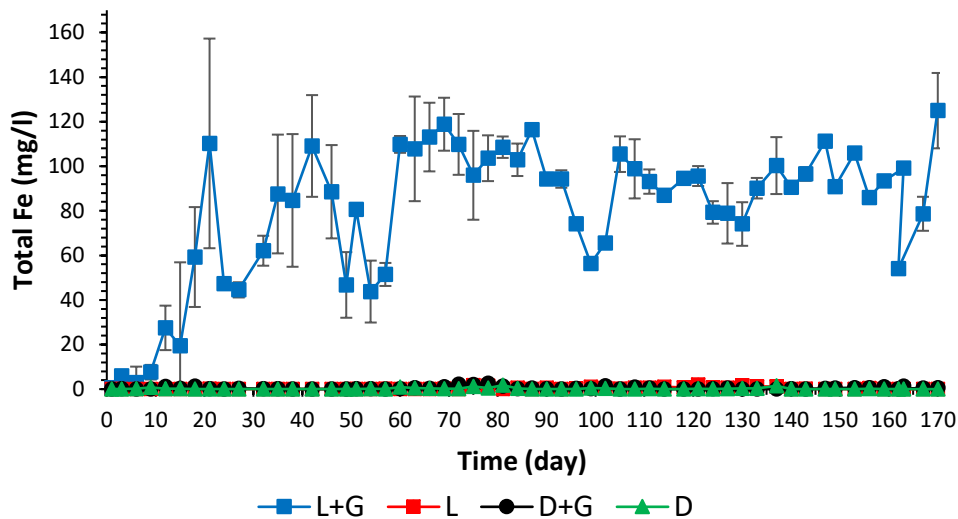
**Figure 5-8 Total Fe concentration during phase one textile wastewater experiment.**
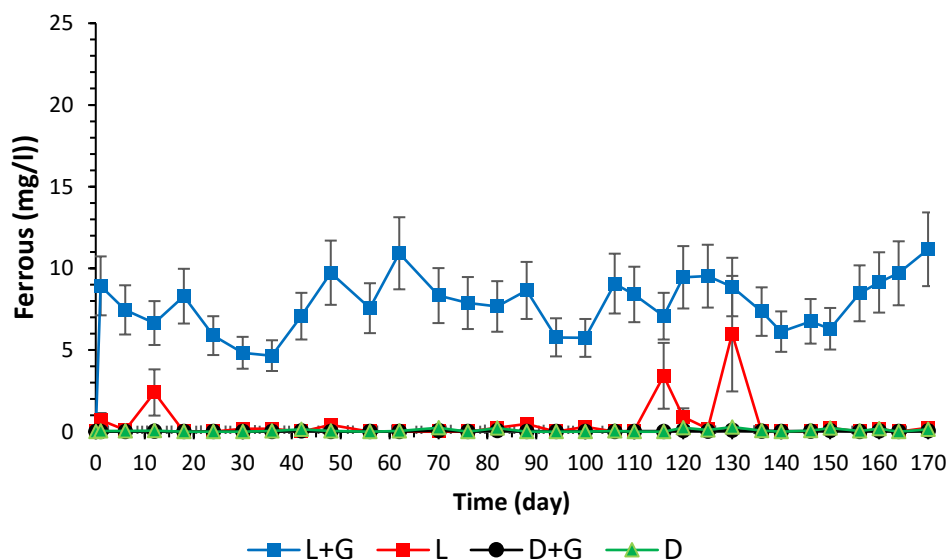


**Figure 5-9  Ferrous concentration during phase one textile wastewater experiment.**

## 5.6    Methyl orange biodegradation fragments by LC-MS

Liquid chromatography (LC-MS) was used to detect the MO degradation products during phase one textile wastewater experiment. Samples were prepared as described in section 3.12. The influent wastewater (15 mg/l MO with glycerol) was compared with column effluents after 170 days to investigate any organic compounds, which were highlighted as peaks in the LC-MS spectrum, as shown in Figure 5-10. The MO in the influent wastewater

was eluted at retention time (RT) (12.1-12.7 min) and 18.9-19.2 min, as highlighted in Figure 5-10A. These peaks were dropped dramatically in L+G and L column effluents while it retreated in D+G and D column effluents. The MWT sludge microbial community degraded Mo, and the degradation products were highlighted as new generation peaks in LC-MS spectrum column effluents. In L+G column effluents, new peaks were generated at RT 1.2 min and 10.2 min (Figure 5-10 B). The significant peak in L column effluents was highlighted at RT 1.2 min, as shown in Figure 5-10C. D+G and D column effluents had the same degradation products at RT 1.2 min and 12.1-12.7 min, as seen in Figure 5-10 D and Figure 5-10 E. All the highlighted peaks in LC-MS spectrum in Figure 5-10 had a unique m/z value (mass to charge ratio). This value was used to draw the compound chemical structures by ChemDraw software, as shown in Table 5-1. LC-MS spectrum was used to determine MO degradation products as highlighted in the diagrams in Figure 5-11. This diagram confirmed that no aromatic amines were detected during this analysis and so it likely that the microbial community within the MWT sludge was able to degrade MO without generating a detectable quantity of aromatic amines. Thus, MWT microorganisms degraded both the azo dye double bond and the aromatic benzene ring by reducing the azo bond and then oxidising the aromatic ring. Furthermore, the microbial community was able to degrade MO as a sole carbon source according to starved L column degradation pathway in Figure 5-10C. Most studies, such as (Fu et al. 2019) note the aromatic amines, N,N-dimethyl-p-phenylenediamine (DPD) and 4-aminobenzene sulfonic acid (4-ABA) were identified as MO biodegradation products by LC-MS. The LC-MS spectrum confirmed that MWT indigenous consortia mineralised MO without generated aromatic amines, whereas the majority of literature reported aromatic amines generation during MO biodegradation in Table 2-4.
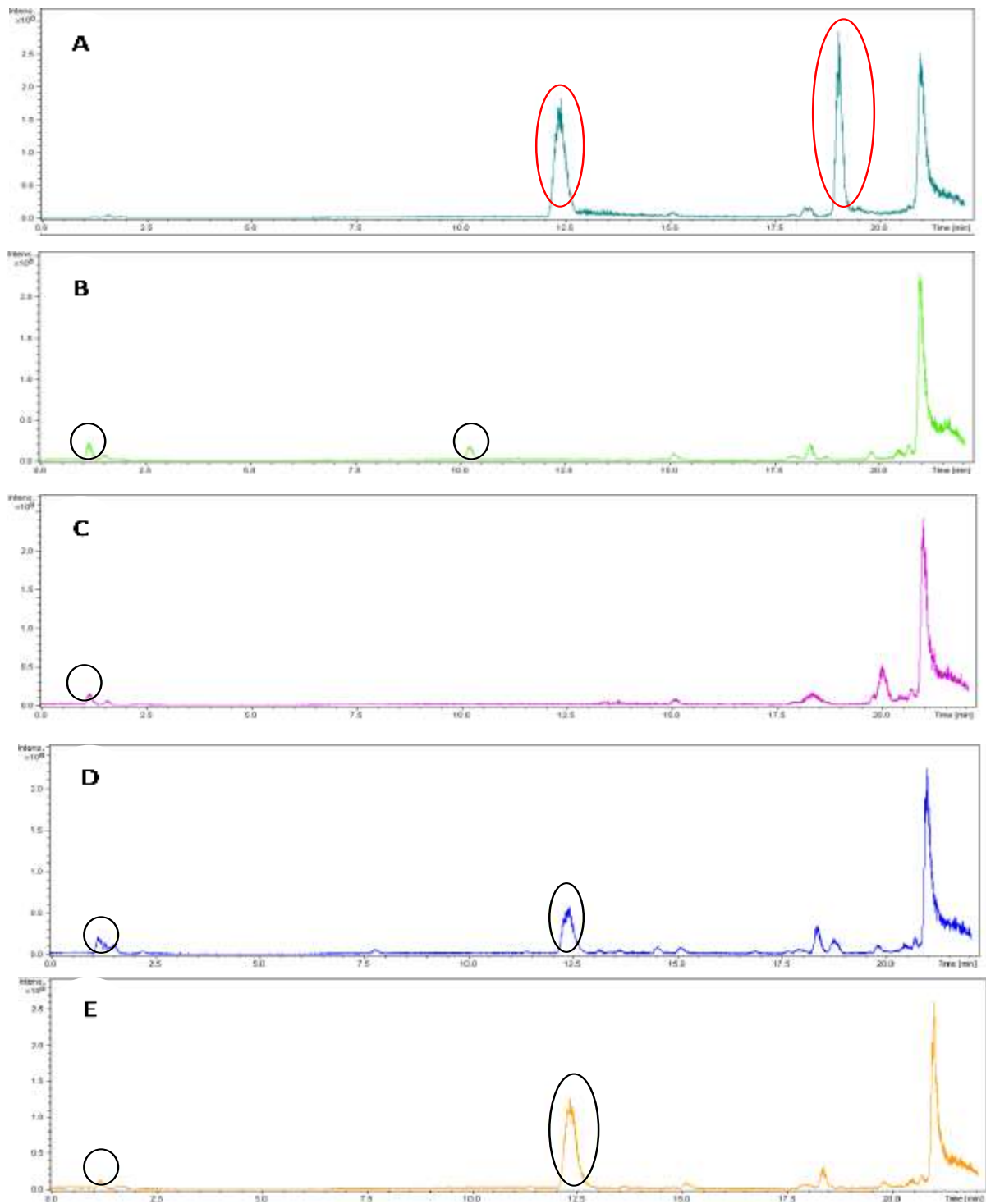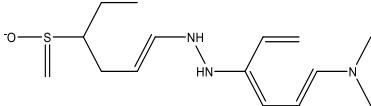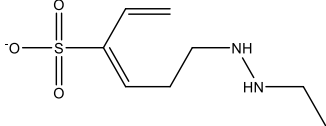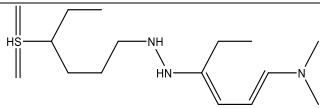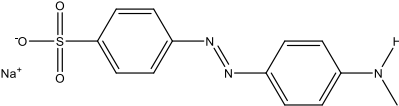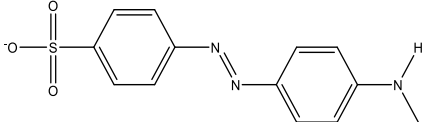
**Figure 5-10 LC-MS spectrum for phase one textile wastewater experiment where: (A) influent dye with glycerol, (B) L+G effluent, (C) L effluent, (D) D+G effluent, and (E) D effluent.**

**Table 5-1 MO degradation products for phase one textile wastewater experiment based on LC-MS and ChemDraw software.**

| RT (min) | m/z | Structure |
|----------|-----|-----------|
| 1.2(L+G) | 296 | Chemical Formula: $C_{15}H_{26}N_3OS^-$<br>Exact Mass: 296.18<br>Molecular Weight: 296.45<br>m/z: 296.18 (100.0%), 297.18 (16.2%), 298.18 (4.5%), 298.19 (1.2%), 297.18 (1.1%) |
| 1.2(L) | 219 | Chemical Formula: $C_8H_{15}N_2O_3S^-$<br>Exact Mass: 219.08<br>Molecular Weight: 219.28<br>m/z: 219.08 (100.0%), 220.08 (8.7%), 221.08 (4.5%) |
| 10.2 | 299 | Chemical Formula: $C_{16}H_{33}N_3S$<br>Exact Mass: 299.24<br>Molecular Weight: 299.52<br>m/z: 299.24 (100.0%), 300.24 (17.3%), 301.24 (4.5%), 301.25 (1.4%), 300.24 (1.1%) |
| 12.1-12.7 | 315.4/ 337 | Chemical Formula: $Na^+$<br>Exact Mass: 22.99<br>Molecular Weight: 22.99<br>m/z: 22.99 (100.0%)    Chemical Formula: $C_{13}H_{12}N_3O_3S^-$<br>Exact Mass: 290.06<br>Molecular Weight: 290.32<br>m/z: 290.06 (100.0%), 291.06 (14.1%), 292.06 (4.5%), 291.06 (1.1%) |
| 18.9-19.2 | 290.4 | Chemical Formula: $C_{13}H_{12}N_3O_3S^-$<br>m/z: 290.06 (100.0%), 291.06 (14.1%), 292.06 (4.5%), 291.06 (1.1%) |
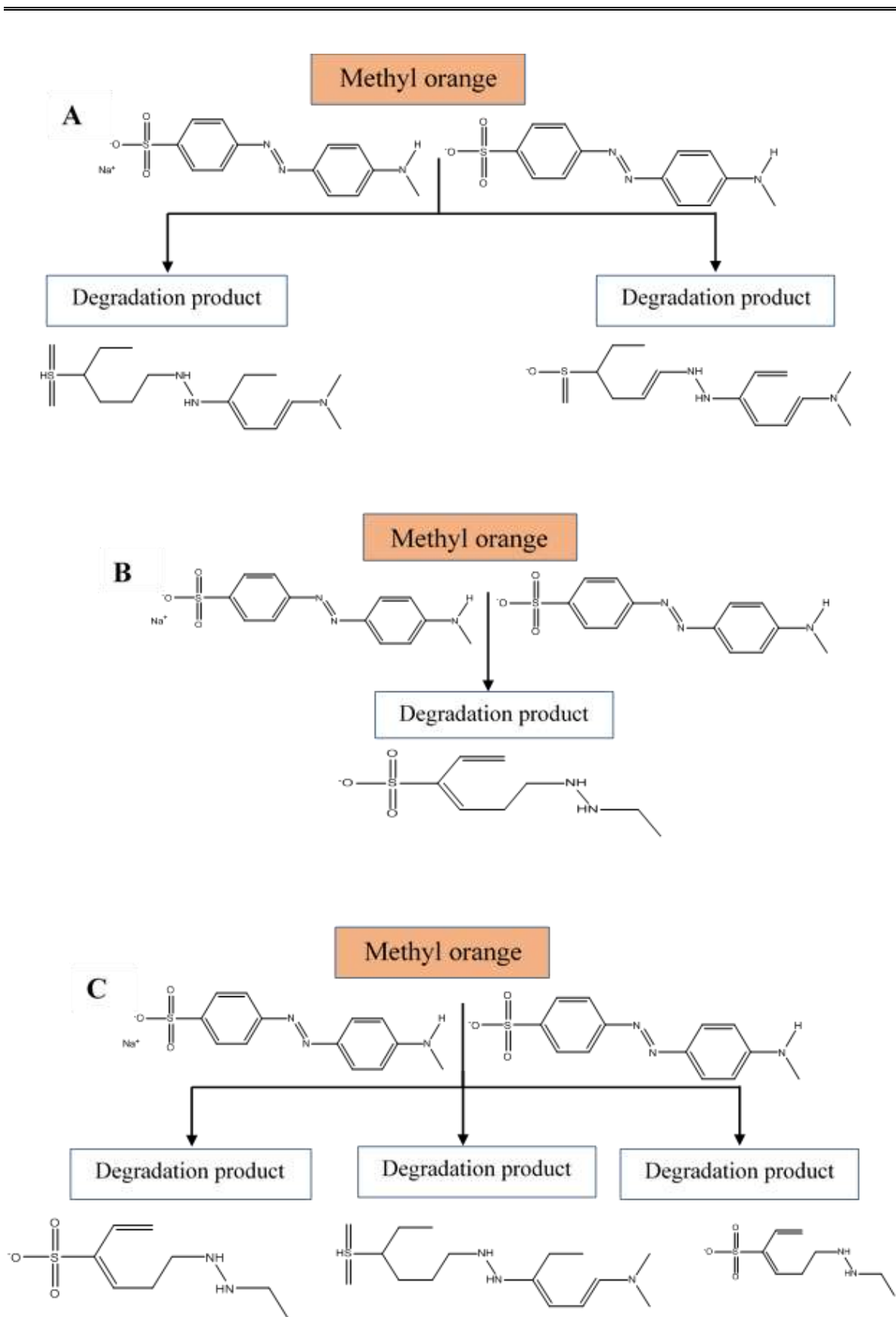
**Figure 5-11 MO degradation pathway during phase one textile wastewater experiment were: (A) L +G effluents, (B) L effluents and (C)  D+G, and D effluents.**

## 5.7    Methyl orange biodegradation fragments by GC-MS

Gas chromatography (GC-MS) was also used to detect any aromatic amines generated during MO biodegradation by the MWT columns substrate. A specific aromatic amines GC-MS column was used for this purpose, as reported in section 3.13. The influent wastewater (15 mg/l MO) was compared with column effluents (L+G, L, D+G and D) after 170 days, as shown in

Figure 5-12. The GC-MS spectrum highlighted only one significant peak at 8.5 min retention time (RT) in the L+G samples, and it was identified as 2 Ethyl 1-hexanol ($C_8H_{18}O$) based on the GC-MS library while all the peaks after RT 12.75 min were considered as a noise peak according to GC-MS technician. 2 Ethyl 1-hexanol is alcohol, and it was probably generated during glycerol biodegradation by MWT bacterial species. The reason for not detected 2 Ethyl 1-hexanol in D+G effluents might because these species probably were killed during autoclaving. Shen et al. (2015) highlighted that N,N-dimethyl-p-phenylenediamine (DPD) and 4-aminobenzene sulfonic acid (4-ABA) were identified as MO aromatic amines generated during anaerobic biodegradation. However, phase one textile wastewater GC-MS spectrum did not detect any of these compounds even though a specific GC-MS column was used to distinguish aromatic amines compounds because the MWT indigenous consortia probably degraded these compounds. Previous studies confirmed that LC-MS is more accurate technique than GC-MS to detect aromatic amines during MO degradation. It detects both DPD and 4-ABA while GC-MS detects only DPD and it was unable to detect 4-ABA because it has a boiling point out of the GC-MS range (Cai et al. 2012; Murali et al. 2013b). However, the GC-MS spectrum in this experiment did not detect DPD during MO bioremediation by MWT indigenous consortia. Based on the reported data from LC-MS (in the previous section 5.6) and the above GC-MS spectrum, it can be confirmed that iron oxides bearing waste (MWT sludge) were appropriate substrate to degrade MO with no evidence for generated aromatic amines.
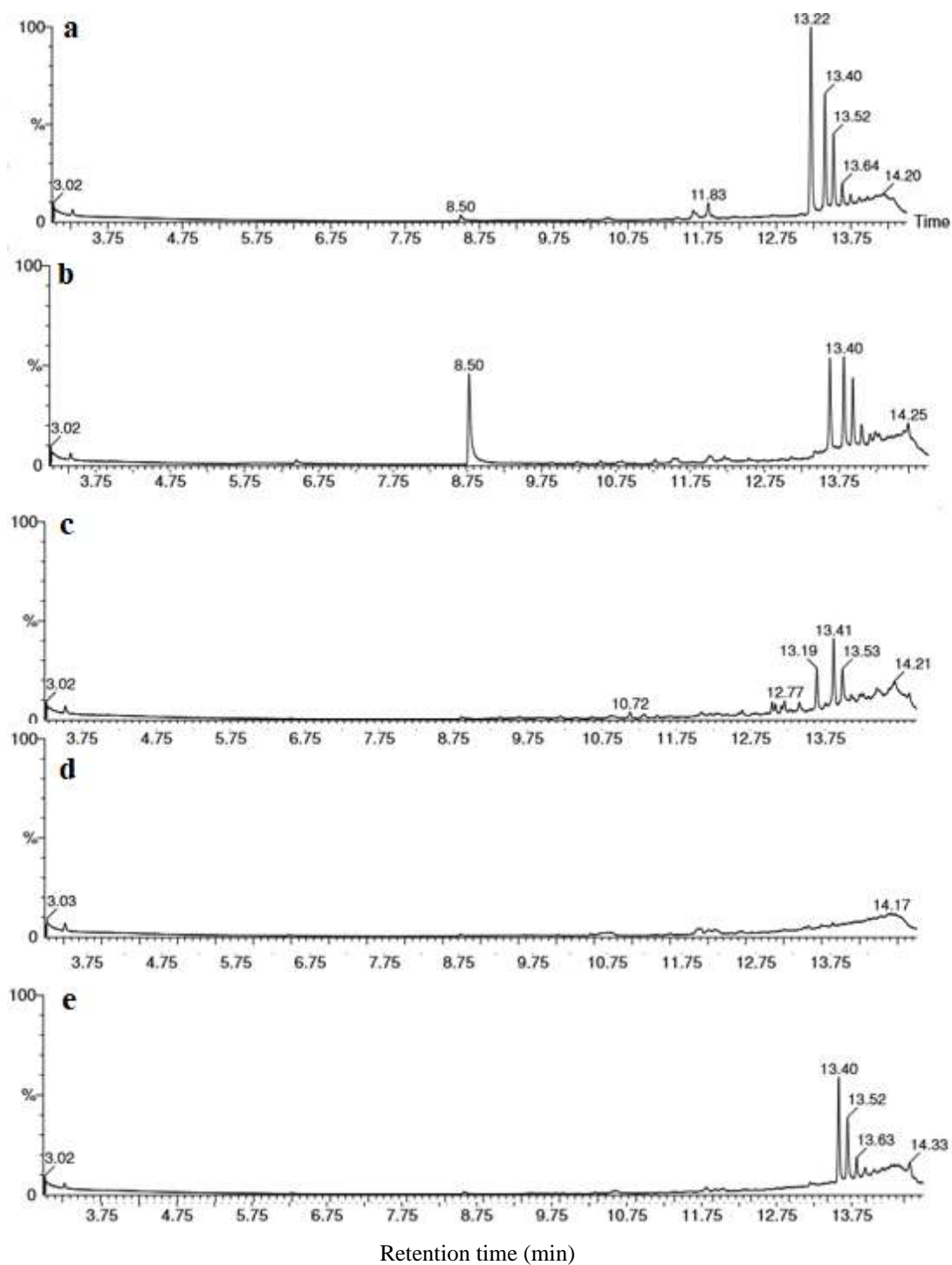
**Figure 5-12 GC-MS spectrums for phase one textile wastewater experiment after 170 where: (a) influent, (b) L+G column effluents, (c) L column effluents, (d) D+G column effluents, and (e) D column.**

## 5.8    Experiment parameters

During phase one textile wastewater experiment, several parameters were monitored: pH, temperature, and oxidation-reduction potential. The influent synthetic dye wastewater pH was 4.5±0.1. Thus, it raised after passing through the MWT sludge column. From the first few days, the pH trendline rose to about 8, and during the experiment, it varied between 6.8 and 8.3 except in L+G. It declined sharply to about 5.5, and it was maintained at approximately within this value (± 0.5) until the end of the experiment, as demonstrated in Figure 5-13. In this experiment, MO biodegraded was in a slightly acidic pH range in L+G columns and in a slightly alkaline range for the other columns. Furthermore, it considered as an indication for the diversity of MO mechanism in the utilised columns. This finding agreed with Du et al. (2015a), who reported that MO could be degraded within a 3-7 pH range. pH 7 is typically the most favourable pH for anaerobic microorganisms (Isık and Sponza 2008; Wang et al. 2013). Azo dye biodegradation might generate organic acids which could decrease the environment pH (Liu et al. 2012). Willmott (1997) highlighted when aromatic amines generated during azo dye biodegradation it raised the treated water pH while, in this experiment, the decline of the pH and the glycerol breakdown boosted MO biodegradation, especially in L+G columns. The decline of pH in the L+G effluents was probably by the influence of organic acid generated during glycerol metabolism by MWT indigenous microorganisms  (Schröder and Südekum 1999).

The environment temperature has a vital impact on microorganisms' enzymes. Figure 5-14 shows that the columns experiment was conducted in a temperature ranging between 15 and 24.5 °C. This range was convenient for MW sludge indigenous microorganism to degrade MO. Du et al. (2015) reported that single bacteria species decolourised MO at a temperature range between 5 to 45 °C. Wang et al. (2013) stated the optimal temperature for azo dye biodegradation is from 35 to 40 °C. Dye biodegradation flourished in warm conditions (Guo et al. 2007). In general, The temperature changes could also affect microorganism acclimatisation, enzyme activity (Chang et al. 2011) and cell growth (Yu et al. 2001; Angelova et al. 2008). Usually, MO mineralised at a constant temperature, as noticed in Table 2-4 while in this phase, MO degraded at different temperature range (15 to 24.5 °C).

Oxidation-reduction potential (ORP) was measured relative to a standard hydrogen electrode (SHE) by added 200 mV to the collected readings. ORP in column effluents included (L+G,

L, D+G and D) were varied between zero to -50 mV as highlighted in Figure 5-15. This condition was convenient for efficient azo dye reduction using indigenous MWT consortia. Liu et al. (2011) noticed that ORP range of -270 to -370 mV was an appropriate environment for anaerobic microorganisms. Added additional organic carbon source as an electron donor may help to maintain the ORP between -380 to -240 mV under obligatory anaerobic conditions (Işik & Sponza 2008). Cervantes (2011) reported that the redox potential should be in harmony with the range of the ecology system for dynamic electron shuttles activity, which is one of the expected mechanisms for azo dye biodegradation.
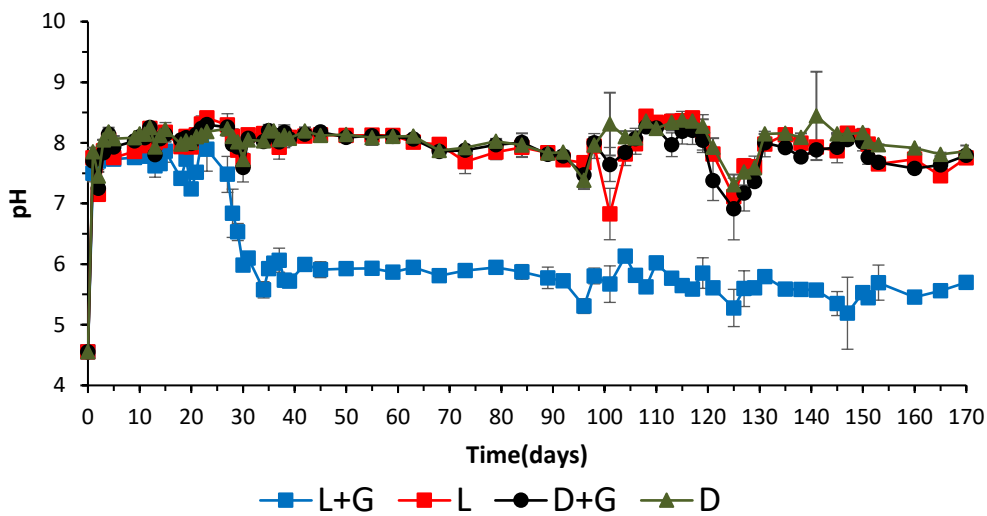


**Figure 5-13 The pH trendline during phase one textile wastewater experiment.**
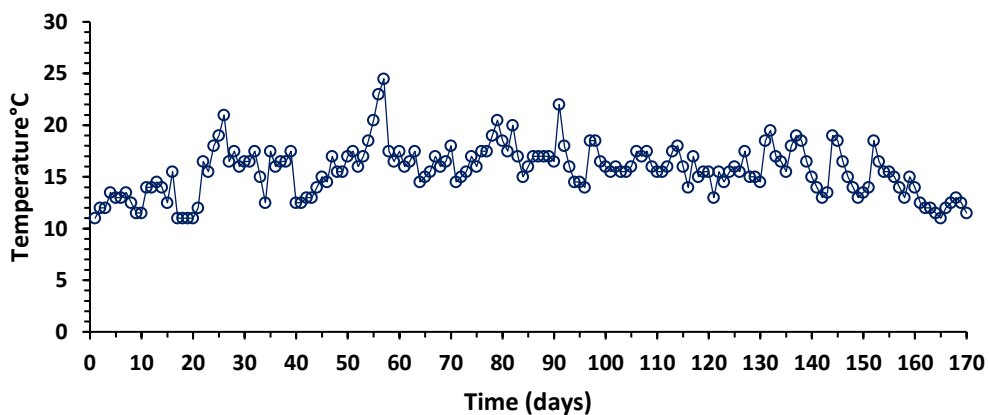


**Figure 5-14 The temperature change during phase one textile wastewater experiment.**
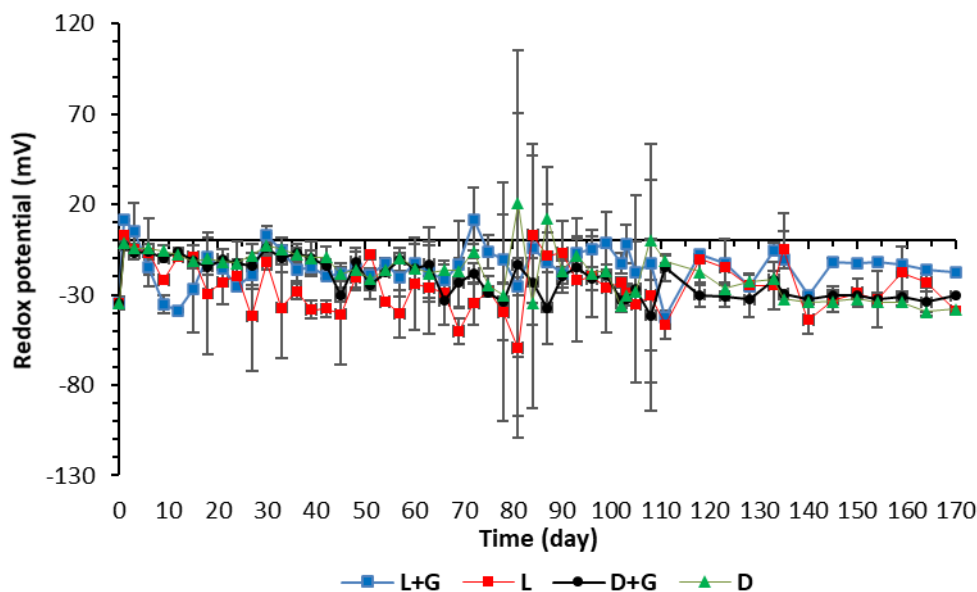
**Figure 5-15 The redox potential correlated to SHE trendline during phase one textile wastewater experiment.**

## 5.9 Parameters correlation for phase one experiment

IBM SPSS statistic software (version 20) was used to find the bivariate correlation between phase one textile wastewater parameters. The parameters data were not normally distributed according to the test of normality using Shapiro-Wilk ($p < 0.05$). Therefore, Spearman's rho was used to determine the correlation of the parameters. The statistical analysis highlighted a negative correlation between MO decolourisation in L+G column and pH with -0.56 correlation coefficient while no correlation was noticed in other columns (L, D+G and D). The statistical results also explored that ORP has negatively correlated with MO decolouration with -0.60 correlation coefficient for D+G columns only as no correlation was found in other columns. A negative correlation was found between MO decolourisation and TOC in L+G (-0.48), and L (-0.57) and D+G (-0.65) columns depend on the correlation coefficient value. The correlation between MO decolourisation and the temperature was positive in L+G, L, and D+G columns with 0.41, 0.43 and 0.43 correlation coefficient respectively, while no correlation was noticed in the D columns. In L+G, there was a correlation between ferrous and MO decolourisation (0.35) while no correlation was highlighted in other columns. The statistical analysis agreed with general pH trendline (in Figure 5-13) where the MO decolourisation increased with decreased pH in the L+G columns.

## 5.10 Microbial community changes in pre-test and post-test MWT column substrates

The next-generation sequencing was used to generate a taxonomic classification (16S rRNA) to distinguish the microbial change in mine water treatment sludge (MWT) indigenous consortia before and after phase one textile wastewater experiment after 170 days of treatment (see section 3.14 for details). In the pre-test MWT, 17 phyla were demonstrated including 16 bacterial phyla with 99.41 % relative abundance and one archaea phylum while in the post-test MWT sludge, the distribution of bacterial phyla declined dramatically by about 50% and the archaea dropped below the detection range except in the L+G substrate as shown in

Figure 5-16. *Proteobacteria* (61.24 %) had the highest density of all the bacterial phyla in the pre-tested MWT sludge. It was detected at 60.25 % relative abundance in the L columns and declined to 34.01 % and 23.24 % in the D+G and D columns, respectively. Furthermore, *Proteobacteria* dropped sharply to 5.05 % relative abundance in the L+G columns. *Acidobacteria* (9.98 %) was the second most abundant bacterial phylum in the pre-test MWT sludge. It resisted the effect of the azo dye, and it was marginally affected in both the L+G (9.19 %) and D+G (8.60 %) columns, while it increased to 14.04 % and 29.02 % relative abundance in the L and D columns. *Chloroflexi* (7.44 %) dropped to 2.71 % in L, 0.22 % in L+G and 0.1% in D+G but it was below the detection limit in the D columns. *Bacteroidetes* consisted of 5.56 % of pre-test MWT sludge relative abundance. It doubled in D (10.43 %), and it rose to 8.03 % in L then, it retreated to 3.28 % and 0.33 % in D+G and L+G respectively. *Firmicutes* flourished in L+G (71.76 %), D+G (45.55 %), D (36.25 %) and in L (6.42 %), while it represented 0.42 % of the pre-test MWT sludge relative abundance. Other phyla in the pre-test MWT sludge included: *Planctomycetes* (3.85 %), *Actinobacteria* (3.09 %), *Nitrospirae* (1.89 %), *Spirochaetes* (1.68 %). The remaining phyla with low relative abundance (relative abundance >1%) were: *Armatimonadetes* (0.74), *Gemmatimonadetes* (0.45 %), *Chlorobi* (0.43 %), *Caldiserica* (0.31 %), *Verrucomicrobia* (0.2 %) as bacterial phyla. Thus, *Crenarchaeota* (0.59 %) was the only *Archaea* detected.

Figure 5-17 highlights the intrinsic genus distinguished in pre-test and post-test MWT. The genera presented had a high relative abundant (>1 %). *Gallionella* was found at 5.82 % in pre-test MWT sludge, and it was distinguished in L (5.34 %), D+G (1.28 %), and D (1.01

%) but not elsewhere. In addition, *Proteobacteria* genus includes *Anaeromyxobacter* (1.77 %) detected in pre-test MWT sludge. This genus was decreased by about 50% in L columns (0.83). *Geothrix* (1.39 %) identified in the pre-test MWT sludge as iron-reducing bacteria, it flourished in D (29.12 %), D+G (7.09 %), and L (7.51 %) columns substrates. Thus, it retreated marginally to a relative abundance of 1.27 % in the L+G substrates. *Rhodoferax* was isolated in the pre-test MWT sludge (4 %), L (5.74 %), and in D+G (1.28 %). *Devosia* was detected only in the pre-test MWT sludge and in L (0.83 %) substrates. *Prevotella* (2.86 %) and *Bradyrhizobium* (1.91 %) were found in the pre-test MWT sludge, but it was undetectable after treatment in column substrates. There was a variety of low-abundance bacterial genera in the pre-test MWT sludge and it consisted of 35.61 % of the overall relative abundance.

In the L+G substrates, Figure 5-17 represents the bacterial genera with relative abundance higher than 1%, which included *Acetobacterium* (31.00 %), *Pelosinus* (6.61 %), *Fusibacter* (7.63 %) *Sporomusa* (4.17 %) and *Clostridium* (1.48 %), these bacteria represented the *Firmicutes* genus. *Proteobacteria* was represented by *Geobacter* (2.89 %), *Desulfovibrio* (1.04 %). *Salinibacterium* (3.64 %) represented the *Actinobacteria* genus, and *Methanospirillum* (6.95 %) was the only *Archaea* presented. In the live mine water treatment sludge (L), the dominance genera (relative abundance >1 %) including *Geobacter* (11.51 %), *Rhodoferax* (5.74 %), *Gallionella* (5.34 %), and *Xanthobacter* (*1*.61 %) as *Proteobacteria* genera. *Clostridium* (1.35 %) represented the *Firmicutes* genus. *Flavobacterium* (2.94 %) was the only *Bacteroidetes* genus identified, *Geothrix* (7.51 %) as the *Acidobacteria* genus. The low-abundance (relative abundance < 1 %) bacterial genus reduced to 3.26 %. The effective genera (relative abundance >1%) in D+G are shown in Figure 5-17. The genera divided into *Pelosinus* (7.42 %) which is a *Firmicutes* genus, and *Proteobacteria* genera classified to *Xanthobacter* (8.07 %), *Azospirillum* (3.30 %), *Sulfurospirillum* (2.92 %), *Sphingomonas* (2.35 %). *Desulfovibrio* (4.39 %), *Methylobacterium* (1.05 %). *Geothrix* (7.10 %) and *Flavobacterium* (3.65 %) representing the *Acidobacteria* and *Bacteroidetes* genera. The genera classified from the D column substrates revealed that the dominant bacterial genus (relative abundance >1%). *Geothrix* (29.13 %) was the most abundant genus. *Bacteroidetes* represented by the *Flavobacterium* genera (13.09 %). *Firmicutes* included *Gracilibacter* (7.31 %), *Anaerovorax* (2.80 %). *Proteobacteria genus divided into Caulobacter* (2.66 %), *Tolumonas* (1.32 %), *Janthinobacterium* (1.90 %), *Sulfurospirillum* (1.01 %), *Desulfovibrio* (1.18 %) and *Gallionella* (1.01 %).

*Proteobacteria* was the abundant bacterial phyla in pre-test MWT sludge. This phylum retreated after treatment while *Firmicutes* flourished in all post-test MWT sludge. *Firmicutes* affiliated with other bacterial phyla. This consortium degraded MO efficiently as a sole carbon source by break the MO azo bond and the aromatic hydrocarbon ring according to the LC-MS data in Figure 5-11. Rasool et al. (2016) noticed *Bacteroidetes, Proteobacteria* and *Firmicutes* were involved in anaerobic azo dye biodegradation. *Proteobacteria* degraded azo dye as a sole of carbon and nitrogen substrates (Govindaswami et al. 1993; Coughlin et al. 1999). Yu et al. (2015) reported that *Firmicutes* efficiently reduced MO at iron-reducing conditions and adding organic carbon as a substrate (as an electron donor) could enhance azo dye biodegradation. Zhang et al. (2013a) demonstrated, *Firmicutes* mineralises organic compounds to the simplest form. *Firmicutes* is a spore generating bacterium, and this may explain the presence of this phylum in the autoclaved column substrates in D and D+G (Schuppert et al. 1990). Iron oxidation bacteria as *Gallionella* was found in MWT sludge. This genus oxidised Fe (II) to Fe (III) (Tay et al. 2008; Ionescu et al. 2015). *Gallionella* was isolated from mine ochre, and it was found in aquatic iron-rich habitats (Harder 1919). This genus was also highlighted in the starved (L) columns, and the generated Fe (III) might be precipitated in column's sludge, it might be the reason for low ferrous concentration in the L effluent. Ivanov (2010) also observed that Fe (III) was precipitated in the column substrate. Iron reducing bacteria *Geothrix* was found in all post-test columns sludge. *Geothrix* was also isolated from rich iron sediments (Luu and Ramsay 2003). It resisted the MO toxicity during phase one textile wastewater treatment. *Geothrix* reduced Fe (III) to Fe (II) by direct and indirect contact (Luu and Ramsay 2003). It also degrades complex aromatic hydrocarbon to $CO_2$ (Rosenberg et al. 2013). It survived with or without additional carbon sources (Weber et al. 2006). *Geobacter* is another anaerobic iron-reducing bacterium. It flourished in post-test column substrates. It mineralised organic aromatic contaminants (as an electron donor) to $CO_2$ while reduces Fe (III) as an electron acceptor (Lovley et al. 1993). A *Clostridium iron-reducing bacterium was* highlighted in some post-test column media, especially in L+G and L columns. Dafale et al. (2010) noticed *Clostridium* acclimatised with various bacterial genera to decolourise azo dye. This genus uses electron shuttle mechanism to reduces Fe (III) anaerobically as an electron acceptor (Fuller et al. 2014). Fe (III) reduces by iron-reducing bacteria either directly by direct contact with bacteria outer membrane or indirect by electron shuttle (Marsili et al. 2008; White et al. 2013). *Pelosinus* is a metal-reducing bacterium. It was one of the competent *Firmicutes* genera, especially in the L+G and D+G

column substrates. This bacteria is a stringent anaerobic species, and it utilises glycerol and organic carbon as a substrate (Moe et al. 2012; León et al. 2015). Other bacterial species, *Acetobacterium* which is acetogeneic *Firmicutes* bacteria. It was isolated from diverse sediments (Krumholz et al. 1999; Rosenberg et al. 2013). This genus was one of the influences bacterial taxa in the L+G column substrates, but it retreated below the detection range in the other columns. *Sporomusa* is other anaerobic acertogenic bacteria identified in L+G. *Sporomusa* and *Acetobacterium* might degrade any aromatic amines generated during azo dye degradation as an electron donor. Rosenberg et al. (2013) noticed *Sporomusa* degrades aromatic organic compounds. Furthermore, Delforno et al. (2016) found that *Sporomusa* degraded aromatic hydrocarbons at the iron-reducing condition. *Flavobacterium* acclimatised with iron-reducing bacteria in post-test column substrates. It could degrade MO and the generated aromatic amines. It was noticed that *Flavobacterium* degrades azo dye and the generated aromatic amines as a sole carbon source (Cao et al. 1993). The column biodegradation mechanism may be associated with the predominant bacteria (Khelifi et al. 2009; Rosenkranz et al. 2013). However, low abundance bacteria may contribute a substantial taxon in azo dye biodegradation (Cervantes and Santos 2011; Prato-garcia et al. 2013). Single microorganism species was used to decolourise azo dye, but it generated aromatic amines (Paper et al. 2009; Parshetti et al. 2010; Cai et al. 2012; Du et al. 2015; Yu et al. 2016). Nevertheless, the collaboration of various microorganisms as a consortium is essential to degrade aromatic amines (Poonam et al. 1996; Chang et al. 2011). Khehra et al. (2005) noticed complementary azo dye biodegradation could be done by utilised synergetic of microorganisms. Natural habitats such as sludge waste and soil are feasible substrates for azo dye degradation because it contains various indigenous species (Ayed et al. 2010; Yu et al. 2011). The utilised MWT sludge via the iron-reducing microorganisms and the affiliated genera considered an efficient biological substrate to mineralised MO.
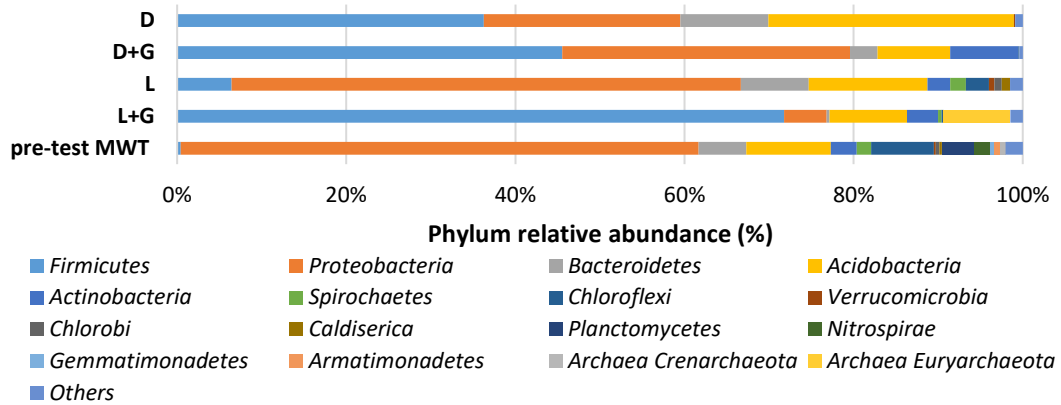
**Figure 5-16 Taxonomic classification of the 16S RNA gene at the phylum level for pre-test and post-test MWT sludge.**
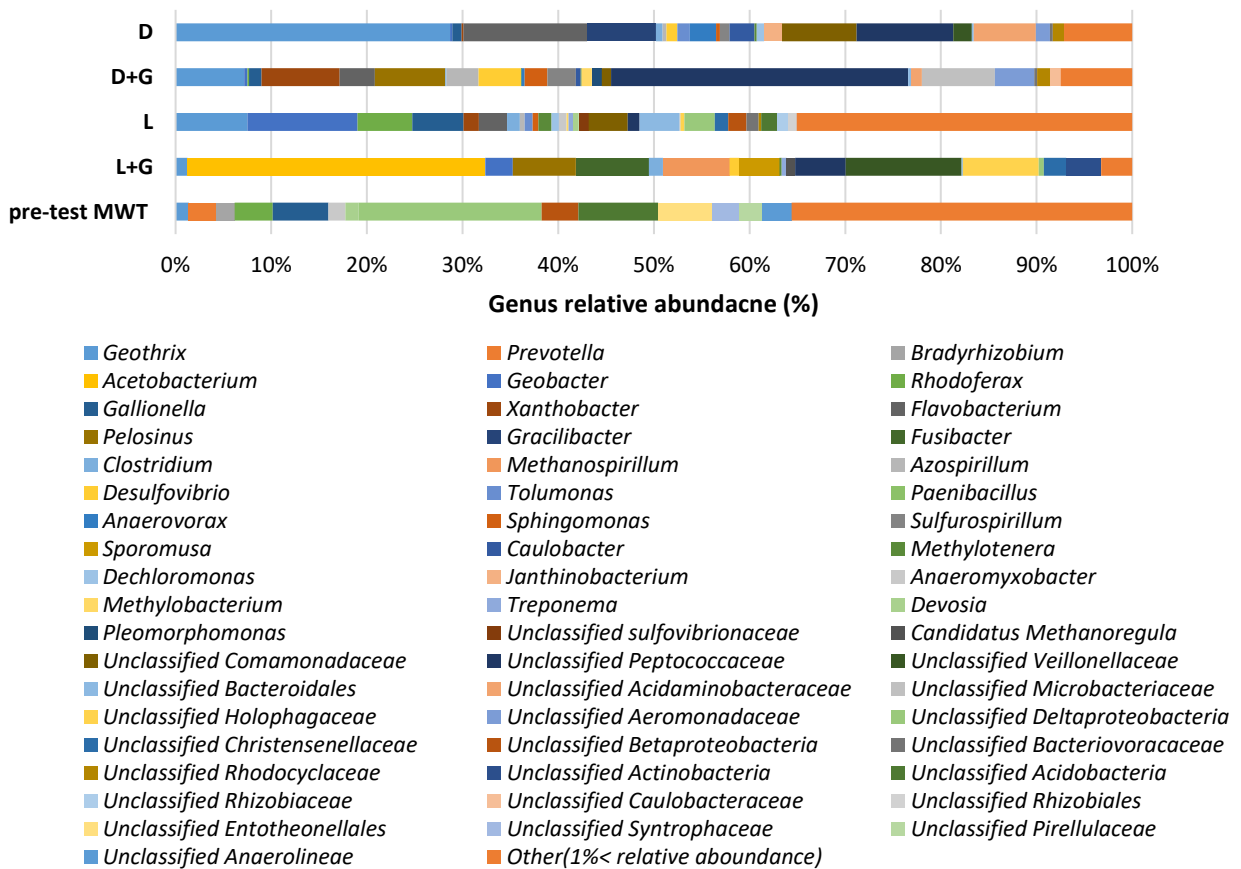


**Figure 5-17 Taxonomic classification of the 16S RNA gene at the genus level in pre-test MWT sludge and post-test MWT.**

## 5.11     Conceptual model

Phase one textile wastewater experiment was the first experiment conducted to distinguish the ability of mine water treatment sludge (MWT) as a substrate to degrade 15 mg/ MO textile wastewater. MWT adsorption capacity was 3.50 mg/g (calculated in chapter four). It was used to estimate the maximum amount of MO removed by adsorption during phase one based on the weight of dried MWT column's substrate. The MWT had a low MO adsorption capacity compared with the literature review studies in Table 2-4. The experiment was run continuously for 170 days to ensure that the amount of MO passed through the column (255 mg) was more than the adsorption capacity of the column's substrate (115 mg MO) see section 5.2. However, TC in pre-test and post-test column substrates in Figure 5-7 confirmed that the sludge had a low TC concentration, and any amount of carbon might adsorb during the experiment was probably degraded. According to that, the MO removal by adsorption can be excluded, and bioremediation was the dominant mechanism for MO removal.

During phase one textile wastewater experiment, the MO decolourisation peaked was about 99 % when additional organic carbon was added while it varied between 66 % to 95 % when MO was the sole carbon source. The highest normalised MO removal rate was about 29 $g/m^3$/day. MO removal efficiency during this experiment was within the range of the reported studies in Table 2-4 while the MO removal rate was not reported in these studies. The flow rate used in this experiment generated 28.7 hrs retention time, which was comparable with the reported studies in Table 2-4. The pH range varied between about 4.5 to 8.3, and the redox potential was between zero to -50 mV. The experiment runs over a temperature range between 15 to 24 °C while the vast majority of the reported literature in Table 2-4 conducted MO removal experiment at a specific temperature. LC-MS and GC-MS spectrum in Figure 5-11 confirmed that MWT indigenous consortia degraded MO without generated aromatic amines. The Spectrophotometer analysis in Figure 5-4 also confirmed this conclusion.

Figure 5-18 presents the hypothesised mechanisms of MO degradation by MWT microorganisms based on LC-MS data. In this mechanism, the MWT microbial consortia probably reduced MO in two steps; first, it utilised azo reductase to reduce azo bond by transfer four electrons from bacterial NADH to cleavage azo dye double bond and generated aromatic amines. In this reaction, azo dye was reduced as an electron acceptor while NADH

represents the electron donor; $NAD^+$ can be regenerated using the available organic carbon generated from MO degradation in reaction B or by metabolised additional organic carbon added as glycerol. Any aromatic amines generated from reaction A were oxidised to simplest MO degradation products in reaction B and during this step, Fe (III) was reduced to Fe (II).
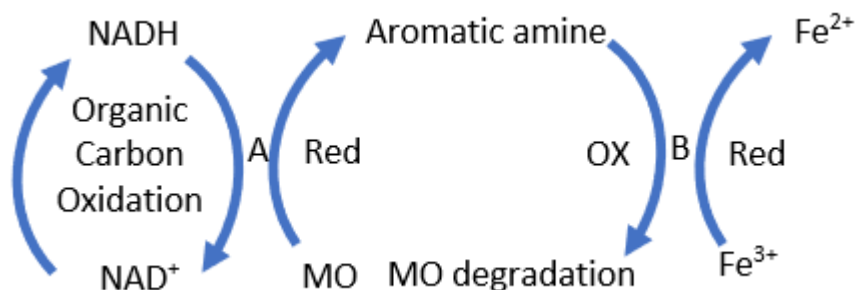


**Figure 5-18 Schematic diagram for MO degradation using iron-reducing microorganism. A: azo dye cleavage, B: degraded aromatic amines where: Ox: oxidation, Red: reduction.**

The next-generation sequencing for post-test MWT sludge highlighted that iron-reducing bacteria as *Geothrix*, *Geobacter* and *Clostridium* were affiliated with other bacterial genera (see section 5.10). The post-test MWT sludge flourished consortium degraded MO as a sole carbon source or an additional carbon source (using glycerol) to simplest compounds. The presence of glycerol as additional organic carbon source accelerated the MO decolourisation as shown in Figure 5-1. *Geobacter* used azo reductase to degrade MO by breakdown the azo bond to generate aromatic amines (Liu et al. 2017b). This finding agreed with other researchers who noticed that azo reductase was responsible for azo dye cleavage to generate aromatic amines (Yoo et al. 2001; Chacko and Subramaniam 2011). Lovley et al. (1993) noticed *Geobacter* coupling aromatic hydrocarbons contaminant oxidation and reduction of Fe (III) to Fe (II).  Du et al. (2015) confirmed that N, N-dimethyl- p-phenylenediamine and 4-aminobenzene sulfonic acid are the aromatic amines generated from MO mineralisation by azo reductase. Due to MWT microbial diversity and because of the unrestricted anaerobic condition, which could stimulate various microbial species. The flourished bacterial species in post-test MWT sludge degraded azo dye double bond and mineralised any aromatic amines generated.

The flourished MWT indigenous consortia were able to mineralise MO as a sole carbon source, which is uncommon behaviour in textile wastewater treatments because all the reported studies in Table 2-4 used additional carbon source to initiate MO biodegradation.

Furthermore, the generated aromatic amines are easy to notice as a drawback in most of the literature in the same table. Microbial pre-acclimatisation did not consider during the conducted experiment whereas it was highly recommended in other studies which were essential to conduct efficient MO degradation (Yu et al. 2011; urali et al. 2013a; Murali et al. 2013b). The diversity of the MWT microbial community is beneficial as it contained bacterial species can degrade azo efficiently by cleavage the azo bond and the aromatic benzene ring as a sole carbon source and without pre-acclimatisation.

.

# Chapter 6 : Phase two textile wastewater results and discussions

## 6.1 Introduction

This chapter presents phase two textile wastewater experiment results. It included a comparison of MO degradation using anaerobic and sequential anaerobic-aerobic reactors and the effects of MO removal by adsorption. A spectrophotometer method was used to determine any aromatic amines generated during MO bioremediation in the column effluents. Furthermore, LC-MS was used to elucidate the MO degradation products included aromatic amines. Different parameters were examined as pH, dissolved oxygen, redox potential, and organic carbon removed. Gene sequencing was used to distinguish any change in mine water treatment sludge (MWT) indigenous genera after treatment compared with the pre-test MWT indigenous microorganisms. A conceptual model was used to describe the MO mineralisation mechanism.

## 6.2 Methyl orange adsorbed by mine water treatment sludge column substrate

In phase two textile wastewater experiment, MWT adsorption capacity might be different from phase one because the wastewater recipe was changed. According to that, another batch experiment was conducted to study the MWT adsorption performance. Mine water sludge sample (MWT) (500 g) was poured in a Pyrex glassware (2 l) and covered with aluminium foil before autoclaved for a 30 min at 121 °C. After autoclaved the sludge sample, it was dried in the oven at 40 °C for 48 hrs as reported by Schwertmann and Cornell (2000). One gram of the dried autoclaved MWT sludge (121 °C for 30 min) was mixed with 100 ml phase two textile wastewater recipe contains 15 mg/l MO under shaking condition (150 rpm) for 20 days. A control sample contained only textile wastewater without adsorbent material was used for monitoring. Samples were withdrawn daily and filtered by 0.45 µm a syringe filter before measured the absorbance using a spectrophotometer at 464 nm. The MO calibration curve was used to calculate the concentration at time t (see section 4.2). Figure 6-1 shows that the amount of MO adsorbed by MWT was quite low under the experiment conditions. The low adsorption was probably because of the high pH of the used textile wastewater. A similar observation was noticed by Namasivayam and Sumithra (2005) during textile wastewater.
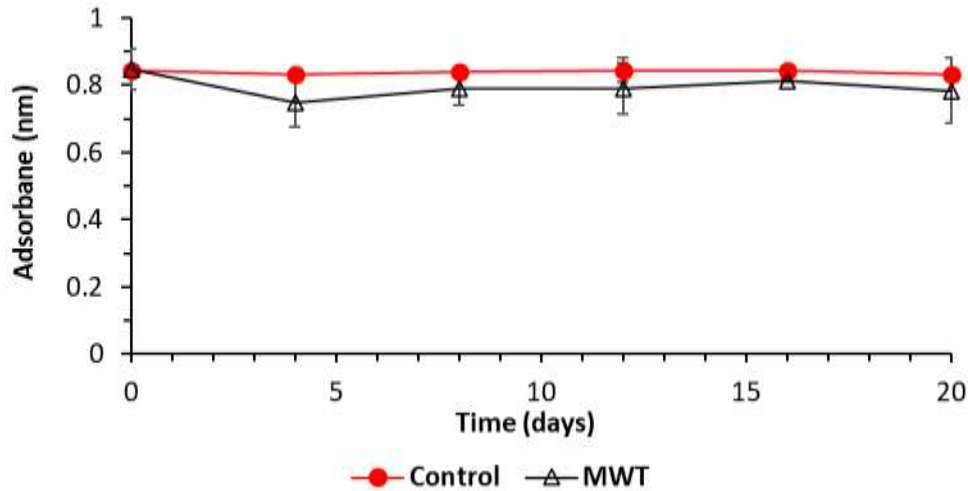
**Figure 6-1 MWT sludge batch experiment to measure the adsorbance with time compared with the control sample contain textile wastewater only.**

## 6.3    Methyl orange decolourisation and colour removal rate

The experiment was set up, as highlighted in section 3.5.2. In phase two textile wastewater experiment, MO was decolourised by anaerobic and sequential anaerobic-aerobic reactors. Figure 6-2A demonstrates that both systems degraded about 97% of the influent MO after four weeks. The MO removal rate was calculated as reported in section 3.10 using Equation 17 see Appendix 2 to clarify. According to that, the dye normalised removal rate was comparable in both reactors, which was about 178 g/m$^3$/day see Figure 6-2 B. According to the literature, it was reported that using sequential anaerobic-aerobic reactors improved azo dye biodegradation, as the aerobic reactor is a complementary process to the anaerobic reactor. The aerobic step degrades aromatic amines which generated during the anaerobic process (Amaral et al. 2014). The experiment runs at 300 ml/day flow rate for each column, this flowrate generated a hydraulic retention time (HRT) equal to two hrs based on the volume of voids in Table 3-1. It was lower than the majority of textile wastewater studies reported in Table 2-4 and Table 2-5, and it was also lower than the HRT in phase one, because the flow rate was raised, and the amount of column substrate was decreased. The MO removal rate in this phase was higher than phase one textile wastewater (see section 5.2). It was probably because the temperature was constant in this phase (25 $^\circ$C). The appropriate retention time has a substantial effect for efficient azo dye degradation

100

(Van Der Zee and Villaverde 2005a; Isık and Sponza 2008). Franca et al. (2015) reported that azo dye could be degraded at eight hrs RT in sequencing sludge batch bioreactor.
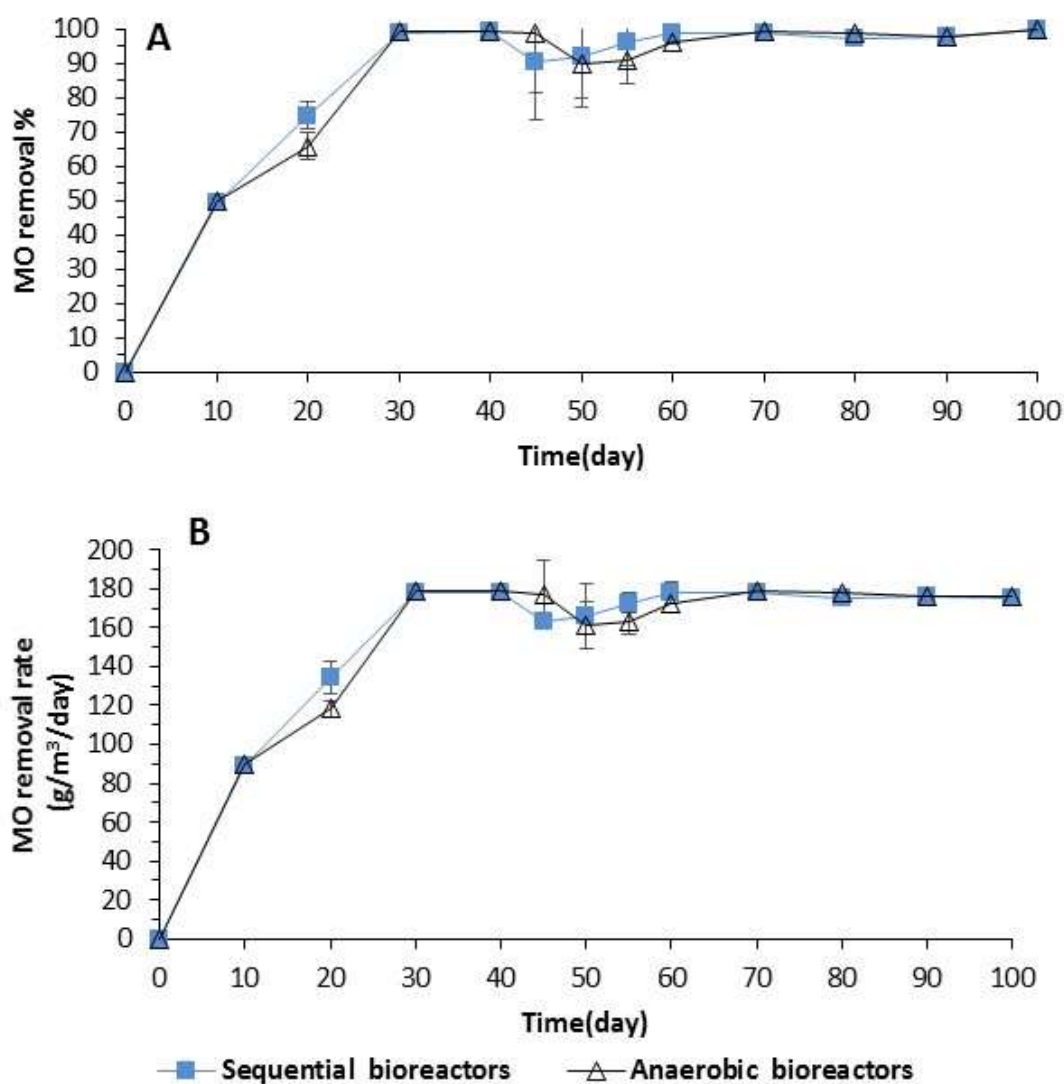


**Figure 6-2 (A) MO removal efficiency, and (B) MO removal rate.**

## 6.4    Aromatic amines detection by spectrophotometer

In phase two textile wastewater experiment, the influent and column effluents were scanned by a spectrophotometer after 100 days of the continuous experiment. They were compared with 4-aminobenzene sulfonic acid (4-ABA) and N,N-dimethyl-p-phenylenediamine (DPD) stock solutions which represented MO aromatic amines degradation standards at 15 mg/l as a concentration for each compound (Haque et al.

2011; Shen et al. 2015). A wide scan range (200 to 700 nm) was used to include the visible and ultraviolet light range. It was used for two purposes, first to detect the decline in MO which cover the visible range, and to highlight any breakdown aromatic amines generated during textile wastewater treatment by anaerobic and sequential anaerobic-aerobic columns which can be detected in the ultraviolet range. Figure 6-3 demonstrates that 300 and 464 nm were the main peaks in the influent textile wastewater in this experiment. The second peak represents the MO, it was almost removed in both sequential anaerobic-aerobic and anaerobic effluents, and the peak at 300 nm could not be identified. However, it was attenuated by about 50%, in column effluents spectrophotometer scan. It can be noticed that there were no new generated aromatic amines peaks in column effluents. It was reported in previous studies, aromatic amine was identified at 250-300 nm wavelength as a new peak (Murali et al. 2013b; Murali et al. 2013a; Amaral et al. 2014). The spectrophotometric scan for phase two textile wastewater effluents highlighted that MWT indigenous consortia decolourised MO without generated generating aromatic amines.
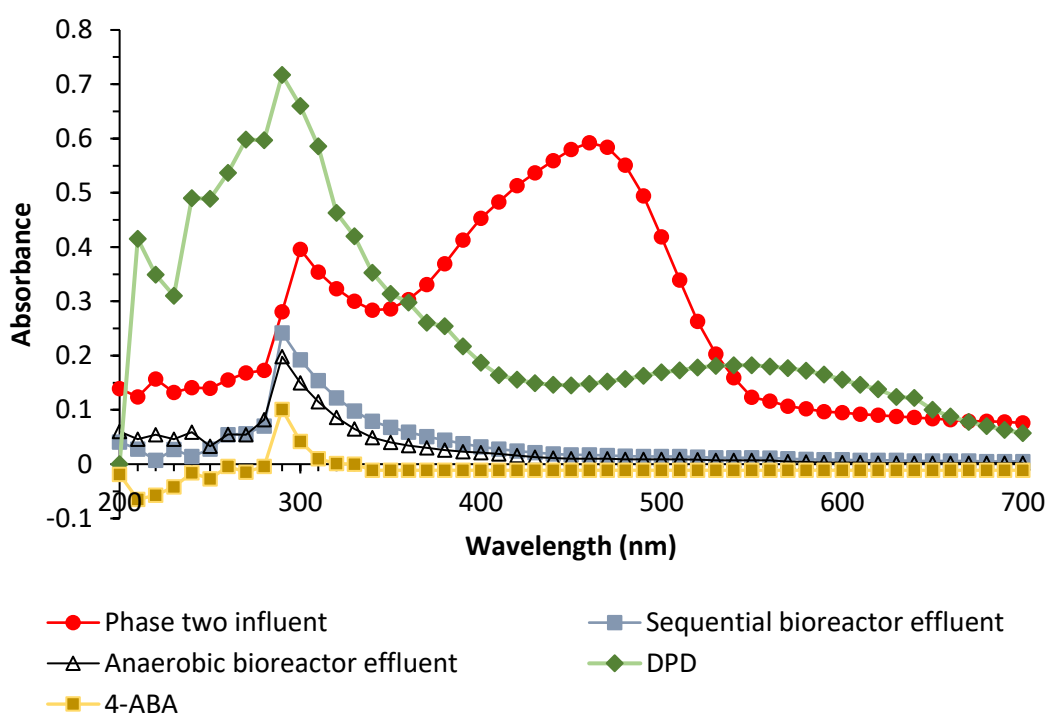


**Figure 6-3 Spectrophotometer scan for phase two textile wastewater influent and effluents after 100 days compared with MO standard degradation products, 4-aminobenzene sulfonic acid (4-ABA) and N, N-dimethyl-p-phenylenediamine (DPD) at 15 mg/l.**

## 6.5    Total carbon removal

Total carbon (TC) was measured in the column effluents during phase two textile wastewater experiment (see section 3.8 for more details). The TC concentration in the influent textile wastewater was $1675 \pm 5$ mg/l. During the first week, about 44 % of the TC was removed by both anaerobic and sequential anaerobic-aerobic columns. In anaerobic columns, TC removed efficiency fluctuated from 22 to 47 % while it was between 25 to 51 % in sequential anaerobic-aerobic columns highlighted in Figure 6-4 A. The normalised total carbon removal rate was also calculated as reported in section 3.10 (see Appendix 2 to clarify). According to that, the highest TC removal rate was about 3000 $g/m^3$/day in both reactors while the lowest value highlighted was 1353, and 1536 $g/m^3$/day in anaerobic, and in sequential anaerobic-aerobic columns respectively see Figure 6-4 B.

It was important to determine the amount of carbon adsorbed in column substrates during the experiment by compared pre-test and post-test samples. Figure 6-4 C shown that TC in pre-test MWT was 1.53 %, and after treatment, it was raised to 6.85 % in post-test MWT that indicated that some of the carbon was adsorbed in MWT sludge during phase two experiment. The amount of carbon removed during phase two experiment varied between 25-50 % of the influent by MWT sludge via the indigenous microorganisms and the performance of both anaerobic and sequential reactors were similar. It was probably because of the inefficient aeration system used in the aerobic reactor, which did not raise the dissolved oxygen concentration to aerobic level to stimulate aerobic microorganisms. The carbon removal rate was not reported in the majority of textile wastewater literature in Table 2-4 and Table 2-5. Nevertheless, García-martínez et al. (2015) highlighted that organic carbon enhanced azo dye biodegradation, and it was noticed that 50 % of TC could be degraded by sequential anaerobic-aerobic bioreactor. O'Neill et al. (2000b) reported that about 77 % of azo dye was decolourised when additional organic carbon was detected in textile wastewater. The additional carbon source is a prerequisite for functional azo dye mineralisation (Anjaneyulu et al. 2005). Microorganism metabolises organic carbon as an electron donor during azo dye mineralisation (Carmen et al. 2010).
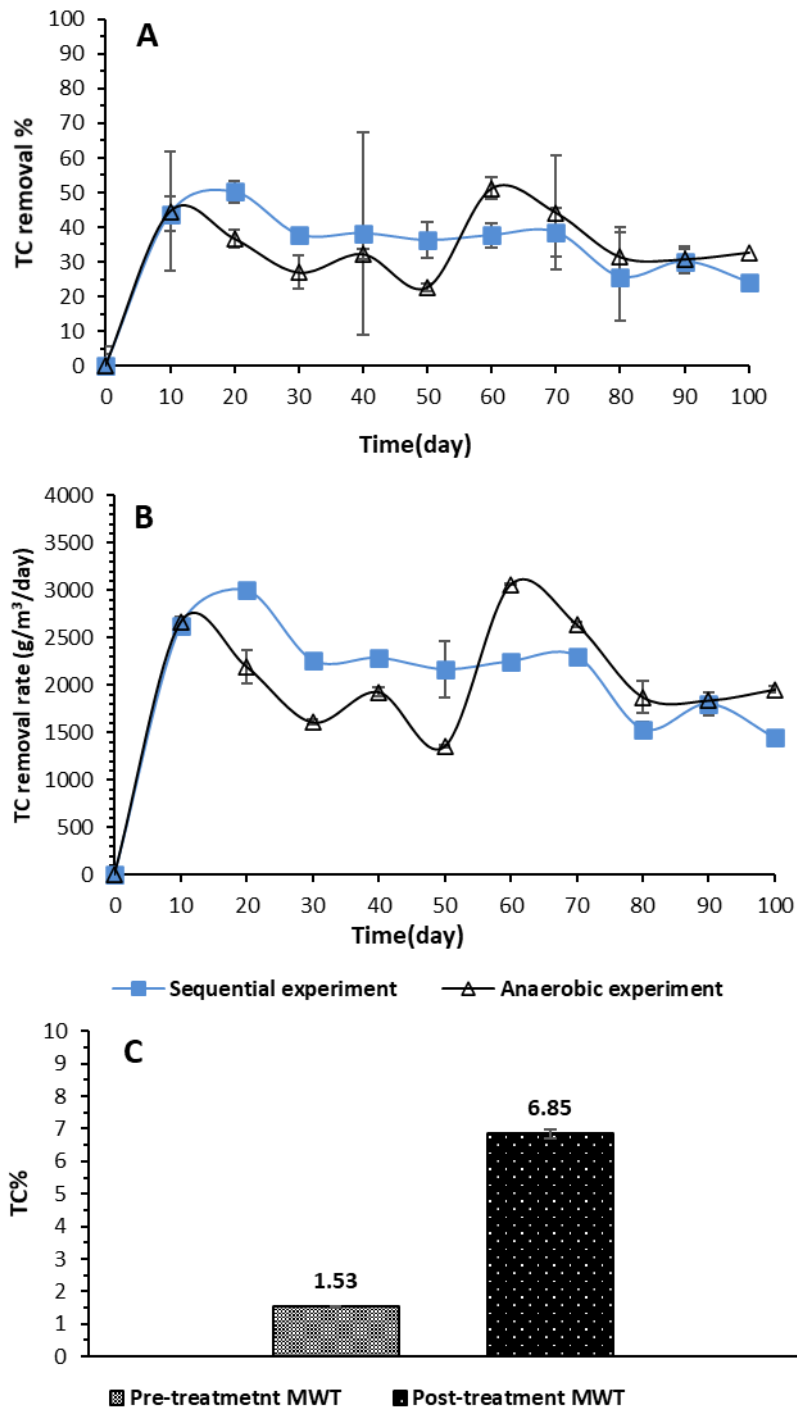
**Figure 6-4 (A)Total carbon removal efficiency, (B) TC removal in the column effluents, and (C) TC concentration in pre-test and post-test MWT sludge.**

## 6.6      Nitrogen removal

Total nitrogen included nitrogen concentration in ammonia, nitrite, and nitrate, which was measured by the methods reported in section 3.8. The normalised total nitrogen removal rate was also monitored during phase two textile wastewater, as shown in Figure 6-5 (A). It was calculated as reported in section 3.10 and using Equation 17. (see Appendix 2 to clarify). In the sequential anaerobic-aerobic reactors, the total nitrogen removal rate dramatically fluctuated with time, 216 $g/m^3/day$ was the highest nitrogen removal rate, which was equal to 12.34 $g/m^2/day$ (as the cross-section area of the column was 4.9 $cm^2$) and 0.71 $g/m^3/day$ was the lowest nitrogen removal rate. Similarly, the highest TN removal rate by anaerobic columns was 127.91 $g/m^3/day$, while the lowest was 7.97 $g/m^3/day$. Ammonia nitrogen concentration ($NH_3$-N) was 60 ± 0.5 mg/l in the influent textile wastewater. The $NH_3$-N removal efficiency fluctuated between 2.5 to 43 % in anaerobic columns, and 1.66 to 47 % in sequential anaerobic-aerobic columns as shown in Figure 6-5 (B), Nitrate concentration in textile wastewater influent was 3.90 mg/l, as shown in Figure 6-5 (C). In sequential anaerobic-aerobic columns, nitrate decreased with time during the first month to 0.97 mg/l then it raised to 8.45 mg/l, by the end of the experiment, it declined gradually to 3.25 mg/l. In anaerobic columns, the lowest nitrate concentration was 2.55 mg/l, and the highest concentration was 11.60 mg/l during the experiment. Figure 6-5 (D) reported the nitrite concentration during MO decolourisation. Nitrite concentration was zero in the influent textile wastewater. During the first-month nitrite concentration increased to 17.50 mg/l in sequential anaerobic-aerobic columns compared with 10.32 mg/l in anaerobic columns, then it dropped to zero again in both column effluents.

Nitrification occurred during azo dye biodegradation when oxygen is available (Xiao et al. 2011). This mechanism probably involved in nitrogen conversion over days 0-20 during phase two textile wastewater experiment, during this time, the dissolved oxygen concentration was high according to Figure 6-11 A. Chen et al. (2003) demonstrated that nitrogen compounds in textile wastewater stimulate azo dye biodegradation. Furthermore, nitrogen compound as nitrite initiates anaerobic ammonium oxidation (Anammox) (Isaka et al. 2007). However, Liu et al. (2016) argued that nitrite might obstruct dye biodegradation. According to the reported information, there might be an influence between the MO decolourisation in this phase

and the nitrogen concentration, which was probably the reason for low decolourisation as noticed in Figure 6-2 during the first month due to high nitrite concentration (Figure 6-5 D). During nitrification, nitrite was generated. Nitrogen bacteria are affected by dye degradation products which might be the reason for fluctuated the TN removal rate with time (Ganesh and Boardman 1994a). The abundance of iron oxides and nitrogen compounds is a favourable environment for anaerobic ammonium oxidation coupled to Fe (III) reduction, which becomes recently known as Feammox. In this mechanism, iron oxides reacted with ammonium to remove nitrogen and generate nitrogen or nitrite as shown in Equations 22 and 23 (Yang et al. 2012)

$$3Fe(OH)_3 + 5H^+ + NH_4^+ \rightarrow 3Fe^{2+} + 9H_2O + 0.5N_2 \hspace{2cm} \text{(Equation 22)}$$

$$6Fe(OH)_3 + 10H^+ + NH_4^+ \rightarrow 36Fe^{2+} + 16H_2O + NO_2^- \hspace{2cm} \text{(Equation 23)}$$
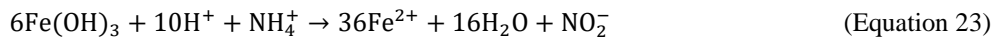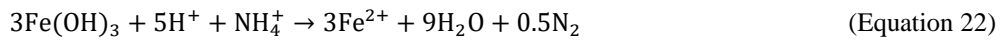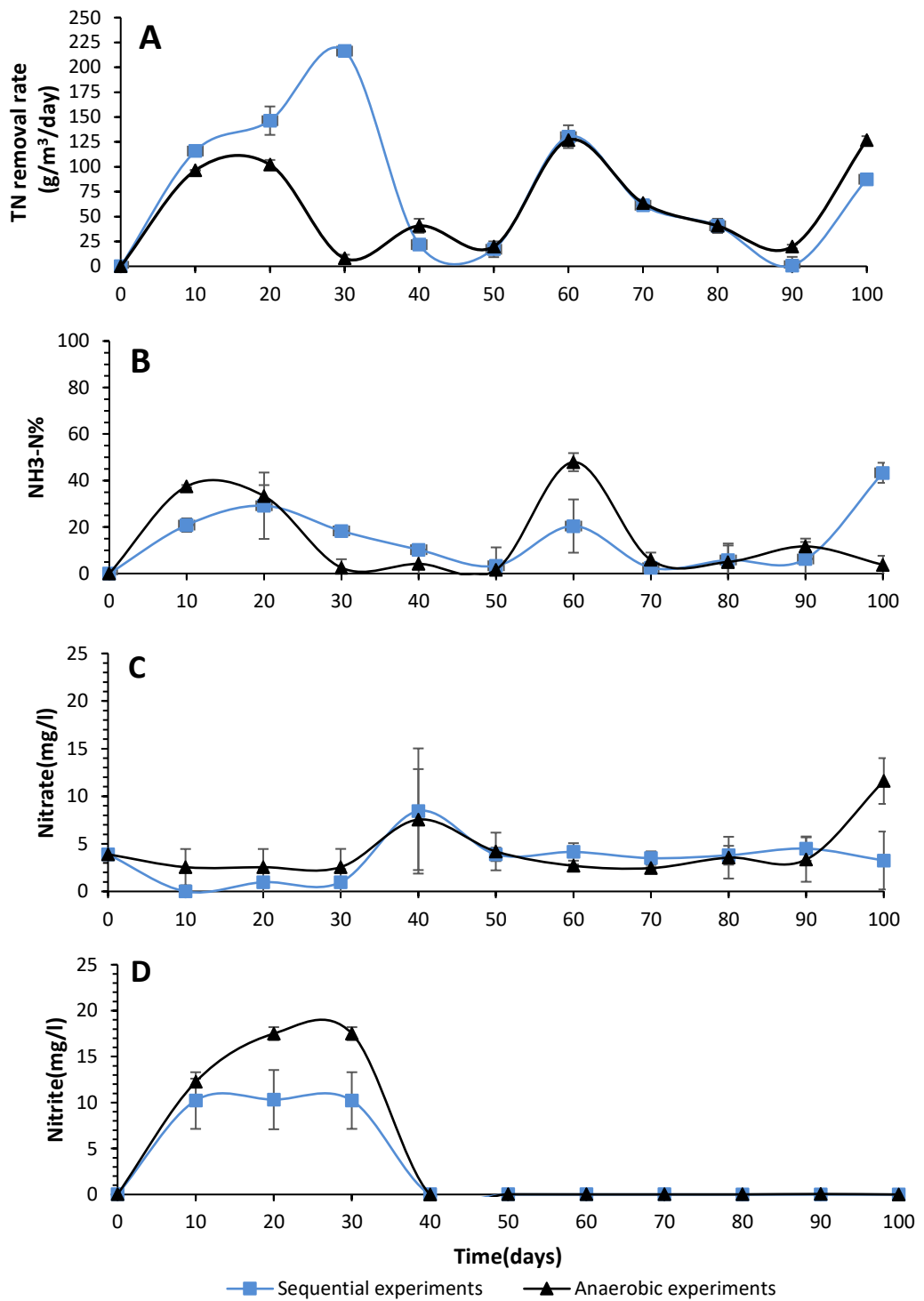
**Figure 6-5 Nitrogen concentration during phase two textile wastewater, (A) the total nitrogen removal rate, (B) ammonia- nitrogen removal efficiency, (C) nitrate concentration in column effluents and (D) nitrite concentration in column effluents.**

## 6.7 Total iron and ferrous iron concentrations

Total iron and ferrous concentrations were measured in the influent and column effluents, as reported in section 3.8. Figure 6-6 A shown that the iron concentration in the influent textile wastewater was 0.82 mg/l. In the sequential anaerobic-aerobic reactor effluents, the highest Fe concentration was 5.08 mg/l compared with 4.16 mg/l in the anaerobic reactor. Ferrous concentration in sequential anaerobic-aerobic effluents was below 1mg/l during the first 40 days, and then it raised gradually to 2.49 mg/l. In anaerobic columns, ferrous concentration was lower than 0.50 mg/l during the first 70 days, then it increased gradually to 1.80 mg/l, as highlighted in Figure 6-6 B. Ferrous iron generated during phase two textile wastewater experiment could be an indication for iron-reducing bacteria activity. this species plays a vital role in azo dye biodegradation (Lier et al. 2008). Albuquerque et al. (2005) reported that at iron reduction conditions, Fe (III) reduced to Fe (II), and the latter reacted with other elements as sulphur to generate FeS. The generated FeS could be precipitated in column substrates. The mentioned Fe (II) precipitation reaction could be the reasonable justification for low Fe (II) generated in column effluents, and this might be confirmed by noticed the sulphate concentration was decline during phase two experiment as shown in Figure 6-7. Van der Zee et al. (2001) emphasised that biological iron oxidation-reduction mechanism could support azo dye biodegradation as an electron shuttle. This finding agreed with Diniz and Lopes (2002), who found ferrous raised azo dye decolourisation rate.
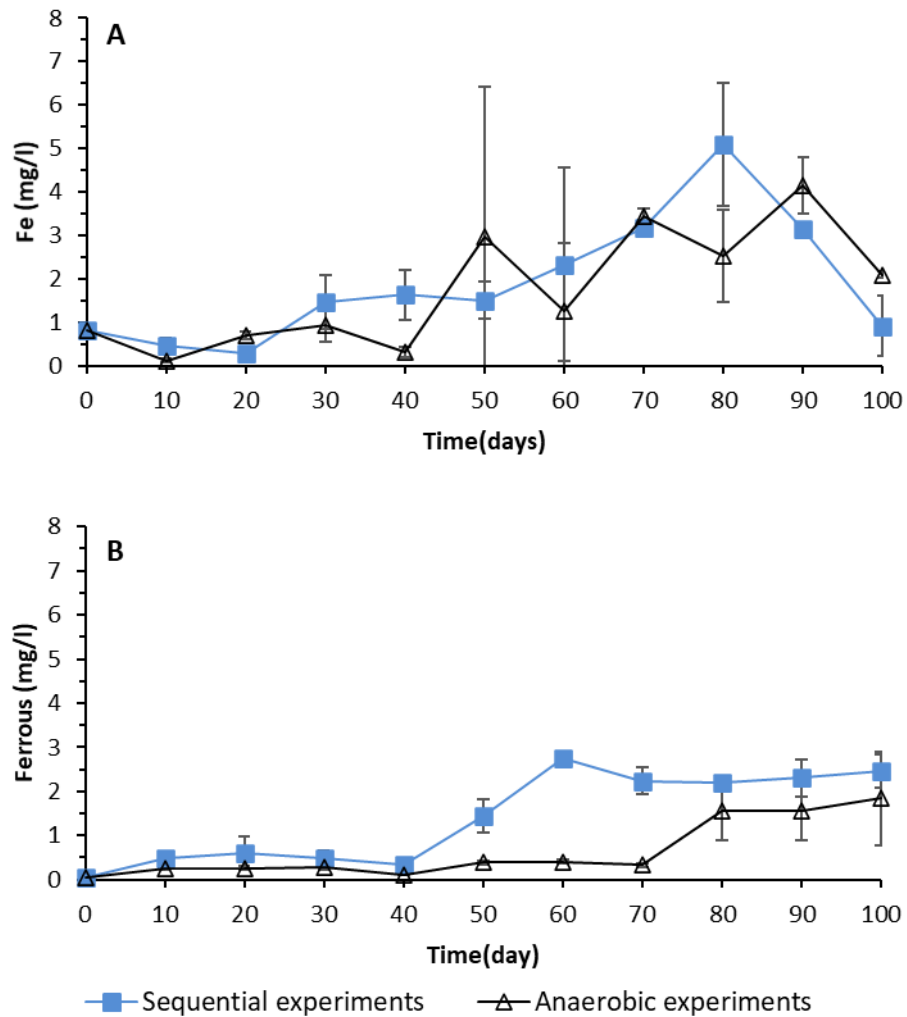
**Figure 6-6 (A) Iron concentration in column effluents (the influent concentration was 0.82 mg/l), (B) Ferrous concentration in the column effluents (the influent was under detection range).**

## 6.8    Sulphate concentration

Sulphate was measured according to the procedure reported in section 3.8. Sulphate concentration in the influent textile wastewater was 200 mg/l, as shown in Figure 6-7. In the anaerobic columns, sulphate concentration levelled off during the first month, after this point, it dropped to about 50 %, and the lowest concentration was 89 mg/l. In the sequential anaerobic-aerobic reactor, sulphate concentration declined during the first 10 days to 178 mg/l. The general trendline was similar to the anaerobic reactor, and it dropped to 90 mg/l as the minimum sulphate concentration. Sulphate-reducing bacteria (SRB) were probably involved in sulphate concentration decline during phase

two textile wastewater experiment. Comeau et al. (2016) found that SRB anaerobically mineralises organic contaminants. Ganesh and Boardman (1994a) reported that high sulphate concentration could inhibit azo dye colour removal. This conclusion was agreed with the current experimental data as it was noticed that MO decolourisation was low during the first month, as shown in Figure 6-2 compared with high sulphate concentration during the same period Figure 6-7. SRB plays an essential role in azo dye biodegradation; it fermented organic carbon and reduced sulphate to sulphide (Manu and Chaudhari 2002b). SRB mineralised organic carbon as starch, and it also decreased environment redox potential (Kudlich et al. 1996; Diniz and Lopes 2002). SRB might provide an electron equivalent to reduce azo bond (Zeng et al. 2017). Thuar et al. (1977) reported that the affinity of sulphate to act as an electron acceptor and reduced to sulphide is weaker than the azo bond due to the high redox potential value of the latter. Yoo, Libra (2000) assumed that SRB reduced sulphate to sulphide as a redox mediator (electron shuttle) during azo dye biodegradation. Amaral et al. (2014) reported that about 50% of sulphate could be removed during anaerobic textile wastewater. Sulphide reacts with metal, and sulphur reacts with oxygen to regenerate sulphate. Amaral et al. (2014) noticed that SRB synergetic with other indigenous species to cleavage aromatic amines (Togo et al. 2008). Plumb et al. (2001) found that during azo dye anaerobic biodegradation SRB bacteria was one of the effective genera.
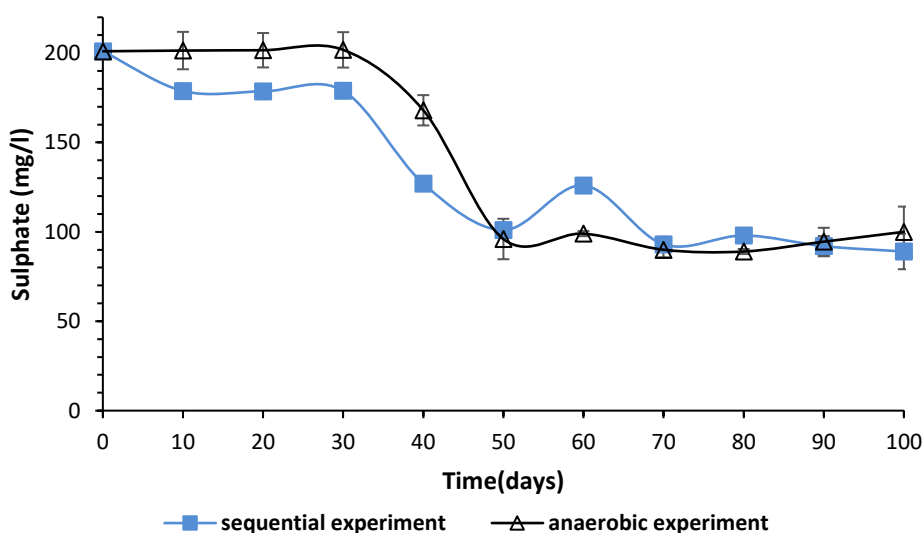


**Figure 6-7 Sulphate concentration during phase two textile wastewater experiment.**

## 6.9 MO biodegradation fragments by LC-MS

Liquid chromatography-mass spectrometry (LC-MS) was used to analyse the influent and column effluents for phase two textile wastewater experiment after 100 days to detect MO degradation products (details reported in section 3.12). LC-MS detection range based on extended retention time (0-22) min. Furthermore, Figure 6-8 A shown that MO was highlighted at retention time (RT) equal to 16.8 min, 17.6 min and 20 min. Sequential anaerobic-aerobic and anaerobic effluents shared similar MO degradation products at RT 3 min and 13.8 min to 14.6 min. Nevertheless, the sequential anaerobic-aerobic effluents generated a unique compound at RT 7 min while anaerobic generated a different peak at RT (8-8.5) min, as demonstrates in Figure 6-8 B, and C. ChemDraw software was beneficial to draw the chemical structures using the m/z ratio obtained from LC-MS spectrum. It interpreted LC-MS peaks into a chemical structure, as shown in Table 6-1. The MO degradation pathway in both sequential anaerobic-aerobic and anaerobic MO in Figure 6-9 and Figure 6-10 confirmed that MWT sludge via the indigenous consortia was efficiently mineralised MO azo dye by degraded the azo bond and breakdown the benzene aromatic ring. This finding confirmed that azo dye can be mineralised without generated aromatic amines using an aerobic column via MWT indigenous microorganisms and the additional aerobic column was ineffective, the reason beyond that might because the diversity of indigenous MWT microorganism, which could include iron-reducing bacteria and other, affiliated genera. Furthermore, an unrestricted anaerobic condition in the utilised anaerobic reactor could enable more diverse microorganism species to flourished during MO mineralisation. However, Ganesh and Boardman (1994a) reported, it is essential to combine aerobic degradation unit after the anaerobic bioreactor to degrade aromatic amines generated during azo dye biodegradation. In addition, Pandey et al. (2007a) who mentioned that aromatic amines required further aerobic biodegradation to make it low toxic chemicals. The LC-MS finding is additional conformation for the ability of MWT to mineralise MO without generated aromatic amines.
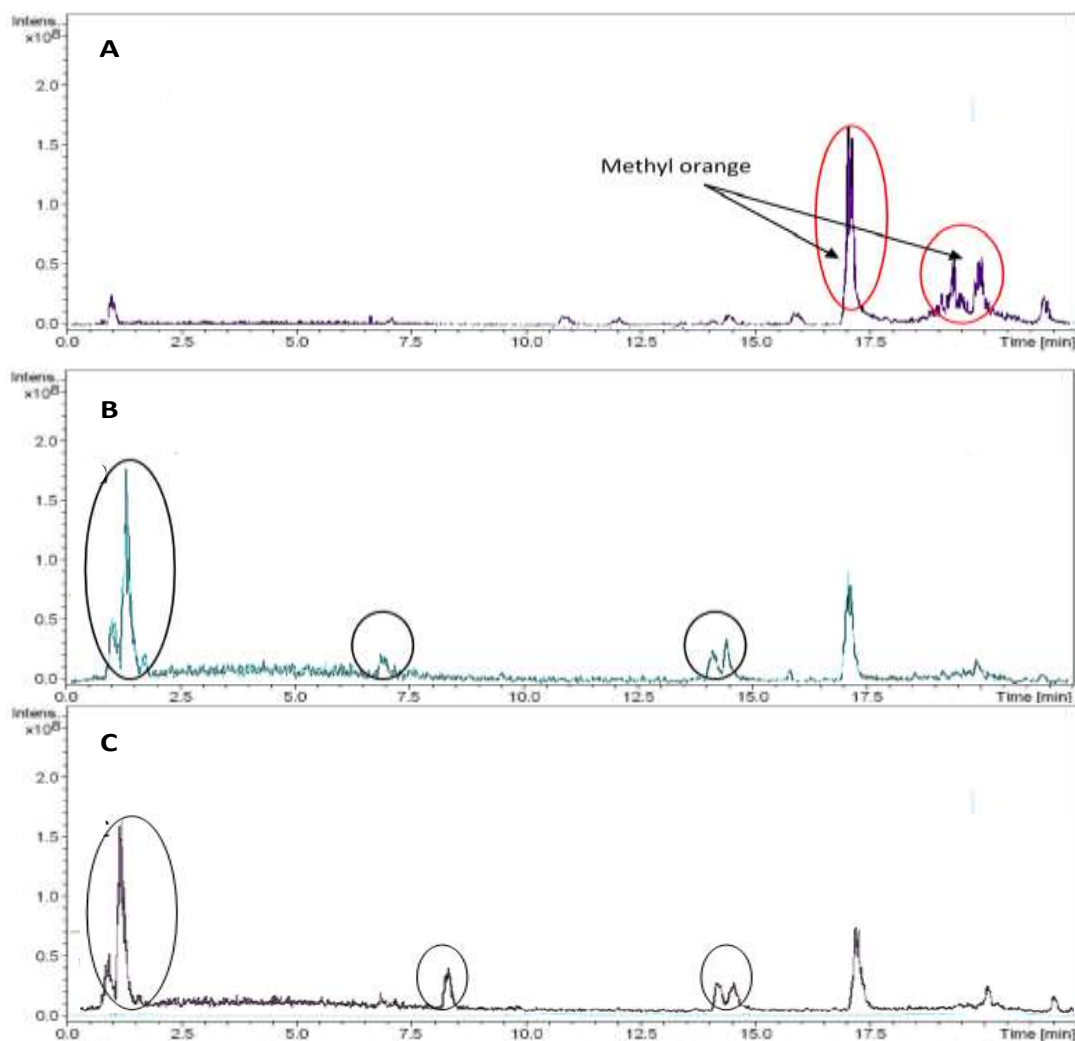
**Figure 6-8 The LC-MS spectrum at a retention time range 0 to 22 min,(A) the influent synthetic wastewater, (B) the sequential anaerobic-aerobic reactor, and (C) the anaerobic reactor.**
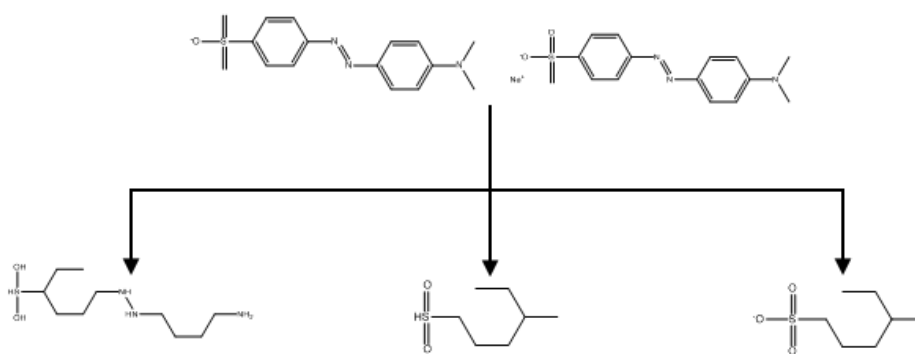


**Figure 6-9 MO degradation products by the sequential anaerobic-aerobic reactors.**

112
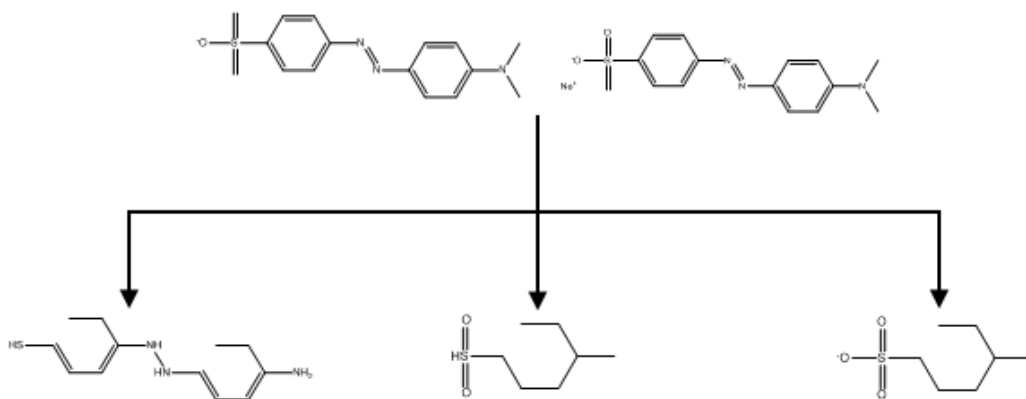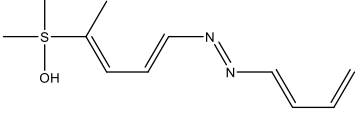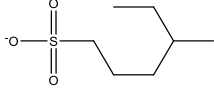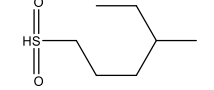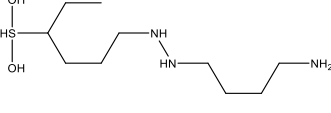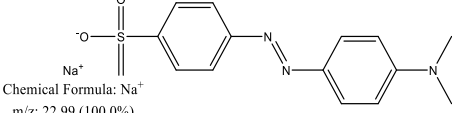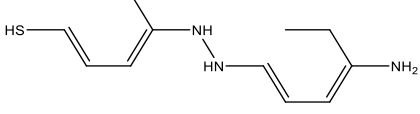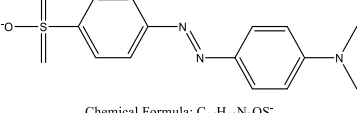
**Figure 6-10 MO degradation products by the anaerobic reactors.**

**Table 6-1 MO degradation fragments according to ChemDraw software.**

| RT(min) | m/z | Structure |
|---|---|---|
| **1** | 226.8 |  Chemical Formula: $C_{11}H_{18}N_2OS$ <br> m/z: 226.11 (100.0%), 227.12 (11.9%), 228.11 (4.5%) |
| **1.3** | 179 |  Chemical Formula: $C_7H_{15}O_3S^-$ <br> Exact Mass: 179.07 <br> m/z: 179.07 (100.0%), 180.08 (7.6%), 181.07 (4.5%) |
| **1.3** | 164 |  Chemical Formula: $C_7H_{16}O_2S$ <br> Exact Mass: 164.09 <br> m/z: 164.09 (100.0%), 165.09 (7.6%), 166.08 (4.5%) |
| **7** | 253 |  Chemical Formula: $C_{10}H_{27}N_3O_2S$ <br> m/z: 253.18 (100.0%), 254.19 (10.8%), 255.18 (4.5%), 254.18 (1.1%) |
| **8-8.5** | 325.1 |  Chemical Formula: $Na^+$ <br> m/z: 22.99 (100.0%) <br> Chemical Formula: $C_{15}H_{16}N_3O_2S^-$ <br> m/z: 302.10 (100.0%), 303.10 (16.2%), 304.09 (4.5%), 304.10 (1.2%), 303.09 (1.1%) |
| **13.8-14.6** | 239.1 |  Chemical Formula: $C_{12}H_{21}N_3S$ <br> m/z: 239.15 (100.0%), 240.15 (13.0%), 241.14 (4.5%), 240.14 (1.1%) |
| **16.8-17.6** | 301 |  Chemical Formula: $C_{16}H_{18}N_3OS^-$ <br> m/z: 300.12 (100.0%), 301.12 (17.3%), 302.11 (4.5%), 302.12 (1.4%), 301.11 (1.1%) |

## 6.10     Experiment parameters

The experiment parameters were measured according to section 3.8. Dissolved oxygen (DO) concentration in the influent textile wastewater was $3.50 \pm 5$ mg/l, as shown in Figure 6-11**A**. After 20 days, it was dramatically decreased to about zero in both column effluents. The low DO concentration in the sequential anaerobic-aerobic reactor emphasised, that the spiral dripping tube system was an impractical aeration technique because it was unable to raise the oxygen concentration to aerobic level. According to dissolved oxygen concentrations in both column effluents, the environment inside the anaerobic reactor and sequential anaerobic-aerobic reactor was probably the anaerobic condition, and this could be confirmed by microbiology evidence in 6.12. Ekici et al. (2001) noticed that oxygen could supress in anaerobic bacteria enzymes.

The influent pH for textile wastewater was about 10. It was within range of real textile wastewater pH (Sandhya et al. 2008; Igor et al. 2010). The pH of the anaerobic and sequential anaerobic-aerobic effluents was gradually declined with time to about 7, as shown in Figure 6-11 (B). Singh and Arora (2011) found that azo dye adsorption is related to pH, and the adsorption of MO (anionic dye) decreased at alkaline pH. It might be another reason for low MWT adsorption capacity. The presence of organic carbons as starch in textile wastewater could decrease the pH solution because it degraded to acetic, propionic and butyric acids during azo dye degradation (Amaral et al. 2014). It was probably the reason for decreased the pH during MO mineralisation. Chen et al. (2003) reported that pH range 6.5-10 was convenient for textile wastewater treatment. Anaerobic consortia flourished at neutral to slightly acidic pH during the azo dye biodegradation (Manu and Chaudhari 2002b). Nevertheless, during phase two textile wastewater experiment, MO was efficiently decolourised within neutral to alkaline pH range. This pH range was similar to the reported literature in Table 2-5.

The oxidation-reduction potential (ORP) was demonstrated, as shown in Figure 6-11 (C). It was correlated to SHE by added 200 mV to the recorded ORP measurement**.** The influent textile wastewater ORP was $-122 \pm 10$ mV while MO decolourisation was conducted at ORP range between -50 mV to -180 mV. The reported ORP range was appropriate for MO microbial mineralisation. Georgiou et al. (2004), who reported that textile wastewater was degraded at a redox potential between -270 mV to -360 mV.

Knapp et al. (2000) demonstrated that negative ORP is intrinsic to flourish azo dye decolourisation. Manu and Chaudhari (2003) asserted that during textile wastewater by the anaerobic reactor, ORP range was between -66 mV to -290 mV. Beydilli et al. (1998) found that anaerobic consortia contributed to reducing the environment redox potential.
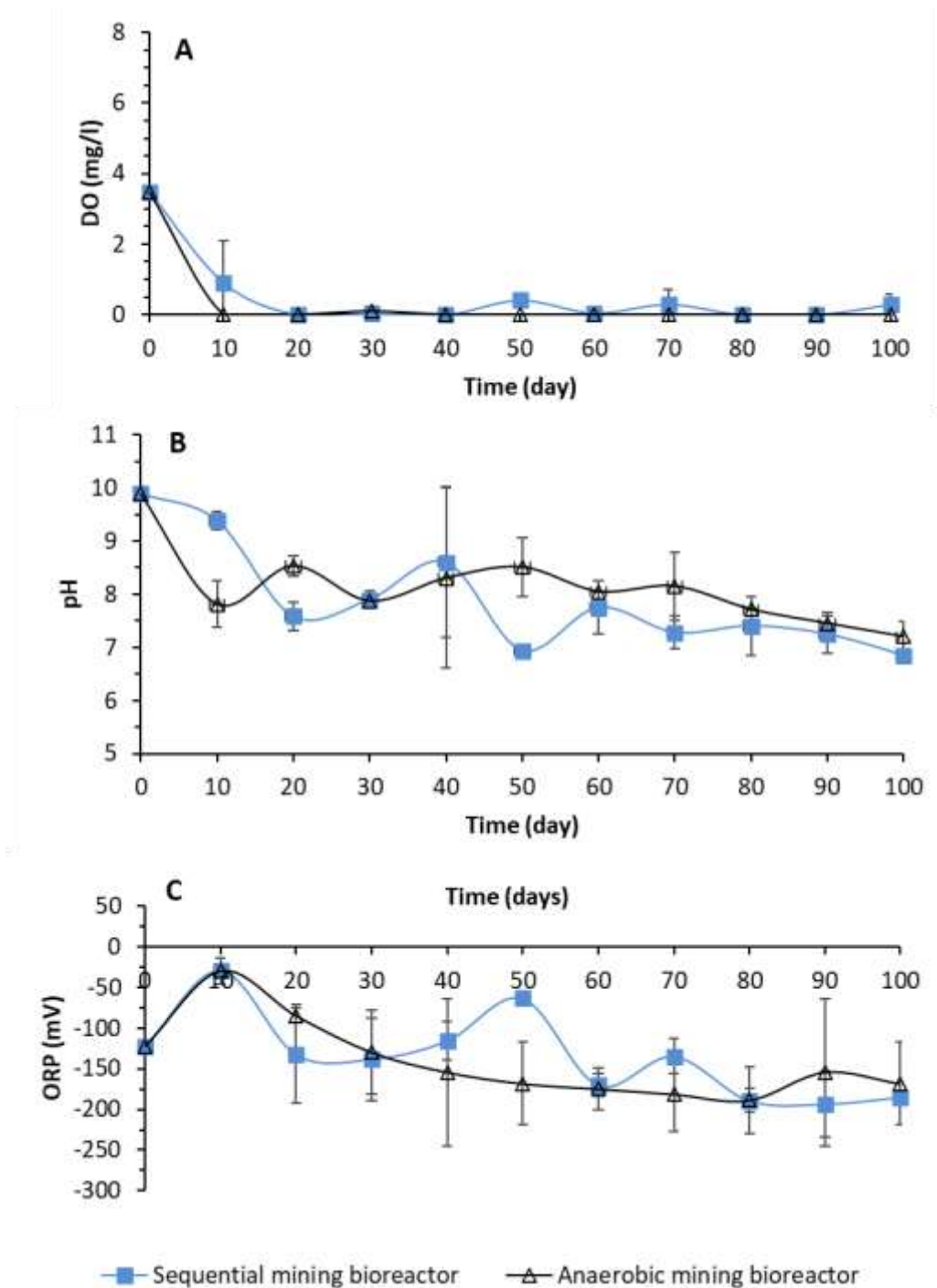


**Figure 6-11 Phase two textile column effluents parameters, (A) dissolved oxygen concentration, (B) pH, and (C) redox potential.**

## 6.11    Parameters correlation for phase two experiment

IBM SPSS statistic software (version 20) was used to determine the correlations between phase two parameters by bivariate correlation analysis. Spearman's rho was used because experiment parameters were not normally distributed ($p < 0.05$). The statistical analysis highlighted that there was a significant negative correlation between MO removal rate and pH in both anaerobic and sequential anaerobic-aerobic reactors with -0.81 and -0.75 correlation coefficients. Statistically, no correlation was highlighted between MO removal rate and TC removal rate in both reactors. While a significant positive correlation was found between TC removal rate and TN removal rate in sequential anaerobic-aerobic columns with 0.88 correlation coefficient, and no correlation was found in the anaerobic reactor. There was no statistical correlation between MO removal rate and ferrous concentration and between TC, TN removal rate and pH in this experiment.

## 6.12    Microbial community changes in pre-test and post-test MWT column substrates

The next-generation sequencing was used to distinguish which bacterial species flourished in MWT in both anaerobic and aerobic column substrates compared with pre-test MWT. (see procedure reported in section 3.14). In pre-test MWT, bacteria were the dominant microorganisms with 17 phyla while archaea consisted only 0.59 % of the relative abundance. In post-test MWT in both aerobic and anaerobic MWT column substrates, bacterial diversity decreased to 5 phyla as highlights in Figure 6-12. *Proteobacteria* (61.24 %) was the highest phylum in pre-test MWT. Thus, it was marginally declined in anaerobic columns to 53.88 %, while it raised to 77.60 % in aerobic columns. *Firmicutes* was the second-highest bacterium phyla in anaerobic (34.24 %) and anaerobic (12.52 %) columns compared with only 0.42 % in pre-test MWT sludge. *Bacteroidetes* was detected at 5.56 %, 7.00 % and 7.92 % in pre-test MWT sludge, aerobic, and anaerobic samples, respectively. *Actinobacteria* declined from 3.09 % in pre-test MWT sludge to 1.94 % in aerobic, and it was distinguished at 3.92 % in anaerobic columns.

The identified bacterial genera in the pre and post-test MWT is shown in Figure 6-13. In pre-test MWT sludge the high relative abundance genera (1%> relative abundance) include *Gallionella* (5.72 %), *Rhodoferax* (4.00 %), *Prevotella* (2.86 %), *Bradyrhizobium* (1.91 %), *Anaeromyxobacter* (1.77 %), *Geothrix* (1.39 %), and *Devosia* (1.39 %). These genera were declined under the detection range after MO bioremediation, as it did not tolerate the textile wastewater harsh environment.

In anaerobic post-test MWT, the dominance taxon (relative abundance >1%) was identified as *Proteobacteria* genera. It included *Citrobacter* (12.88 %), *Enterococcus* (10.92 %), *Sporomusa* (6.65 %), *Dysgonomonas* (4.19 %) and *Dietzia* (3.37 %). Additionally, *Exiguobacterium* (4.80 %), and *Acetobacterium* (1.42 %) were represented the *Firmicutes* genera. In aerobic post-test MWT, the high abundance genera are *Ochrobactrum* (23.44 %), *Brevundimonas* (13.83 %) *Proteiniclasticum* (6.06 %), *Citrobacter* (2.70 %), *Sporomusa* (1.50 %), *Dysgonomonas* (1.48 %), and *Achromobacter* (1.64 %).

*Proteobacteria* and *Firmicutes* were the flourished bacterial phyla in post-test MWT in both anaerobic and aerobic MWT sludge. These phyla were effective in MO mineralisation as it included intrinsic bacterial species which remediated MO to the simplest compounds (see Figure 6-9 and Figure 6-10). Plumb et al. (2001) reported that *Proteobacteria* and *Firmicutes* were the main phylogenetic bacterial detected during azo dye biodegradation. *Ochrobactrum* was one of the dominances *Proteobacteria* species during MO biodegradation. It flourished in the aerobic post-test MWT sludge. It acclimatised with other species as *Brevundimonas, Proteiniclasticum* and *Citrobacter* to degrade MO by cleavage the azo bond and mineralised the aromatic amines. *Ochrobactrum* was isolated from mineral contaminated soil (Pandey et al. 2010; Keharia 2012). Khan et al. (2014a) highlighted *Ochrobactrum* was synergetic with other species as *Citrobacter* to decolourise azo dye. *Ochrobactrum is* classified as a facultative anaerobic bacteria, it can be found in various aquatic sediments, and it reduces iron while fermented organic carbon (Kim et al. 2005). Zhu et al. (2018b) mentioned that *Proteiniclasticum* mineralised MO and the generated aromatic amines. This could be the reason for not detection aromatic amines in column effluent during MO mineralisation by MWT sludge. *Citrobacter*, *Enterococcus*, *Sporomusa* and *Dysgonomonas* where the dominance flourished genera in anaerobic MWT columns.

These genera mineralised MO by cleavage the azo bond and the aromatic benzene ring. *Citrobacter* and *Enterococcus* were the effective bacterial species during azo dye biodegradation (Khan et al. 2014a). *Citrobacter* was an efficient bacterial genus during MO biodegradation. It decolourised MO and the intermediate degradation products (Chung et al. 1978; Wang et al. 2014). Li et al. (2011) demonstrated that *Enterococcus* synergetic with other iron-reducing bacteria to reduce Fe (III) to Fe (II). It degraded azo dyes and the generated aromatic amines (Chen et al. 2004; Bafana et al. 2009). The highlighted bacterial genera in post-test column sludge in both aerobic and anaerobic MWT sludge efficiently degraded MO during phase two textile wastewater without generated aromatic amines.
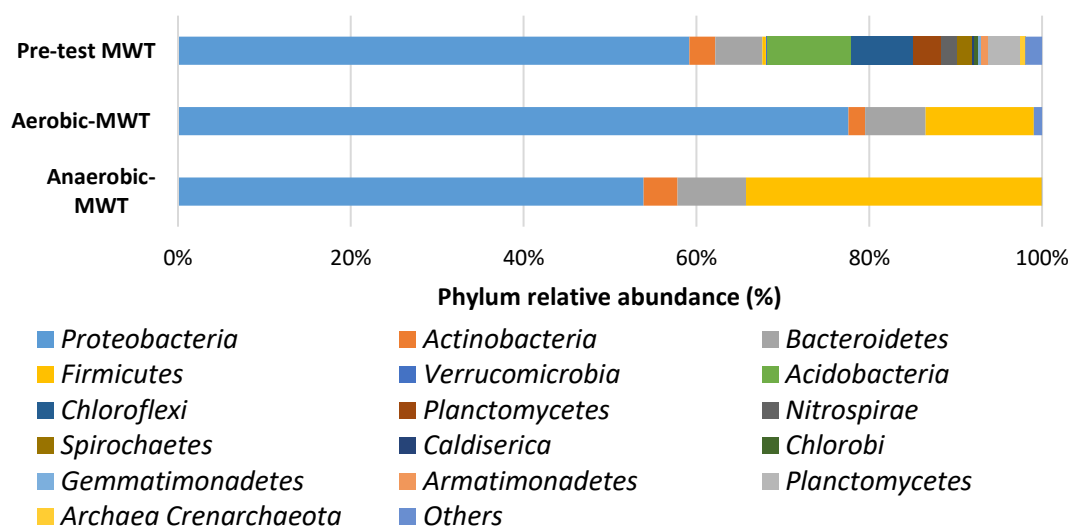


**Figure 6-12 Taxonomic classification of 16S RNA gene at the phylum level for pre-test and post-test (aerobic and anaerobic) MWT.**
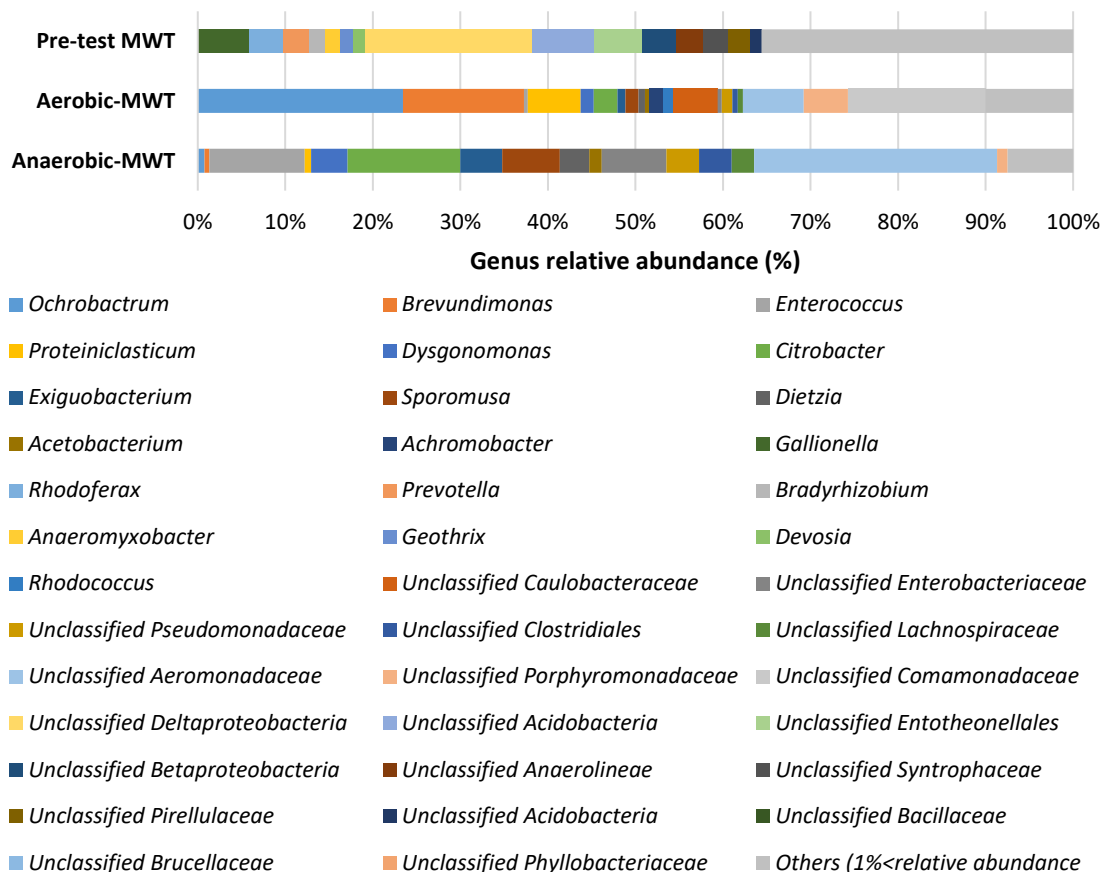
**Figure 6-13 Taxonomic classification of 16S RNA gene at the genus level for pre-test and post-test (aerobic and anaerobic) MWT.**

## 6.13    Conceptual model

In phase two textile wastewater experiment, mine water treatment sludge (MWT) was the column substrates to degrade textile wastewater. The amount of MWT media in each column was decreased to 28 g wet sludge compared with 128 g in phase one while the flowrate was increased for practical reasons, as explained in section 3.2. The textile wastewater recipe becomes more complicated (similar to real textile wastewater recipe) than what was in chapter five, as it contained more chemicals to determine the microorganism tolerance. However, MO, at 15 mg/l still represented the azo textile dye. The MWT adsorption for MO was declined based on experimental conditions, as highlighted in Figure 6.1. In this experiment, MO was degraded by anaerobic and sequential anaerobic-aerobic reactor for comparison. MO decolourisation was 97 % by both anaerobic and sequential anaerobic-aerobic reactor, and dye removal rate was

about 178 g/m$^3$/day by both reactors. Dye removal rate did not report in the majority of the textile wastewater studies in Table 2-4 and Table 2-4. Nevertheless, MO removal rate in this experiment provided information to understand the system capacity. The highest normalised TC and TN removal rates were 3000 g/m$^3$/day and 216 g/m$^3$/day, respectively. The nitrogen removal rate was not reported in textile wastewater literature (see Table 2-4) However, the detected nitrogen removal rate in phase two was competitive with the nitrogen removal rate in municipal wastewater literature (see Table 2-8). The temperature was maintained at 25 °C, pH was between 7 to 10 during the experiment and ORP was between -50 mV to -180 mV. The flow rate used in this experiment generated 2 hrs RT which was lower than what was reported in other studies (see Table 2-4). The flourished iron-reducing bacteria and other genera in post-test MWT sludge (see Figure 6-13) degraded MO without generated aromatic amine as confirmed by the spectrophotometer scan (Figure 6-3). These species degraded azo dye double bond and the aromatic hydrocarbon ring without generated aromatic amines according to LC-MS spectrum and ChemDraw software (Figure 6-9 and Figure 6-10).

Figure 6-14 highlighted the expected MO mineralisation mechanism based on LC-MS data. In this mechanism, MO was mineralised by two steps. In the first step, MO azo bond was reduced by azo reductase to generate aromatic amines (reaction A). The bacterial NADH was the electron donor for this step. It was regenerated by metabolised organic carbon compounds as starch or MO degradation products. In the second step, the generated aromatic amines were oxidised as electron donors by cleavage the aromatic benzene ring to generate MO degradation products ( reaction B) and Fe (III) was reduced to Fe (II) as electron acceptors. Anaerobic ammonium oxidation at iron-reducing condition (Feammox) might be the main mechanism for nitrogen removal during this experiment. In this mechanism, ammonium anaerobically oxidised to nitrogen, nitrite and nitrate, and Fe (III) reduced to Fe (II) (reaction C). Other nitrogen mechanisms could also present as anaerobic ammonium oxidation (Anammox) because of the MWT sludge microbial diversity. In this mechanism (reaction D), ammonium was converted to nitrogen by utilised the generated nitrate from Feammox. Nitrification was probably involved in nitrogen removal by converted ammonium to nitrite (see reaction E). Additional nitrogen compounds were present in the influent in this phase of experiments (see Section 3.5.3) compared to the first phase of

experiments. As such the conceptual model includes possible nitrogen transformations including feammox, anammox and nitrification.
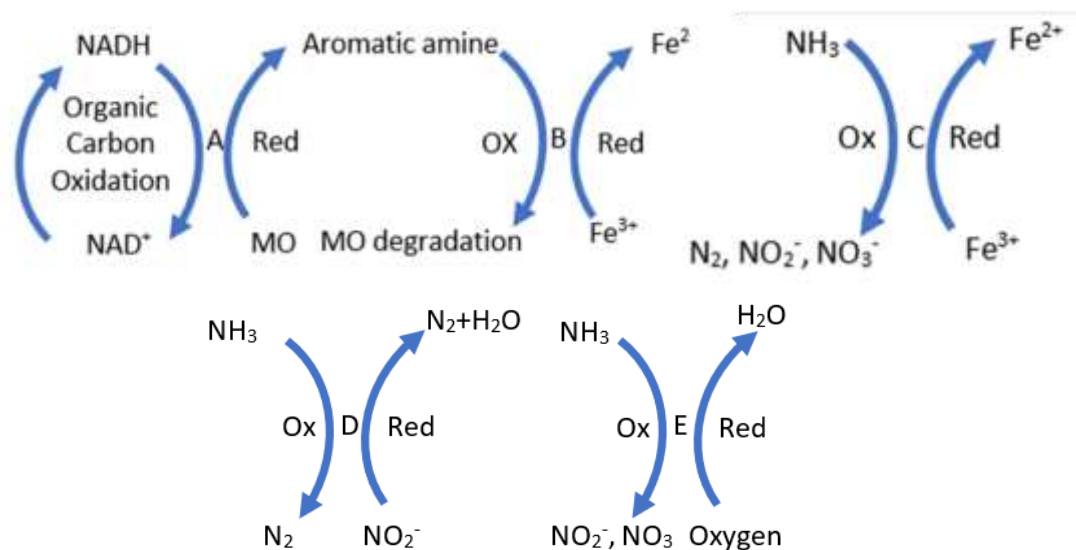


**Figure 6-14 Schematic diagram for MO degradation using iron-reducing microorganism. A: Reduction of MO azo bond, B: Oxidised aromatic amines, C: Feammox reaction, D: Anammox reaction, and E: nitrification where Ox: oxidation reaction, Red: reduction reaction.**

During microbial azo dye bioremediation, azo reductase and NADH as a co-substrate involved in azo dye degradation in various textile wastewater studies (Solís et al. 2012b). This enzyme was active during azo dye biodegradation (Liu et al. 2017b). Parshetti et al. (2010) noticed that azo reductase mineralized MO to aromatic mines where NADH participated in this mechanism. This mechanism was also highlighted by Du and his group during azo dye biodegradation (Du et al. 2015). Even though this enzyme cannot further degrade the generated aromatic amines and here, the microbial diversity of the MWT was substantial to metabolise these recalcitrant compounds.

Phase two textile wastewater experiment confirmed that MWT sludge was an efficient microbial substrate to remediate MO without detected aromatic amines, which considered the main limitation in previous studies (Table 2-4). The MWT flourished genera also decrease nitrogen and carbon contaminants to minimum concentration that makes it a competent substrate for textile wastewater bioremediation.

# Chapter 7 : Phase three textile wastewater results and discussions

## 7.1 Introduction

This chapter discusses phase three textile wastewater experiment results. The dye removal by adsorption was highlighted, and the decolourisation dye efficiency was studied. The total carbon and nitrogen removal rate were highlighted during the experiment. Other parameters as pH and dissolved oxygen were demonstrated. The spectrophotometer was used to measure the dye decolourisation, and any aromatic amines generated. Additional to that, LC-MS was used to determine dye degradation products. Gene sequencing analysed the pre-test and post-test column substrates to highlight the microorganism variations. A conceptual model was used to describe the dye degradation mechanism.

## 7.2 Spectrophotometric analysis to determine the appropriate wavelength for real textile wastewater

In phase three textile wastewater experiment, mine water treatment sludge (MWT), mixed sludge (MX), and water treatment sludge (WT) were used as column substrates to treat real textile wastewater. The wastewater was supplied by Blackburn Yarn Dyers Ltd, the company was unable to determine the types, and the concentrations of dyes used because the wastewater was collected from collection tank which received wastewater from various dyeing facilities. According to that, the spectrophotometer was used to detect the highest absorbance via wavelength by tested the wastewater over the visible range from 350 to 700 nm. Figure 7-1A shown, the wavelength at 470 nm had the highest absorbance (1.54) and this wavelength will be used to calculate the dye intensity during this experiment. The extent of dye decolourisation was determined using the wavelength at which maximum absorption measured for the influent. This method was chosen because of the unknown influent composition. It can be considered an estimation to assess the dye decolourisation during the experiment. The use of a single wavelength to determine dye decolourisation was reported in previous studies (Kuai et al. 1998; Nilsson et al. 2006; Manenti et al. 2014). Furthermore, additional sophisticated analyses using LC-MS was conducted (Section 7.11) to identify the dye degradation which was the goal of the experiment.

124
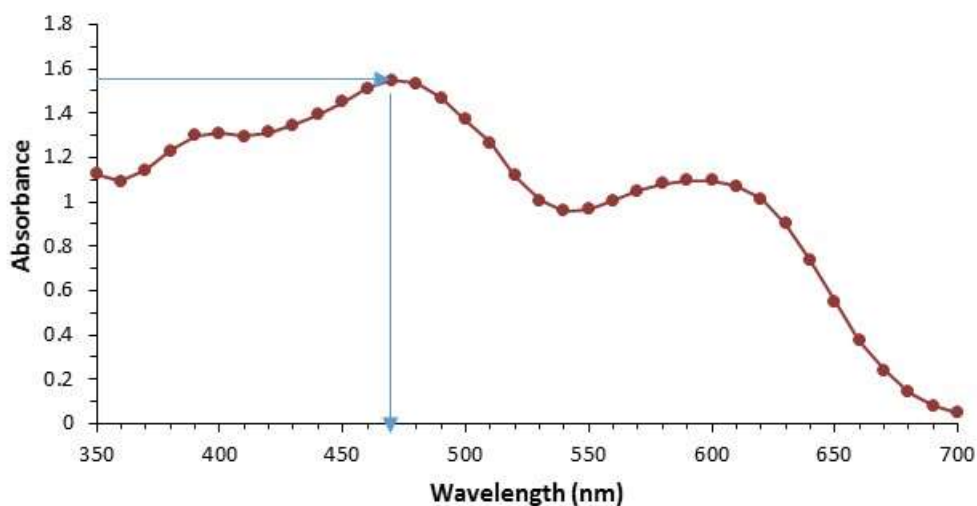
**Figure 7-1 Real textile wastewater spectrophotometer scan 350-700 nm.**

## 7.3 Dye adsorption by column substrates

A batch experiment was conducted to estimate the effect of adsorption of real textile wastewater by the used sludge (MWT, MX and WT). These sludges represent column substrates for phase three textile wastewater experiment, and it is essential to study the influence of dye removal by adsorption during the biodegradation process. From each sludge sample, 500 g was poured in a Pyrex glassware (2 l) and it was covered with aluminium foil before autoclaved it for a 30 min cycle at 121 °C. The autoclaved sludge samples were dried in the oven at 40 °C for 48 hrs as recommended by Schwertmann and Cornell (2000). One gram of the dried autoclaved sludge (MWT, MX, and WT) was mixed with 100 ml of real textile wastewater using 100 ml plastic containers with screw lids. Control samples contained only the textile wastewater were used for monitoring. The batch experiment was run in duplicate for 70 days under shaking condition (150 rpm). Absorbance of the samples were monitored daily; 3ml was withdrawn from each sample and it was filtered by 0.45 µm syringe filter before measure the absorbance by spectrophotometry at 470 nm as highlighted in Figure 7-2. Data collected revealed that the colour removal by adsorption using MWT, MX, and WT had a minor influence because the colour adsorbance did not change noticeably during the experiment. According to that, the dye removal by can be neglected during the experiment in this chapter. The real textile wastewater and high pH might attenuate

ion-exchange force, which could be the main adsorption driving force in iron oxides bearing waste (Namasivayam and Arasi 1997). Rasool et al. (2016) emphasised that biodegradation was the main reason for textile wastewater removal. In azo dye biodegradation, the dye structure is either destroyed or degraded to small fragments (Khan et al. 2013). Biodegradation is the main reason for dye decolourisation using iron oxides bearing sludge via the indigenous consortia.
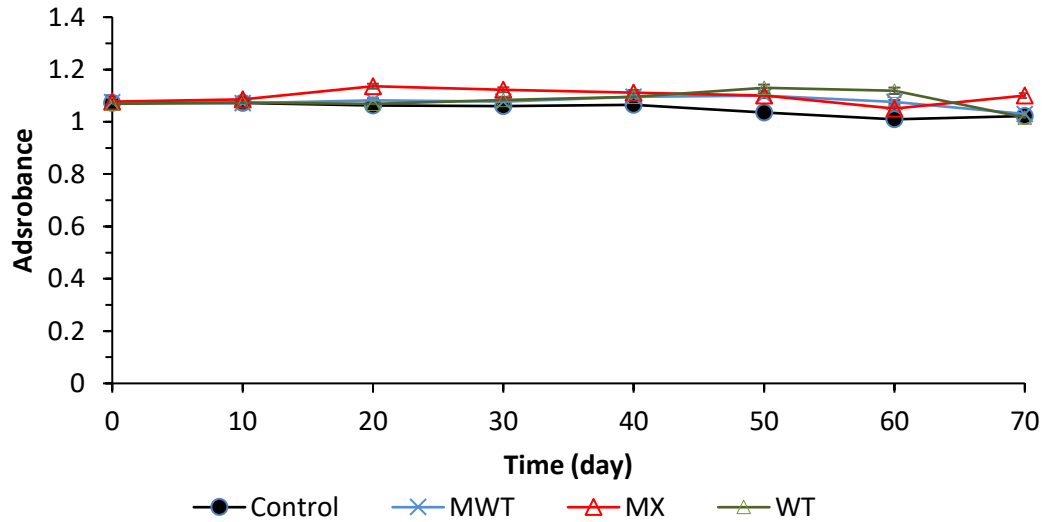


**Figure 7-2 Batch adsorption of 1 g MWT, MX and WT sludge solid samples using real textile wastewater.**

## 7.4 Decolourisation of real textile wastewater

The experiment was set up as explained in section 3.5.3. The dye wastewater depletion with time was measured by spectrophotometer at 470 nm wavelength to detect dye intensity changes (as reported in section 7.2). The dye decolourisation efficiency was calculated using the following Equation:

**Dye decolourisation** $\% = \frac{A_0 - A_t}{A_0} \times 100$ (Equation 24)

Where $A_0$ is the absorbance of the influent and $A_t$ is the absorbance at time t.

In the first 10 days, the textile wastewater decolourisation efficiency increased to 40 % in MX column effluents compared with 20 % in MWT column effluents while it was about 2.5 % in WT column effluents as shown in Figure 7-3. The dye removal

efficiency raised with time, and by the end of the experiment, the MX effluents were more efficient than the other columns as it decolourised 81 % of the influent dye comparing with 68 % and 63 % by MS and WT effluents respectively. The gradual increased in column performance over the first two months and particularly the delay in dye decolourisation in the early 10 days could be the evidence for slow microbial acclimatisation with textile wastewater harsh condition. Although, microbes in MX column substrates might be acclimatised faster than MWT and WT microorganisms because of the nutrients available in the wastewater sludge added. Possibly nutrients and humic materials in MX sludge could boosted the microbial acclimatisation, and enhanced the decolourisation. Khan et al. (2013) noticed that in a new environment, microorganisms developing a new resistance generation that can breakdown contaminants using new mechanisms which did not exist in the earlier generation. It was reported that adaptation of single bacterial species for three months was acceptable to acquire efficient dye biodegradation (Chen et al. 2003). Whereas, in this experiment, the dye removal was efficiently acclimatised after two months. Dye adsorption in longe term textile wastewater experiment could be neglected as it reached to saturation (Kalathil et al. 2011; Kalathil et al. 2012). Colour removal during phase three textile wastewater experiment was generally related to microbial biodegradation by iron oxides bearing sludge indigenous consortia because the adsorption effects can be ignored according to the batch experiment result in Figure 7-2. The comparison between various textile wastewater biodegradation studies is difficult due to various parameters, e.g. dye concentration, microorganisms used, degradation technique and dye removal calculations included: percentage and concentration in each study (Santos et al. 2007). However, retention time (RT) can be used as an indication to determine the process efficiency. In this experiment columns, RT was 5.48 hrs in the WT columns, and it was about 6.25 hrs in MWT and MX. The reported retention time was lower than the vast majority of the reported literature in Table 2-4. Furthermore, dye decolourisation was comparable to review studies in Table 2-5. The mentioned information makes the utilised iron oxides sludge are appropriate substrates to degrade textile wastewater.
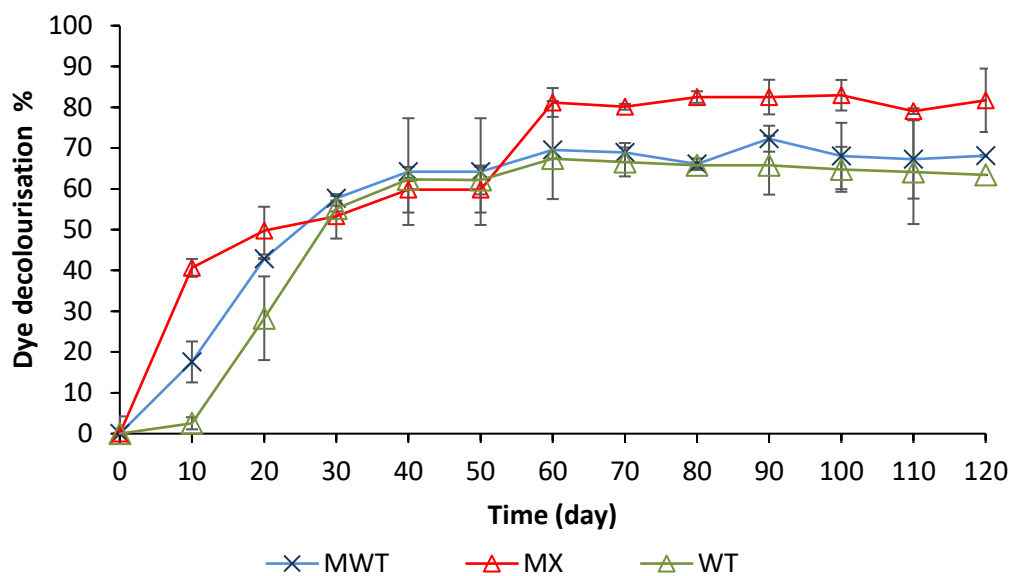
**Figure 7-3 Dye decolourisation efficiency during phase three textile wastewater experiment.**

## 7.5 Aromatic amine detection by spectrophotometer scan

In phase three textile wastewater experiment, influent and column effluents (after 120 days) were scanned by spectrophotometer at a wavelength range (200 nm -700 nm) to detect the dye decolourisation decline and any aromatic amines generated as new peaks. Figure 7-4 shown that iron oxides bearing wastes as column substrates were efficiently decolourised textile wastewater. Column effluents declined compared with influent wastewater see Figure 7-5. The absorbance of the treated water by MX column retreated from about 1.54 to 0.36 compared with 0.58 and 0.71 for MWT and WT column effluents respectively as shown in Figure 7-5. The peak at wavelength 300 nm was not identified. The spectrophotometer analysis showed that no new peaks were generated over the ultraviolet range (200 nm -400 nm) where aromatic amines should be noticed. Researchers confirmed that aromatic amines could be detected by a spectrophotometric method as new generation peaks (Pinheiro et al. 2004; Somasiri et al. 2008; Amaral et al. 2014; Manenti et al. 2014). Aromatic amines are the expected degradation product generated during anaerobic azo dye biodegradation (Brosillon et al. 2008). He et al. (2004) was unable to highlight aromatic amine in the ultraviolet range, which indicated that azo dye was degraded to aliphatic hydrocarbons. Işik and Sponza (2005) and Balapure et al. (2015) found that microorganism consortia could degrade aromatic amines by synergism between different bacterial species. Moreover,

128

some bacterial species can mineralise aromatic amines as an energy source, e.g. *Pseudomonas* (Kulla et al. 1983; Stolz 2001). Detection aromatic amines are the main drawback for azo dye biodegradation; these toxic chemicals were detected in the vast majority of the reported literature in Table 2-5. The main reason for dye decolourisation in this experiment is iron oxides bearing sludge microbial activity because the dye removal by adsorption had a minor influence, as highlighted in Figure 7-2. These microorganisms degraded azo dye without generated aromatic amines.
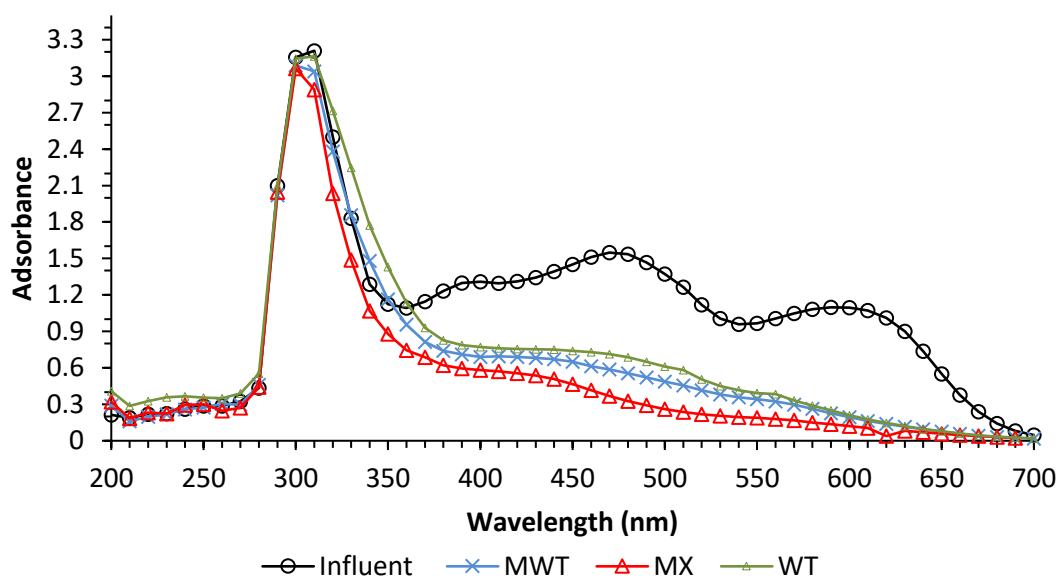


**Figure 7-4 Phase three textile wastewater column effluents scan after 120 days.**



| WT effluents | MX effluents | MWT effluents | Real textile wastewater (Influent) |
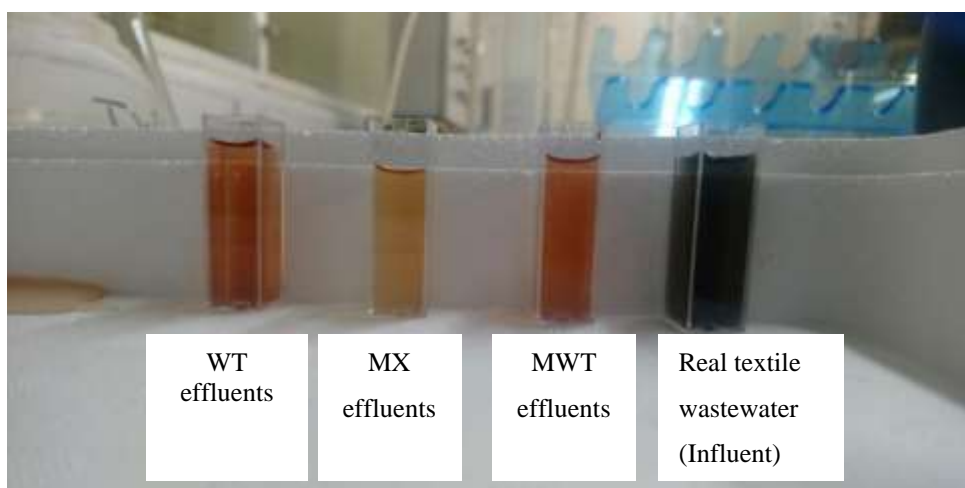
**Figure 7-5 Phase three textile wastewater samples after 120 days.**

## 7.6 Chemical oxygen demand (COD) and total carbon (TC) removal

Chemical oxygen demand (COD) was measured according to the procedure reported in section 3.8. The COD of the influent textile wastewater was about $1397 \pm 10$ mg/l. In the first week, both MWT and MX column effluents removed about 30 % of the influent COD, while COD removal was quite low in WT column effluents. The COD removal efficiency was about 36 % by the end of the experiment in all column effluents (see Figure 7-6). Total carbon (TC) concentration in the influent textile wastewater was about 736 mg/l. The TC removal efficiency raised gradually with time to about 51 % in MX column effluents compared with 48 % and 50 % for WT and WT column effluents, as shown in Figure 7-7A. The normalised TC removal rate was calculated as explained in Appendix 2. The highest normalised TC removal rate conducted was 1394 g/m$^3$/day, 1390 g/m$^3$/day, and 1376 g/m$^3$/day by MWT, MX and WT column effluents, as demonstrated in Figure 7-7 B. Furthermore, the total carbon concentration was detected for pre-test and post-test column substrates to highlight any carbon precipitated during phase three textile wastewater experiment. Figure 7-8 shown that there was no carbon precipitated in the column substrates according to TC % highlighted. The carbon lost from the column substrates was probably degraded to $CO_2$ that might release from the collection tanks, and no further step was taken to manage the released gas from the collection tanks. COD can be an indicator of pollutants removal during wastewater treatments (Yadav et al. 2012). Dye toxicity during textile wastewater treatment could decrease the COD removal efficiency because it affects microbial growth (Li et al. 2014). During textile wastewater treatment, dye degradation intermediate compounds could also retreat the COD removal efficiency (Singh et al. 2006; Li et al. 2010). This might be the reason for not exceeded the COD removal by more than 40 % during this phase. Furthermore, textile wastewater salinity could also decrease organic carbon biodegradation and COD removal (Kargi and Dincer 1996; Bassin et al. 2011). Additional to that, inadequate microbial acclimatisation could be another reason for incompetent COD removal (Bell et al. 2000; Kong et al. 2014), because harsh textile wastewater condition might inhibit some column's substrate indigenous consortia due to lack the adaptation; this might reduce the biological biomass involved in biodegradation (Talarposhti et al. 2001). It was reported that low COD removal is the main drawback for anaerobic dye biodegradation (Sponza 2002;

Kapdan and Alparslan 2005). This drawback could be overcome either by, increasing the hydraulic retention time or adding carbon source to support the microbial growth (Dafale et al. 2008; Jonstrup et al. 2011). Işik and Sponza (2005) found that hydraulic retention time could dramatically influence the COD removal ; for example, COD efficiency dropped from 80 % to 29 % when HRT was decreased from 100 hrs to 6 hrs. Alternatively, added an aerobic reactor as a complementary process which is known as a sequential anaerobic-aerobic bioreactor could raise the COD removal (Kumar et al. 2006; Farabegoli et al. 2010). Distinguish the total concentration during textile wastewater treatment is beneficial to assess dye biodegradation progress (Chang et al. 2011). In this phase, the decline in total carbon might be associated with microbial biodegradation activity. It means that iron oxides bearing sludge via the indigenous microorganisms mineralised approximately 50 % of the influent carbon compounds, and the COD data could confirm this conclusion see Figure 7-6. Stolz (2001) reported that some microorganism degrades azo dyes as a sole carbon source, as demonstrated in chapter five. However, most microorganisms metabolise additional organic carbon to degrade dye see Table 2-4. Thus, Telke et al. (2009) argued that metabolises azo dye as a sole organic carbon usually is insufficient to be the main nutrient for microbial growth. Therefore, additional substrates are fundamental to conduct efficient azo dye degradation. More and above, an additional carbon source assists the microorganism to tackle textile wastewater harsh environment (Franciscon et al. 2015).
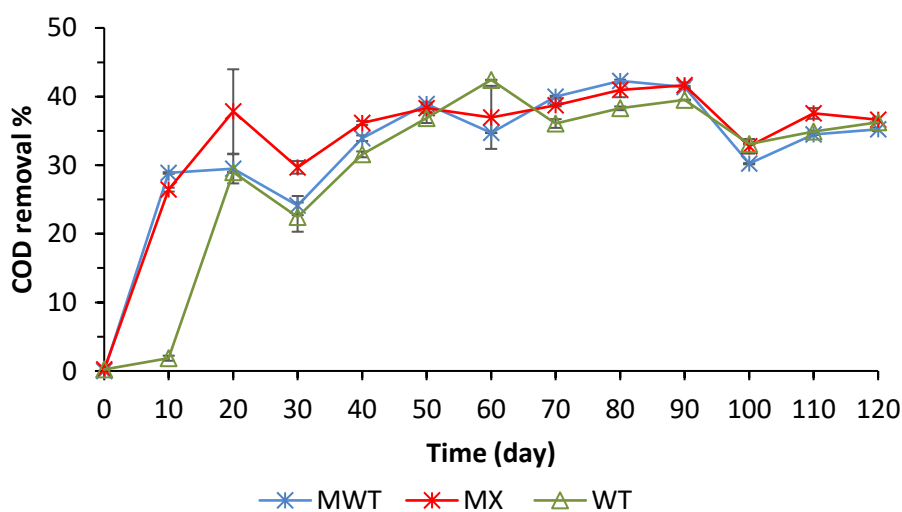


**Figure 7-6 Chemical oxygen demand removal efficiency during phase three textile wastewater experiment.**
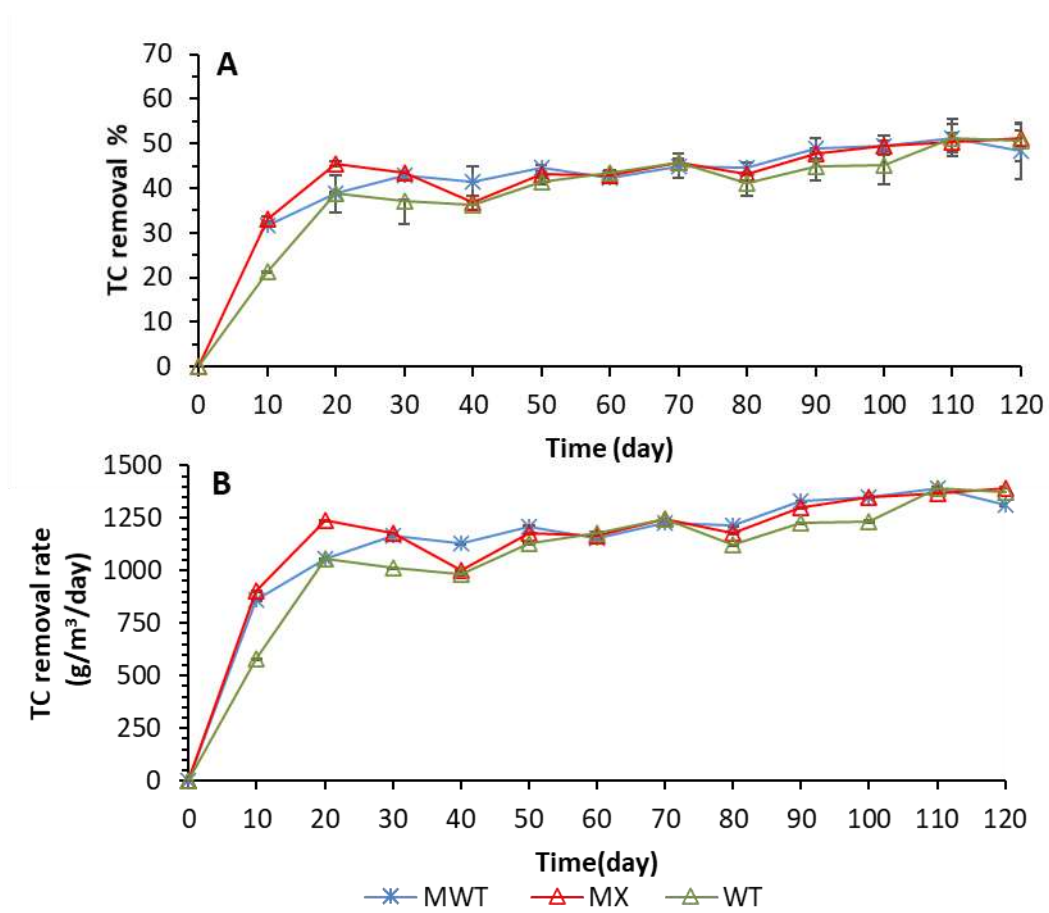
**Figure 7-7  Total carbon (TC) measurement during phase three textile wastewater experiment, (A) TC removal efficiency, (B) TC removal rate.**
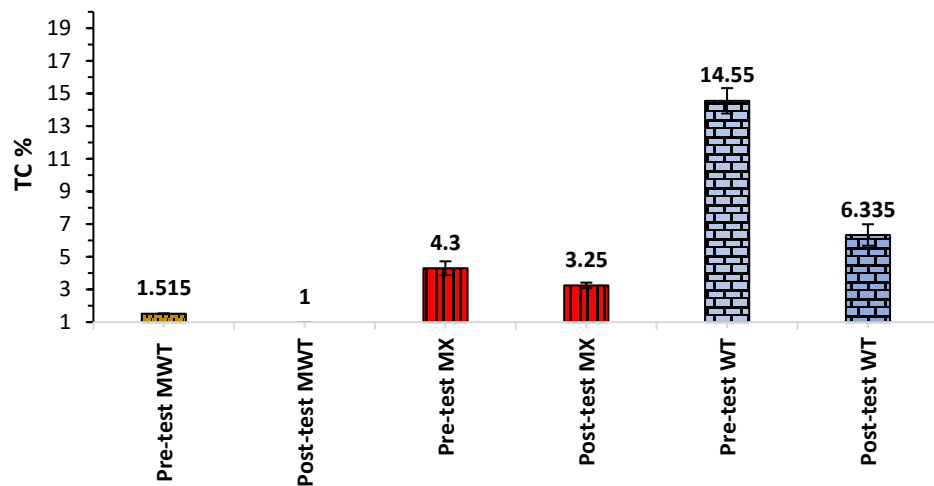


**Figure 7-8 Total carbon concentration in pre-test and post-test column substrates.**

## 7.7　Ammonia-nitrogen (NH$_3$-N), nitrite, and nitrate

Ammonia-nitrogen, nitrate, and nitrite concentrations were measured as reported in section 3.8. They were measured in column effluents to study the fate of nitrogen during phase three textile wastewater experiment. Ammonia–nitrogen concentration in the influent textile wastewater was $10 \pm 0.2$ mg/l. After ten days, it sharply dropped to about 0.50 mg/l in MWT and MX column effluents. While it was 2 mg/l in WT effluent. after this point, ammonia–nitrogen concentration fluctuated with the time between 0 to 5.50 mg/l as presents in Figure 7-9 A. Nitrate concentration in the influent textile wastewater was $4.60 \pm 0.20$ mg/l. Nitrate concentration in WT effluents fluctuated with time while the nitrate concentrated general trendline was gradually decreased with time as shown in Figure 7-9 B. Nitrate concentration in all column effluents dropped to approximately to 0.92 mg/l by the end of the experiment. Nitrite concentration over the first month was under the detection limit in all column effluents as presents in Figure 7-9 C. Even though nitrite was generated from days 50, but it did not exceed more than 5 mg/l. The normalised TN removal rate included the nitrogen concentration in ammonium, nitrite, and nitrate only was calculated as reported in section 3.10 using Equation 17 (see Appendix 2 for more information). The volume of the sludge used in each column was used to calculate the nitrogen removal rate. The highest normalised nitrogen removal rate was 39 g/m$^3$/day by MX columns followed by 36 g/m$^3$/day, and 31 g/m$^3$/day by WT and MWT columns respectively, as shown in Figure 7-9 D.

Nitrogen is an essential element during azo dye biodegradation because microorganisms need it to regenerate NADH which is a vital component for microorganism growth (Chang et al. 2000). It was reported that environment dissolved oxygen (DO) plays a fundamental role in nitrogen removal (Gerardi 2003; Ong et al. 2010b; Ong et al. 2010a). Oxygen concentration level effects on nitrification, where nitrite oxidised to nitrate (Spychała and Starzyk 2015). According to that, the dissolved oxygen concentration during phase three textile wastewater in Figure 7-12 could divide the experiment into three sections based on oxygen concentration level, the aerobic period was monitored from days 1 to 30, the anoxic period was highlighted during 30 to 80 days and anaerobic period determined over days 80 to 120. The NH$_3$-N depletion during the aerobic period 1-30 days was probably conducted by nitrification (Cuervo-

López et al. 2009). During this period, ammonium oxidised to nitrate via nitrite (Singer and Little 1975; Prosser 1990; Texier and Zepeda 2012). There are two types of microorganisms that might involve in nitrification, ammonium oxidation bacteria (AOB), and nitrite-oxidising bacteria (NOB). AOB converts ammonium to nitrite and the latter oxidised nitrite to nitrate. AOB is more productive compared with the NOB due to different energy yields (Singer and Little 1975; Wiesmann 1994). These microorganisms are highly sensitive to any alteration in pH, dissolved oxygen, temperature, ammonia, and nitrate concentration. Moreover, these microorganisms have a slow growth rate, and it might be inhibited by organic pollutants (Li and Bishop 2002; Bernet and Spérandio 2009). Batool et al. (2015) highlighted that several parameters could influence these microbes, e.g., the type and the concentration of pollutants as it suppresses the nitrification enzymes. Zepeda et al. (2006) found that the concentration of the pollutants could decrease nitrification. Furthermore, researchers noticed that the intermediate dye biodegradation products could impede nitrification mechanism by inhibiting the related enzymes (Tong and Young 1974; Yongjie and Bishop 1994; Brandt et al. 2001; Amor et al. 2005).

The anaerobic ammonia oxidation (Anammox) is expected to be one of the dominated mechanisms during phase three-textile wastewater experiment, especially over the period 30 - 120 days as it considered as anoxic and anaerobic conditions. In this mechanism, ammonium reduces to $N_2$ gas when oxygen is almost not available (Jetten et al. 2001). Anammox is a common mechanism in column units, especially in anaerobic columns, and it flourished in column substrates (Tang et al. 2013). Van Dongen et al. (2001) asserted that about 80% of the ammonia could be mineralised to dinitrogen gas. Tang et al. (2017) reported that Anammox is an efficient process to remove ammonia under shortage of oxygen concentration. Anaerobic ammonium oxidation at iron-reducing condition (Feammox) is another highly expected mechanism, which might be occurred in MWT, MX and WT as they are rich iron oxides sludge and they expected to be the indigenous environment for iron-reducing bacteria. In such environments, ammonium anaerobically oxidised to nitrogen gas by iron-reducing microorganisms which simultaneously reduced Fe (III) to Fe (II) (Yang et al. 2012; Ding et al. 2014; Li et al. 2018). The conducted nitrogen removal rate during phase two textile wastewater was within the range of nitrogen removal by municipal wastewater literature review in Table 2-8. It could confirm that the iron

oxides bearing sludge indigenous consortia included iron-reducing bacteria can remove nitrogen contaminants efficiently during textile wastewater treatment, which considered an advantage for remediating azo dye by iron-bearing wastes.
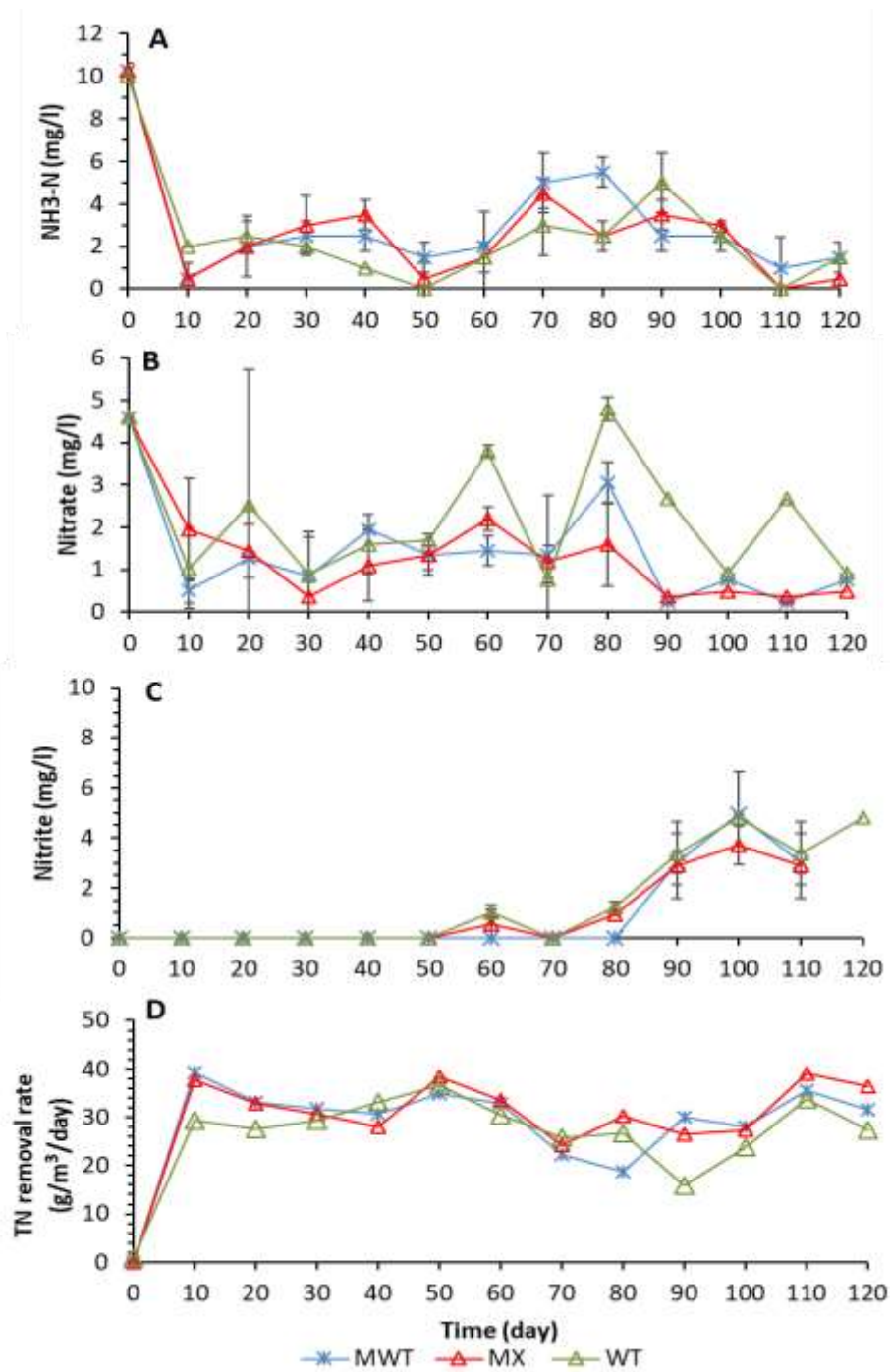


**Figure 7-9  Nitrogen concentration during phase three textile wastewater, (A) Nitrogen-ammonia, (B) Nitrate, (C) Nitrite, and (D) Total nitrogen removal rate.**

135

## 7.8　　　Total iron and ferrous iron concentrations

Total iron and ferrous iron were measured during the dye removal experiment, as reported in section 3.8. Iron concentration in the influent textile wastewater was 0.11 mg/l. After ten days, it rose to 3.99 mg/l in WT effluents. While it declined to less than 2 mg/l in both MWT and MX effluents, by the end of the experiment iron concentration was marginally lower than 2 mg/l in all column effluents as shown in Figure 7-10 (A). Ferrous concentration was zero in the influent textile wastewater. It rose to 0.50 mg/l by the end of the first month. Ferrous kept fluctuated over the experiment in all column effluents. However, it did not exceed 0.50 mg/l, 1 mg/l and 1.70 mg/l in MS, WT and MX effluent, respectively, as shown in Figure 7-10 (B).

Iron is oxidised to either ferrous or ferric or both (Hem and Cropper 1962). Iron oxides are abundant in nature (Cornell and Schwertmann 2003). Fe (III) is used as an electron donor during azo dye remediation (Farrell et al. 2000). It provided a reductive environment (Van Der Zee and Villaverde 2005b). Iron oxide improved azo dye biodegradation (Ghasemi et al. 2015). More and above, dye removal by substrate containing iron oxides might be sufficient that no further treatment is needed (Shih et al. 2010). Iron reducing-bacteria is an essential microorganism for environmental bioremediation. It is one of the expected species in iron oxides bearing wastes. It degraded aromatic organic carbon, and it reduced Fe (III) to Fe (II) (Lovley and Lonergan 1990; Lovley et al. 2002). Iron-reducing bacteria flourished at anaerobic conditions, though Bridge and Johnson (1998) noticed that some iron-reducing bacteria, e.g. *Shewanella,* is a facultative bacteria. The reason of low ferrous generation from the columns used for textile wastewater biodegradation might because the generated ferrous reacts with the generated nitrite during nitrogen transformation to regenerate Fe (III) which precipitated in column sludge as shown in this reaction (Otiteley et al. 1997). It might be the reason for low ferries detection in column effluent during this phase**.**

$$6\text{Fe(II)} + 2NO_2^- + 8H_2O \rightarrow 6FeOOH + N_2 + 10H^+$$
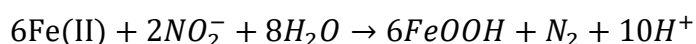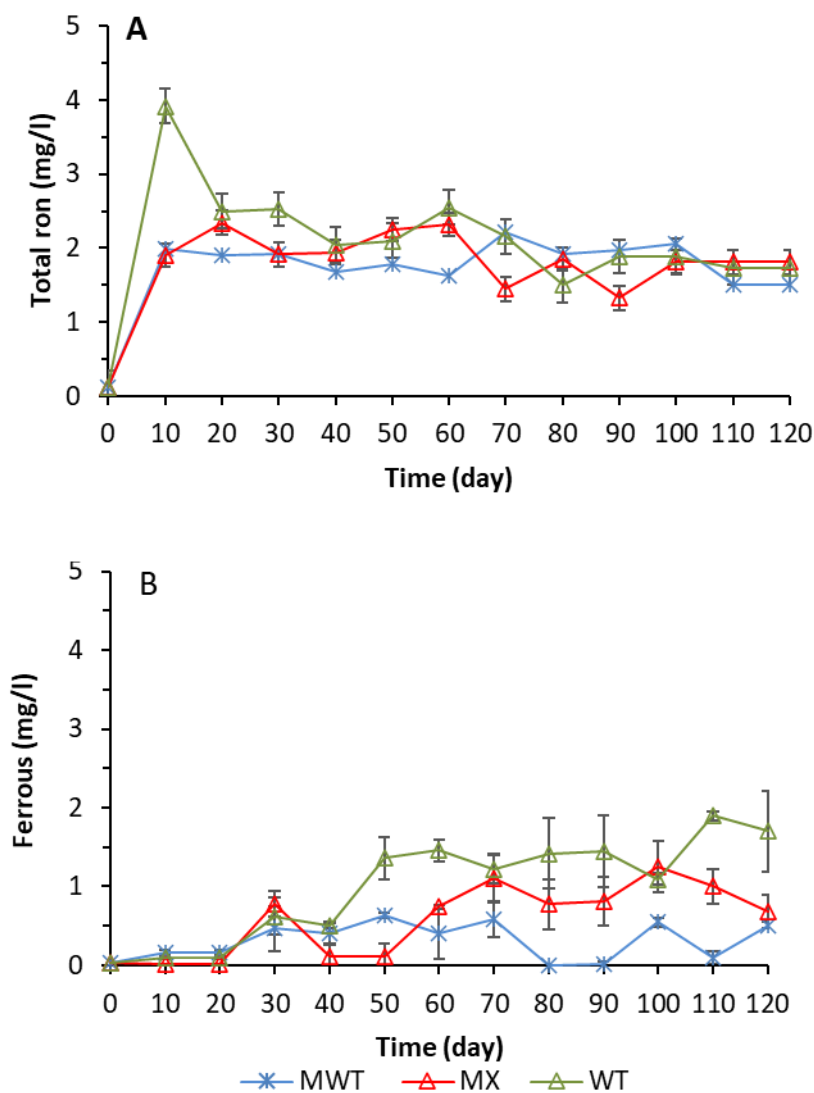
**Figure 7-10 (A) Total iron, and (B) ferrous iron concentrations in column effluents**

## 7.9 Experimental parameters

Experiment parameters were measured as described in section 3.8. In this experiment, the inlet wastewater pH was $9.5 \pm 0.2$. After about one week, the MWT column effluents declined to pH 8. In contrast, it was slightly shifted to pH 8.8 and 9.1 in WT and MX effluents, respectively. For the remained time, general pH trendline of effluent columns was about $8.5 \pm 0.5$, as shown in Figure 7-11. In this phase, real dye biodegradation occurred at alkaline pH range. Chemical additives during the dyeing

process, e.g. sodium hydroxide and other chemicals raise the textile wastewater pH to alkalinity range (Santos et al. 2007). Vimonses et al. (2010) found that azo dye adsorption declined at alkaline pH range. Furthermore, pH of textile wastewater has a significant impact on dye biodegradation. It affects on microorganism metabolism and enzyme activity (Khan et al. 2013). Some microorganisms degraded textile wastewater at a wide pH range (6-10) (Guo et al. 2007; Kiliç et al. 2007). The ability of microbial species to tolerate alkaline condition is essential for efficient dye biodegradation (Wang et al. 2009). Joe et al. (2008) confirmed that *Clostridium bifermentans* degrades azo dye at alkaline pH. While *Aspergillus fumigatus* degrades azo dye at a wide pH range (Jin et al. 2007), the abundance of iron oxides during azo dye biodegradation could buffer the pH by the influence of ferrous generation (Chang et al. 2006; Yu and Amrhein 2006; Zhang et al. 2012b). The minor changes in pH trendline during textile wastewater might be a piece of evidence for not generation aromatic amine during dye degradation (Erguder et al. 2003). This finding was confirmed by Wijetunga et al. (2010) and Balapure et al. (2015) as they asserted that the aromatic amines generation during azo dye degradation raised the pH.

Dissolved oxygen (DO) concentration was measured in the column effluents. The DO in the feeding textile wastewater was $10 \pm 1$ mg/l, as shown in Figure 7-12. DO dramatically dropped to about 1 mg/l after 10 days in all columns. After 30 days, it declined to about 0.5 mg/l, and it kept decreasing until it reached zero by the end of the experiment. DO concentration over the first 30 days had a negative impact on dye mineralisation and oxygen depletion after two months associated with significant dye decolourisation, as shown in Figure 7-3. It could be due to the influence of oxygen on anaerobic biodegradation enzymes (Kalyani et al. 2009). Oxygen might be either an inhibitor or a booster parameter during textile wastewater treatment depends on the microorganism involved (Solís et al. 2012a). Zimmermann et al. (1982), and Banat et al. (1997b) emphasised that the anaerobic condition was appropriate for azo dye degradation due to the negative impact of oxygen on the involved biodegradation enzyme. Bardi and Marzona (2010) highlighted that oxygen controls dye biodegradation directly, by influence microbial growing or indirectly, by hindering the degradation enzyme. Van Der Zee and Villaverde (2005a) reported that azoreductase enzyme in bacteria degrades azo dye bond. Wuhrmann et al. (1980) found that *Pseudomonas* enzymes mineralised azo dye to carbon dioxide under anaerobic

condition. These enzymes breakdown the dye chromophores (Santos et al. 2007). Under anaerobic conditions, dye chromophores could be cleaved by accepting two pairs of electrons (Gingell and Walker 1971; Santos et al. 2007). Nevertheless, some dyes had a low degradation rate even in anaerobic condition (Brown and De Vito 1993; Dos Santos et al. 2005). It could be attributed to the toxicity of these dye which inhibited the microorganism growth even at low concentration, this probably the reason for the partial dye mineralisation during this experiment even under anaerobic condition (60-120 days) (van der Zee et al. 2001; Fontenot et al. 2003; Lee et al. 2006).

A HANNA data logger monitored the temperature during textile wastewater treatment. The textile treatment was conducted during a various temperature range (1 °C to 19.5 °C) as demonstrated in Figure 7-13. In the first two weeks, the temperature range did not raise more than 5 °C. The highest temperature recorded during the experiment was 19 °C. Temperature is one of the controlled parameters in dye biodegradation. It affects the microorganism growth, enzymes activity, and biodegradation mechanism (Angelova et al. 2008; Solís et al. 2012a). Pearce et al. (2003) found that dye biodegradation could be processed at a temperature range between 10 °C to 30 °C. This might explain the low dye degradation in the experiment for early days (see Figure 7-3). This finding agreed with Ramachandran et al. (2013), who found that 30 °C was a convenient temperature for dye degradation. Dye biodegradation increase with temperature increase to the optimum species temperature, and it retreated when it exceeded the optimum condition due to denaturation of the relevant enzymes (Asad et al. 2007; El Ahwany 2008). Shih et al. (2010) and Khan et al. (2013) reported that temperature raised during dye decolourisation enhanced dye biodegradation. Shih et al. (2010) reported that raising the temperature from 7 °C to 25 °C increased the dye removal efficiency from 48% to 83%.
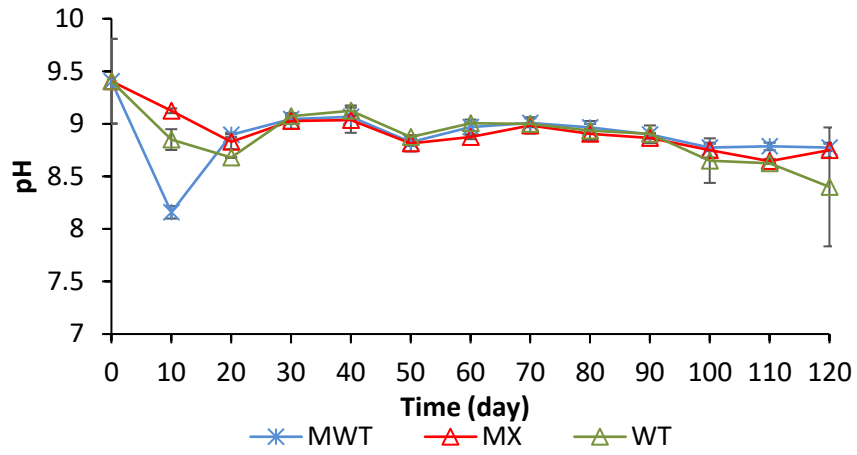
**Figure 7-11  pH during phase three textile wastewater experiment.**
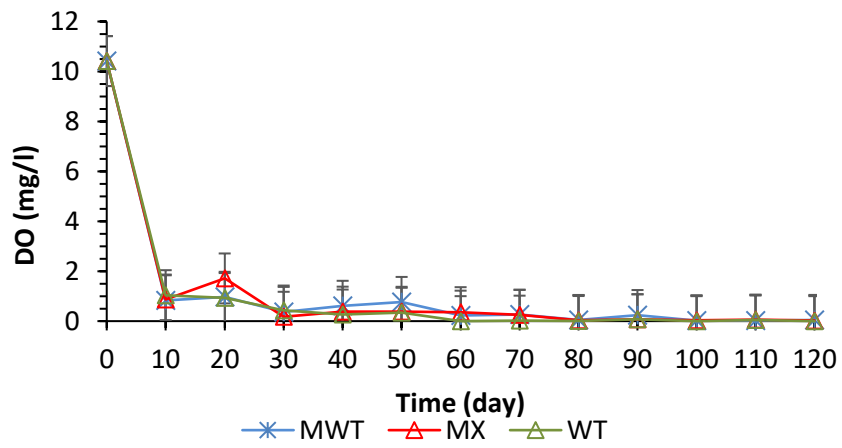


**Figure 7-12 Dissolved oxygen concentration during phase three textile wastewater experiment.**
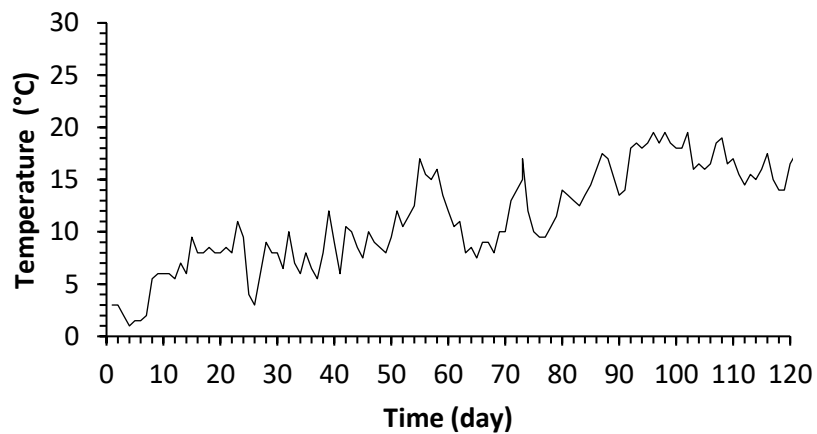


**Figure 7-13 Temperature profile during phase three textile wastewater experiment.**

## 7.10    Parameters correlation for phase three textile wastewater experiment

IBM SPSS statistic software (version 20) was used to highlight the correlation between phase three textile wastewater parameters using bivariate correlation analysis. Pearson analysis was used to determine the correlation between experiment parameters because it was normally distributed ($p < 0.05$). A significant negative correlation was found between dye decolourisation and the pH in MX columns only (-0.81) while no correlation was noticed in other columns. The correlation between dye decolourisation and TC removal rate was significantly positive for MWT (0.92), MX (0.89) and WT (0.87) respectively, according to the calculated correlation coefficient. Furthermore, the only significant correlation between dye decolourisation and TN removal rate was positive in MX columns (0.59) while no correlation was found in MWT and WT column effluents. TC removal rate in phase three textile experiment was significantly negatively correlated with pH in both MX (-0.90) and WT (-0.69) column effluents while no correlation was found in MWT. A significant negative correlation was found between the TN removal rate and pH in MWT (-0.72) and MX (-0.74) column effluents. The correlation between TN and TC removal rate was described as a significant positive in MWT (0.70) MX (0.80) and WT (0.64). There was a significant correlation between dye decolourisation and ferrous generation in MX (0.74) and WT (0.82) columns, while no correlation was found in MWT. The temperature has a positively correlated with dye decolourisation only in MX columns (the correlation coefficient was 0.57). Furthermore, no significant correlation was found between temperature and TN removal rate. The correlation between TC removal rate and the temperature was highlighted as a positive correlation in MWT (0.57) only.

## 7.11    Dye degradation detected by LC-MS

The main challenge in this experiment was the unknown dyes influent chemical structure because the textile company was unable to determine the types and concentrations of dyes and chemicals in real textile wastewater. However, liquid chromatography-mass spectrometry (LC-MS) was used to detect the organic compounds in the influent textile wastewater and column effluents to highlight dye breakdown products (see section 3.12 for more details). Influent real textile wastewater

was compared with the column effluents after 140 days. Positive and negative LC-MS spectrum was used in all tested samples. The positive LC-MS spectrums are shown in Figure 7-14 and Figure 7-15. Each figure covered a specific retention time range. Figure 7-14 demonstrated a retention time between 8 min -20 min. In this spectrum, peaks at 9.38 min, and 9.69 min were disappeared in the influent, and the dye intensity dropped to zero (see the highlighted red circle). Peaks at retention time 11.62 min, 12.37 min, and 12.73 min were also degraded. Figure 7-15 demonstrates organic compounds over retention time between 13 min to 31 min. In this spectrum, peaks highlighted at 13.56 min, 14.7 min, 20.24 min, and 27.46 min were declined in all column effluents. The negative spectrum was demonstrated in Figure 7-16. It included retention time from zero to 11 min. The peaks labelled at the 3.26 min, 3.35 min, 3.50 min, 3.56 min, 7.08 min, 8.3 min, and 8.4 min retention time (RT), they disappeared from the MWT, MX, and WT effluents. Figure 7-17 shown that the intensity of the general signal detection was dropped by about 50 % compared with the influent textile wastewater as highlighted by the red arrows. Under each spectrum, there is a table elucidates the relationship between the detected retention time and m/z ratio to identify the chemical formula, for instance, the expected chemical structure formula for the first positive spectrum at RT equal to 9.38 min was $C_{22}O_2N_2$ or $C_{14}H_{29}N_{12}Na$ or $C_{15}H_{35}O_5N_5Na$. Remote analyser software was used to identify the chemical structure, as shown in RT 20.24 min, which was $C_{24}H_{35}N_2Na$., the LC-MS software was able to identify the spectrum peak as a chemical formula; however, it was unable to give the chemical name of these chemical structures.
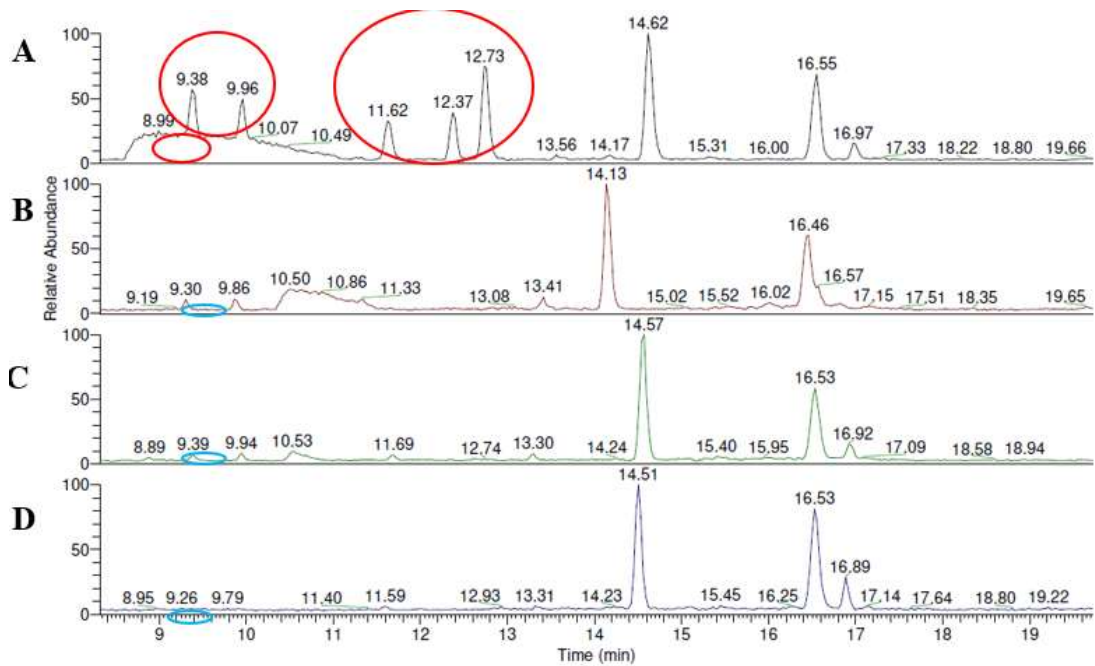
| RT (min) | M/Z | Chemical structure |
|----------|-----|--------------------|
| 9.38 | 323.99/ 388.25 | $C_{22}O_2N_2/C_{14}H_{29}N_{12}Na/ C_{15}H_{35}O_5N_5Na$ |
| 9.69 | 323.99/432.27 | $C_{22}O_2N/C_{15}H_{34}O_4N_{11}/ C_{16}H_{40}O_9N_4$ |
| 11.62 | 453.34/609.38 | $C_{15}H_{46}O_2N_{10}NaS/C_{35}H_{53}O_3N_4S$ |
| 12.37 | 475.32/453.34 | $C_{22}H_{50}O_2N_3NaS_4/C_{22}H_{43}O_3N_7$ |
| 12.72 | 566.42 | $C_{28}H_{57}O_5N_5Na/C_{27}H_5N_{12}Na$ |

**Figure 7-14 Positive LC-MS spectrums (RT 8-20 min), (A) the influent textile wastewater, (B) WT effluent, (C): MWT effluent, and (D) MX effluent.**
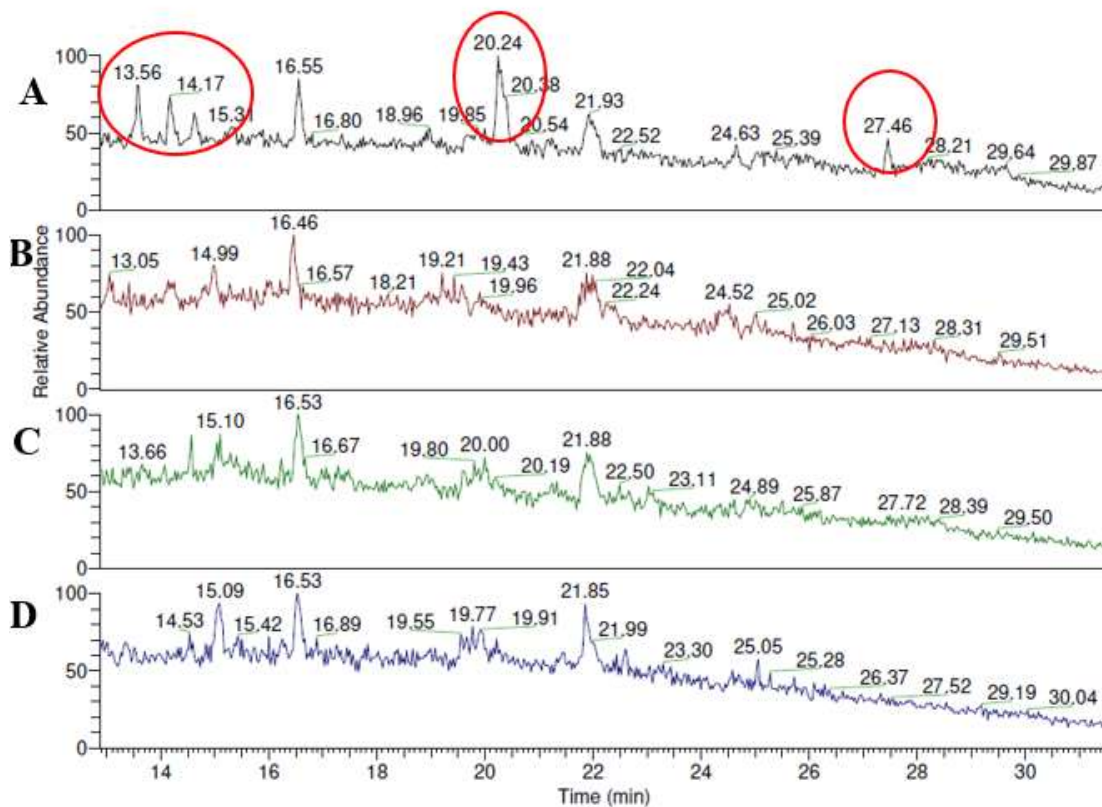
| RT (min) | M/Z | Chemical structure |
|---|---|---|
| 13.65 | 679.50 | $C_{26}H_{69}O_7N_{11}S/C_{42}H_{72}O_2NS$ |
| 20.24 | 290.26 | $C_{17}H_{35}N_2Na$ |
| 27.46 | 332.33 | $C_{22}H_{42}N$ |

**Figure 7-15 Positive LC-MS spectrums (RT13-31 min), (A) is the influent textile wastewater, (B) WT effluent, (C) MWT effluent, and (D) MX effluent.**

144
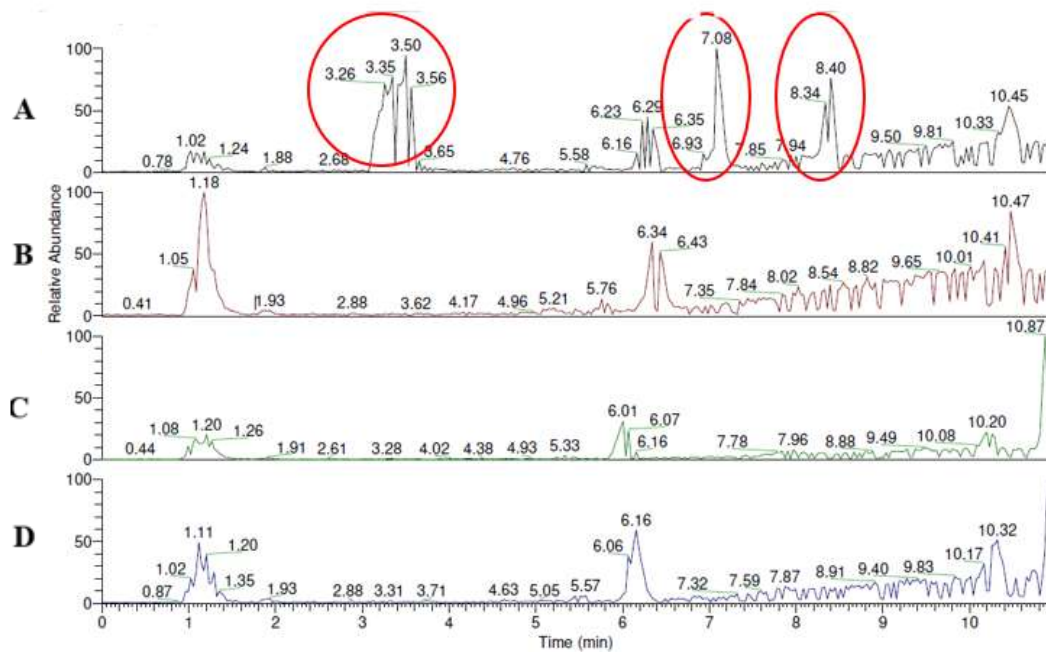
| RT | M/z | Chemical structure |
|-----------|---------------|------------------------------------------------|
| 3.26-3.56 | 201.98 | $C_6H_4O_5NS$ |
| 7.8 | 336.53 | $C_{41}H_{15}O_2N_5S_2$ |
| 8.34-8.40 | 441.05/336.53 | $C_8H_{13}O_{10}N_{10}S_2/C_{41}H_{15}O_2N_5S_2$ |

**Figure 7-16 Negative LC-MS spectrums (RT 0-11 min), (A) is the influent textile wastewater, (B) WT effluent, (C) MWT effluent, and (D) MX effluent.**
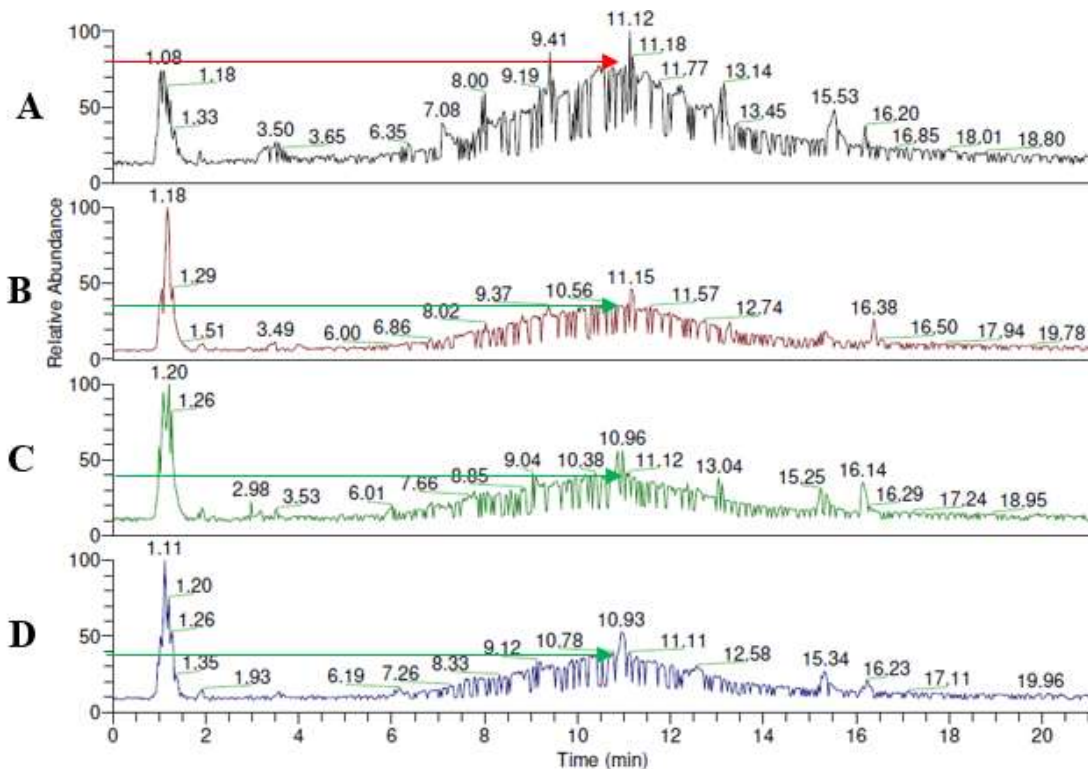
**Figure 7-17 Negative LC-MS spectrums (RT 0-20 min), (A) is the influent textile wastewater, (B) WT effluent, (C) MWT effluent, and (D) MX effluent.**


## 7.12    Microbial community changes in pre-test and post-test column substrates

Taxonomic classification at phylum and genus level was conducted for pre-test and post-test column substrates used in real textile wastewater experiment. (see details in section 3.14). In MWT sludge, the phylum diversity (relative abundance >1 %) was retreated dramatically from nine in pre-test MWT sludge to two in post-test MWT as highlights in Figure 7-18. *Proteobacteria* relative abundance was the highest bacterial phyla in pre-test MWT sludge (61.24 %), it retreated by about 50 % in post-test MWT (31.62 %.) While *Firmicutes* prospered to 67.47 % in post-test MWT compared with 0.49 % in pre-test MWT sludge. *Proteobacteria* (64.45 %) was the highest bacterial phylum in pre-test MX. However, in the post-test MX, it dropped sharply to 17.82 %. *Firmicutes* (14.79 %) was the second abundance phylum in pre-test MX while it raised to 62.09 % to be the dominant bacterial phyla in post-test MX. *Bacteroidetes* gradually increased from 8.91% in pre-test MX to 10.55 % in post-test MX. Similarly,

146

*Actinobacteria* raised from 4.46 % to 7.18 %. *Chloroflexi* was 6.12 % in pre-MWT. It reduced lower than the detection limit in post-test MWT (see Figure 7-19). In the post-test water treatment substrate, *Firmicutes* was sharply increased from 0.7 % in pre-test WT to cover 50.91 % of the total relative abundance in post-test WT. *Proteobacteria* declined in pre-test WT from 36.5 % to 32.67 %. *Verrucomicrobia* dropped from 17.19 % to 1.35 %. *Acidobacteria* and *Bacteroidetes* highlighted in pre-test WT at 12.82 % and 8.10 % respectively. However, it could not be distinguished in post-test WT. *Actinobacteria* (12.08 %) retreated to 10.54 % in post-test WT, as shown in Figure 7-20.

At the genus level, the dominance genera in pre-test and post-test MWT sludge with relative abundance >1 % can be shown in Figure 7-21. *Proteobacteria* genus in pre-test MWT sludge included *Gallionella* (5.82 %), *Rhodoferax* (4.00 %) *Bradyrhizobium* (1.91 %), *Anaeromyxobacter* (1.77 %), and *Devosia* (1.39 %). *Geothrix* (1.39 %), and *Prevotella* (2.86 %) represented *Acidobacteria* and *Bacteroidetes* genera. The entire reported genus in pre-test MWT sludge retreated below the detection range in the post-test MWT. Alternatively, *Firmicutes* genus flourished in post-test MWT *Alkaliphilus* (19.22 %), *Dethiobacter* (15.81 %), *Proteiniclasticum* (7.39 %), *Enterococcus* (6.37 %), *Natronobacillus* (2.47 %), *Exiguobacterium* (4.78 %), *Acetobacterium* (3.9 6%), *Alkalibacterium* (3.29 %) and *Trichococcus* (1.66 %). A substituted *Proteobacteria* genus included *Ochrobactrum* (14.81 %), *Agrobacterium* (9.77 %), *Pseudomonas* (2.11 %), and *Brevundimonas* (1.67 %).

Figure 7-23 highlights genus variation (relative abundance>1) in pre-test and post-test MX sludge. *Proteobacteria* genera in pre-test MX are *Devosia* (10.01 %), *Mycoplana* (10.23 %), *Rhodoferax* (9.63 %), *Achromobacter* (8.56 %), and *Brevundimonas* (16.66 %). Additionally, *Sporosarcina* (3.66 %), *Paenibacillus* (4.61 %), and *Alkaliphilus* (1.89 %), and *Solibacillus* (2.09 %) were the distinct *Firmicutes* genus. *Sphingobacterium* (3.68 %) classified as *Bacteroidetes* genus. *Actinobacteria* included *Leucobacter* (1.41 %). The bacterial genus in pre-test MX was suppressed by the influence of the real textile wastewater harsh environment. Therefore, another *Firmicutes* genus was flourished in post-test MX included: *Alkaliphilus* (21.43 %), *Proteiniclasticum* (12.91 %), *Alkalibacter* (4.75 %), *Dethiobacter* (6.64 %), *Exiguobacterium* (4.60 %), *Enterococcus* (3.91 %), *Trichococcus* (3.08 %), *Coprococcus* (2.05 %), *Sedimentibacter* (1.75 %), *Facklamia* (1.42

%) *Clostridium* (1.31 %) and *Acetobacterium* (4.58 %). The resistance *Proteobacteria* identified *Ochrobactrum* (7.95 %), *Agrobacterium* (2.33 %), *and Pseudomonas* (2.24 %). *Actinobacteria Corynebacterium* represented 3.41 % relative abundance. *Actinobacteria Dietzia* highlighted at 3.07 % *Bacteroidetes* genus highlighted was *Dysgonomonas* (2.78 %), and *Bacteroides* (1.65 %). *Archaea Methanolobus* comprised 1.32 % of the total post-test MX relative abundance.

Figure 7-23 represents the genus classification (with relative abundance > 1% ) in pre-test and post-test WT sludge. *Methylibium* (12.82 %) and *Geothrix* (9.33 %) were the abundance genus. Followed by *Flavobacterium* (2.46 %), *Polynucleobacter* (2.04 %), *Synechococcus* (1.10 %) *Prevotella* (2.41 % ). This taxon dropped lower than the detection limit in post-test WT. Thus, *Alkaliphilus* (17.07 %), *Enterococcus* (14.02 %), *Epulopiscium* (6.03 %), and *Natronobacillus* (5.90 %), were the flourished resistance *Firmicutes* genera, which tackled with the extreme condition of textile wastewater. High relative abundance *Proteobacteria* genus included: *Ochrobactrum* (12.78 %). Other genera (1 % > relative abundance) included *Nesterenkonia* (10.19 %), and *Dysgonomonas* (2.26 %) represent *Actinobacteria,* and *Bacteroidetes,* respectively.

It was clearly noticed that *Proteobacteria* was the dominance of bacterial phyla in all the pre-test iron oxides sludge. This phylum retreated in post-test column sludge while *Firmicutes* flourished remarkably. Wang et al. (2018) reported that Azo dye was anaerobically mineralised by bacterial consortium contained *Firmicutes*. *Alkaliphilus* was one of the functional *Firmicutes* genera during azo dye biodegradation. It increased dramatically in all the post-test column substrates used in this experiment. It is anaerobic iron-reducing bacteria, and it is spore generation bacterial species (Zhilina et al. 2009). Yang et al. (2011) reported *Alkaliphilus* was efficient genera in azo dye mineralisation. In post-test column substrates, *Ochrobactrum* synergetic with other genera to degrade azo dye. It reduces Fe (III) by redox mediator, and it enriched in metallic iron contaminated soil (Pandey et al. 2010; Keharia 2012). *Ochrobactrum* remediated azo dye by azo reductase, and it metabolised starch used as an electron donor, redox mediator transfer electron to dye molecule (electron acceptor) to generate the aromatic amines which were also degraded to simplest structure (Khan et al. 2014b).

Additional to iron-reducing bacteria, other species as *Dethiobacter* sulphate reducing bacteria were able to grow in post-test column substrates. It distinguished in rich iron soil as an obligate *Firmicutes* genus (Sorokin et al. 2008a). *Proteiniclasticum* and *Pseudomonas* were identified during dye biodegradation; they reduced azo dye by cleavages the double bond and mineralised the intermediated aromatic amines to $CO_2$ and $H_2O$ (Zhu et al. 2018a). Perei et al. (2001) Agreed that *Pseudomonas* could mineralise azo dye intermediate aromatic amines (Zhu et al. 2018a). *Nesterenkonia* was highlighted in post-test WT sludge. It was found in lakes mud (Collins et al. 2002). It breakdown the azo bond at high pH and salinity condition (Bhattacharya et al. 2017). *Natronobacillus* was described as nitrogen fixation bacteria. It was isolated from soil, it was probably metabolised mono organic carbon and starch anaerobically (Sorokin et al. 2008b). *Achromobacter* was found in post-test MX sludge. It degraded azo dye (Min et al. 2011; Jin et al. 2015). *Corynebacterium* was used to degrade dye in textile wastewater into non-toxic compounds. This genus utilises starch as a growth substrate (Aftab et al. 2011). *Enterococcus* is a facultative anaerobic bacterium. This genus was active during dye degradation as it increased in post-test column substrates. It uses azo reductase to degrade azo dye (Punj and John 2009; Ivanov 2010).

*Agrobacterium, Exiguobacterium, Alkalibacterium and Trichococcus* were detected in post-test iron oxides bearing sludge. Blümel et al. (1998) found that *Agrobacterium* degrades the generated aromatic amines during azo dye biodegradation. *Firmicutes Exiguobacterium* degraded azo dye under high salinity conditions (Dhanve et al. 2008; Forss et al. 2013). *Alkalibacterium* is a facultative anaerobic bacterium, salt-tolerant species. It decolourised azo dye. It can be found in various soils and aquatic sediments (Nakajima et al. 2005). *Trichococcus* is a facultative anaerobic genus (Pikuta et al. 2006). It was one of the dominated genus detected during azo dye degradation at iron-reducing condition (Wang et al. 2018). The flourished Iron-reducing bacterial genera and the affiliated microorganisms in post-test iron oxides bearing sludge were able to degrade azo dye without generated aromatic amines.
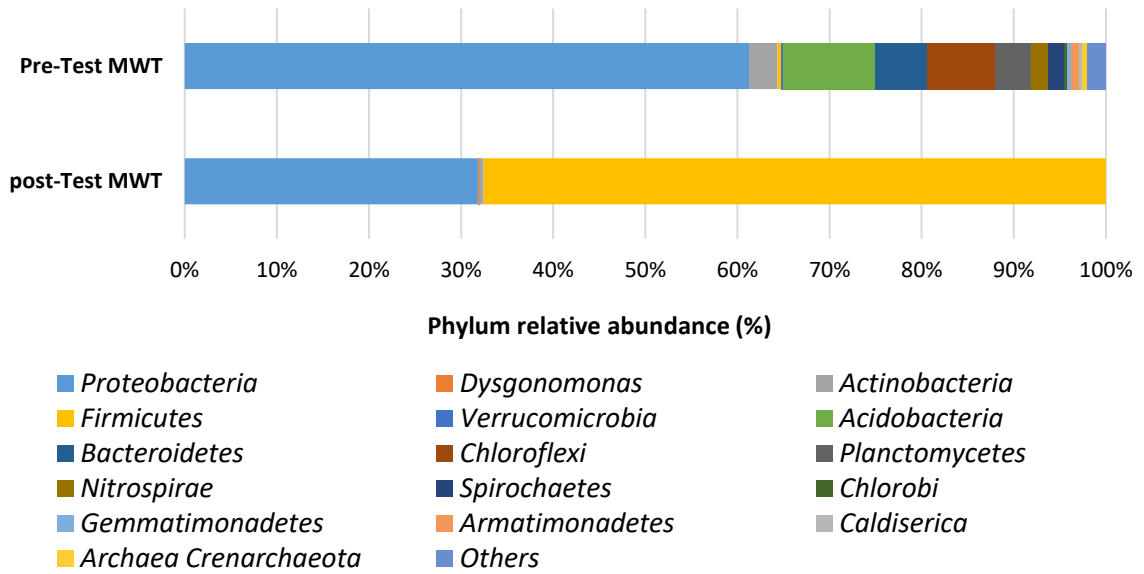
**Figure 7-18 Taxonomic classification of 16S RNA gene at the phylum level for pre-test and post-test MWT sludge.**
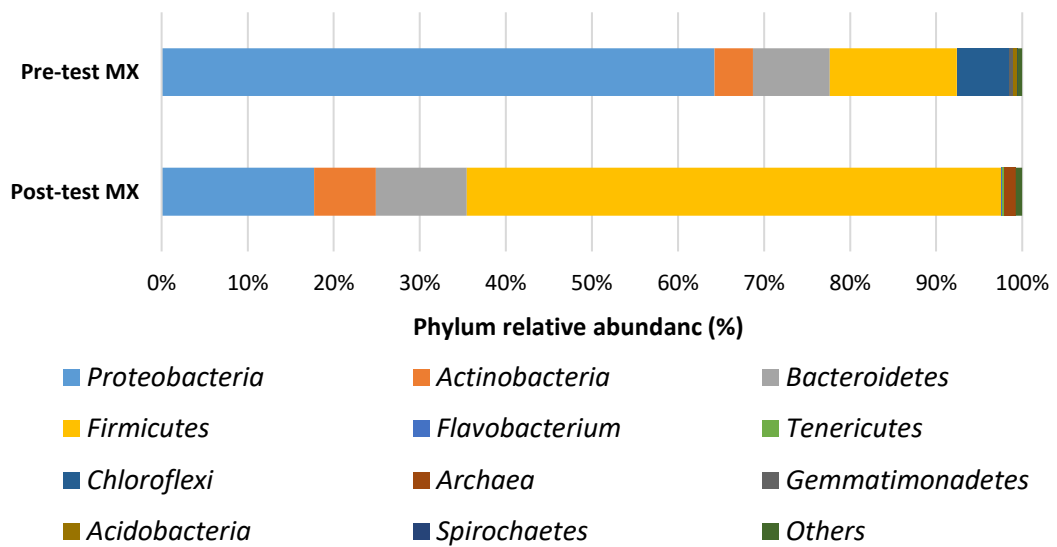


**Figure 7-19 Taxonomic classification of 16S RNA gene at the phylum level for pre-test and post-test MX sludge.**
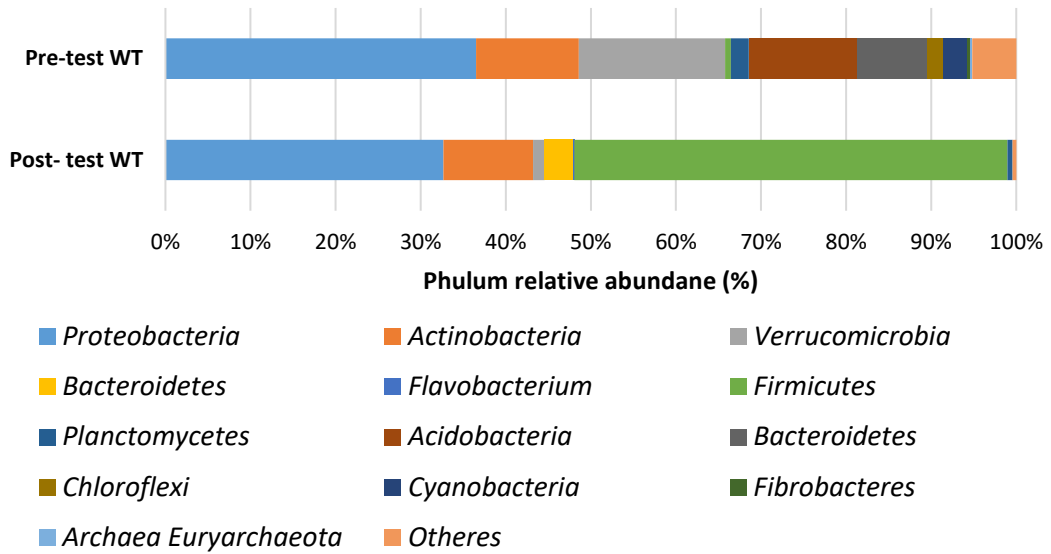
**Figure 7-20 Taxonomic classification of 16S RNA gene at the phylum level for pre-test and post-test WT sludge.**
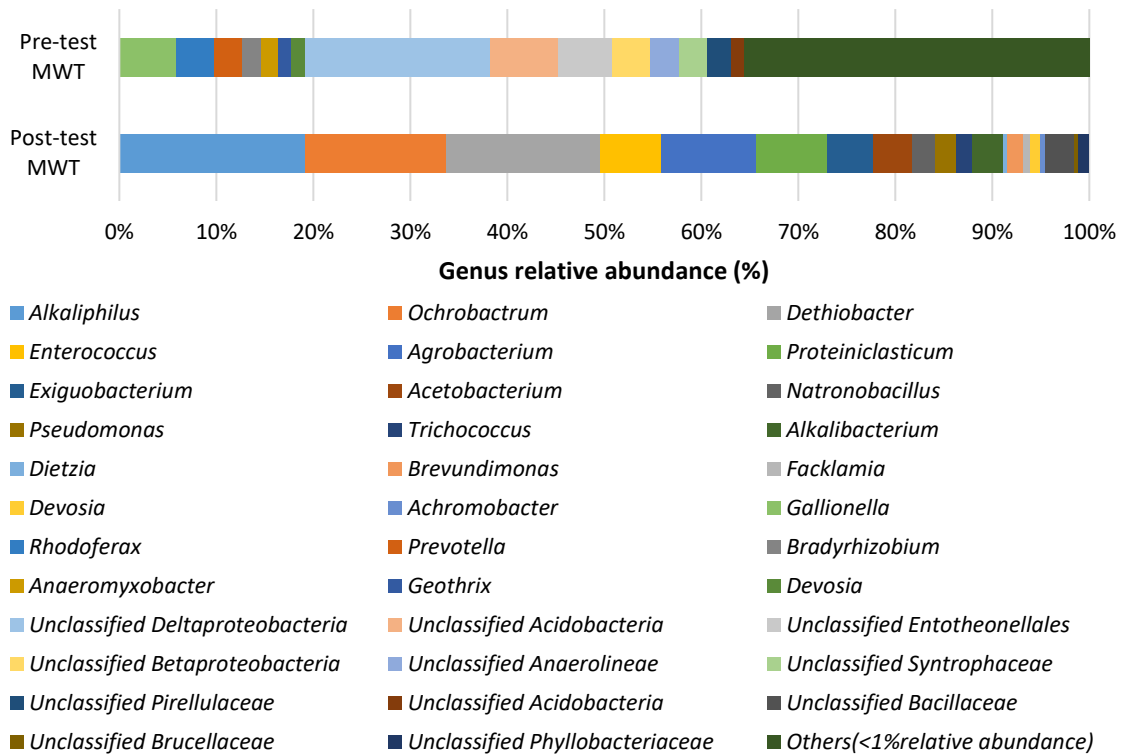


**Figure 7-21 Taxonomic classification of 16S RNA gene at the genus level for pre-test and post-test MWT sludge.**
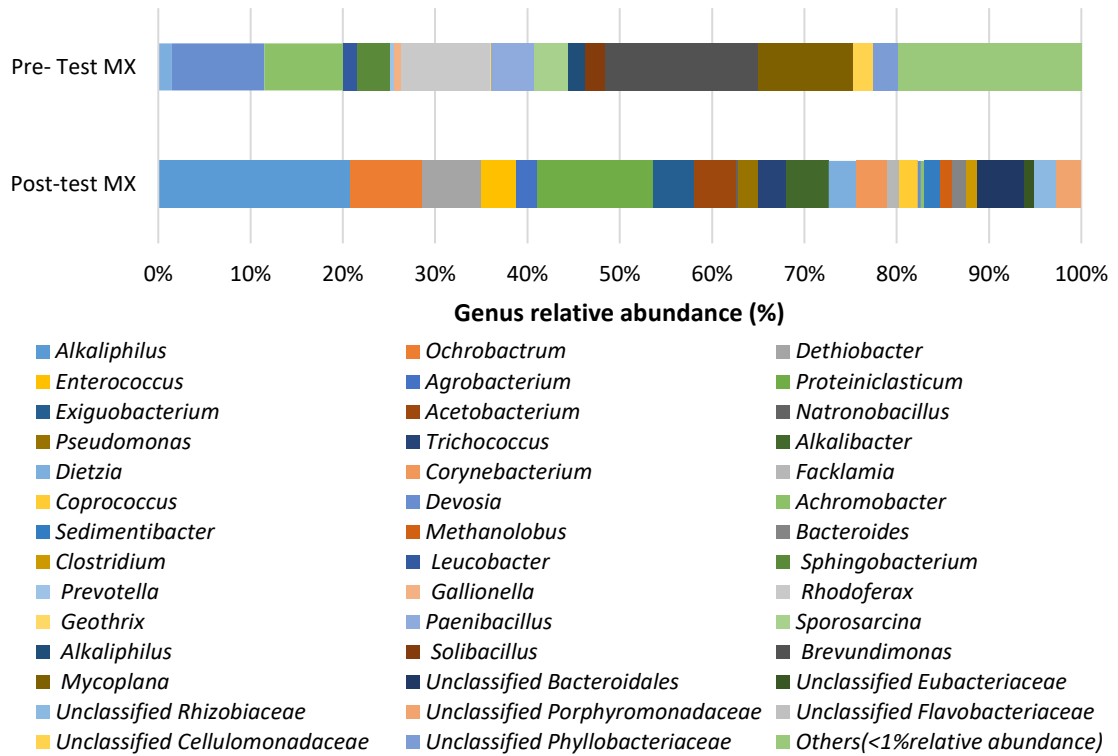
**Figure 7-22 Taxonomic classification of 16S RNA gene at the genus level for pre-test and post-test MX sludge.**
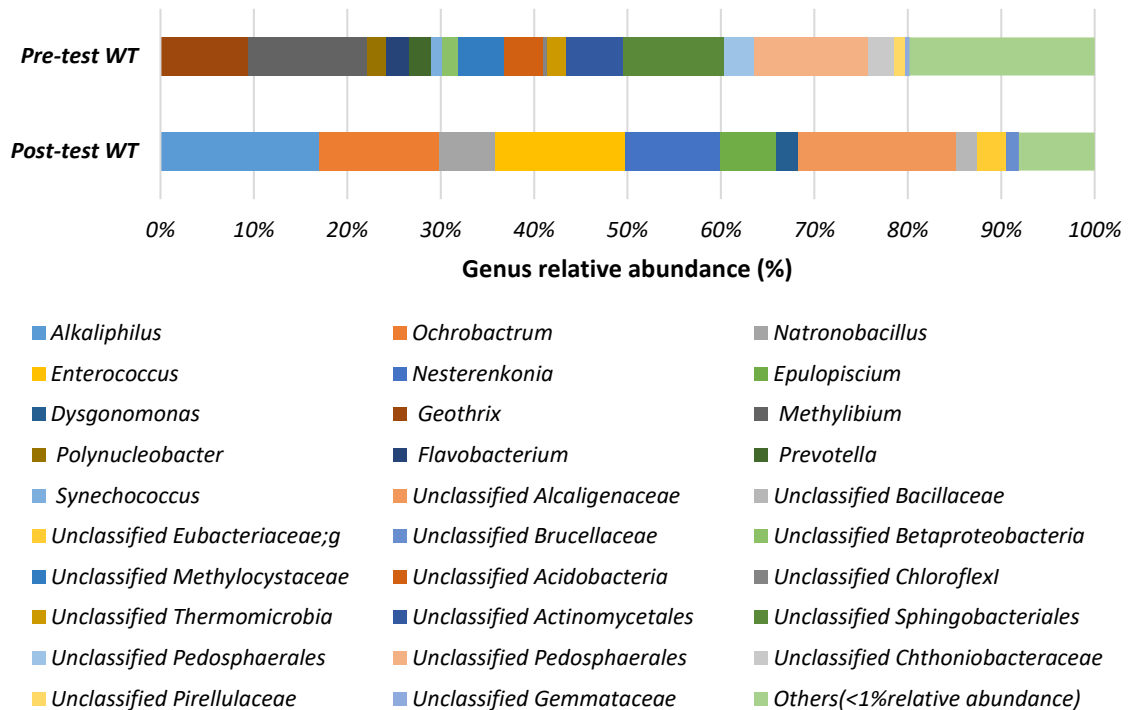


**Figure 7-23 Taxonomic classification of 16S RNA gene at the genus level for pre-test and post-test WT sludge.**

## 7.13    Conceptual model

In this phase, real textile wastewater was degraded by MWT, MX and WT via iron-reducing bacteria and the affiliated microbes by continuous columns experiment. The flourished bacterial genera in post-test column sludge decolourised 81 % of the influent textile wastewater (see Figure 7-3). Biodegradation was the main mechanism for dye removal by iron oxides bearing sludge because these sludges had a low affinity to adsorbed real textile wastewater under experiment conditions (Figure 7-2). These microorganisms also degraded carbon and nitrogen contaminants, and the highest normalised TC and TN was 1394 $g/m^3/day$ and 39 $g/m^3/day$ by MX sludge. The amount of TC removed by adsorption into the column sludge was low at experiment conditions as seen in Figure 7-8 according to that biodegradation was the main reason for TC decline during the experiment. The amount of nitrogen removal was competent with literature in Table 2-5.

According to next-generation sequence, *Firmicutes* was the abundance of bacterial phylum and iron-reducing bacteria were affiliated with other genera in post-test sludge, as shown in Figure 7-21 to Figure 7-21. The flourished bacterial species degraded azo dye without generated aromatic amines as highlighted by the spectrophotometer scan (see Figure 7-4). These species also partially mineralised the influent textile wastewater dyes as highlighted by LC-MS spectrums (see Figure 7-15 to Figure 7-17).

Figure 7-24 clarify the expected mechanism for azo dye and contaminants biodegradation by the flourished iron oxides bearing sludge microorganisms. In reaction A, azo reductase was probably the main enzyme for azo dye degradation as it reduced the azo dye double bone to generate aromatic amines using NADH as a source of electrons. $NAD^+$ was regenerated by oxidised organic carbon or any simple azo dye degradation products generated in the latter reaction. In reaction B, the generated aromatic amines oxidised as electron donor and during that iron-reducing bacteria reduced Fe (III) to Fe (II). Electron shuttles might be abundance in the MX sludge because the amount of wastewater sludge added. It could enhance the dye removal mechanism. Anaerobic ammonium oxidation at iron-reducing condition, which is known as Feammox might be the dominance mechanism for nitrogen removal where ammonium converted to nitrogen simultaneously with Fe (III) reduction to Fe (II) as highlighted in C. Anaerobic ammonium oxidation at nitrite condition (Anammox) is

another nitrogen transformation mechanism. In this reaction, ammonia anaerobically oxidised by reacted with nitrite to generate nitrogen (see reaction D). Nitrification also might occur because of the diversity of the indigenous microorganisms in iron oxides bearing wastes (reaction E).
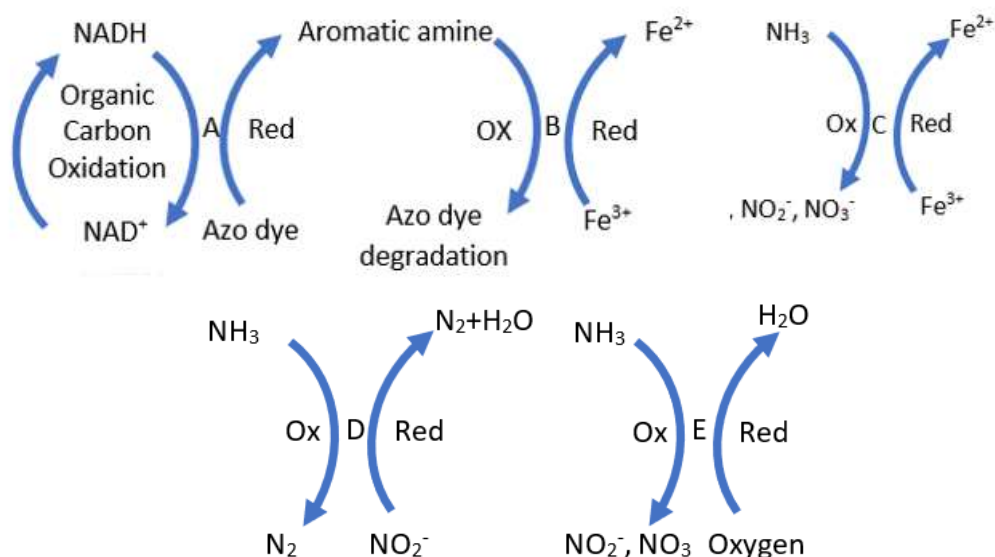


**Figure 7-24 Schematic diagram for dye degradation using iron-reducing microorganism. A: azo dye reduction, B: Oxidised aromatic amines, C: Feammox reaction. D: Anammox reaction, and E: nitrification where Ox: oxidation reaction, Red: reduction reaction.**

Microbial acclimatisation was usually noticed in real textile wastewater experiments. Şen and Demirer (2003) asserted that anaerobic sludge should be acclimatised for 24 days before treated textile wastewater. Chinwetkitvanich et al. (2000) reported that acclimatised microorganisms for five years were used to mineralise real textile wastewater, while Igor et al. (2010) conducted textile wastewater treatment using acclimatised microorganism for 30 days. In the above-mentioned studies, the dye decolourisation did not exceed more than 70 %. In contrast, the utilised iron oxides bearing sludge had removal efficiently up to 81 % removal efficiency without pre-acclimatisation.

All the evidence reported in this conceptual model and other conceptual models in chapter five and six provided sufficient evidence for the ability of MWT, MX and WT sludge as a microbial substrate to remediate textile wastewater. In addition, it decreased the nitrogen and carbon contaminants because of the diversity of iron-reducing bacteria and the affiliated genera in these sludges.

Chapter 8 : Municipal wastewater experiment results and discussions.

## 8.1    Introduction

This chapter presents and discusses the municipal wastewater treatment results, including chemical oxygen demand, total carbon removal, nitrogen removal mechanism, phosphorus and sulphate removal rate and other operation parameters. Gene sequencing was used to identify the microbial change in column substrates before and after treatment to highlight the effective bacterial gene. A conceptual model was used to demonstrate the mechanisms involved.

## 8.2    Experimental parameters

All experiment parameters were measured as reported in section 3.8. In this experiment, the influent wastewater pH was 7.8 ± 0.2. The general trend lines for all column effluents were varied between 7.2 to 8.2 (Figure 8-1). The experiment pH range suggests that all column sludge could be an appropriate environment for nitrogen biodegradation according to previous studies (Painter and Loveless 1983; Alleman 1985; Antoniou et al. 1990; Van Dongen et al. 2001). Sylvia et al. (1998) reported that any drastic change in pH could suppress microbial enzyme activity, and it could deactivate some intrinsic biodegradation enzymes and might obstruct microorganism metabolisms. Dissolved oxygen (DO) was monitored in Figure 8-2. In the first ten days, DO was dropped from 7.00 ± 0.5 mg/l which was the influent concentration to 4.32 mg/l, 4.69 mg/l and 2.32 mg/l in MWT, MX and WT effluents, respectively. DO was below 4.50 mg/l during the first 80 days. From this point, it decreased gradually, and the lowest DO concentration was measured on day 80 days at 2.87 mg/l, 2.46 mg/l and 2.20 mg/l for MWT, MX and WT columns, respectively. Figure 8-3 demonstrates the temperature distribution during municipal wastewater treatment. The experiment was conducted in a relatively low-temperature range (3 °C to 11 °C) in the first month. Temperature gradually increasing with time but did not exceed 15 °C until the second month. This temperature was a conducive environment for a psychrophilic microorganism (microorganism lives in low temperature < 15 °C environment). After the second month, the highest temperature recorded was 24.5 °C on day 99, which was a conducive environment for a mesophilic microorganisms whose optimal temperature for growth is  20 °C to 45 °C (Batstone et al. 2002). In wastewater treatment, temperature could be influenced either by the seasonal change or because of treating

more than one type of wastewater in the same plant. The temperature changes has an adverse effect on nitrogen transformation and organic carbon biodegradation which are the main mechanisms for municipal wastewater treatment (Van Dongen et al. 2001; Wang et al. 2017).
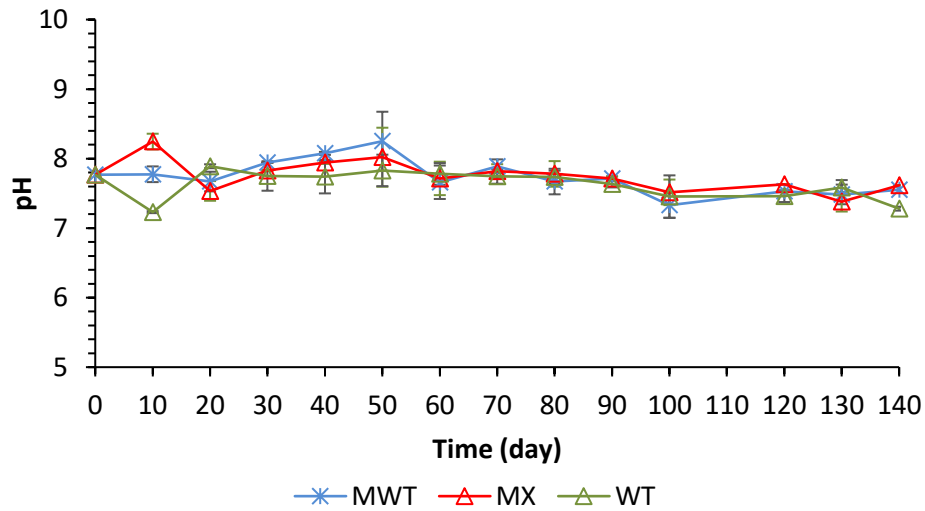


**Figure 8-1 the pH trend line in column effluents during municipal wastewater experiment.**
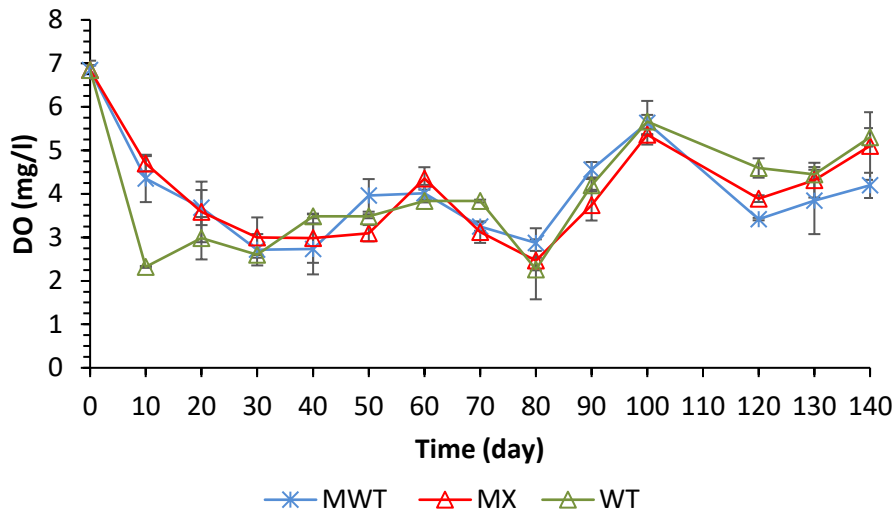


**Figure 8-2 Dissolved oxygen concentration in column effluents during municipal wastewater experiment.**
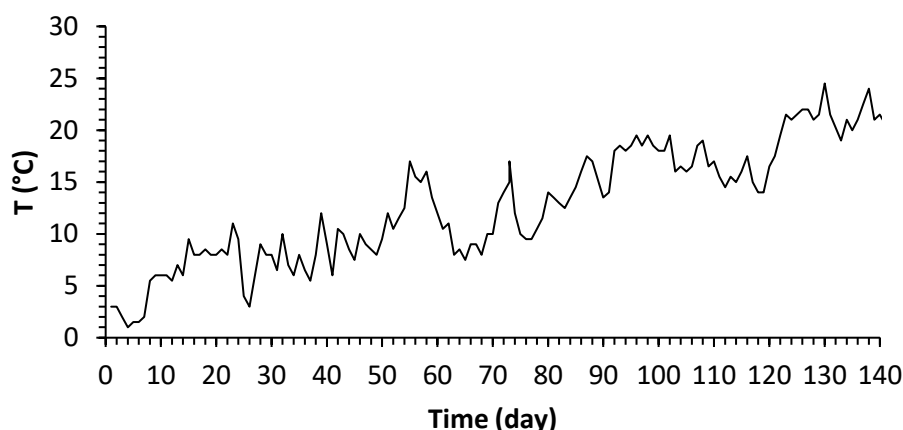
**Figure 8-3. Average daily temperature recorded during municipal wastewater experiment.**

## 8.3 Chemical oxygen demand (COD) and Total carbon (TC) removal

Chemical oxygen demand (COD) and total carbon were measured as reported in section 3.8. The COD concentration for influent municipal wastewater was $236 \pm 5$ mg/l as shown in Figure 8-4. After ten days, it declined to 93.90 mg/l and 99.40 mg/l in MWT, and MX effluents respectively while WT needed three folds this time to achieve a comparable result. From this point onward, the COD concentration continued to decline, and the lowest COD was 22 mg/l in MX effluents, it was followed by MWT (32 mg/l), and WT (53 mg/l). COD is a common parameter used to assess wastewater treatment processes (Von Sperling and Chernicharo 2005; Sperling 2007). Hernández Leal et al. (2007) reported that the highest COD removal using anaerobic reactor for treating wastewater did not exceed more than 50 % while in this experiment, about 80 % of the COD was removed using rich iron substrates via the indigenous microbial consortia.

Total carbon (TC) concentration in the influent municipal wastewater was $104.30 \pm 0.50$ mg/l, as shown in Figure 8-5 A. TC retreated gradually with time and by the end of the experiment, it decreased to 12.40 mg/l, 19.24 mg/l, and 27.44 mg/l in MWT, MX, and WT, respectively. The carbon removal rate was calculated, as highlighted in Appendix 2. The highest normalised TC removal rate was 301 g/m$^3$/day by MWT, it was followed by MX (279 g/m$^3$/day) and WT (259 g/m$^3$/day) as shown in Figure 8-5 B. The total carbon TC was also monitored in the pre-test and post-test column

substrates is shown in Figure 8-5 C to estimate any carbon adsorbed during municipal wastewater experiment. TC in pre-test MWT, MX and WT sludge were 1.52 %, 4.30 %, and 14.55 % respectively while it was 1.01 % 4.71 %, and 12.40 % in MWT, MX, and WT post-test sludge samples. The difference between TC in sludge samples before and after treatment confirmed that the carbon adsorption or precipitation could be ignored in this experiment. TC removal in column effluents referred that about 80 % of the influent organic carbon was removed. The low TC and COD removal noticed during the first two weeks (see Figure 8-3) was probably because of the low-temperature range (see Figure 8-3) and lack of microbial acclimatisation for sludge indigenous microorganisms. These microorganisms need sufficient time for adaptation with the new environment. MWT and MX column's microorganisms tolerated low temperature and were able to degrade the municipal wastewater contaminants. At the same time, carbon removal increased in WT only when the temperature rose, indicating that the MWT indigenous microbes acclimatised faster than the WT column's microbial consortium.
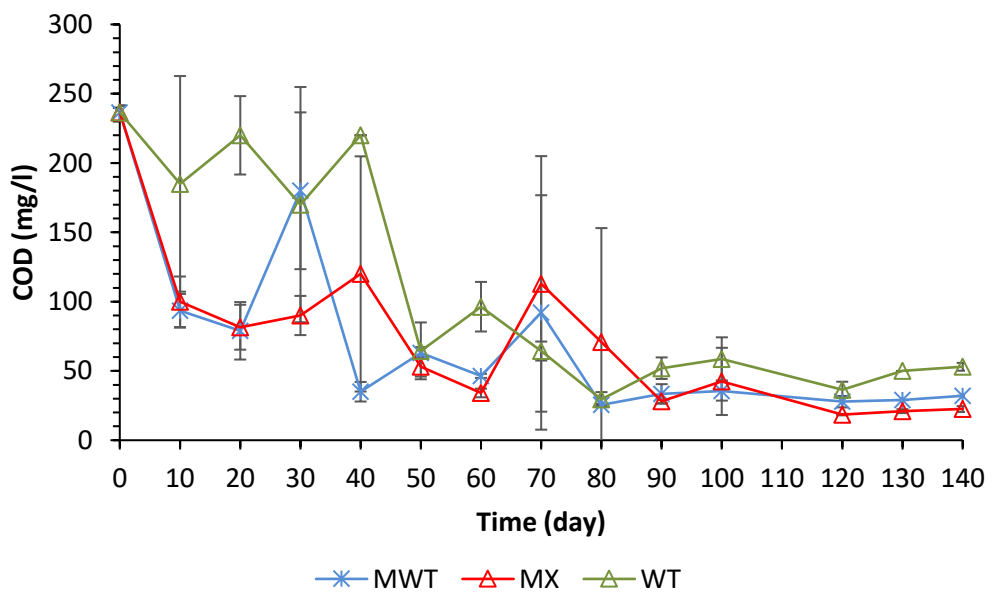


**Figure 8-4 Chemical Oxygen Demand (COD) detected during municipal wastewater experiment.**
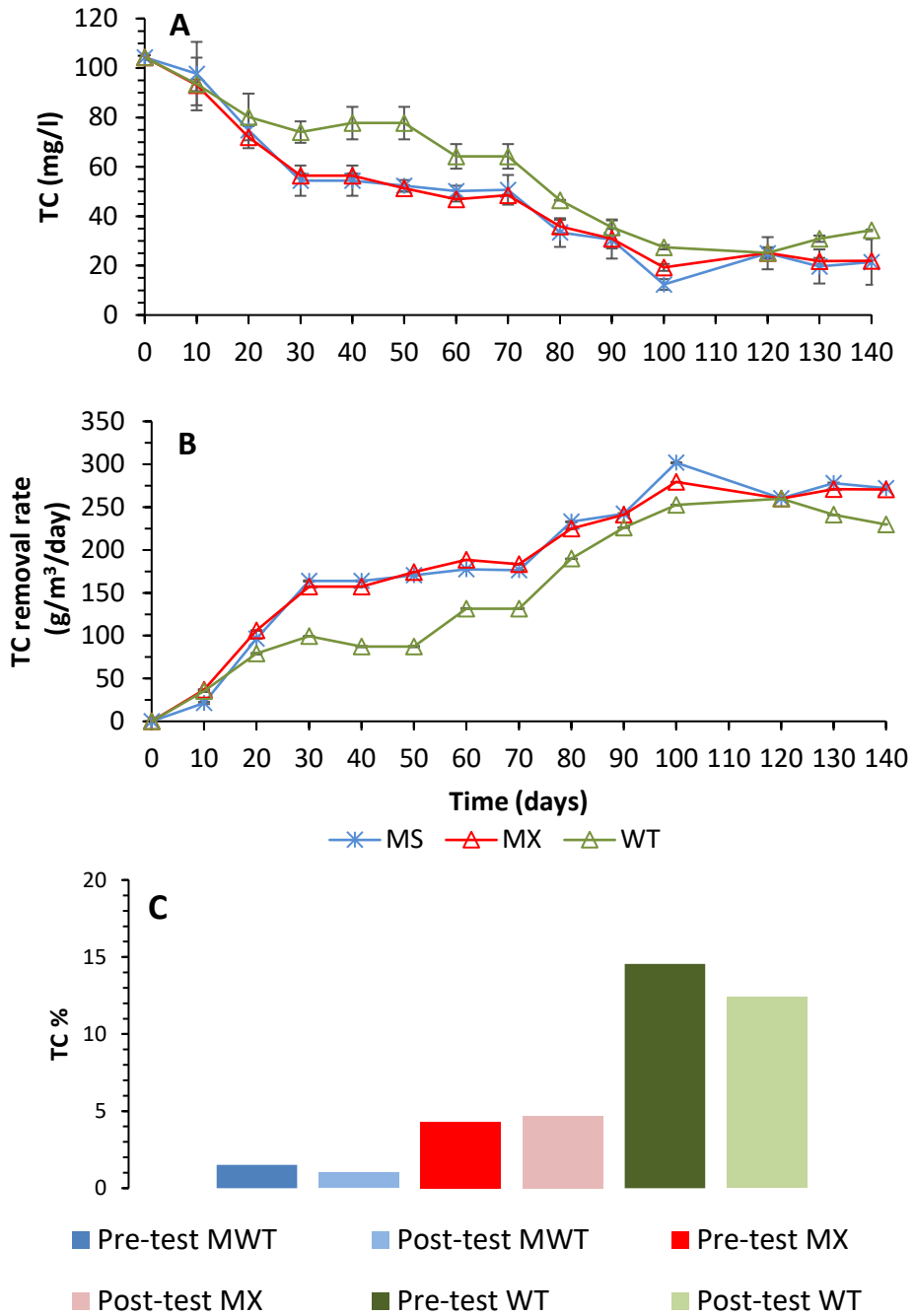
**Figure 8-5** **(A)** Total carbon concentration in column effluents, **(B)** Total carbon removal rate in column effluent, and **(C)** Total carbon in pre-test and post-test column substrates.

## 8.4　Nitrogen removal

Ammonia-nitrogen ($NH_3$-N), nitrate and nitrite were measured as reported in section 3.8. The ammonia-nitrogen ($NH_3$-N) concentration was $60 \pm 1$ mg/l in the influent wastewater as shown in Figure 8-6 A. It was a comparable concentration to the highest nitrogen-ammonia concentration range in real municipal wastewater (Sedlak 1991). After ten days, $NH_3$-N decreased in all columns, especially in MX (35.50 mg/l), and recovered during the first two months. From this point, $NH_3$-N decreased until the end of the experiment in MWT (18.50 mg/l), MX (23.50 mg/l) and WT (15.50 mg/l). Nitrite concentration was highlighted in Figure 8-6 B. This figure shows that the highest nitrite concentration was at days 90 in MWT (42 mg/l), MX (29 mg/l) and WT (27 mg/l). At this time, nitrate highest concentration was 6 mg/l in WT effluent, followed by 3.20 mg/l in MX, and 2.40 mg/l in MWT effluents, see Figure 8-6 C. The highest normalised nitrogen removal rate was 159, 142.44 and 141.84 g/m$^3$/day by MX, WT and MWT as reports in Figure 8-6 D see Appendix 2 for calculations.

In this experiment, a comparison of temperature trendline (Figure 8-3) with nitrogen removal rate (Figure 8-6 D) highlighted that the nitrogen removal rate increased when temperature increased. Nitrification is the conventional mechanism for nitrogen transformation. In this reaction ammonia oxidised to nitrite and nitrite oxidised to nitrate, nitrification bacteria are sensitive to temperature changes (Van Dongen et al. 2001; Wang et al. 2017). Additionally, nitrification bacteria has a low growth rate during municipal wastewater treatment, and it affects by temperature changes (Kuschk et al. 2003; Von Sperling 2007; Dotro et al. 2017). Also, comparing the $NH_3$-N (Figure 8-6 A) with COD and TOC figures (Figure 8-5 A and B) revealed that $NH_3$-N decline was related with TOC decrease during the period (70-140 days). It might because the microbial community required about two months to acclimatise with municipal wastewater condition. The delay noticed in $NH_3$-N removal during the first term of the experiment covering days 1 to 70 might because adsorption was the main mechanism for nitrogen removal, especially over 10 to 20 days (Figure 8-6 D). Nevertheless, as Dotro et al. (2017) point out, $NH_3$-N removal by adsorption can be neglected as a significant removal mechanism in long term wastewater treatment.

The column effluent pH (Figure 8-1) was an appropriate range for microbial nitrogen transformation (Painter and Loveless 1983; Alleman 1985; Antoniou et al. 1990; Van

Dongen et al. 2001). Oxygen initiates nitrification bacteria while anaerobic conditions are a prerequisite to start denitrification (Suarez et al. 2010). Other nitrogen removal mechanisms such as Feammox and Anammox might be involved in nitrogen removal during this experiment because column substrates are rich in both iron-reducing microorganism and iron oxides, which is the appropriate condition for these mechanisms. Ammonium can be anaerobically oxidised to dinitrogen and nitrite by Feammox. The generated nitrite used to reduce ammonium (Li et al. 2018). It might be the reason for not detecting large concentrations of nitrite in the column effluents. During Feammox iron-reducing bacteria spontaneously remove nitrogen contaminants and reduced Fe (III) to Fe (II) (Ding et al. 2014). Feammox is a natural phenomenon to reduce ammonium in diverse habitats (Shrestha et al. 2009; Ding et al. 2014), and it can be described by equations 25 to 27 (Yang et al. 2012; Ding et al. 2014; Li et al. 2018):

$$3Fe(OH)_3 + 5H^+ + NH_4^+ \rightarrow 3Fe^{2+} + 9H_2O + 0.5N_2 \qquad \text{(Equation 25)}$$

$$6Fe(OH)_3 + 10H^+ + NH_4^+ \rightarrow 6Fe^{2+} + 16H_2O + NO_2^- \qquad \text{(Equation 26)}$$

$$8Fe(OH)_3 + 14H^+ + NH_4^+ \rightarrow 8Fe^{2+} + 2H_2O + NO_3^- \qquad \text{(Equation 27)}$$
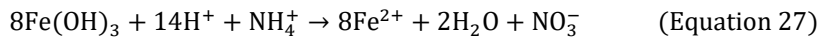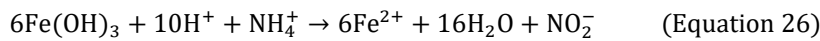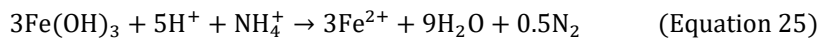
Nitrite reacted with Fe (II) according to the reactions below (see equations 28 to 35) to regenerated Fe (III). The generated Fe (III) might be precipitated in the column substrates (equation 30 – 35). In other studies, it was noticed that the generated Fe (II) is re-oxidised to Fe (III) during Feammox mechanism (Li et al. 2018; Yang et al. 2019). It may be the reason for not detecting ferrous iron at high concentration in the column effluents during municipal wastewater experiment (see Figure 8-7 B).

$$6Fe(II) + 2NO_2^- + 8H_2O \rightarrow 6FeOOH + N_2 + 10H^+ \qquad \text{(Equation28)}$$

$$9Fe(II) + 2NO_2^- + 8H_2O \rightarrow 3Fe_3O_4 + N_2 + 16H^+ \qquad \text{(Equation29)}$$

$$4Fe(II) + 2NO_2^- + 5H_2O \rightarrow 4FeOOH + N_2O + 6H^+ \qquad \text{(Equation30)}$$

$$6Fe(II) + 2NO_2^- + 5H_2O \rightarrow 2Fe_3O_4 + N_2O + 10H^+ \qquad \text{(Equation31)}$$

$$6Fe(II) + NO_2^- + 10H_2O \rightarrow 6FeOOH + NH_4^+ + 10H^+ \qquad \text{(Equation 32)}$$

$$9Fe(II) + NO_2^- + 10H_2O \rightarrow 3Fe_3O_4 + NH_4^+ + 16H^+ \qquad \text{(Equation33)}$$

$$Fe(II) + NO_2^- + H_2O \rightarrow FeOOH + NO + H^+ \qquad \text{(Equation34)}$$

$$3Fe(II) + NO_2^- + 3H_2O \rightarrow Fe_3O_4 + NO + 6H^+ \qquad \text{(Equation35)}$$
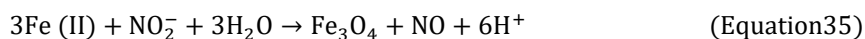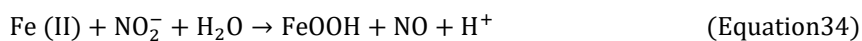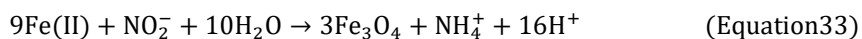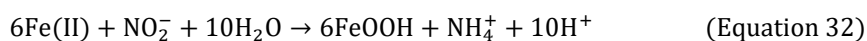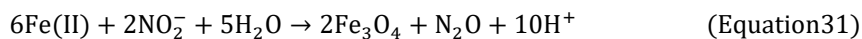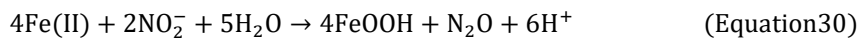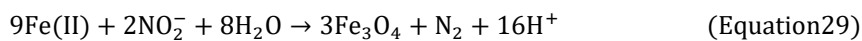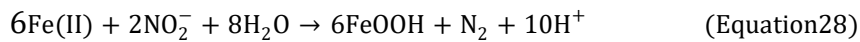
Nitrate dependent Fe (II) oxidation (NDFO) is another mechanism could occur at iron-reducing conditions when the generated Fe (II) from iron-reducing bacteria reacts with nitrate to generates nitrogen (Yang et al. 2019) (see equations 36, and 37). This could be additional evidence for not detected ferrous in high concentration in column effluents during municipal wastewater experiment.

$$2NO_2^- + 6Fe^{2+} + 8H^+ \rightarrow 6Fe^{3+} + N_2 + 4H_2O \qquad \text{(Equation 36)}$$

$$2NO_3^- + 10Fe^{2+} + 12H^+ \rightarrow 10Fe^{3+} + N_2 + 6H_2O \qquad \text{(Equation 37)}$$
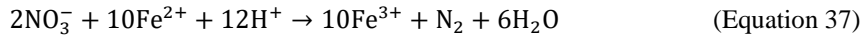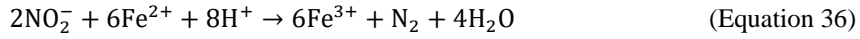
NDFO and Feammox is a complimentary co-mechanism, Fe (III) generated by NDFO is used by Feammox, and NDFO uses Fe (II) generated by Feammox. Li et al. (2018b). Li et al. (2017b) found that Feammox mechanism can be stimulated by adding iron oxides to anammox sludge while the utilised iron oxides bearing sludge probably natural habitats for Feammox and Anammox. The normalised nitrogen removal rate using iron oxides bearing sludge by indigenous microorganisms (Figure 8-6 D) was acceptable compared with the literature in Table 2-8.
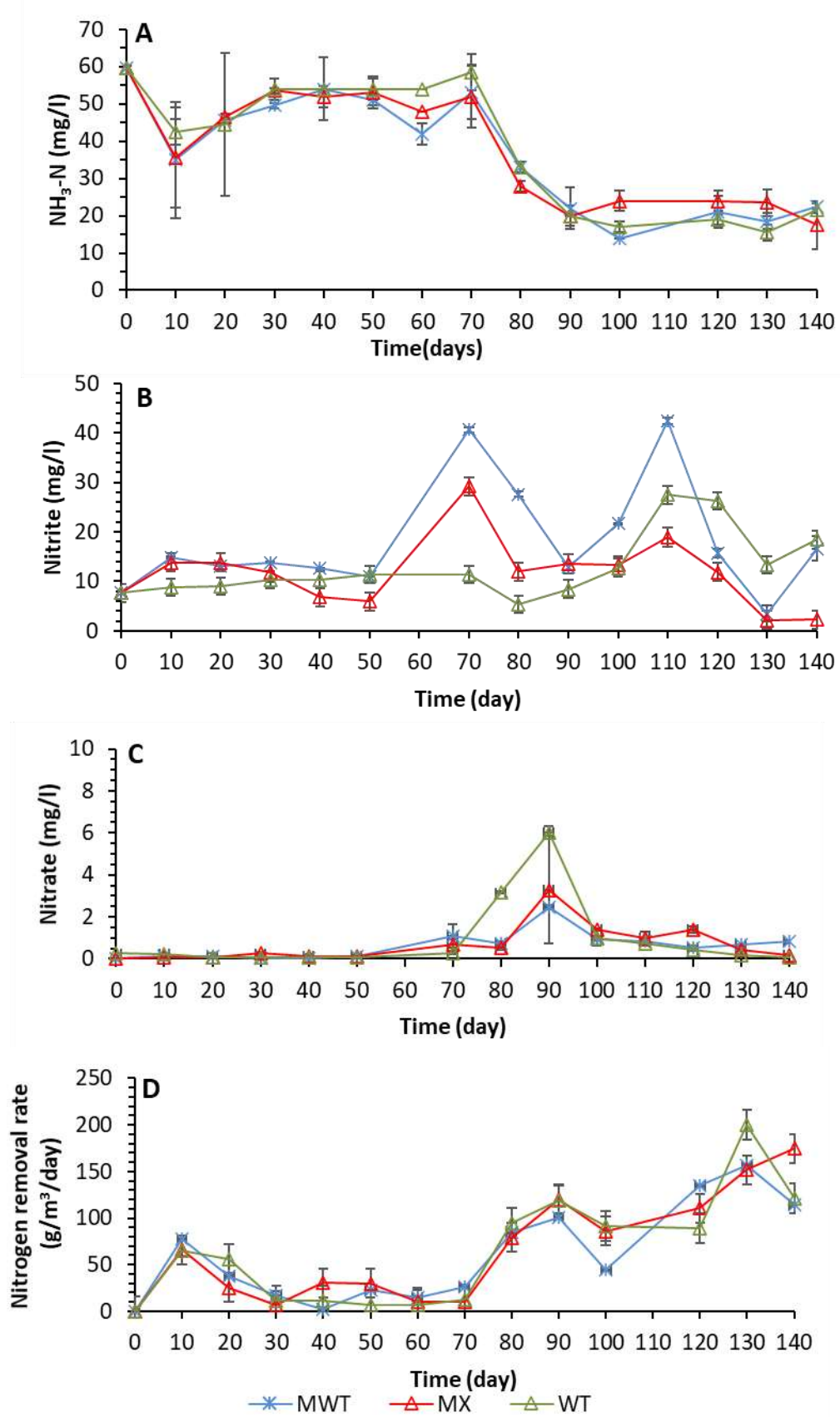
**Figure 8-6 Nitrogen concentration in column effluents during municipal wastewater experiment, (A) NH₃-N, (B) Nitrite, (C) Nitrate, and (D) Nitrogen removal rate.**

## 8.5　Total iron and ferrous iron concentrations

Total iron and ferrous iron were measured as reported in section 3.8. Iron concentration in WT effluent was higher than the other columns, the highest iron concentration was detected in WT (8.70 mg/l) in days 130 while it did not exceed more than 2 mg/l in both MWT and MX effluents (see Figure 8-7A). Ferrous concentration was about 0.36 mg/l in the influent wastewater. The highest ferrous concentration was 1.50 mg/l in WT effluents, while it was below the detected range in other columns, as highlighted in Figure 8-7 B. Iron bearing sludge are rich substrate with iron oxides, and it could be natural habitats for iron-reducing bacteria. These bacteria affiliated with other species as demonstrated in previous chapters (chapter five, six and seven). Detection of ferrous is probably an indication for the activity of iron-reducing bacteria. However, some of the generated ferrous could be re-oxidised to Fe (III), or it might precipitate in the column sludge, as mentioned in section 8.4. Iron reducing bacteria reduces Fe (III) to Fe (II) either by direct contact or by electron shuttles as indirect contact (Lovley et al. 1996; Nevin and Lovley 2002b). Watanabe et al. (2009) reported that electron shuttles could be found in a natural environment, or it can be synthesised by microorganisms. Humic acids which probably found in MX sludge as it contained municipal sludge are considered as electron shuttles (Lovley et al. 1996; Hayes et al. 1998).
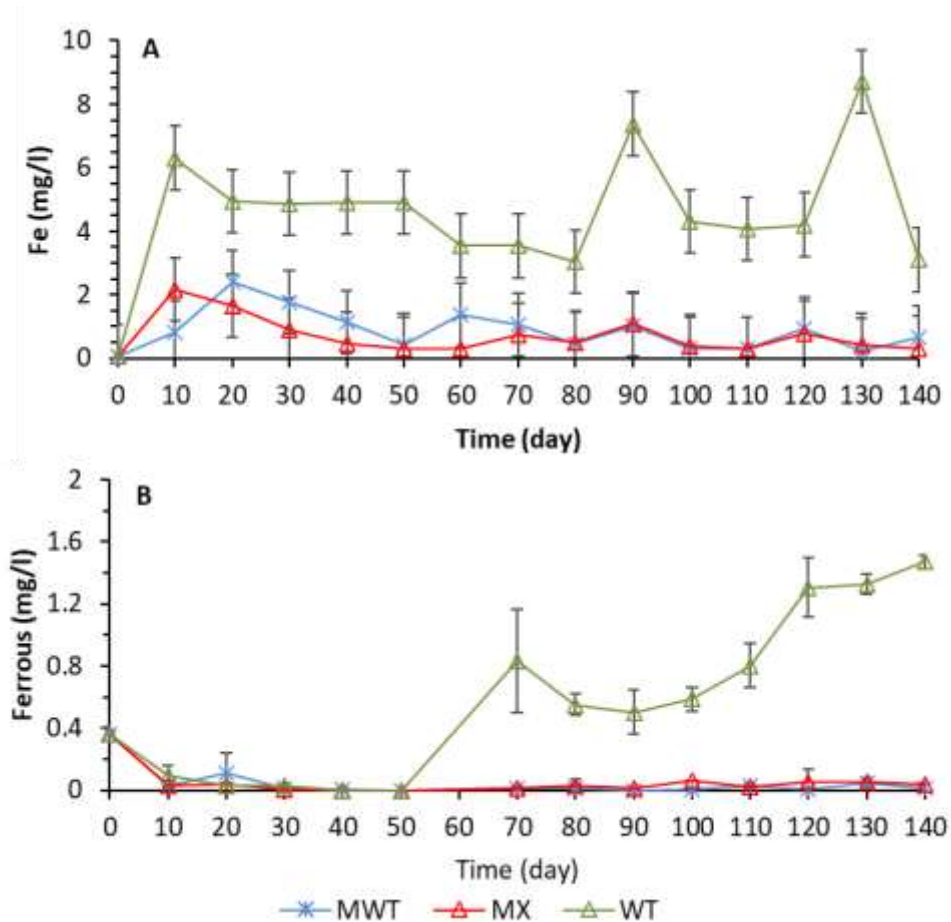
**Figure 8-7 (A) total iron, (B) ferrous iron concentrations during municipal wastewater experiment.**

## 8.6    Phosphorus removal

Phosphorus concentration was $14.29 \pm 0.2$ mg/l in the influent wastewater (see section 3.4 for more details). After two weeks, it declined dramatically by MWT (0.37 mg/l), MX (0.47 mg/l), and WT (2.91 mg/l) as shown in Figure 8-8A. From this point, phosphorus concentration gradually increased with time, and the average phosphorus removal was less than 50 % by the end of the experiment. Figure 8-8B shows that the phosphorus removal rate by the end of the experiment was about 25 $g/m^3/day$ in all columns used. Biological phosphate removal is probably involved because one of the flourished bacterial genera detected in section 8.9 is sulphate accumulation bacteria. Polyphosphate (polyp) in the form of P accumulated by microorganisms. In conventional wastewater processes, phosphorus removal efficiency by adsorption does not exceed 20 % using activated sludge which should be reactivated to be reuse

(Blackall et al. 2002). Furthermore, Lötter (1985) mentioned that even by using pure phosphorus bacterial strains phosphorus removal was below 40 %. While in this process, about 50 % of phosphorus was removed without pre-acclimatised (Figure 8-8). Polyphosphate accumulating organisms (PAOs) and Glycogen accumulating organisms (GAOs) are the two types of microorganism responsible to uptake phosphorus as polyphosphate (Barnard 1976; Nicholls and Osborn 1979; Groenestijn et al. 1989; Blackall et al. 2002). Ge et al. (2013) noticed that high phosphorus concentration might affect biological nitrogen removal. Nevertheless, in this experiment, high phosphorus did not affect nitrogen removal (Figure 8-6 D). Adsorption is another mechanism for phosphorus removal using iron oxide (Zhang and Pan 2014; You et al. 2015). Jørgensen et al. (2017) reported that iron sludge had a low adsorption capacity, it adsorbed 0.2 mg/l of phosphorus. Torrent et al. 1992 found that an initial 1 mg/l phosphorus concentration, the amount of P adsorbed by iron oxides was 2.04 µmol/m$^2$ after 24, and it raised to 3.18 µmol/m$^2$ after 75 days. Based on the reported evidence, the amount of phosphorus removed during the experiment was probably a combination of biological and physical effects.
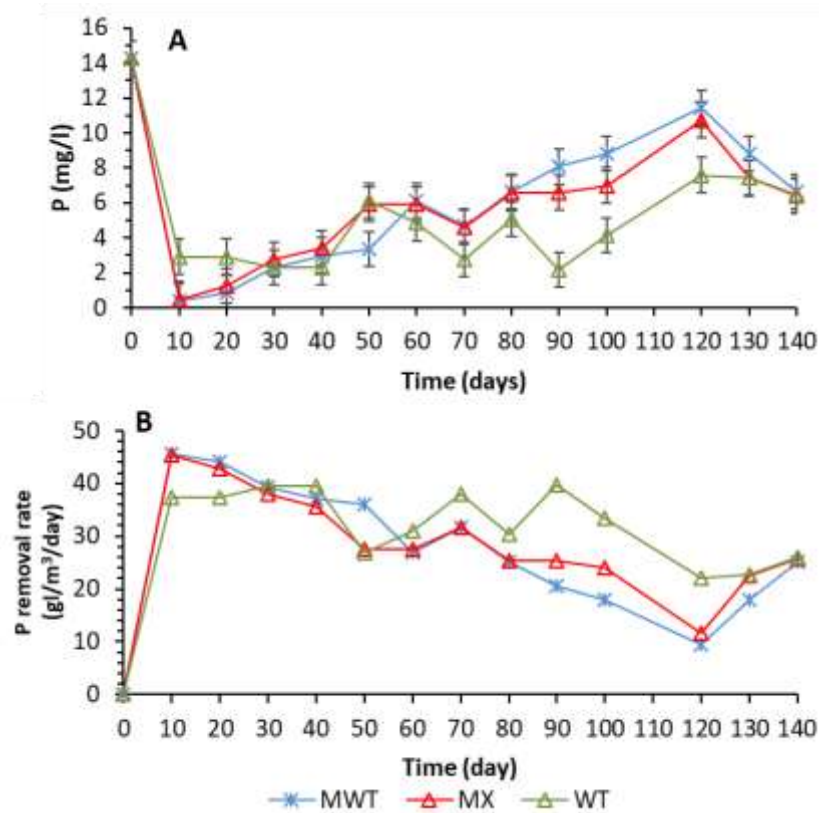


**Figure 8-8 (A) Phosphorus concentration during municipal wastewater experiment, and (B) Phosphorus removal rate.**

## 8.7 Sulphate removal

Sulphate concentration ($SO_4$) was $2.5 \pm 1$ mg/l in the influent wastewater, during the municipal wastewater treatment it fluctuated with the time between 2.50 mg/l - 0.25 mg/l as highlighted in Figure 8-9. Koch and Mendelssohn (1989) reported that sulphate could suppress the growth of various microorganisms even though iron-reducing bacteria and the affiliated microorganism tolerated sulphate concentration during municipal wastewater experiment.
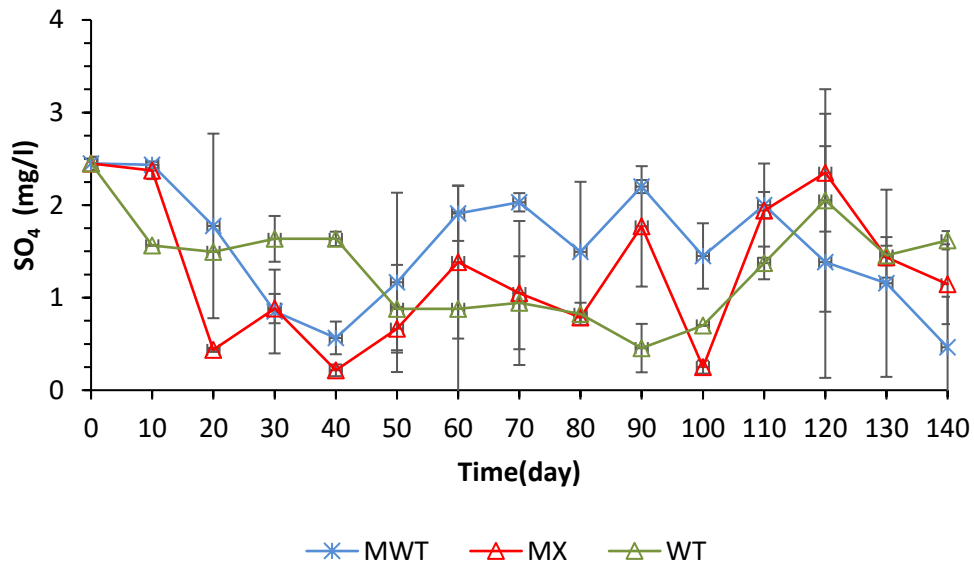


**Figure 8-9 Sulphate concentration in column effluents during municipal wastewater experiment, influent concentration was $2.5 \pm 1$ mg/l.**

## 8.8 Parameters correlation for municipal wastewater experiment

IBM SPSS statistic software (version 20) was used to find the correlation between municipal wastewater parameters using bivariate analysis. These parameters were invalidated the normal distribution assumptions ($p < 0.05$). Therefore, Spearman was used to determining the significant correlation for these parameters. The correlation between TC and TN removal rate was a significant positive in MWT (0.68), MX (0.76) and WT (0.70) according to the determined correlation coefficient value. In contrast, a significant negative correlation was demonstrated between TC removal rate and pH

in MWT (-0.73) and MX (-0.65) column effluents. It was found that the correlation between TN removal rate and pH was significant negative in MWT (-0.69) and WT (-0.69) columns. The correlation between TC and TP removal rates was significant negative for MWT (-0.55) and MX (-0.54). The temperature was positively correlated with TC removal rate for MWT (0.76), MX (0.76) and WT (0.78) effluents. Similarly, the correlation was significantly positive for TN removal rate and temperature in MWT (0.72), MX (0.66) and WT (0.66). There was no correlation between TC and TN removal rate and ferrous in MWT and MX columns while it was significantly positive at 0.78 and 0.62 for WT columns.

## 8.9 Microbial community changes in pre-test and post-test column sludge

In pre-test MWT sludge, 17 phyla were detected included *Crenarchaeota* (0.59%) as the only archaea phyla, and the others were identified as bacteria phyla. In post-test MWT, bacterial phyla declined to 11, and archaea were below the detection range (Figure 8-10). *Proteobacteria* (61.24 %) was the highest abundance phylum in pre-test and post-test MWT. Thus, it declined to 41.04 % in post-test MWT. *Acidobacteria* (9.98 %) was the second abundance phylum in pre-test MWT sludge, and it raised to 10.62 % relative abundance in post-test MWT. *Chloroflexi* dropped dramatically from 7.44 % in pre-test MWT sludge to 0.15 % in post-test MWT. *Firmicutes* was the second highest bacterial phylum in post-test MWT as it was highlighted at 28.05 % compared with only 0.42 % relative abundance in pre-test MWT sludge. *Bacteroidetes* raised from 6.65 % to 15.32 % relative abundance in post-test MWT. *Actinobacteria* retreated in pre-test MWT from 3.09 % to 1.02 % in post-test MWT. Another phylum presented in pre-test MWT sludge as: *Planctomycetes* (3.85 %), *Nitrospirae* (1.89 %), *Spirochaetes* (1.68 %) *Verrucomicrobia* (0.2 %), *Chlorobi* (0.43 %), *Gemmatimonadetes* (0.45 %), and *Caldiserica* (0.31 %). Bacterial genera affiliated with *Bacteroidetes* and *Proteobacteria* in pre-test MWT sludge were included *Gallionella* (5.82 %), *Prevotella* (2.86 %), *Bradyrhizobium* (1.91 %), *Anaeromyxobacter* (1.77 %), and *Devosia* (1.39 %) were below the detection range in post-test MX. The genus taxonomic classification for post-test MWT found that *Geobacter* (12.24 %) was the highest *Proteobacteria* genera (Figure 8-11). *Rhodoferax* was another *Proteobacteria* genus. It existed in both pre-test MWT sludge (8.77 %) and post-test MWT (4.00 %). *Trichococcus* (10.21 %) was the second-

highest genus in post-test MWT, and *Geothrix* increased from 1.39 % in pre-mining to 9.66 % in post-test MWT. Anther flourished taxon in post-test MWT are *Rhodocyclus* (7.75 %), *Clostridium* (2.90 %), *Fusibacter* (2.97 %), *Desulfosporosinus* (2.14), *Proteiniclasticum* (2.12 %), and *Brevundimonas* (1.15 %).

Figure 8-12 highlights the bacterial phylum in pre-test and post-test MX sludge. *Proteobacteria* relative abundance was sharply declined from 64.23 % in pre-test MX sludge to 5.24 % in post-test MX. *Proteobacteria* abundance *genus in* pre-test MX (relative abundance>1%) included *Brevundimonas* (16.66 %), *Mycoplana* (10.23 %), *Devosia* (10.01) and *Achromobacter* (8.56 %) (see Figure 8-13). *Geobacter* (3.75 %) and *Dechloromonas* (1.44 %) were the only *Proteobacteria* genera in post-test MX. *Firmicutes* relative abundance was increased significantly in post-test MX (83.90 %) compared with pre-test MX (14.79 %). It became the dominance phylum in post-test MX. The high abundance *Firmicutes* genus in mixed sludge after treatment are *Trichococcus* (21.33 %), *Clostridium* (7.63 %), and *Proteiniclasticum* (3.10 %). *Actinobacteria* (4.48 %), and *Chloroflexi* phylum (6.12 %) were distinguished in pre-test MX while it reduced dramatically (lower than < 1 % relative abundance) in the post-test MX. The abundance of low bacterial genera of (relative abundance < 1% ) had a higher ration in pre-test MX (19.70 %) compared with post-test MX (4.36 %).

The phylum classification for pre-test and post-test WT media as elucidates in Figure 8-14. *Proteobacteria* was the highest bacterial phylum in both pre-test WT (36.76 %) and post-test WT (40.38 %). Thus, the genus classification was dramatically differentiated, the dominance bacterial taxon (1 > relative abundance) in post-test WT are *Brevundimonas* (5.67 %), *Rhodocyclus* (5.14 %), *Geobacter* (4.26 %), and *Thiobacillus* (1.42 %), while the abundance genus in pre-test WT was: *Polynucleobacter* (2.46 %), *Flavobacterium* (2.41 %), and *Methylibium* (2.40 %). *Rhodoferax* was the only *Proteobacteria* genera found in both pre-test WT (9.33 %) and post-test WT (7.15 %) (Figure 8-15). Phylum as *Firmicutes* (0.7 %), *Bacteroidetes* (8.10 %) and *Chloroflexi* (1.99 %) was distinguished in pre-test WT, and it raised to 12.29 %, 12.70 %, and 3.44 % respectively in post-test WT. In pre-test WT, *Clostridium* (1.94 %), and *Desulfosporosinus* (1.42 %) were the only highly abundance (relative abundance > 1 %) *Firmicutes taxon*. Furthermore, *Verrucomicrobia* (17.19 %), *Acidobacteria* (13.35 %), and *Actinobacteria* (12.08 %) were the influenced phyla during the municipal

treatment. It dropped after treatment to 8.90 %, 8.45 %, and 3.60 % respectively. *Acidobacteria Geothrix* declined from 12.82 % in pre-test WT to 7.77 % in post-test WT. Low bacterial genera (relative abundance < 1 %) was 36.58 % in pre-test WT and 18.05 % in post-test WT columns media.

*Proteobacteria* and *Firmicutes* were the abundant bacterial phyla in post-test iron oxides bearing sludge, and they were affiliated with other bacteria genera. *Proteobacteria* retreated after treatment and *Firmicutes* flourished in the post-test column substrates. These phyla included various bacterial genera that are known to contribute to municipal wastewater treatment. Li et al. (2016) highlighted *Proteobacteria* and *Firmicutes* flourished at the iron-reducing condition. These two bacterial phyla detected during municipal wastewater treatment (Miura et al. 2007). These dominance phyla included several bacterial species were highlighted in the post-test column sludge. *Geobacter* is one of the *Proteobacteria* species that flourished. It is classified as an iron-reducing bacterium; it was highlighted in all column substrates. *Geobacter* simultaneously reduces iron oxides and oxidises organic contaminants to carbon dioxide (Reviews 1991; Luu and Ramsay 2003). It *uses* flagella as micro wires to transfer electrons to reduces Fe (III) to Fe (II) (Childers et al. 2002). *Rhodoferax* is another *Proteobacteria* genus which was found in post-test MWT and WT sludge. It was found in freshwater sediments (Finneran et al. 2003). It reduces Fe (III) and nitrate and oxidised organic carbon (Prade and Penninckx 2004). It also can accumulate phosphate as a phosphate accumulative organism (PAO) (Kong et al. 2005). *Trichococcus is* one of the flourished *Firmicutes* genera in both post-test MX and MWT sludge. It is a facultative anaerobic bacteria which tolerates low-temperature (Pikuta et al. 2006). *Geothrix* was found in the majority of pre-test and post-test column sludge. It is classified as an iron-reducing bacteria found in aquatic sediments (Luu and Ramsay 2003). *Geothrix* used organic carbon as an electron donor to reduced Fe (III) as an electron acceptor (Nevin and Lovley 2002a). From the gene sequencing analysis, it was noticed that *Geothrix* acclimatised with *Geobacter*. A similar observation was noticed by Rooney-varga et al. (1999), as he highlighted that *Geothrix* synergetic with *Geobacter* during organic carbon bioremediation. Other effective bacteria as *Proteiniclasticum* was found in MWT and MX column substrates. It is known as nitrate-reducing bacteria (Li et al. 2016). Sulphate-reducing bacteria as *Desulfosporosinus* (Robertson et al. 2001; Coates et al. 2002). It was highlighted in

both MWT and WT sludge. It degrades organic hydrocarbon compounds (Ivanov 2010). *Dechloromonas* presented in MX sludge. It is anaerobic bacteria used organic pollutants as an electron donor and nitrate as an electron acceptor (Wolicka and Borkowski 2012). It considered a denitrification genus as it transformed nitrate to dinitrogen gas (Coates et al. 2001). *Dechloromonas* reduces $NO_3$ to $N_2$ simultaneously with Fe (II) oxidation (Weber et al. 2006; Li et al. 2016). The flourished bacterial genera in the utilised iron oxides bearing sludge is an indication for the diversity of the used sludge and the condition inside the tested sludge can be aerobic and anaerobic because the highlighted bacterial species included anaerobic and facultative bacterial genera. These microorganisms mineralised organic carbon and other contaminants efficiently without pre-acclimatised.
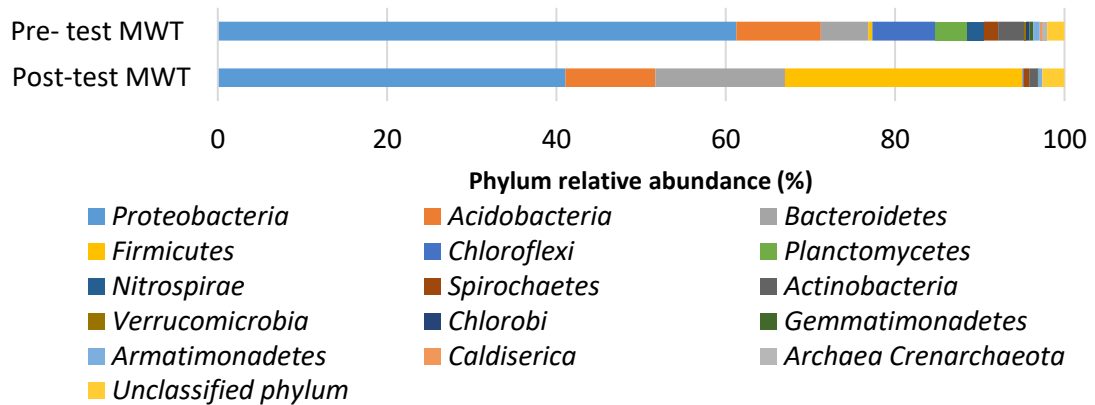


**Figure 8-10 Taxonomic classification of 16S RNA gene at phylum level for pre-test and post-test MWT column substrates.**
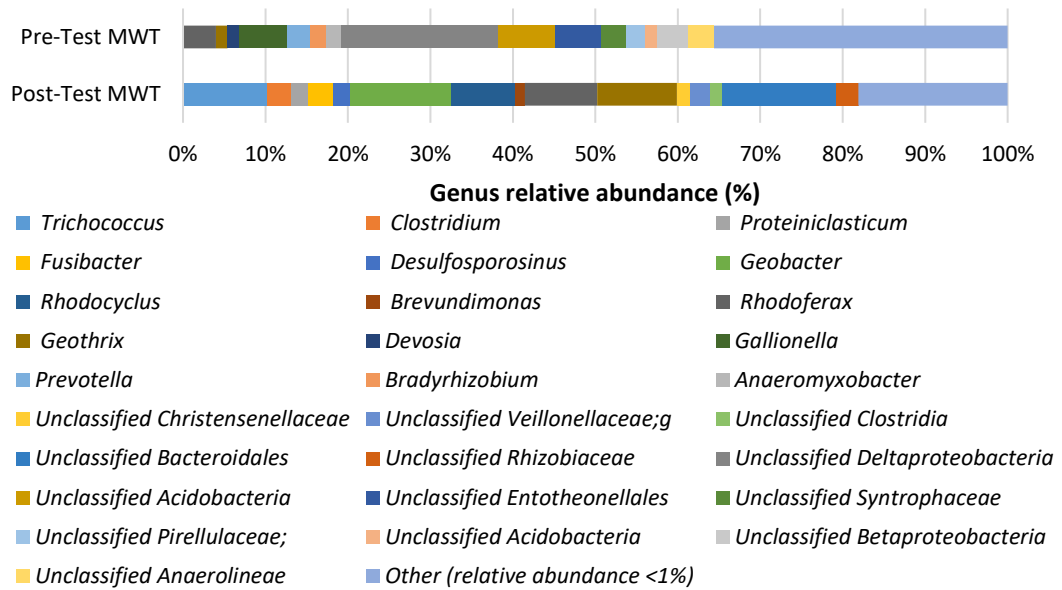
**Figure 8-11 Taxonomic classification of 16S RNA gene at the genus level for pre-test and post-test MWT column substrates.**
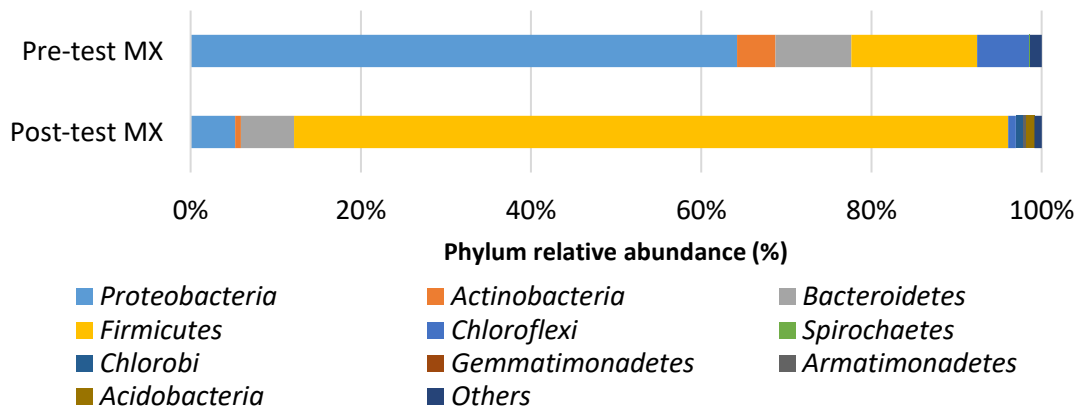


**Figure 8-12 Taxonomic classification of 16S RNA gene at phylum level for pre-test and post-test MX column substrates.**
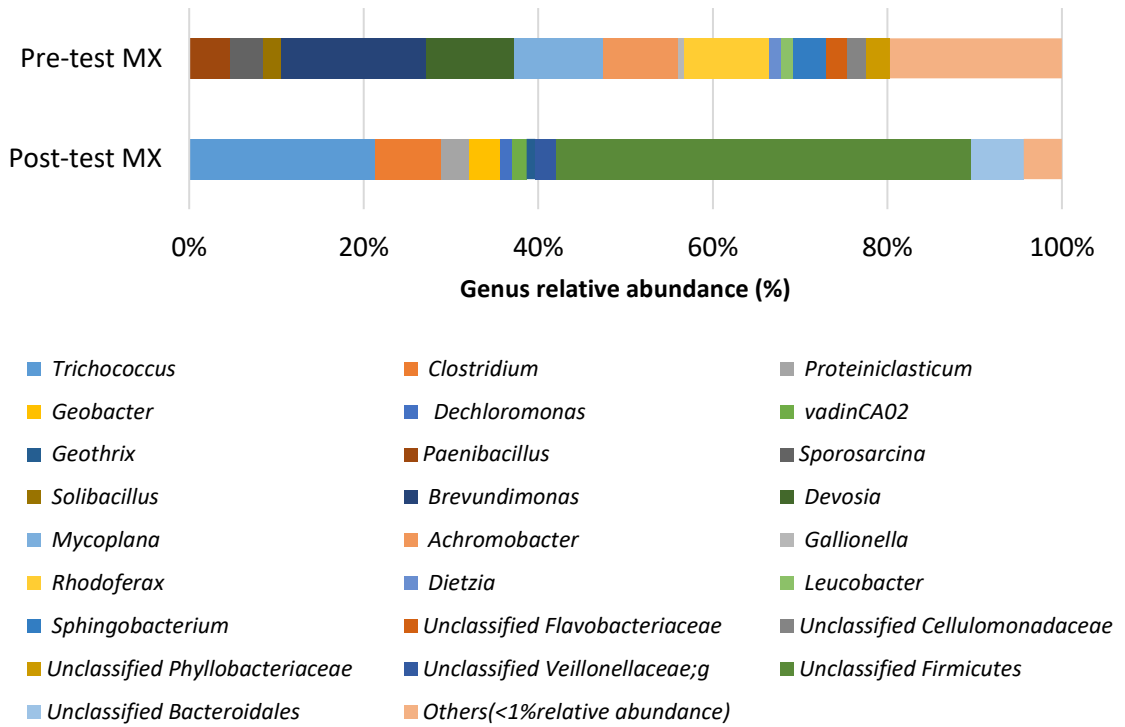
**Figure 8-13 Taxonomic classification of 16S RNA gene at the genus level for pre-test and post-test MX column substrates.**
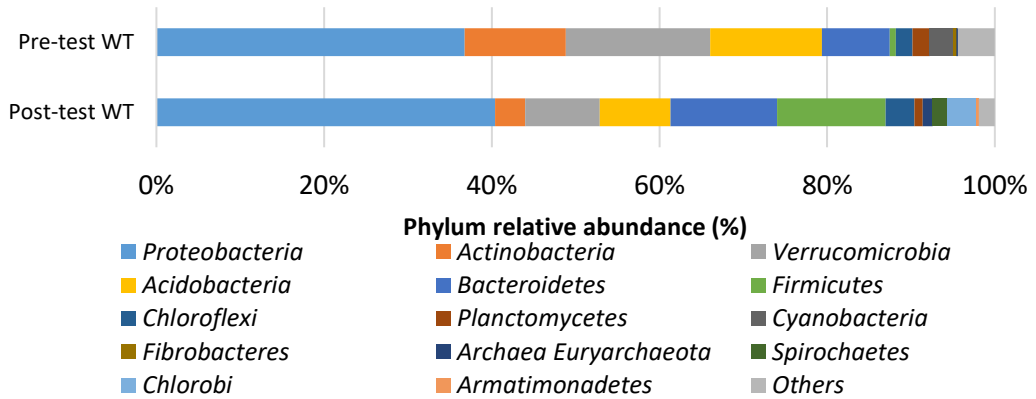


**Figure 8-14 Taxonomic classification of 16S RNA gene at the phylum level for pre-test and post-test WT column substrates.**

175
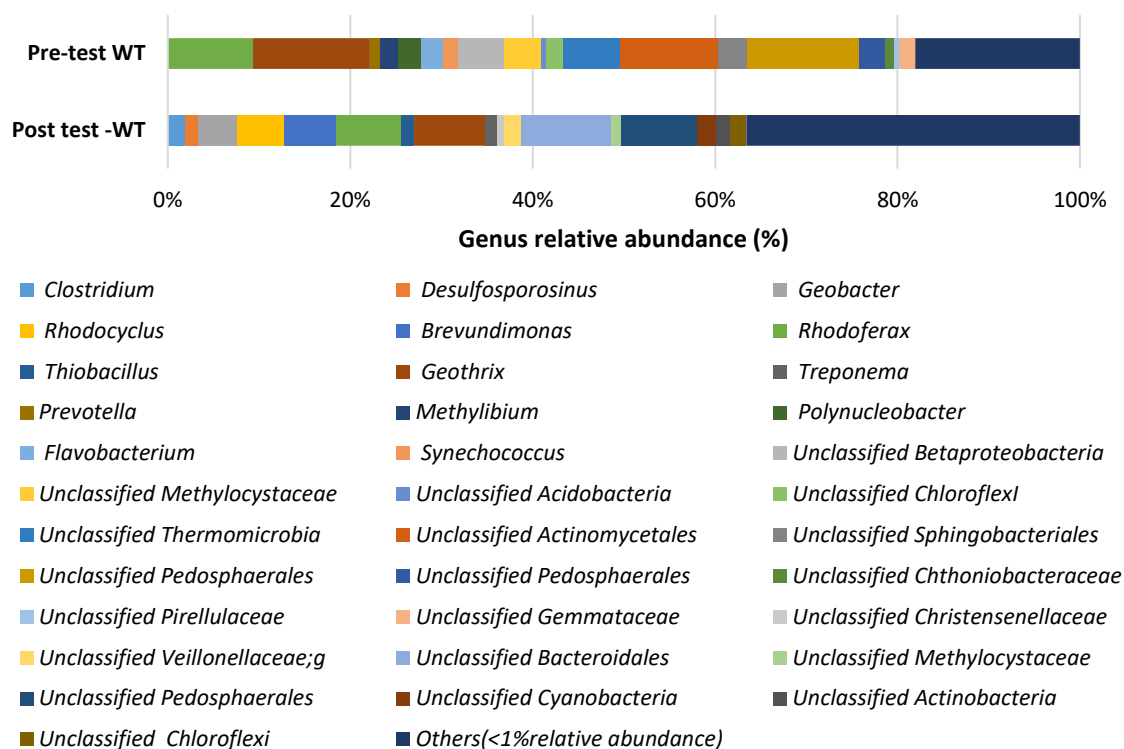
Figure 8-15 Taxonomic classification of 16S RNA gene at the genus level for pre-test and post-test WT column substrates.

## 8.10    Conceptual  model

In this experiment, iron oxides bearing sludge (MWT, MX and WT) were used as column substrates to treat municipal wastewater. Biodegradation was the main reason for carbon decline during the experiment because the TC in the post-test column substrates confirmed that there was no carbon was precipitated in theses sludge compared with per-test sludge samples as shown in Figure 8-5 C. The highest normalised TC and TN removal rate was 301 g/m$^3$/day by MWT sludge and 159 g/m$^3$/day by MX columns. Chemical oxygen demand declined from 236 $\pm$ 5 mg/l to 12.40 mg/l.  The pH range during the experiment was between 7.2 to 8.2, which highlighted that the microorganisms involved remediated the wastewater contaminants at neutral to slightly alkaline pH conditions. In the utilised iron oxides bearing sludge, iron-reducing bacteria were affiliated with other genera as confirmed by the gene sequencing data in Figure 8-10 to Figure 8-15. These flourished genera were

176

efficiently decreased organic carbon and nitrogen contaminants to lower concentrations which proved the availability of the iron oxides bearing sludge as a biomaterial to remediate municipal wastewater by simple and practical technique.

Figure 8-16 elucidated the expected mechanism in column sludge during municipal wastewater treatment. In reaction A, the flourished consortia oxidised organic carbon as an electron donor, and within the flourished genera, iron-reducing bacteria reduced Fe (III) to Fe (II). Anaerobic ammonium oxidation at iron-reducing condition (Feammox) is highlighted as reaction B where ammonia oxidised to nitrite, nitrate and nitrogen simultaneously with Fe (III) reduction. Anaerobic ammonium oxidation at nitrite condition (Anammox) might occurred to convert ammonia to nitrogen (see reaction C). In reaction D, nitrification transformed ammonia to nitrite and nitrite.
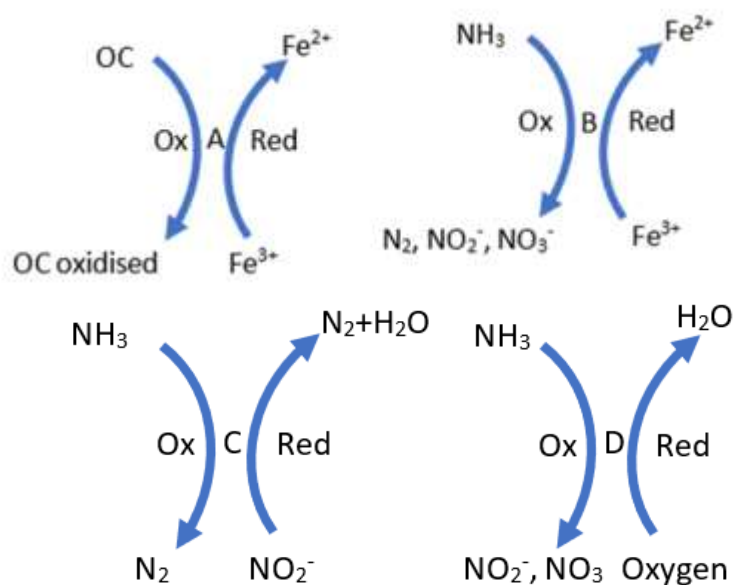


**Figure 8-16 Schematic diagram for municipal wastewater degradation using iron-reducing microorganism. A: oxidation of organic carbon, B: Feammox reaction, C: Anammox reaction, and D: nitrification where, Ox: oxidation reaction, Red: reduction reaction, OC: organic carbon.**

In the conducted municipal wastewater experiment, the nitrogen removal rate by Feammox and other mechanism was normalised from 159 $g/m^3/day$ to 8.11 $g/m^2/day$ and to 0.15 g/kg/day (see Appendix 2 for calculations) to be validated for comparison with nitrogen removal rates in the literature in Table 2-8). It was reported that the amount of nitrogen removed by Feammox and Anammox was 0.59 mg/kg/day while

it was 0.04 mg/kg/day by conventional nitrification and denitrification mechanisms (Ding et al. 2014). In another study, the nitrogen removal rate was 0.37 mg/kg/day where *Geobacter* was identified as one the flourished Feammox genera (Ding et al. 2017). Long et al. (2013) found that the amount of nitrogen removal rate by nitrification and denitrification was about 0.003 $g/m^3$/day, this rate increased to 0.01 $g/m^3$/day when Anammox involved. Nitrogen removal rate by iron oxides bearing sludge microorganisms was competitive compared with the reported studies.

Feammox is a novel mechanism for nitrogen conversion. It is described as a part of the natural nitrogen cycle (Yang et al. 2012). However, it has a low nitrogen removal efficiently, which can be enhanced by added electron shuttles (Yang et al. 2019). Iron reducing bacteria as *Geobacter* and *Geothrix* were highlighted in post-test column sludge and these genera were affiliated with other species as *Desulfosporosinus*. *Geobacter* flourished and affiliated with *Desulfosporosinus* during Feammox mechanism to transform nitrogen contaminants (Yang et al. 2019). Li et al. (2018) also highlighted that *Geobacter* was identified as one of the essential iron-reducing bacteria during Feammox. *Actinobacteria* was prosperous in all post-test column substrate during municipal wastewater experiment. It classified as iron-reducing, which highlighted in Feammox, and it affiliated with *Geobacter* (Ruiz-urigüen et al. 2018). The utilised iron oxides bearing sludge via iron-reducing bacteria and the affiliated genera degraded organic carbon and nitrogen contaminants without pre-acclimatisation. All the mentioned evidence confirmed that these sludges were appropriate substrates to treat municipal wastewater.

# Chapter 9 : BTEX bearing wastewater results and discussions

## 9.1 Introduction

This chapter discusses BTEX bearing wastewater experiments results using microcosms containing mine water treatment sludge (MWT), mixed sludge (MX) and water treatment sludge (WT) as substrates to remediate BTEX under initial aerobic and anoxic conditions. The BTEX adsorption by the used sludges were determined, GC-MS was used to measure BTEX biodegradation with time. Experiments parameters were also monitored and discussed. Taxonomic classification was used to distinguish any change in indigenous consortia in column substrates at genus level before and after treatment. A conceptual model explained the mechanism involved.

## 9.1 Adsorption experiments

It was important to determine the amount of BTEX adsorbed by MWT, MX and WT substrates because these sludges were used as substrates to mineralise BTEX. Two tests were conducted using open and sealed glass vials. In the open lid experiment, quick-fit glass lid containers were used while GC-MS 20 ml sealed glass vials with PTFE gas-tight aluminium silicone crimp lids were used in the sealed vials experiment. A gas-tight syringe was used to withdraw samples for GC-MS analysis to determine the BTEX concentration. 100 g wet sludge (MS, MX, and WT) were autoclaved (121 °C for 30 min) to exclude any microbial influence, and the autoclaved samples were dried at 40 °C for 48 hrs as reported by Schwertmann and Cornell (2000).

In the adsorption experiment, each sample contained 0.25 g of the autoclaved dried sludge mixed with 21 ml BTEX solution ("BTEX bearing wastewater"). Experiments were run in duplicates for 25 days in the dark, at shaking condition (150 rpm) to avoid light influence (Kelly et al. 1996). Control samples contained only BTEX bearing wastewater. The experiment was run on a small scale because the gas-tight GC-MS vials were the only available sealed container, microcosms were used in previous studies for BTEX biodegradation (Nales et al. 2010).

### 9.1.1 Open vial adsorption experiment

Figure 9-1 shows the changes in BTEX concentration with time for open lid containers. The BTEX concentration was measured using ppb unit based on GC-MS, which was

used to determine the BTEX concentration. In this experiment MWT, MX, WT, and control samples (contained only BTEX bearing wastewater) were monitored for 25 days. The general trendline for all samples included the control samples were dramatically declined with time from 45000 ppb to about 7000 ppb after 25 days. The sharp decline of BTEX concentration in control samples confirmed that the BTEX volatility was the main contribution for concentration declined because these samples did not contain any sludge. Sharmasarkar et al. (2000) asserted that volatility was a critical issue during the BTEX adsorption experiment.
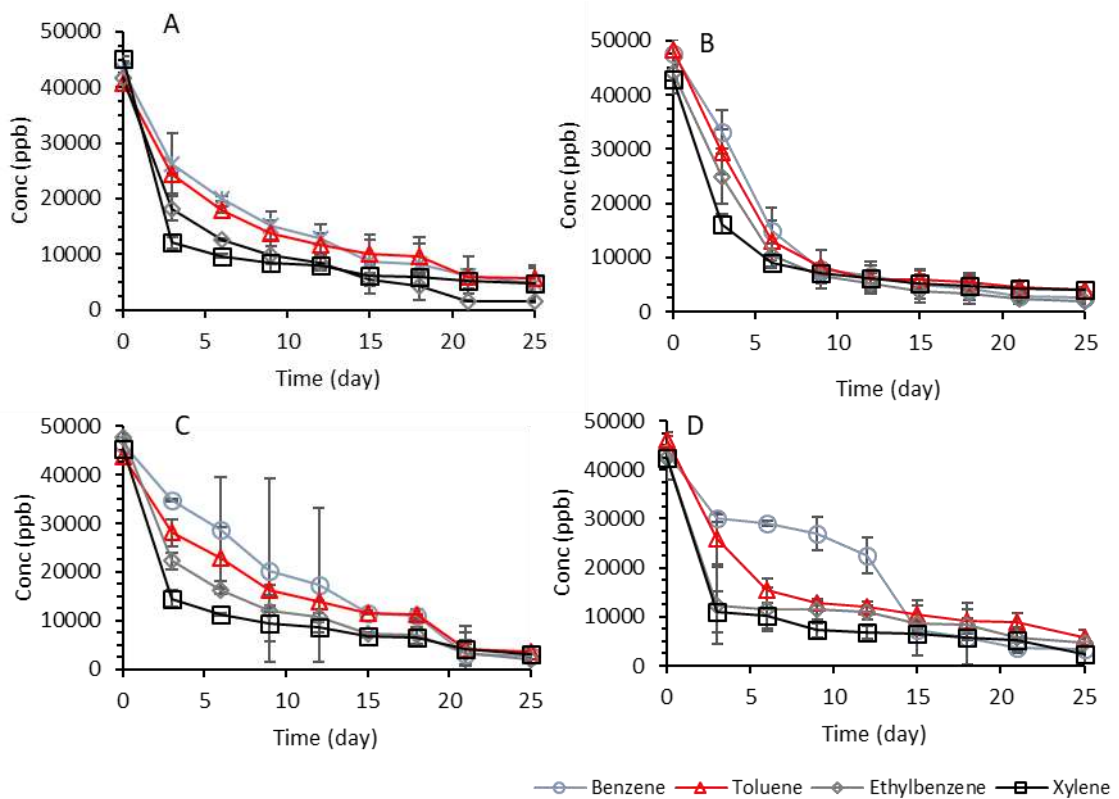


**Figure 9-1 BTEX open vials batch adsorption experiment, (A) mine water treatment sludge, (B) control, (C) mixed sludge, and (D) water treatment sludge.**

### 9.1.2 Sealed vials adsorption experiment

In this experiment, The BTEX concentration in control samples was almost stable during the 25 days (Figure 9-2 C). In MWT and MX samples, benzene, toluene and ethylbenzene concentration declined from 45,000 ppb to about 40,000 ppb. In comparison, xylene concentration declined by about 50 % compared with the initial concentration as shown in Figure 9-2 A and B. In WT samples the BTEX concentration

181

declined by the end of the experiment to 40,283 ppb, 42,629 ppb 34,505 ppb and 20,280 ppb for benzene, toluene, ethylbenzene, and xylene respectively. The adsorption in WT samples was the highest compared with MWT and MX. Data collected confirmed that benzene, toluene, and ethylbenzene had a low adsorption affinity to the substrate used, unlike xylene, which adsorbed in a higher concentration. The batch adsorption experiment lasted for 25 days, even though Aivalioti et al. (2010) and Seifi et al. (2011) argued that two days were sufficient to determine the BTEX adsorption. This experiment also highlighted that sealed GC-MS without headspace can be used as a microcosm for BTEX biodegradation.
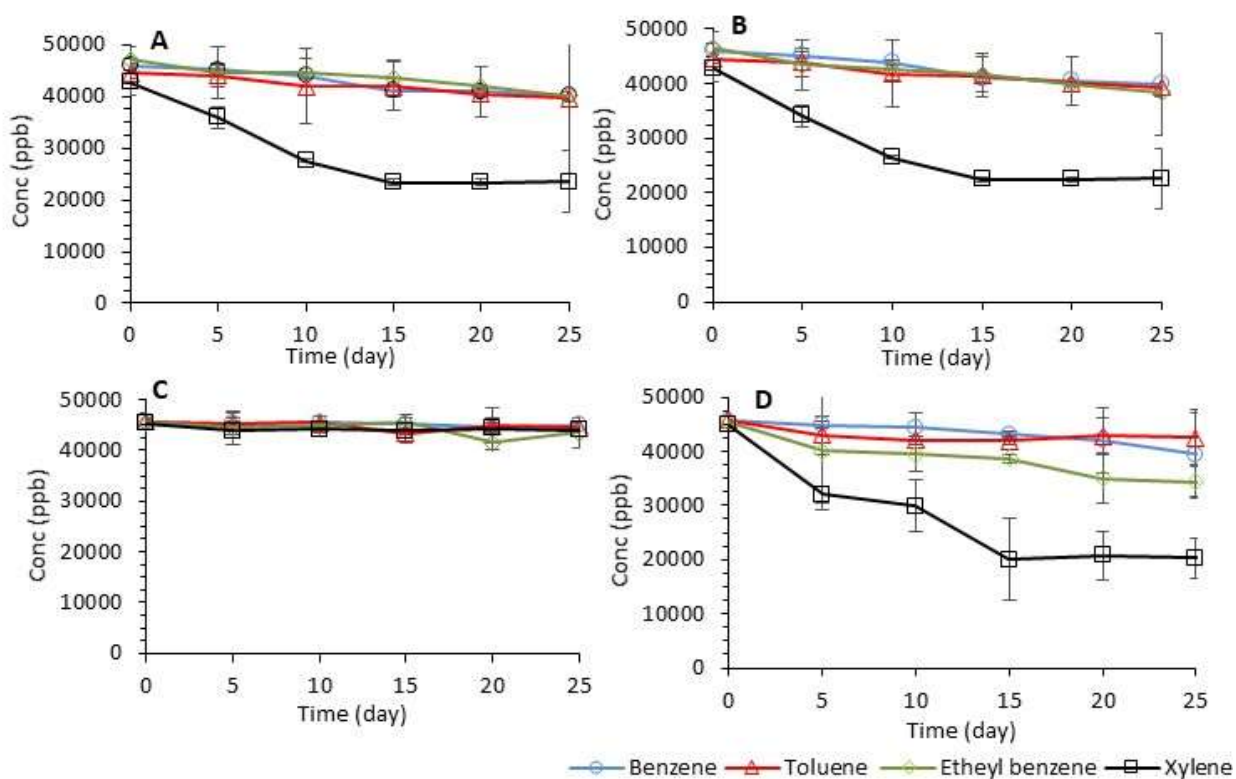


**Figure 9-2 BTEX sealed vials batch adsorption experiment, (A) mine water treatment sludge, (B) mixed sludge, (C) control, and (D) water treatment sludge.**

## 9.2    BTEX biodegradation using initial aerobic and anoxic microcosms

Microcosm samples were prepared, as described in section 3.7. These microcosms were labelled according to the substrate used, aerobic mine water treatment sludge (AMWT), aerobic mixed sludge (AMX), and aerobic water treatment sludge (AWT). The experiment started with 45,000 ppb as a concentration for each BTEX compound, as shown in Figure 9-3. After 20 days, a sharp decline was highlighted in AMX, ethylbenzene decline to 4,638 ppb, and toluene decreased to 15,146 ppb while benzene was 28,472 ppb and xylene 33,233 ppb as shown in Figure 9-3 C. In AMWT, xylene (11,271 ppb) and ethylbenzene (24,733 ppb) retreated more than toluene (36,985 ppb) and benzene (36,802 ppb) see Figure 9-3 A. During the same duration, BTEX decreased in AWT to 25,049 ppb, 27,204 ppb, 37,100 ppb, 33,587 ppb in ethylbenzene, toluene, benzene, and xylene as can be distinguished in Figure 9-3 B. By the end of the initially aerobic experiment, the concentration of xylene (38.5 ppb), toluene (106 ppb), ethylbenzene (2977 ppb) and benzene (20053 ppb) in AMX was lower than other substrates. In this experiment, it can be highlighted that benzene was the most recalcitrant monoaromatic compound with other mono aromatic hydrocarbons and aerobic mixed substrate (AMX) degraded BTEX more efficient than AMWT and AWT.

Figure 9-4 highlights the BTEX biodegradation under anoxic condition. The anoxic microcosms were labelled according to the substrate used, anoxic mine water treatment sludge (UMWT), anoxic mixed sludge (UMX), and anoxic water treatment sludge (UWT). It can be noticed that both anoxic mine water treatment sludge (UMWT) and anoxic mixed sludge (UMX) had comparable performance. Efficient BTEX removal was notified after about three weeks by UMWT and UMX while, UWT needed more than two folds this time to conduct a similar trendline. In UMWT, toluene was efficiently declined to 5,287 ppb followed by ethylbenzene (8950 ppb), xylene (13,322 ppb) and benzene (14,009 ppb) see Figure 9-4 A. In UMX microcosms, xylene (36,903ppb), benzene (8,138 ppb), ethylbenzene (277 ppb) and toluene (280 ppb) were highly degraded during the same period as elucidates in Figure 9-4 B. After 160 days xylene was completely degraded by UMX followed by ethylbenzene (1,413 ppb), toluene (1,400 ppb) and benzene (6,513 ppb). While xylene, ethylbenzene, toluene and

benzene decline to 95 ppb, 1,154 ppb, 1,879 ppb, and 6,115 ppb respectively in UMX. Compared with 4,113 ppb, 2,978 ppb, 815 ppb, and 10,053 ppb respectively in UMWT.

It is important to estimate the amount of BTEX adsorbed by microcosms sludge during BTEX bioremediation. Figure 9-5 represents the total carbon concentration (TC %) in pre-test microcosms compared with post-test sludge after 160 days of BTEX biodegradation. TC % in post-test MWT did not increase during the experiment compared with pre-test MWT. TC in post-test MX raised slightly compared with pre-test MX as it was 4.83 % and 6.07 % in AMX and UMX, respectively. WT was probably adsorbed the highest amount of BTEX, and TC was 17.75 % and 16.15 % in AWT and UWT compared with 14.55 % in pre-test WT. The reported information highlighted that WT sludge adsorbed BTEX more than MWT and MX sludge. Data presented in Figure 9-5 confirmed that the adsorption influence during BTEX mineralisation had a stronger influence on water treatment sludge (WT) compared with mine water treatment sludge (MWT) and mixed sludge (MX).

By comparing the initially aerobic and anoxic BTEX biodegradation (Figure 9-3 and Figure 9-4), it could be highlighted that the BTEX degraded more efficient and faster at initial anoxic condition than initially aerobic condition. Biodegradation was the main contribution of BTEX concentration decline, rather than adsorption. This conclusion could be confirmed by compared BTEX adsorption trend line in Figure 9-2 with concentration declined in Figure 9-3 and Figure 9-4. This finding was in agreement with Müller et al. (2017) who reported that microbial biodegradation was the dominated mechanism to degrade BTEX over adsorption when iron-reducing bacteria involved. The indigenous microorganism in the tested sludge (MWT, MX, and WT) were efficiently reduced the concentration of BTEX as a sole carbon source.

In this experiment, benzene was the most recalcitrant compound, followed by toluene and xylene. This finding agreed with Kelly et al. (1996), who notice the same behaviour. Gibson (1978) argued that the R-Group in toluene, ethylbenzene, and xylene could accelerate the biodegradation rate. Kelly et al. (1996) highlighted that about 25% of the BTEX was degraded to $CO_2$. Jo et al. (2008) highlighted that BTEX had a synergistic or antagonistic impact when it degrades as a mixture with BTEX. It means that increase one BTEX compound concentration can either increased or

decreased the degradation of other BTEX compounds, for examples increased xylene concentration from 15 mg/l to 75 mg/l in a mixture of BTEX raised the BTEX removal while increased benzene over the same concentration decreased the BTEX biodegradation. BTEX could be utilised as a sole carbon source by microbial consortia, even though at a concentration above 30 mg/l it could suppress microorganism involved (Cerniglia 1993), while the tested substrate in this experiment mineralised BTEX at 45 mg/l for each compound. The BTEX intermediate compounds could impede microbial metabolism (Müller et al. 2017), while some microorganism could be acclimatised and degraded BTEX as a sole carbon (Hamed et al. 2003; El-Naas et al. 2014). The lack of acclimatisation could be the reason for low aerobic BTEX biodegradation in the first 20 days by aerobic microcosms while in anoxic microcosms BTEX degraded more efficiently during the same duration. The reason beyond that maybe because the anoxic condition is similar sludge original condition where indigenous microorganism natural environment. Harayama and Timmis (1992) revealed that BTEX mineralised by cleavage the aromatic ring and mineralised the degradation products to $CO_2$. The utilise iron oxides bearing wastes via the indigenous iron-reducing bacteria and the affiliated microorganisms degraded BTEX as a sole carbon source. Furthermore, added nutrients could support BTEX biodegradation (El-Naas et al. 2014). This is the reason for added MX sludge in this experiment as it contained wastewater sludge. This sludge contains nutrients and humic substances which could be used as electron shuttles by iron-reducing bacteria.
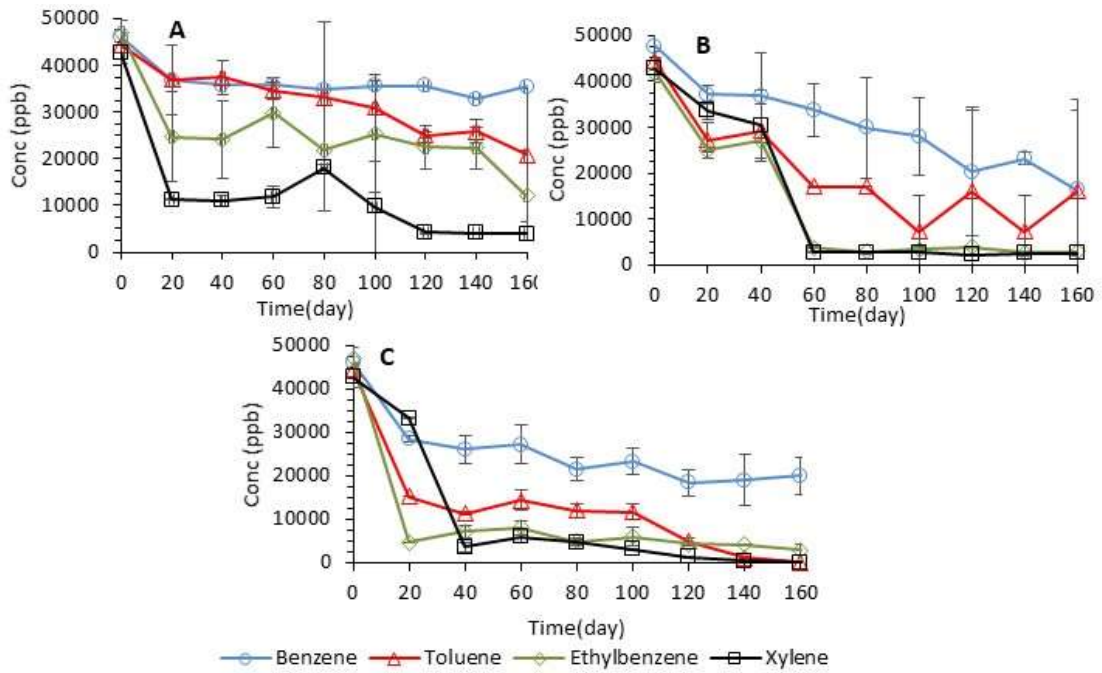
**Figure 9-3 BTEX concentration during initially aerobic microcosms biodegradation for (A) aerobic mine water treatment sludge, (B) aerobic water treatment, and (C) aerobic mixed sludge.**
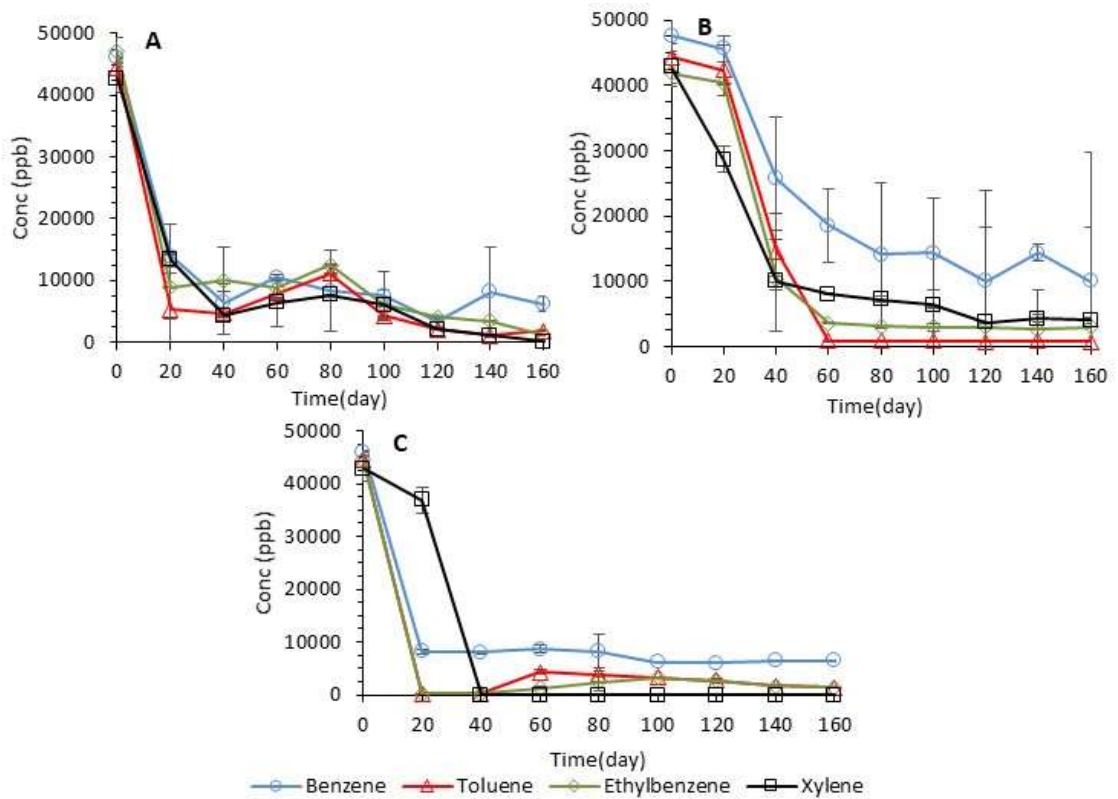


**Figure 9-4 BTEX concentration during anoxic microcosms biodegradation for (A) anoxic mine water treatment sludge (B) anoxic water treatment, and (C) anoxic mixed sludge.**

186
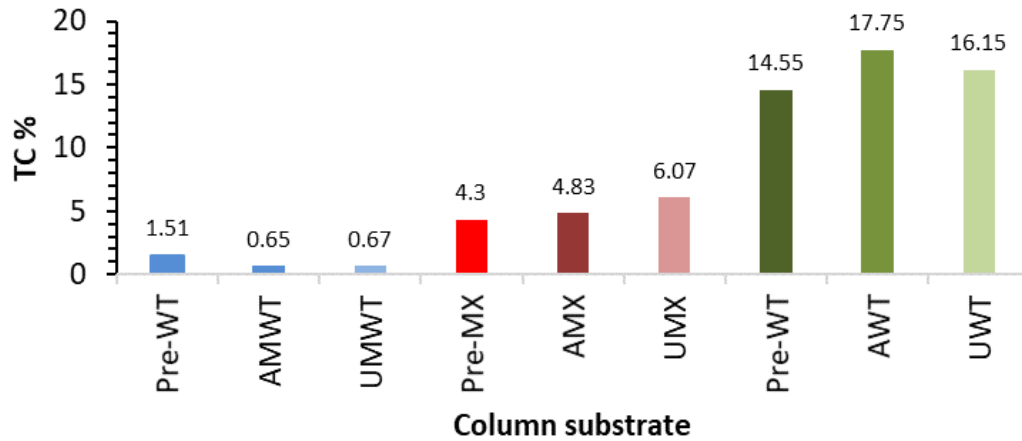
**Figure 9-5 Total carbon concentration in pre-test and post-test (after 160 days) microcosm substrates.**

## 9.3 Experiment microcosms parameters during BTEX biodegradation

The pH for aerobic BTEX bearing wastewater was 7.07, and the pH of AMX samples maintained at the neutral range while both AMWT (pH 6.25) AWT (pH 4.80) samples shifted the pH trend line to the acidic range, as shown in Figure 9-6 A. In the anoxic experiment, pH raised with time in all tested columns from pH 4.71 to 7.79 for UMX while it was pH 6.20 and 6.65 for UMWT, and UWT respectively (Figure 9-6 B). Providenti et al. (1993) reported that BTEX bioremediation was influenced by pH and temperature changed as it related to the type of microorganism used in the study. It was found that efficient BTEX biodegradation was noticed at the neutral pH range (Firmino et al. 2015a). In this experiment, BTEX degraded at acidic to neutral pH range by the iron oxides bearing sludge indigenous microorganisms.

Dissolved oxygen (DO) was $9.1 \pm 0.2$ mg/l in the aerobic microcosm samples. After three weeks, it was dramatically declined in AMWT (2.96 mg/l) and AMX (2.65 mg/l) while it was 6.33 mg/l in AWT as shown in Figure 9-7 A. The lowest DO concentration detected was in AMX (0.86 mg/l), AMWT (1.08 mg/l) and AWT (2.34 mg/l) by the end of the experiment. In the anoxic microcosm samples, the initial DO concentration was 2.03 mg/l $\pm 0.1$. The general trend for UMWT and UMX was below 2 mg/l while

in UWT, it dropped to zero as monitored in Figure 9-7 B. Providenti et al. (1993) mentioned that oxygen is vital for aerobic microorganisms for oxygenase enzymes to breakdown the aromatic ring. Lovley and Lonergan (1990) reported that oxygen has a minor effect for iron-reducing bacteria where iron becomes the substituted electron acceptor. Hutchins (1991) found that at a limited oxygen level, aromatic hydrocarbons mineralise to $CO_2$ and $H_2O$ when an alternative electron acceptor available. The diversity of iron oxides bearing sludge microorganisms perhaps the reason for degraded BTEX over different DO concentrations.

The electrical conductivity (EC) of the porewater was measured during BTEX biodegradation for both initial aerobic and anoxic condition, as shown in Figure 9-8. EC for BTEX bearing wastewater was 98.80 µS/cm. After 20 days, EC was dramatically increased in both AMX (2565 µS/cm) and UMX (2615 µS/cm). Though, it retreated with time to 1761 µS/cm and 1556 µS/cm for AMX and UMX, respectively. EC was raised in AMWT, and UMWT to 1510 µS/cm, and 929 µS/cm respectively. In initially aerobic samples, porewater EC did not exceed 961 µS/cm for AW, and in  UW it increased to 1455 µS/cm by the end of the experiment. The increased noticed in EC during BTEX biodegradation was probably associated with the bacteria growth included iron-reducing bacteria.

The temperature was monitored during BTEX biodegradation. It gradually increased with time, as shown in Figure 9-9. In the first 20 days, it was between 1 to 9.5 °C, which was the lowest range detected during the BTEX experiment. However, it increased gradually to 24.5 °C, which was the highest temperature recorded on day 160. Firmino et al. (2015a) experimented BTEX removed by bacterial at room temperature (27  °C). In general, BTEX biodegradation conducted at temperature range 27 °C to 33 °C (Shim and Yang 2002; Farhadian et al. 2008b). Data collected highlighted the ability of iron oxides indigenous consortia to remediate BTEX at different temperature range.
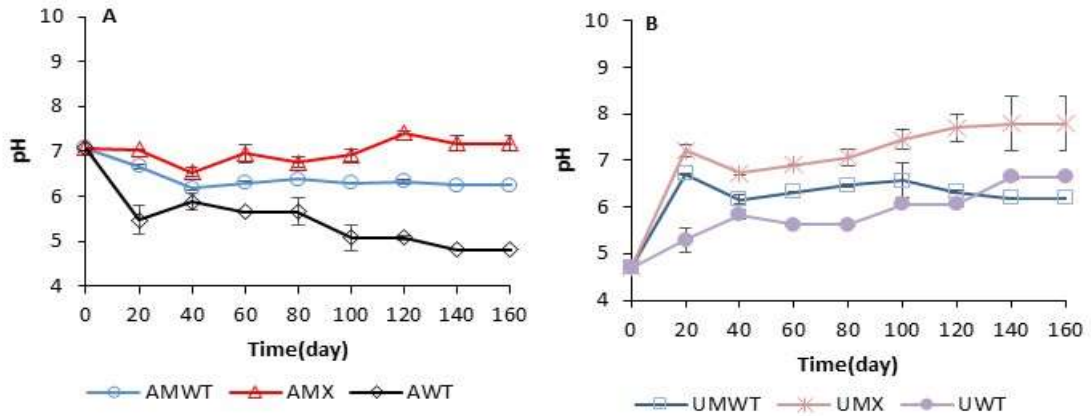
**Figure 9-6 pH trend line, (A) initially aerobic and (B) anoxic BTEX biodegradation experiments.**
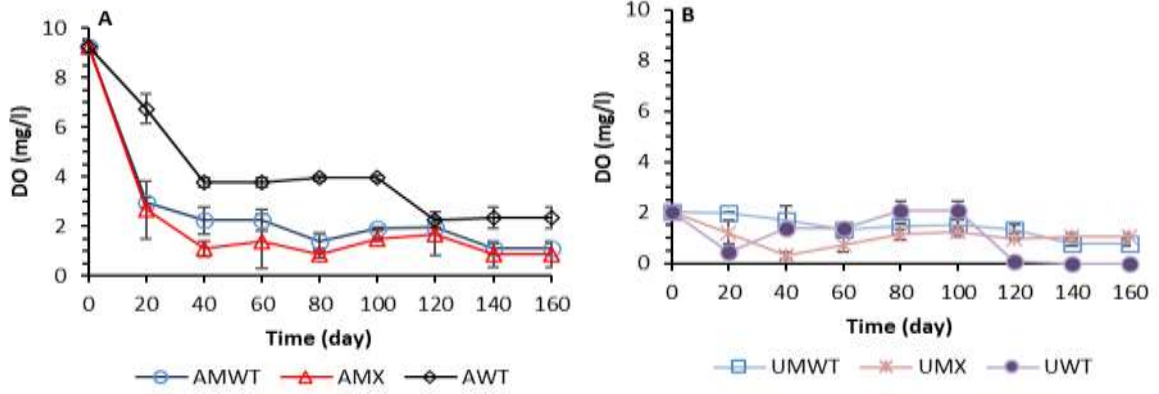


**Figure 9-7 Dissolved oxygen concentration, (A) initially aerobic and (B) anoxic BTEX biodegradation experiments.**
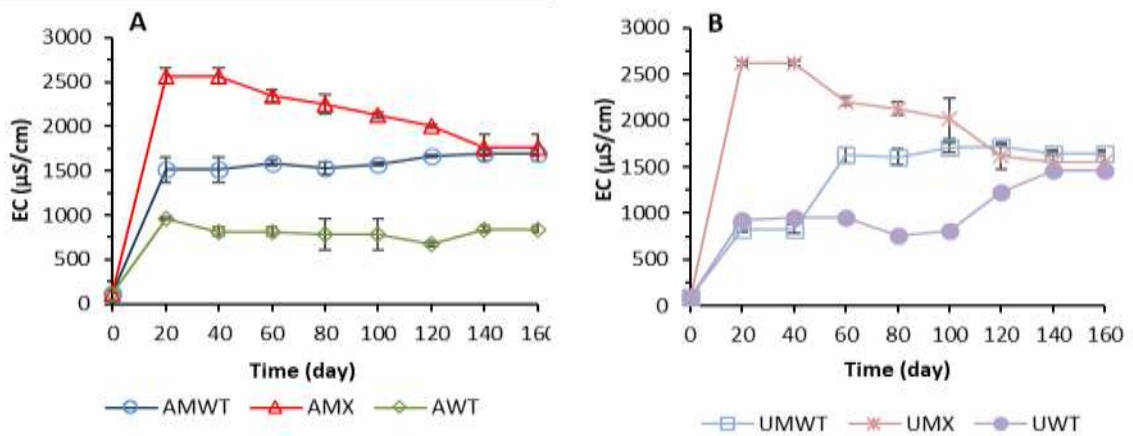


**Figure 9-8 Electrical conductivity, (A) initially aerobic, and (B) anoxic BTEX biodegradation experiments.**

189
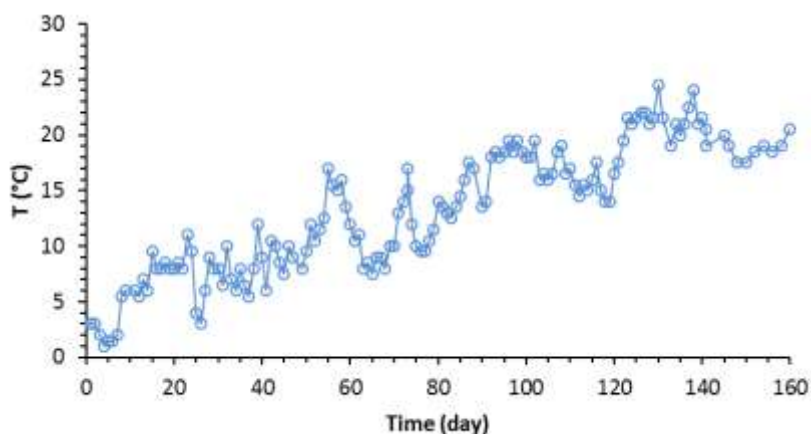
**Figure 9-9 Temperature changes with time during BTEX biodegradation experiments.**

## 9.4      Total iron and ferrous iron concentrations

Total iron and ferrous iron concentration were monitored, as mentioned in section 3.8. Duplicate microcosms samples were withdrawn, and the porewater was filtered before measure the total iron and ferrous iron concentrations. Both MWT sludge and MX microcosm samples generated low iron in both initial anoxic and aerobic conditions compared with WT microcosms. In AWT microcosms, total iron concentration in the porewater increased gradually with time to 486 mg/l in days 120, and then it declined to 282 mg/l by the end of the experiment. In AMWT, 9.05 mg/l was the highest iron concentration determined after day 120. While the iron concentration was 58.26 mg/l in AMX at days 80 (see Figure 9-10A). In anoxic microcosms, iron concentration in all examined samples as demonstrated in Figure 9-10 B. The highest iron concentration was 1488 mg/l in UWT after 120 days, followed by 50.38 mg/l in UMX after days 60, and 31.45 mg/in UMWT after 120 days. Ferrous concentration was the highest in AWT (110.41 mg/l), and UWT (151.10 mg/l) compared with 20.91 mg/l, and 3.20 mg/l  in AMX, and AMWT. While it was 19.44 mg/l in UMX and 8.75 mg/l in UM as seen in Figure 9-11. The detection of iron and ferrous during BTEX biodegradation could be an indicator for iron-reducing microorganism activity. Iron reducing bacteria can be used to remediate BTEX, these microorganisms oxidised BTEX as an electron donor and reduced Fe (III) as an electron acceptor (Botton and Parsons 2006; Botton et al. 2007; Farkas et al. 2017).
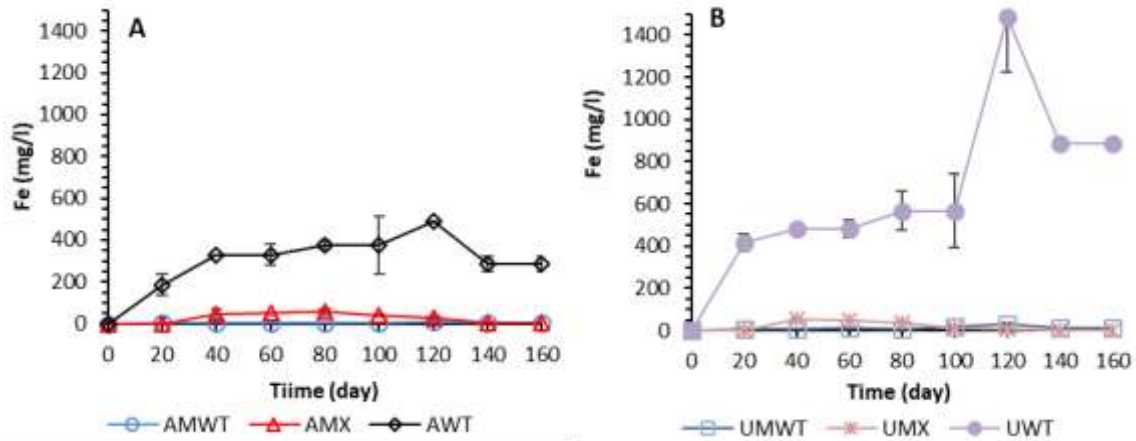
**Figure 9-10 Total iron, (A) initially aerobic, and (B) anoxic BTEX biodegradation experiments.**
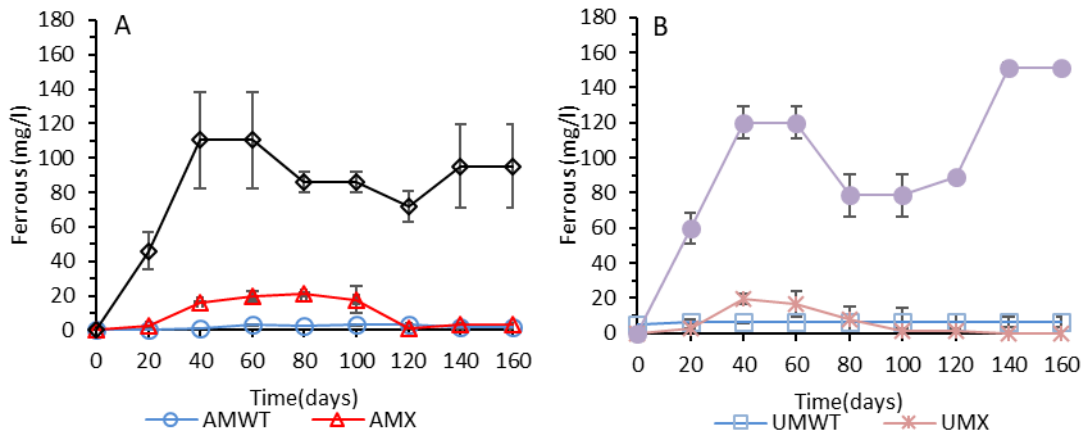


**Figure 9-11 Ferrous concentration, (A) initially aerobic, and (B) anoxic BTEX biodegradation experiments.**

## 9.5 Parameters correlation for BTEX bearing wastewater experiment

Bivariate correlation analysis by IBM SPSS statistic software (version 20) was used to find the correlation between BTEX experiment parameters. These parameters were normally distributed ($p < 0.05$), and therefore Pearson correlation was used to determine the correlation between experiment parameters. For aerobic microcosms experiment, AMWT correlation was significant positive between pH and aerobic degradation for benzene (0.90) toluene (0.68) ethylbenzene (0.80) and xylene (0.86) according to the reported correlation coefficient. The correlation was also distinguished between the mono aromatic hydrocarbons, for example, it was

significant positive between benzene and toluene (0.70), benzene and ethylbenzene (0.85), and benzene and xylene (0.91). In AMX microcosms, no correlation was found between pH and the aerobic biodegradation for benzene, toluene, ethylbenzene, and xylene. The correlation between mono aromatic hydrocarbons was significant positive between benzene and toluene (0.97), benzene and ethylbenzene (0.93) and benzene and xylene (0.87) according to the reported correlation coefficient. In AWT microcosms, the correlation was significant positive between pH and aerobic degradation of benzene (0.91), toluene (0.89), ethylbenzene (0.83) and xylene (0.76). Also, the correlation was significant positive between benzene and toluene (0.81), benzene and ethylbenzene (0.85) and benzene and xylene (0.83). In MWT, the correlation between BTEX and ferrous was significant negative in benzene (-0.59), toluene (-0.57), ethylbenzene (-0.41) and xylene (-0.53). In AX, no correlation was noticed between BETX removal and ferrous generated. In AWT, a negative correlation was noticed between ferrous and toluene (-0.69), ethylbenzene (-0.70) and xylene (-0.67). No correlation was found between temperature and aerobic BTEX biodegradation.

At anoxic microcosms condition, a significant negative correlation was demonstrated in UMWT microcosms between pH and the anoxic degradation of benzene (-0.88) toluene (-0.89) ethylbenzene (-0.88) and xylene (-0.82). Furthermore, a positive correlation was highlighted between benzene and toluene (0.96), benzene and ethylbenzene (0.96), and benzene and xylene (0.98). In UMX, the correlation between pH and BTEX degradation was significant negative in benzene (-0.93), toluene (-0.92), ethylbenzene (-0.90) and xylene (-0.69). While the correlation was significant positive between benzene and toluene (0.992), benzene and ethylbenzene (0.99) and benzene and xylene (0.73). In UWT the correlation significant positive between pH, and benzene (-0.82), toluene (-0.78), ethylbenzene (-0.78) and xylene (-0.85). The correlation was significant positive between benzene and toluene (0.98), benzene and ethylbenzene (0.97) and benzene and xylene (0.95) based on the calculated correlation coefficient. The correlation of BTEX anoxic biodegradation was significant negative with ferrous generation in UMWT for benzene (-0.66), toluene (-0.65), ethylbenzene (-0.78) and xylene (-0.72). Similar notice was highlighted in UMWT for benzene (-0.71), toluene (-0.73), ethylbenzene (-0.75) and xylene (-0.82). While no correlation

was found in UMX. Also, no correlation was found between temperature and anoxic BTEX biodegradation.

## 9.6    Microbial community changes in pre-test and post-test microcosm sludge

The taxonomic classification for pre-test MWT sludge was compared with post-test MWT sludge included initially aerobic mine water treatment sludge (AMWT) and anoxic mine water treatment sludge (UMWT) at phylum level as shown in Figure 9-12. The phylum diversity dropped from 16 in pre-test MWT sludge to 7 in post-test MWT (AMWT, and UMWT). However, *Proteobacteria* was the abundant bacterial phyla before and after treatment. It consisted of 61.24 % of the pre-test MWT sludge relative abundance, while it decreased in UMWT (51.51 %) and AMWT (39.67 %). *Firmicutes* (0.42 %) and *Bacteroidetes* (5.65 %) were identified in pre-test MWT sludge. Thus, it was the second and the third dominant phylum in AMWT at 30.32 % and 21.80 % respectively. Though, *Bacteroidetes* and *Firmicutes* were distinguished at 23.76 % and 17.98 % relative abundance in UMWT as the second and third dominated phyla. Phylum as *Planctomycetes* (8.58 %), *Actinobacteria* (3.09 %) and *Spirochaetes* (1.68 %) was unable to tolerate the wastewater, and they declined dramatically (relative abundance < 1%) in both aerobic and anoxic conditions. Bacterial genera were highlighted for pre-test and post-test MWT microcosm substrates as shown in Figure 8-10. The highlighted genus (relative abundance > 1%) in pre-test MWT sludge was *Gallionella* (5.82 %), *Rhodoferax* (4.00 %), *Prevotella* (2.86 %), *Bradyrhizobium* (1.91 %), *Anaeromyxobacter* (1.77 %), *Devosia* (1.39 %), and *Geothrix* (1.39 %). Some bacterial genera were recognised in initially aerobic and anoxic samples. *Escherichia* was the first abundance bacterial genus in UMWT (32.47 %) and AMWT (20.76 %). Similarly, *Prevotella* flourished in UMWT (17.17 %) and AMWT (13.26 %). *Archaea Methanobacterium* distinguished in UMWT (11.48 %) and AMWT (4.22 %). Furthermore, *Veillonella* relative abundance was 3.96 % in UMWT compared with 1.22 % in AMWT. Others abundance genera in UMWT are: *Enhydrobacter* (5.32 %), *Flavobacterium* (3.64 %), *Geobacter* (2.61 %), *Longilinea* (2.54 %), *Clostridium* (1.40 %), *Butyrivibrio* (1.12 %), and *Stenotrophomonas* (1.01 %). The prosperous genus in

AMWT (relative abundance > 1%) was *Proteiniclasticum* (11.37 %), *Streptococcus* (4.37 %), *Crenothrix* (4.22 %), *Haemophilus* (3.48 %), *Granulicatella* (2.75 %), *Sedimentibacter* (2.07 %), *Porphyromonas* (1.58 %), *Rubrivivax* (1.50 %), *Pseudomonas* (1.29 %), *Fibrobacter* (1.27 %), *Legionella* (1.11 %) and *Thauera* (1.04 %). Other low abundance genera (relative abundance > 1%) consisted 35.61 %, 7.22 % and 13.00 % in Pre-test MWT sludge, UMWT, and AMWT respectively.

Figure 9-14 shows that *Proteobacteria* was dominant in the pre-test MX (64.23 %) compared with 6.62 % in AMX, and 3.61 % in UMX,. *Firmicutes* was the second most abundant phylum in AMX (59.28 %) and UMX (37.05 %) compared with 14.59 % in pre-test MWT sludge. *Bacteroidetes* contributed 27.81 %, and 29.07 % of AMX, and UMX relative abundance. Others bacterial phylum as *Actinobacteria* (4.48 %) was noticed in AMX and *Chloroflexi* (6.12 %) in UMX. *Archaea* were detected in pre and post mixes sludge under the initially aerobic condition at 1.45 % and 1.71 % respectively, while it was below the detection range in the anoxic substrate.

Figure 9-15 represents the bacterial genus highlights in the pre-test, and post-test MX microcosms sludge included anoxic and initially aerobic conditions. The abundance *proteobacteria* genera in pre-test MX included *Brevundimonas* (16.66 %), *Mycoplana* (10.23 %), *Devosia* (10.01 %), *Rhodoferax* (9.63 %) and *Achromobacter* (8.56 %). Additionally, *Paenibacillus* (4.61 %), *Sporosarcina* (3.66 %), *Solibacillus* (2.09 %), and *Alkaliphilus* (1.89 %) represented the *Firmicutes* bacterial genus. *Bacteroidetes Sphingobacterium* contributed by 3.68 % of the total pre-test MX genus relative abundance. There were extensive changes at the genus level for both AMX and UMX related with the BTEX biodegradation, all the dominated bacteria genera in pre-test MX retreated sharply under the detection limit in both AX and UMX. Thus, several alternative genera were highlighted in both initially aerobic and anoxic mixed substrates such as *Prevotella*. It was the highest genus in AMX (25.73 %) and UMX (27.91 %). It was followed by *Clostridium* as the second highest bacteria genera in AMX (11.34 %) and UMX (6.27 %). *Proteiniclasticum* was found in AMX (10.00 %) thus. It dropped by about 50 % in UMX (4.13 %). *Geobacter* relative abundance was highlighted at 6.22 % in AMWT while in UMX it retreated sharply to 1.01 %. *Acetobacterium* was the highest in UMX (2.33 %). Nevertheless, *Anaerovorax* was found in AMX (2.64 %) compared with 0.71 % relative abundance in UMX. A genus

with low abundance (1 < 1 %) consisted of 12.87 % of the overall relative abundance in AMX, and it was raised to 18.49 % in UMX.

In pre-test WT, there were 12 phylum included *Euryarchaeota* (0.19 %) as the only *archaea* phylum and the others are bacterial phyla, as shown in Figure 9-16. *Proteobacteria* (36.76 %) was the most abundant phylum; it was followed by *Verrucomicrobia* (17.19 %), *Acidobacteria* (13.35 %), *Actinobacteria* (12.08 %), and *Bacteroidetes* (8.10 %). After BTEX treatment, the phylum distribution was considerably changed. *Verrucomicrobia* became the dominant bacterial phylum in AWT (38.32 %) and UWT (39.07 %). *Bacteroidetes* increased to 20.02 % and 11.81 % relative abundance in AWT and UWT substrates. *Proteobacteria* dropped in AWT (15.41 %) and UWT (10.73 %). Other phylum (1 % > relative abundance) in AWT were *Actinobacteria* (11.52 %), *Cyanobacteria* (5.75 %), *Acidobacteria* (4.24 %), *Chloroflexi* 91.55 %), and *Firmicutes* (1.23 %). Thus, the remained phylum in UWT classified into; *Acidobacteria* (10.38 %), *Chloroflexi* (7.59 %), *Actinobacteria* (4.56 %), *Firmicutes* (4.19 %), *Planctomycetes* (4.10 %), and *Cyanobacteria* (1.66 %). Figure 9-17 referred to bacterial genus detected in pre-test and post-test WT microcosm sludge. The highlighted bacterial genus in pre-test WT were distributed as: *Geothrix* (12.82 %), *Rhodoferax* (9.33 %), *Polynucleobacter* (2.46 %), *Flavobacterium* (2.41 %), *Methylibium* (2.04 %), Synechococcus (1.67 %), and *Prevotella* (1.10 %). The genus available in post-test WT substrates indicates that *Geothrix* and *Methylibium* were the only bacterial genera resisted BTEX. It was distinguished in both AWT and UWT. *Geothrix* declined in AWT (4.07 %), and UWT (8.51 %) while *Methylibium* raised to 6.01 % relative abundance in AWT compared with 3.96% relative abundance in UWT. Other bacterial genera in AWT identified *as Escherichia* (3.75 %), and *Veillonella* (1.16 %) were classified as *Proteobacteria and Firmicutes* genera. While *Prevotella* (10.02 %), *Geobacter* (3.69 %), *Desulfosporosinus* (2.84 %) represented *Bacteroidetes*, *Proteobacteria* and *Firmicutes* bacterial genera in UWT. Furthermore, the diversity of low abundance genus (1 % < relative abundance) was more diversity in AWT (35.05 %) compared with UWT (15.52 %) and pre-test WT (18.05 %).

*Proteobacteria, Firmicutes, Chloroflexi* and *Bacteroidetes* represented the bacterial phylum that flourished in post-test iron oxides bearing sludge during BTEX

bioremediation. Within these phyla, there are several bacterial genera highlighted. In previous BTEX biodegradation studies, *Proteobacteria, Firmicutes,* and *Bacteroidetes* represented the dominant bacterial phyla (Siddique et al. 2012; Dang et al. 2013; Aburto-Medina and Ball 2015). *Proteobacteria* degraded monoaromatic carbon as benzene to $CO_2$ and $H_2O$ (Zaan et al. 2012). Takahata et al. (2007) demonstrated that *Firmicutes* could be synergetic with other bacterial phyla to decay aromatic hydrocarbons. *Chloroflexi* degrades aromatic organic carbon such as toluene, and it could be distinguished in various natural environments (Rosenkranz et al. 2013). Several iron-reducing bacterial genera were highlighted during BTEX bioremediation in the utilised iron oxides bearing sludge. Iron-reducing bacteria as *Geothrix* was identified in pre-test MWT sludge (12.68 %) and post-test MWT sludge in both aerobic (4.07 %) and anoxic (8.51 %) microcosms. *Gallionella* iron oxidation bacteria was found in lake sediments (Mouchet 1992; Weber et al. 2006). It highlighted in pre-test MWT sludge (5.82 %), this genus decreased under the detection range after BTEX mineralisation because of the inappropriate growth conditions. *Rhodoferax* is a facultative iron-reducing bacterium. It was characterised in the collected MWT (4 %), MX (9.63 %) and WT sludge (9.33 %). It also found in subsurface aquatic sediments, and it tolerates low-temperature environment (4 ˚C) (Finneran et al. 2003). C*lostridium* was found in UMX (11.34 %), and AMX (6.27 %) while it was in a relatively low concentration in AWT (0.64 %), AMWT (0.84 %), and UMWT (1.40 %). *Clostridium* was able to reduce iron oxides simultaneous with organic carbon fermentation (Park et al. 2001). It was successfully isolated from-mining lakes ochre where iron-reducing condition available (Ku¨sel and Dorsch 2000; Castro et al. 2013; Wei et al. 2015). It degraded BTEX by acclimatised with other bacterial species as *Geobacter* in aquifers (Silva and Alvarez 2002).

*Geobacter* was highlighted in post-test iron oxides sludge. It oxidises monoaromatic hydrocarbons as an electron donor and reduces Fe (III) as an electron acceptor. Anderson et al. (1998) noticed that *Geobacter* mineralises BETX, and aromatic hydrocarbons to $CO_2$ at iron-reducing condition. The reported iron-reducing bacterial genera affiliated with other bacterial species as *Escherichia* which flourished in UMWT (32.47 %), and in AMWT (20.76 %) sludge. It was also found in AWT (3.76%). This genus probably was one of the effective bacterial genera during BTEX biodegradation. Morlett-chávez et al. (2010) reported that *Escherichia* could degrade

BTEX. *Escherichia* was found in MWT sludge as indigenous genera (Wei et al. 2015). It degraded various organic pollutants (Kiernicka et al. 1999; Van der Zee and Cervantes 2009). *Prevotella* was found in all the microcosm substrates as one of the efficient *Bacteroidetes* taxa in BTEX bioremediation. It presented in indigenous MWT sludge as it flourished in AMWT (13.26 %) and UMWT (17.17 %) samples. Thus, it was also highlighted in AMX (25.73 %) and UMX (27.91 %). While it was only found in aerobic AWT (10.02 %). It was classified as one of the functional environmental genus in aquatic sediments ecosystem (Ivanov 2010). It is anoxic-facultative bacteria (Zeikus et al. 1999). It degraded aromatic hydrocarbons to the simplest compounds (Plumb et al. 2001; Zhu et al. 2018a). *Prevotella* tolerated BTEX effectively at iron-reducing condition (Smalley et al. 2003; Tindall 2005). *Methanobacterium* flourished in iron-reducing environments (Shrestha et al. 2014; Holmes et al. 2017). It was the only archaea taxon tolerated BTEX in UMWT (11.48 %) as well as AMWT (4.42 %). It mineralises aromatic pollutants efficiently when iron oxide added (Wang et al. 2018). It reduces aromatic hydrocarbons (Plumb et al. 2001; Sarkar et al. 2016). It degraded complex organic compounds to the simplest compounds (Zhao et al. 2017b). *Firmicutes Proteiniclasticum* was found in soil (Li et al. 2016). It was differentiated in AMWT (11.37 %), AMX (10 %), and UMX (4.13 %). It completely mineralised aromatic hydrocarbons as benzene to $CO_2$, and $H_2O$ (Zhu et al. 2018b). *Proteiniclasticum* and *Prevotella* within a bacterial consortium could efficiently degrade aromatic organic hydrocarbon (Wang et al. 2018; Zhu et al. 2018b). The flourished iron reducing bacteria and the affiliated genera in post-test iron oxides bearing sludge degraded BTEX as a sole organic carbon.
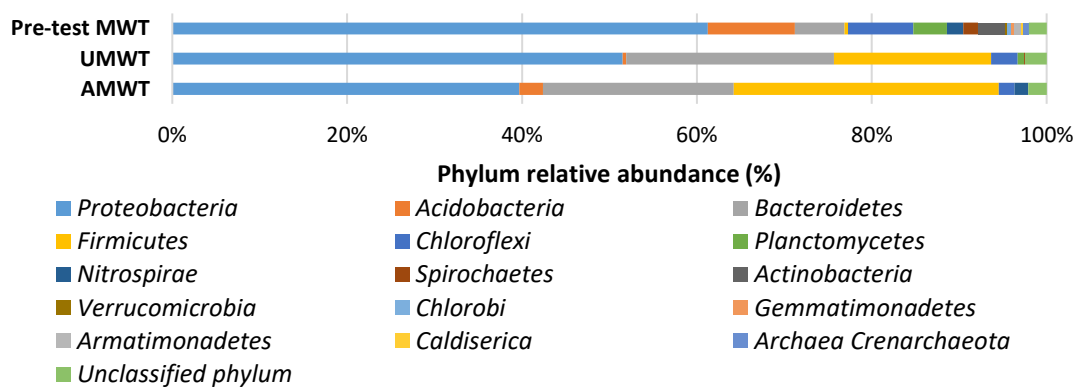


**Figure 9-12 Taxonomic classification of 16S RNA gene at phylum level for pre-test and post-test MWT sludge.**
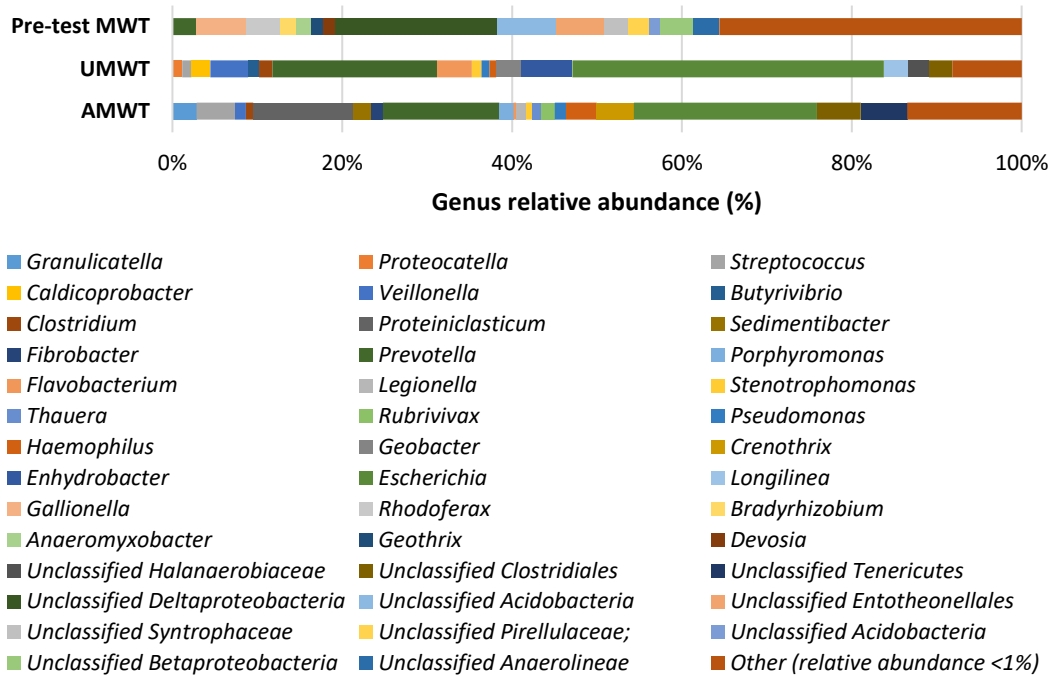
**Figure 9-13 Taxonomic classification of 16S RNA gene at the genus level for pre-test and post-test MWT sludge.**
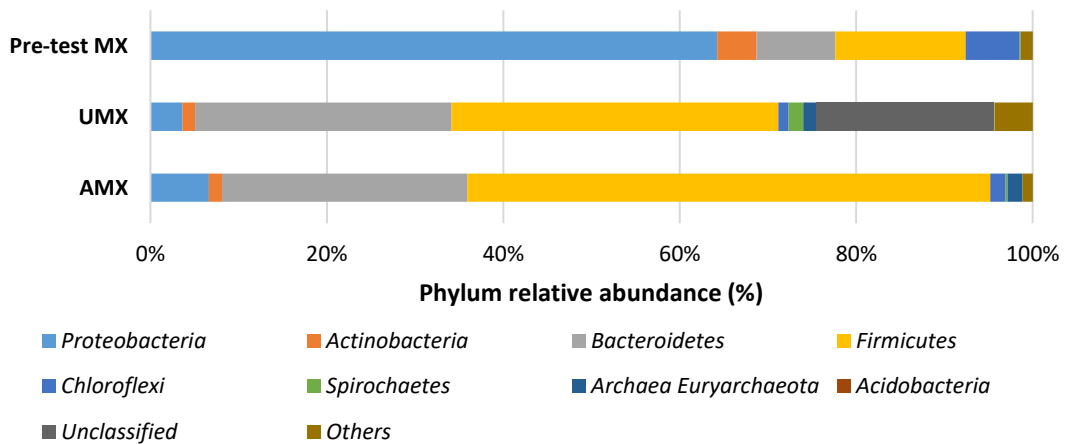


**Figure 9-14 Taxonomic classification of 16S RNA gene at the phylum level for pre-test and post-test MX sludge.**
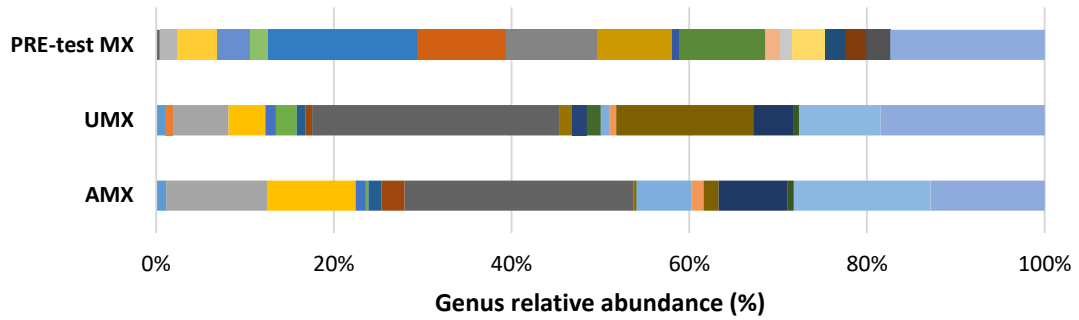
**Figure 9-15 Taxonomic classification of 16S RNA gene at the genus level for pre-test and post-test MX sludge.**
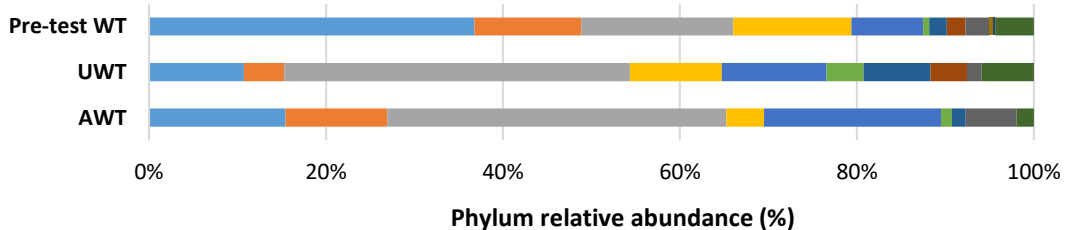


**Figure 9-16 Taxonomic classification of 16S RNA gene at the phylum level for pre-test and post-test WT sludge.**

199
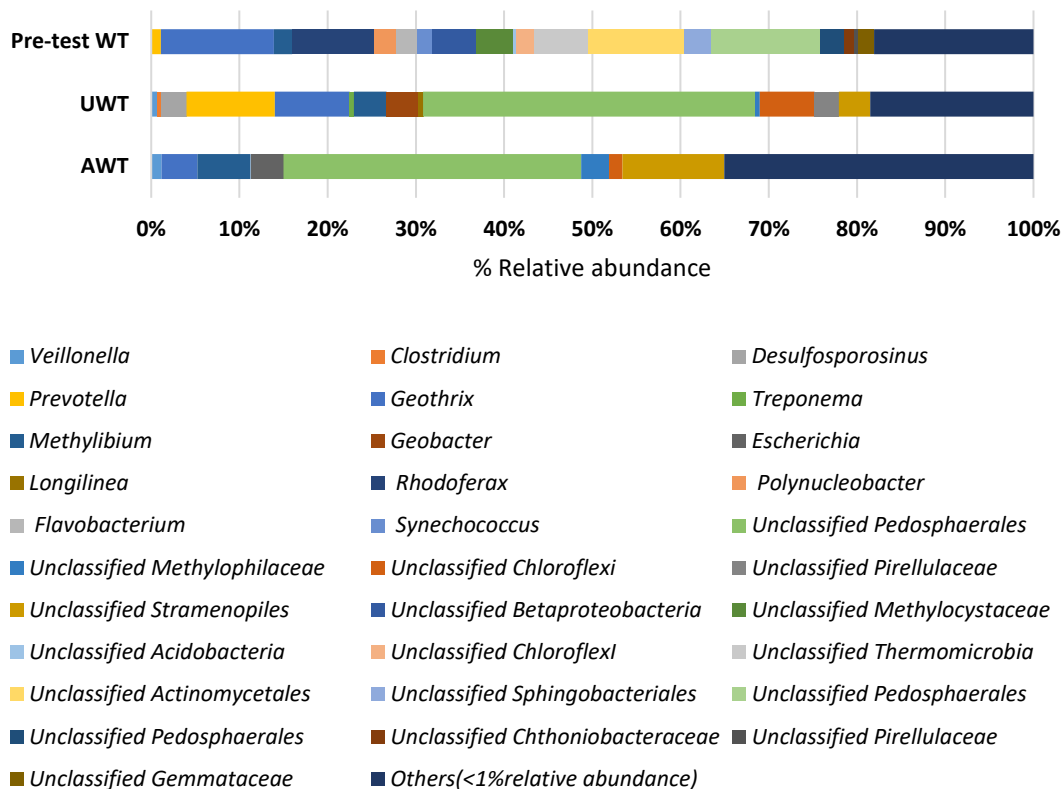
Figure 9-17 Taxonomic classification of 16S RNA gene at the genus level for pre-test and post-test WT sludge.

## 9.7     Conceptual model

Mine water treatment sludge (MWT), mixed sludge (MX), and water treatment sludge (WT) were used as microcosm substrates to degrade BTEX at 45 mg/l for each compound in a batch experiment over 160 days. Volatility was the main reason for the use of sealed 20 ml GC-MS sealed vials without headspace as microcosm reactors. Batch adsorption experiment highlighted that the iron oxides bearing sludge had low adsorption for benzene, toluene and ethylbenzene compared with xylene as noticed in Figure 9-2. BTEX biodegradation was conducted as initial aerobic and initial anoxic conditions for comparison, and data collected confirmed that BTEX was degraded more efficiently at the initial anoxic condition as noticed in Figure 9-4. During the BTEX biodegradation experiment, ferrous iron was detected particularly in MX microcosms which probably an indication for iron-reducing bacteria activity. The

indigenous iron oxides bearing sludge flourished consortia degraded BTEX at a pH range between 4.7 to 7.7, and DO was between 2 mg/l to zero mg/l. Next-generation sequencing confirmed that iron-reducing bacteria, including *Geothrix, Geobacter,* and *Clostridium* flourished in the microcosm substrates. These microorganisms affiliated with other genera as *Escherichia, Prevotella,* and *Proteiniclasticum* to mineralise the BTEX as a sole carbon source (see Figure 9-13, Figure 9-15 and Figure 9-17).

Figure 9-18 elucidates the expected mechanism for BTEX biodegradation by iron oxides bearing sludge microorganisms included iron-reducing bacteria and the affiliated bacterial genera. In this mechanism mono aromatic hydrocarbons, BTEX was oxidised as an electron donor to reduce iron oxide, which is the electron acceptor.
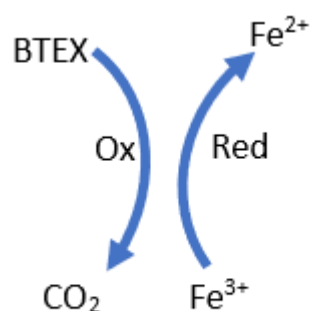


**Figure 9-18 The expected mechanism in microcosm substrates during BTEX biodegradation.**

Under iron-reducing condition, BTEX was oxidised as an electron donor, and Fe (III) was reduced to Fe (II) as an electron acceptor, within this condition BTEX can completely mineralise to $CO_2$ (Botton and Parsons 2006; Kunapuli et al. 2008). Anderson et al. (1998) confirmed that BTEX was degraded by bacterial consortium contained iron-reducing genera as *Geobacter* and *Geothrix.* Single iron-reducing bacteria species as *Geothrix* mineralised BTEX as a sole carbon source (Zhang et al. 2013c). *Geobacter* can degrade BTEX at the iron-reducing condition. It degraded mono aromatic hydrocarbon to $CO_2$ (Botton et al. 2007). *Geobacter* is coupling aromatic hydrocarbon oxidation as a BTEX to $CO_2$ and Fe (III) reduction (Lovley and Lonergan 1990; Botton et al. 2007). Iron-reducing bacteria and the affiliated microorganism in iron oxides bearing sludge mineralised the BTEX as a sole organic carbon without pre-acclimatisation, which considered an advantage for this system.

Some of the literature review studies in Table 2-7 mineralised BTEX as an additional carbon source, and pre-adoption was required. Singh and Celin (2010) utilised bacterial consortium to mineralised BETX as additional carbon source and the microorganisms used were pre-acclimatised before treatment. In this experiment, BTEX degraded over the variable temperature range (1 $^{\circ}$C to 24.5 $^{\circ}$C) while in literature, BTEX mineralisation usually conducted at a constant temperature (25 $^{\circ}$C) (Shim and Yang 2002; Müller et al. 2017; Viggi et al. 2018). The evidence highlighted during BTEX mineralised, confirmed that the tested iron oxides bearing sludge are competitive substrates to degrade mono aromatic hydrocarbon as it contains rich iron-reducing genera which synergetic with other species. These microorganisms degraded BTEX as a sole carbon source and with no acclimatisation needed.

# Chapter 10 Cross-chapters general discussion

Iron oxides bearing wastes included mine water treatment sludge (MWT), mixed sludge (MX) and water treatment sludge (WT) were used as biological-active media to treat textile, municipal and BTEX bearing wastewater. The wastewater experiments were designed to be simple and practical to be applied. These iron oxides can be found as a mining waste which is restricted with mining activity while water treatment sludge is generated from water treatment plants. Mixed sludge was used to study the effect of added additional nutrients as a wastewater sludge to MWT microorganism.

Iron oxides bearing sludge contained indigenous iron-reducing bacteria additional to other bacterial species. These microorganisms degraded wastewater aromatic hydrocarbons, including azo dye and BTEX. The flourished consortia biodegraded the azo dye double bond and aromatic hydrocarbon ring in azo dye without generated aromatic amines. The non-detection of aromatic amines during textile wastewater experiments demonstrated the ability of iron oxides bearing sludge's indigenous consortia to manualised azo dye to simplest chemicals. These microbial consortia degraded aromatic hydrocarbons included azo dye and BTEX as a sole carbon source and without pre-adaptation. Azo dye degraded by reduction of the azo bond as a first step and then oxidation the aromatic amines to the simplest chemicals as a second step. The organic hydrocarbons represent the electron donor, and Fe (III) is the electron acceptor which reduced to Fe (II). The dye decolourisation was high up to 99% during textile wastewater experiments with efficient azo dye removal rate.

Nitrogen removal was also investigated during wastewater experiments. It was determined the ability of iron oxides bearing sludge to transform nitrogen. It expected to involve various mechanisms included: Feammox, Anammox and nitrification. The nitrogen removal rates during the experimented wastewater treatments were promising and competitive with other literature. The highest normalised nitrogen removal rate was 216 g/m3/day, 39 g/m3/day and 159 g/m3/day in phase two, phase three textile wastewater and in municipal wastewater experiments and the highest normalised TC removal rate was 3000 $g/m^3/day$, 1394 $g/m^3/day$, 301 $g/m^3/day$ in phase two, phase three textile wastewater and in municipal wastewater experiments. The variation in nitrogen removal rate over the different experiment might be related to TC

concentration in each wastewater. It was the highest in phase two textile wastewater at 1676 mg/l, followed by 450 mg/l in phase three textile wastewater, and it was only 104 mg/l in municipal wastewater. TC could influence the nitrogen removal rate indirectly as a substrate to increase the microorganism growth during these experiments. It was also noticed that the pH of the conducted wastewater experiment was usually alkaline to neutral range in all wastewater experiments except it was acidic to neutral in the BTEX bearing wastewater experiment. It referred that majority of bioremediation microorganisms in iron oxides bearing sludge flourished in alkaline condition.

The flourished consortia in post-test sludge varied according to the type of wastewater used because some species tolerate the utilised contaminants and adapted with the new conditions while other do not resist these contaminants and retreated under the detection limit. However, there were some bacterial species able to grow in all post-tested sludge for textile, municipal and BTEX bearing wastewater experiments. In general, iron-reducing bacteria were detected in all post-test sludge, and it affiliated with other microorganisms. The gene sequencing confirmed that Bacterial *Firmicutes* and *Proteobacteria* phyla flourished during wastewater treatments in all the post-test sludge. These sludges were rich substrates with iron-reducing bacteria which affiliated with other microorganisms. It was noticed that some iron-reducing bacterial species were detected in most of the tested sludge as *Geobacter*, *Geothrix, Clostridium Alkaliphilus, Ochrobactrum, and Rhodoferax*. These species degraded aromatic hydrocarbons efficiently as it synergetic with other bacterial species during wastewater experiments. The rich microbial diversity of the utilised iron oxides bearing sludge is one of the advantages for used these sludges because they were tackled with various wastewater contaminants and in each experiment, a specific bacteria species was flourished. These species tolerated the contaminants more than other bacterial species which contained the required mechanism to metabolise the recalcitrant contaminants chemical structure to simplest form. Study the contaminants removal rates during the conducted wastewater experiment provided valuable information about the capacity of the system and how much sludge is required to treat wastewater in practical applications.

There were some engineering constraints could be highlighted, the fine iron oxides bearing sludge particles and upflow rate used could clog the columns, it can be avoided by mixing the sludge with other materials as bio-ball to increase the sludge primarily. In phase two textile wastewater experiment, the spiral tube was not efficient to raise the DO to the aerobic range. Alternatively, a mechanical air pump should be used for aeration. Lack of data acquired directly within the columns during wastewater experiments is one of the study limitations. It could infer the physicochemical parameters from effluents tanks. Even though this technique did not consider any changes occurred for column effluents in the collection tanks. Data was collected every 24 hrs, which provides time to alter wastewater properties so that the data collected was not the instant conditions of the columns. Due to experiment design, sludge samples for biological analysis were collected by the end of wastewater experiments. This technique did not give enough information about the microbial developing during the experiment as some species other the dominant genera might proliferate and decline during the treatment without expressed in the post-test sludge samples.

# Chapter 11 Conclusions and recommendations

- The iron oxide bearing wastes microbial consortia (iron-reducing bacteria and the affiliated genera) where demonstrated to efficiently mineralise recalcitrant wastewater contaminants such as azo dye and BTEX. These bacterial consortia also transformed nitrogen contaminants and degraded organic carbon contaminants in municipal wastewater without pre-acclimatisation.

- The MWT sludge's indigenous microbial consortia included iron-reducing bacteria, and the synergetic bacterial genera degraded MO to simple compounds by degrading the azo bond and oxidising the aromatic benzene ring.

- Iron oxide bearing wastes were efficient substrates to remediate dyes in textile wastewater as they decolourised 81 % to 99 % of the influent textile wastewater dye under the experimental conditions.

- Biodegradation is the main mechanism for recalcitrant wastewater contaminants removal as MO and BTEX, iron oxide-bearing wastes (MWT, MX, and WT) had a low adsorption affinity for these contaminants.

- MO azo dye was biodegraded by the indigenous microbial community within the iron oxides bearing sludge without generating aromatic amines. The community included iron-reducing bacteria and the synergetic bacterial species.

- The MWT sludge indigenous microbial consortium degraded MO as a sole organic carbon source. However, adding additional organic carbon as glycerol accelerated the MO decolourisation.

- The highest normalised MO removal rate during phase one and phase two textile wastewater experiments was 29.71 $g/m^3/day$, and 178 $g/m^3/day$ by MWT sludge flourished bacterial consortia.

- The highest normalised carbon and nitrogen removed rate during textile wastewater experiments was 3000 $g/m^3/day$ and 216 $g/m^3/day$ by MWT sludge indigenous consortia.

- The flourished iron-reducing bacteria and the synergetic genera in iron oxide bearing sludge were able to remove organic carbon and nitrogen during the municipal wastewater experiment. The highest normalised carbon removal rate

was 301 g/m$^3$/day by MWT while the nitrogen removal was 159 g/m$^3$/day by MX columns.

- Benzene, toluene, ethylbenzene and xylene degraded more effectively under initially anoxic condition rather than initially aerobic conditions by iron oxides bearing sludge microbial consortia.

- The indigenous iron oxide bearing sludge microbial consortia degrade BTEX as a sole carbon source and without pre-acclimatisation.

- *Proteobacteria*, *Firmicutes,* and *Bacteroidetes* were the dominant bacterial phyla in post-test iron oxide bearing substrates during wastewater experiments. These bacterial species contributed efficiently in recalcitrant wastewater bioremediation.

- Various iron-reducing bacteria as *Geothrix, Geobacter, Clostridium, Alkaliphilus, Ochrobactrum,* and *Rhodoferax* flourished in post-test iron oxide-bearing substrates during wastewater experiment, these genera synergistic with other bacterial species to degrade wastewater contaminants.

# Recommendation for future studies

- Determine the ability of iron oxide bearing sludge and its indigenous microbial consortia to tolerate and degrade different azo dyes at various concentrations instead of using only MO at 15 mg/l.

- Develop a column design that allows for sub-samples of waste to be taken during the experiment to monitor how the indigenous microorganisms changes with time during the experiment instead of using pre-test and post-test biological samples only.

- Use a built-in dissolved oxygen probe which can be attached to the columns to determine the in-situ column conditions accurately

- Undertake experiments to isolate the dominance of iron-reducing species to study the aromatic hydrocarbons mechanism intensively as a single bacteria species and distinguish the role or electron shuttles mechanism.

- Determine the extent of the anaerobic ammonium oxidation at iron-reducing condition (Feammox) in the iron oxides bearing sludge when treating nitrogenous wastewaters.

- .Conduct a field study using iron oxides bearing sludge as a biological substrate to remediate wastewater contaminants in a landfill application.

- Conduct an experimental study for using iron oxides bearing sludge to remediate BTEX contamination in aquifers as a permeable reactive barrier.

- Conduct more experiment using higher nitrogen and carbon concentrations to validate the ability of iron oxides bearing sludge indigenous consortia to remediate wastewater contaminants at various contaminant concentrations.

# References

Abiri, F., Fallah, N. and Bonakdarpour, B. 2017. Sequential anaerobic-aerobic biological treatment of colored wastewaters: Case study of a textile dyeing factory wastewater. *Water Science and Technology* 75(6), pp. 1261–1269.

Aburto-Medina, A. and Ball, A.S. 2015. Microorganisms involved in anaerobic benzene degradation. *Annals of Microbiology* 65(3), pp. 1201–1213.

Aftab, U., Khan, M.R., Mahfooz, M., Ali, M. and Aslam, S.H. 2011. Decolourization and degradation of textile azo dyes by Corynebacterium sp. isolated from industrial effluent. *Pakistan Journal of Zoology* 43(1), pp. 1–8.

Agency, E.P. 1986. *Test methods for evaluating solid waste: physical/chemical methods*. US Environmental Protection Agency. Office of Solid Waste and Emergency Response.

Ahn, Y. and Logan, B.E. 2010. Effectiveness of domestic wastewater treatment using microbial fuel cells at ambient and mesophilic temperatures. *Bioresource Technology* 101(2), pp. 469–475.

El Ahwany, A.M.D. 2008. Decolorization of Fast red by metabolizing cells of Oenococcus oeni ML34. *World Journal of Microbiology and Biotechnology* 24(8), pp. 1521–1527.

Aihara, J. 1992. Why aromatic compounds are stable. *Scientific American* 266(3), pp. 62–69.

Aivalioti, M., Vamvasakis, I. and Gidarakos, E. 2010. BTEX and MTBE adsorption onto raw and thermally modified diatomite. *Journal of Hazardous Materials* 178(1–3), pp. 136–143.

Akmirza, I., Pascual, C., Carvajal, A., Pérez, R., Muñoz, R. and Lebrero, R. 2017. Anoxic biodegradation of BTEX in a biotrickling filter. *Science of the Total Environment* 587–588, pp. 457–465.

Albuquerque, M.G.E., Lopes, A.T., Serralheiro, M.L., Novais, J.M. and Pinheiro,

H.M. 2005. Biological sulphate reduction and redox mediator effects on azo dye decolourisation in anaerobic-aerobic sequencing batch reactors. *Enzyme and Microbial Technology* 36(5–6), pp. 790–799.

Aleghafouri, A., Hasanzadeh, N., Mahdyarfar, M., SeifKordi, A., Mahdavi, S.M. and Zoghi, A.T. 2015. Experimental and theoretical study on BTEX removal from aqueous solution of diethanolamine using activated carbon adsorption. *Journal of Natural Gas Science and Engineering* 22, pp. 618–624.

Alexander, R.R., Tang, J. and Alexander, M. 2002. Genotoxicity is unrelated to total concentration of priority carcinogenic polycyclic aromatic hydrocarbons in soils undergoing biological treatment. *Journal of Environmental Quality* 31(1), pp. 150–154.

Ali, M. and Okabe, S. 2015. Anammox-based technologies for nitrogen removal: Advances in process start-up and remaining issues. *Chemosphere* 141, pp. 144–153.

Alleman, J.E. 1985. Elevated nitrite occurence in biological wastewater treatment systems. *Water Science and Technology* 17, pp. 409–419.

Altschul, S.F., Gish, W., Miller, W., Myers, E.W. and Lipman, D.J. 1990. Basic local alignment search tool. *Journal of Molecular Bology* 215(3), pp. 403–410.

Alzaydien, A.S. 2015. Adsorption behavior of methyl orange onto wheat bran: Role of surface and pH. *Oriental Journal of Chemistry* 31(2), pp. 643–651.

Amaral, F.M., Kato, M.T., Florêncio, L. and Gavazza, S. 2014. Color, organic matter and sulfate removal from textile effluents by anaerobic and aerobic processes. *Bioresource Technology* 163, pp. 364–369.

Anderson, R.T., Gaw, C. V and Lovley, D.R. 1998. Anaerobic benzene oxidation in the Fe (III) reduction zone of petroleum-contaminated aquifers. *Environmental Science and Technology* 32(9), pp. 1222–1229.

Andreoni, V. and Gianfreda, L. 2007. Bioremediation and monitoring of aromatic-polluted habitats. *Applied Microbiology and Biotechnology* 76(2), pp. 287–308.

Angelova, B., Avramova, T., Stefanova, L. and Mutafov, S. 2008. Temperature effect

on bacterial azo bond reduction kinetics: An Arrhenius plot analysis. *Biodegradation* 19(3), pp. 387–393.

Anjaneyulu, Y., Chary, N.S. and Raj, D.S.S. 2005. Decolourization of industrial effluents–available methods and emerging technologies–a review. *Reviews in Environmental Science and Biotechnology* 4, pp. 245–273.

Antoniou, P. et al. 1990. Effect of temperature and ph on the effective maximum specific growth rate of nitrifying bacteria. *Water Research* 24(1), pp. 97–101.

Aravind, P., Selvaraj, H., Ferro, S. and Sundaram, M. 2016. An integrated (electro- and bio-oxidation) approach for remediation of industrial wastewater containing azo-dyes: Understanding the degradation mechanism and toxicity assessment. *Journal of Hazardous Materials* 318, pp. 203–215.

Arsalan, A. et al. 2018. Performance of activated sludge biofilms fluidized process in the biotreatment of real textile wastewater. *Journal of Applied Environmental and Biological Sciences* 7(12), pp. 81–90.

Asad, S., Amoozegar, M.A., Pourbabaee, A.A., Sarbolouki, M.N. and Dastgheib, S.M.M. 2007. Decolorization of textile azo dyes by newly isolated halophilic and halotolerant bacteria. *Bioresource Technology* 98(11), pp. 2082–2088.

Ávila, C., Pelissari, C., Sezerino, P.H., Sgroi, M., Roccaro, P. and García, J. 2017. Enhancement of total nitrogen removal through effluent recirculation and fate of PPCPs in a hybrid constructed wetland system treating urban wastewater. *Science of the Total Environment* 584–585, pp. 414–425.

Ayed, L. et al. 2010. Response surface methodology for decolorization of azo dye Methyl Orange by bacterial consortium: Produced enzymes and metabolites characterization. *Chemical Engineering Journal* 165(1), pp. 200–208.

Ayed, L., Mahdhi, A., Cheref, A. and Bakhrouf, A. 2011. Decolorization and degradation of azo dye Methyl Red by an isolated Sphingomonas paucimobilis: Biotoxicity and metabolites characterization. *Desalination* 274(1–3), pp. 272–277.

Badham, H. and LM Winn 2007. Investigating the role of the aryl hydrocarbon

receptor in benzene-initiated toxicity in vitro. *Toxicology* 229(3), pp. 177–185.

Bafana, A., Chakrabarti, T., Muthal, P. and Kanade, G. 2009. Detoxification of benzidine-based azo dye by E. gallinarum: Time-course study. *Ecotoxicology and Environmental Safety* 72, pp. 960–964.

Bagajewicz, M. 2000. A review of recent design procedures for water networks in refineries and process plants. *Computers and Chemical Engineering* 24(9–10), pp. 2093–2113.

Baiocchi, C. et al. 2002. Characterization of Methyl Orange and its photocatalytic degradation products by HPLC/UV-VIS diode array and atmospheric pressure ionization quadrupole ion trap mass spectrometry. *International Journal of Mass Spectrometry* 214(2), pp. 247–256.

Balapure, K., Bhatt, N. and Madamwar, D. 2015. Mineralization of reactive azo dyes present in simulated textile waste water using down flow microaerophilic fixed film bioreactor. *Bioresource Technology* 175, pp. 1–7.

Banat, I.M., Nigam, P., Singh, D. and Marchant, R. 1997. Microbial decolorization of textile-dye-containing effluents: A review. *Bioresource Technology* 58(1996), pp. 217–227.

Bardi, L. and Marzona, M. 2010. Factors affecting the complete mineralization of azo dyes. In: *Biodegradation of azo dyes*. Springer, Berlin, Heidelberg, pp. 195– 210.

Barnard, J.L. 1976. A Review of biological phosphorus removal in the activated sludge process. *Water S* 2(3), pp. 136–144.

Barragán, B.E., Costa, C. and Carmen Márquez, M. 2007. Biodegradation of azo dyes by bacteria inoculated on solid media. *Dyes and Pigments* 75(1), pp. 73–81.

Bashiri, B., Fallah, N., Bonakdarpour, B. and Elyasi, S. 2018. The development of aerobic granules from slaughterhouse wastewater in treating real dyeing wastewater by Sequencing Batch Reactor (SBR). *Journal of Environmental Chemical Engineering* 6(4), pp. 5536–5543.

Bassin, J.P., Pronk, M., Muyzer, G., Kleerebezem, R., Dezotti, M. and van Loosdrecht,

M.C.M. 2011. Effect of elevated salt concentrations on the aerobic granular sludge process: Linking microbial activity with microbial community structure. *Applied and Environmental Microbiology* 77(22), pp. 7942–7953.

Batool, S., Khalid, A., Jalal, K.C.A., Sarfraz, M., Balkhair, K.S. and Ashraf, M.A. 2015. Effect of azo dye on ammonium oxidation process and ammonia-oxidizing bacteria (AOB) in soil. *The Royal Society of Chemistry* 5(44), pp. 34812–34820.

Batstone, D.J. et al. 2002. The IWA anaerobic digestion model no 1 (ADM1). *Water Science and Technology* 45(10), pp. 65–73.

Bell, J., Plumb, J.J., Buckley, C. a and Stuckey, D.C. 2000. Treatment and decolorization of dyes in anaerobic baffled reactor. *Journal of Environmental Engineering* 126(11), pp. 1026–1032.

Bennett, G.. 1993. *In situ bio-remediation When Does it Work?. Water science and technology board commission on engineering and technical systems national research council*. Academy Press, Washington, DC, 1993, 207 pages, price US.

Berlendis, S. et al. 2010. First evidence of aerobic biodegradation of BTEX compounds by pure cultures of Marinobacter. *Applied Biochemistry and Biotechnology* 160(7), pp. 1992–1999.

Bernet, N. and Spérandio, M. 2009. Principles of nitrifying processes. In: *Environmental technologies to treat nitrogen pollution*. IWA publishing., pp. 23–37.

Beydilli, M.I., Pavlostathis, S.G. and Tincher 1998. Decolorization and toxicity screening of selected reactive azo dyes under methanogenic conditions. *Water Science and Technology* 38(4–5), pp. 225–232.

Bhattacharya, A., Goyal, N. and Gupta, A. 2017. Degradation of azo dye methyl red by alkaliphilic, halotolerant Nesterenkonia lacusekhoensis EMLA3: Application in alkaline and salt-rich dyeing effluent treatment. *Extremophiles* 21(3), pp. 479–490.

Bheemaraddi, M.C., Patil, S., Shivannavar, C.T. and Gaddad, S.M. 2014. Isolation and characterization of Paracoccus sp. GSM2 capable of degrading textile azo dye reactive violet 5. *The Scientific World Journal* 2014, pp. 1–9.

Blackall, L.L., Crocetti, G.R., Saunders, A.M.. and Bond, P.L. 2002. A review and update of the microbiology of enhanced biological phosphorus removal in wastewater treatment plants. *Antonie van Leeuwenhoek* 81(1), pp. 681–691.

Blümel, S., Contzen, M., Lutz, M., Stolz, A. and Knackmuss, H.J. 1998. Isolation of a bacterial strain with the ability to utilize the sulfonated azo compound 4-carboxy-4'-sulfoazobenzene as the sole source of carbon and energy. *Applied and Environmental Microbiology* 64(6), pp. 2315–2317.

Bolden, A.L., Kwiatkowski, C.F. and Colborn, T. 2015. New look at BTEX: Are ambient levels a problem? *Environmental Science and Technology* 49(9), pp. 5697–5703.

Boothman, C. et al. 2006. Reactive azo dye reduction by Shewanella strain J18 143. *Biotechnology and Bioengineering* 95(4), pp. 692–703.

Botton, S., Harmelen, M. Van, Braster, M., Parsons, J.R. and Wilfred, F.M.R. 2007. Dominance of Geobacteraceae in BTX-degrading enrichments from an iron-reducing aquifer. *FEMS Microbiology Ecology* 62, pp. 118–130.

Botton, S. and Parsons, J.R. 2006. Degradation of BTEX compounds under iron-reducing conditions in contaminated aquifers microcosms. *Environmental Toxicology and Chemistry* 25(10), pp. 2630–2638.

Botton, S. and Parsons, J.R. 2007. Degradation of BTX by dissimilatory iron-reducing cultures. *Biodegradation* 18, pp. 371–381.

Bridge, T.A.M. and Johnson, D.B. 1998. Reduction of soluble iron and reductive dissolution of ferric iron- containing minerals by moderately thermophilic iron-oxidizing bacteria. *Applied and Environmental Microbiology* 64(6), pp. 2181–2186.

Brosillon, S., Djelal, H., Merienne, N. and Amrane, A. 2008. Innovative integrated process for the treatment of azo dyes: coupling of photocatalysis and biological treatment. *Desalination* 222(1–3), pp. 331–339.

Brown, M.A. and De Vito, S.C. 1993. Predicting azo dye toxicity. *Critical Reviews in Environmental Science and Technology* 23(3), pp. 249–324.

Bulc, T.G. and Ojstršek, A. 2008. The use of constructed wetland for dye-rich textile wastewater treatment. *Journal of Hazardous Materials* 155(1–2), pp. 76–82.

Bushnell, L.D. and Haas, H.F. 1940. The utililization o fcertain hydrocarbons by microorganisms. *Journal of Bacteriology* 41(5), pp. 653–673.

Caccavo, F., Blakemore, R.P. and Lovleyl, D.R. 1992. A Hydrogen-oxidizing, Fe(III)-reducing microorganism from the Great Bay Estuary, New Hampshire. *Applied and Enviromental Microbiology* 58(10), pp. 3211–3216.

Caccavo, F., Schamberger, P.C., Keiding, K., Hampshire, N. and Hampshire, N. 1997. Role of hydrophobicity in adhesion of the dissimilatory Fe(III)-reducing bacterium Shewanella alga to amorphous Fe(III) oxide. *Applied and Enviromental Microbiology* 63(10), pp. 3837–3843.

Cai, P.J. et al. 2012. Anaerobic biodecolorization mechanism of methyl orange by Shewanella oneidensis MR-1. *Applied Microbiology and Biotechnology* 93(4), pp. 1769–1776.

Caldwell, M.E.M. et al. 1999. Microbial metabolism of benzene and the oxidation of ferrous iron under anaerobic conditions: Implications for bioremediation. *Anaerobe* 5(6), pp. 595–603.

Canstein, H. Von, Ogawa, J., Shimizu, S. and Lloyd, J.R. 2008. Secretion of flavins by Shewanella species and their role in extracellular electron transfer. *Applied and Enviromental Microbiology* 74(3), pp. 615–623.

Cao, W., Mahadevan, B., Crawford, D.L. and Crawford, R.L. 1993. Characterization of an extracellular azo dye-oxidizing peroxidase from Flavobacterium sp. ATCC 39723. *Enzyme Microb. Technol* 15, pp. 810–817.

Caporaso, J.G. et al. 2010. QIIME allows analysis of high-throughput community sequencing data. *Nature* 7(5), pp. 335–336.

Carmen, Z., Daniela, S., Daniel, S., Daniela, S., Daniel, S. and Daniela, S. 2012. Textile organic dyes-characteristics, polluting Effects and separation/elimination procedures from industrial effluents–a critical overview. In: *Organic Pollutants Ten*

*Years After the Stockholm Convention-Environmental and Analytical Update (Vol. 2741, p. 31). Rijeka, Croatia: InTech.*

Castro, L., García-Balboa, C., González, F., Ballester, A., Blázquez, M.L. and Muñoz, J.A. 2013. Effectiveness of anaerobic iron bio-reduction of jarosite and the influence of humic substances. *Hydrometallurgy* 131–132, pp. 29–33.

Cerniglia, C.E. 1993. Biodegradation of polycyclic aromatic hydrocarbons. *Current Opinion in Biotechnology* 4(3), pp. 227–244.

Cervantes, F.J. and Santos, A.B. Dos 2011. Reduction of azo dyes by anaerobic bacteria : microbiological and biochemical aspects. *Reviews in Environmental Science and Biotechnology* 10(2), pp. 125–137.

Chacko, J. and Subramaniam, K. 2011. Enzymatic Degradation of Azo Dyes – A Review. *International Journal of Environmental Sciences* 1(6), pp. 1250–1260.

Chan, Y.J., Chong, M.F., Law, C.L. and Hassell, D.G. 2009. A review on anaerobic-aerobic treatment of industrial and municipal wastewater. *Chemical Engineering Journal* 155(1–2), pp. 1–18.

Chang, J., Kuo, T., Chao, Y., Ho, J. and Lin, P. 2000. Azo dye decolorization with a mutant Escherichia coli strain. *Biotechnology Letters* 22, pp. 807–812.

Chang, J., Chen, B. and Lin, Y.S. 2004. Stimulation of bacterial decolorization of an azo dye by extracellular metabolites from Escherichia coli strain NO3. *Bioresource Technology 91* 91, pp. 243–248.

Chang, J.S., Chou, C., Lin, Y.C., Lin, P.J., Ho, J.Y. and Hu, T.L. 2001. Kinetic characteristics of bacterial azo-dye decolorization by Pseudomonas luteola. *Water Research* 35(12), pp. 2841–2850.

Chang, J.S. et al. 2011. Bacterial decolorization and degradation of azo dyes: A review. *Journal of the Taiwan Institute of Chemical Engineers* 42(1), pp. 138–157. Available at: http://dx.doi.org/10.1016/j.jtice.2010.06.006.

Chang, M., Shu, H., Yu, H. and Sung, Y. 2006. Reductive decolourization and total organic carbon reduction of the diazo dye CI Acid Black 24 by zero-valent iron.

*Journal of Chemical Technology and Biotechnology* 81, pp. 1259–1266.

Chen, G., Li, J., Tabassum, S. and Zhang, Z. 2015. Anaerobic ammonium oxidation (ANAMMOX) sludge immobilized by waterborne polyurethane and its nitrogen removal performance-a lab scale study. *The Royal Society of Chemistry* 5(32), pp. 25372–25381.

Chen, H., Wang, R.F. and Cerniglia, C.E. 2004. Molecular cloning, overexpression, purification, and characterization of an aerobic FMN-dependent azoreductase from Enterococcus faecalis. *Protein Expression and Purification* 34(2), pp. 302–310.

Chen, K., Wu, J., Liou, D. and Hwang, S.J. 2003. Decolorization of the textile dyes by newly isolated bacterial strains. *Journal of Biotechnology* 101, pp. 57–68.

Chen, P. et al. 2012. Simultaneous heterotrophic nitrification and aerobic denitrification by bacterium. *Bioresource Technology* 116, pp. 266–270.

Chequer, F.M.D., Dorta, D.J. and Danielle Palma de Oliveira 2011. Azo dyes and their metabolites: Does the discharge of the azo dye into water bodies represent human and ecological risks ? *Advances in Treating Textile Effluent* , pp. 27–48.

Childers, S.E., Ciufo,  &Stacy and Lovley, D.R. 2002. Geobacter metallireducens accesses insoluble Fe(III) oxide by chemotaxis. *Nature* 416(1996), pp. 767–769.

Chinwetkitvanich, S., Tuntoolvest, M. and Panswad, T. 2000. Anaerobic decolorization of reactive dyebath effluents by a two-stage UASB system with tapioca as a co-substrate. *Water Research* 34(8), pp. 2223–2232.

Chung, K., Fulk, G.E. and Egan, M. 1978. Reduction of azo dyes by intestinal anaerobes. *Applied and Environmental Microbiology* 35(3), pp. 558–562.

Cl'ement, J.C., Shrestha, J., Ehrenfeld, J.G. and Jaffe', P.. 2005. Ammonium oxidation coupled to dissimilatory reduction of iron under anaerobic conditions in wetland soils. *Soil Biology and Biochemistry* 37, pp. 2323–2328.

Claus, H., Faber, G. and König, H. 2002. Redox-mediated decolorization of synthetic dyes by fungal laccases. *Applied Microbiology and Biotechnology* 59(6), pp. 672–678.

Cleverson Vitorio Andreoli, M. von S. and Fernandes, F. 2007. *Sludge treatment and disposal*. IWA publishing.

Coates, J.D., Phillips, E.J.P., Lonergan, D.J., Jenter, H. and Lovley, D.R. 1996. Isolation of Geobacter species from diverse sedimentary environments. *Applied and Enviromental Microbiology* 62(5), pp. 1531–1536.

Coates, J.D., Chakraborty, R., Lack, J.G. and Connor, S.M. 2001. Anaerobic benzene oxidation coupled to nitrate reduction in pure culture by two strains of Dechloromonas. *Nature* 411(6), pp. 1039–1043.

Coates, J.D., Chakraborty, R. and McInerney, M.J. 2002. Anaerobic benzene biodegradation-a new era. *Research in Microbiology* 153(10), pp. 621–8.

Coelho, A., Castro, A. V., Dezotti, M. and Sant'Anna, G.L. 2006. Treatment of petroleum refinery sourwater by advanced oxidation processes. *Journal of Hazardous Materials* 137(1), pp. 178–184. doi: 10.1016/j.jhazmat.2006.01.051.

Cohen, B. 1931. The bacterial culture as an electrical half-cell. *J. Bacteriol* 21(1), pp. 18–19.

Collins, M.D., Lawson, P.A., Labrenz, M., Tindall, B.J., Weiss, N. and Hirsch, P. 2002. Nesterenkonia lacusekhoensis sp. nov., isolated from hypersaline Ekho Lake, East Antarctica, and emended description of the genus Nesterenkonia. *International Journal of Systematic and Evolutionary Microbiology* 52, pp. 1145–1150.

Cornell, R.M. and Schwertmann, U. 2003. *The iron oxides: structure, properties, reactions, occurrences and uses*. John Wiley & Sons.

Cornell, R.M. and Schwertmann, U. 2004. Environmental Significance. In: *The Iron Oxides*., pp. 541–551. doi: 10.1002/3527602097.ch21.

Coughlin, M.F., Kinkle, B.K. and Bishop, P.L. 1999. Degradation of azo dyes containing aminonaphthol by Sphingomonas sp strain 1CX. *Journal of Industrial Microbiology and Biotechnology* 23(4–5), pp. 341–346.

Coughlin, M.F., Kinkle, B.K. and Bishop, P.L. 2002. Degradation of acid orange 7 in an aerobic biofilm. *Chemosphere* 46(1), pp. 11–19.

Cuervo-López, F., M.-H. and Gómez, J. 2009. Principles of denitrifying processes. In: *Environmental technologies to treat nitrogen pollution*. IWA publishing, London, pp. 41-65.

Cui, D., Li, G., Zhao, D., Gu, X., Wang, C. and Zhao, M. 2012. Microbial community structures in mixed bacterial consortia for azo dye treatment under aerobic and anaerobic conditions. *Journal of Hazardous Materials* 221–222, pp. 185–192. doi: 10.1016/j.jhazmat.2012.04.032.

Dafale, N., Wate, S., Meshram, S. and Nandy, T. 2008. Kinetic study approach of remazol black-B use for the development of two-stage anoxic–oxic reactor for decolorization/ biodegradation of azo dyes by activated bacterial consortium. *Journal of Hazardous Materials* 159, pp. 319–328.

Dafale, N., Agrawal, L., Kapley, A., Meshram, S., Purohit, H. and Wate, S. 2010. Selection of indicator bacteria based on screening of 16S rDNA metagenomic library from a two-stage anoxic–oxic bioreactor system degrading azo dyes. *Bioresource Technology* 101(2), pp. 476–484.

Dang, Y., Ye, J., Mu, Y., Qiu, B. and Sun, D. 2013. Effective anaerobic treatment of fresh leachate from MSW incineration plant and dynamic characteristics of microbial community in granular sludge. *Appl Microbiol Biotechnol* 97, pp. 10563–10574.

Das, B., Mondal, N.K., Bhaumik, R. and Roy, P. 2014. Insight into adsorption equilibrium, kinetics and thermodynamics of lead onto alluvial soil. *International Journal of Environmental Science and Technology* 11(4), pp. 1101–1114.

Deeb, R.A. and Alvarez-cohen, L. 2000. Aerobic biotransformation of gasoline aromatics in multicomponent Mixtures. *Bioremdiation Journal* 4(2), pp. 171–179.

Delforno, T.P., Okada, D.Y., Faria, C. V and Varesche, M.B.A. 2016. Evaluation of anionic surfactant removal in anaerobic reactor with Fe(III) supplementation. *Journal of Environmental Management* (3), pp. 3–9.

Dhanve, R.., Shedablkar, U.. and J.P.Jadhav 2008. Biodegradation of Diazo Reactive dye navy blue HE2R (Reactive blue 172) by an isolated Exiguobacterium sp. RD3. *Biotechnology and Bioprocess Engineering* 13, pp. 53–60.

Ding, B., Li, Z. and Qin, Y. 2017. Nitrogen loss from anaerobic ammonium oxidation coupled to Iron (III) reduction in a riparian zone. *Environmental Pollution* 231, pp. 379–386.

Ding, L., An, X., Li, S., Zhang, G. and Zhu, Y. 2014. Nitrogen Loss through anaerobic ammonium oxidation coupled to iron reduction from paddy soils in a chronosequence. *Environ. Sci. Technol* 48, pp. 10641–10647.

Diniz, P.E. and Lopes, A.T. 2002. Anaerobic reduction of a sulfonated azo Dye, Congo Red, by sulfate-reducing bacteria. *Applied Biochemistry and Biotechnology* 97, pp. 147–163.

Doğan, M., Alkan, M., Türkyilmaz, A. and Özdemir, Y. 2004. Kinetics and mechanism of removal of methylene blue by adsorption onto perlite. *Journal of Hazardous Materials* 109(1–3), pp. 141–148.

Van Dongen, U., Jetten, M.S.M. and Van Loosdrecht, M.C.M. 2001. The SHARON-Anammox process for treatment of ammonium rich wastewater. *Water Science and Technology* 44(1), pp. 153–160.

Dotro, G. et al. 2017. *Treatment Wetlands*. London, UK: IWA publishing.

Du, L.-N.N. et al. 2015. Efficient metabolism of the azo dye methyl orange by Aeromonas sp. strain DH-6: Characteristics and partial mechanism. *International Biodeterioration and Biodegradation* 105, pp. 66–72.

Du, R., Peng, Y., Cao, S., Li, B., Wang, S. and Niu, M. 2016. Mechanisms and microbial structure of partial denitrification with high nitrite accumulation. *Appl Environ Microbiol* 100(2), pp. 2011–2021.

E.S. Yoo, J. Libra, U.W. 2000. Reduction of azo dyes by desulfovibrio desulfuricans. *Water Science & Technology* 41(12), pp. 15–22.

Ekici, P., Leupold, G. and Parlar, H. 2001. Degradability of selected azo dye metabolites in activated sludge systems. *Chemosphere* 44, pp. 721–728.

El-Naas, M.H., Acio, J.A. and El Telib, A.E. 2014. Aerobic biodegradation of BTEX: progresses and prospects. *Journal of Environmental Chemical Engineering* 2(2), pp.

1104–1122.

El-Naggar, M.Y. et al. 2010. Electrical transport along bacterial nanowires from Shewanella oneidensis MR-1. *PNAS* 107(42), pp. 18127–18131.

Erguder, T.H., Guven, E. and G.N, D. 2003. The inhibitory effects of lindane in batch and upflow anaerobic sludge blanket reactors. *Chemosphere* 50, pp. 165–169.

Essaid, H.I., Bekins, B.A., Herkelrath, W.N. and Delin, G.N. 2011. Crude oil at the Bemidji Site: 25 years of monitoring, modeling, and understanding. *Grownd Water* 49(5), pp. 706–726.

Evalu. [no date].

F. X. Prenafeta-Boldú, Vervoort, J., Grotenhuis, J.T.C. and Groenestijn, J.W. van 2002. Substrate interactions during the biodegradation of benzene, toluene, ethylbenzene, and xylene (BTEX) hydrocarbons by the fungus Cladophialophora sp. Strain T1. *Applied and Enviromental Microbiology* 68(6), pp. 2660–2665.

Fan, Y., Li, B., Yang, Z., Cheng, Y. and Liu, D. 2018. Abundance and diversity of iron reducing bacteria communities in the sediments of a heavily polluted freshwater lake. *Applied Microbiology and Biotechnology* 102, pp. 10791–10801.

Farabegoli, G., Chiavola, A., Rolle, E. and Naso, M. 2010. Decolorization of Reactive Red 195 by a mixed culture in an alternating anaerobic-aerobic sequencing batch reactor. *Biochemical Engineering Journal* 52(2–3), pp. 220–226.

Farhadian, M., Vachelard, C., Duchez, D. and Larroche, C. 2008a. In situ bioremediation of monoaromatic pollutants in groundwater: A review. *Bioresource Technology* 99(13), pp. 5296–5308.

Farhadian, M., Duchez, D., Vachelard, C. and Larroche, C. 2008b. Monoaromatics removal from polluted water through bioreactors-A review. *Water Research* 42(6–7), pp. 1325–1341.

Farkas, M., Szoboszlay, S., Benedek, T. and Révész, F. 2017. Enrichment of dissimilatory Fe(III)-reducing bacteria from groundwater of the Siklós BTEX-contaminated site (Hungary). *Folia Microbiol* 62, pp. 63–71.

Farrell, J., Kason, M., Melitas, N. and Li, T. 2000. Investigation of the long-term performance of zero-valent iron for reductive dechlorination of trichloroethylene. *Environmental Science and Technology* 34(3), pp. 514–521.

Ferdous Rumky, J., Abedin, Z., Rahman, H. and Hossain, A. 2013. Environmental treatment of dyes: Methyl Orange decolorization using Hog Plum peel and mix-bacterial strains. *Journal of Environmental Science* 5(3), pp. 19–22.

Field, J. and Cervantes, F.J. 2005. Microbial redox reactions mediated by humus and structurally related quinones. In: *In Use of humic substances to remediate polluted environments: from theory to practice*. Springer, Dordrecht., pp. 343–352.

Finneran, K.T., Johnsen, C. V and Lovley, D.R. 2003. Rhodoferax ferrireducens sp. nov., a psychrotolerant, facultatively anaerobic bacterium that oxidizes acetate with the reduction of Fe(III). *International Journal of Systematic and Evolutionary Microbiology* (53), pp. 669–673.

Firmino, P.I.M. et al. 2015a. Engineering and microbiological aspects of BTEX removal in bioreactors under sulfate-reducing conditions. *Chemical Engineering Journal* 260, pp. 503–512.

Firmino, P.I.M. et al. 2015b. Understanding the anaerobic BTEX removal in continuous-flow bioreactors for ex situ bioremediation purposes. *Chemical Engineering Journal* 281, pp. 272–280.

Foght, J. 2008. Anaerobic biodegradation of aromatic hydrocarbons: pathways and prospects. *Journal of Molecular Microbiology and Biothechnology* 9, pp. 93–120.

Fontenot, E.J., Lee, Y.H., Matthews, R.D., Zhu, G. and Pavlostathis, S.G. 2003. Reductive decolorization of a textile reactive dyebath under methanogenic conditions. *Applied Biochemistry and Biotechnology* 109(1–3), pp. 207–225.

Forss, J., Pinhassi, J., Lindh, M. and Welander, U. 2013. Microbial diversity in a continuous system based on rice husks for biodegradation of the azo dyes Reactive Red 2 and Reactive Black 5. *Bioresource Technology* 130, pp. 681–688.

Franca, R.D.G., Vieira, A., Mata, A.M.T., Carvalho, G.S., Pinheiro, H.M. and

Lourenço, N.D. 2015. Effect of an azo dye on the performance of an aerobic granular sludge sequencing batch reactor treating a simulated textile wastewater. *Water Research* 85, pp. 327–336.

Francis, A. and Sosamony, K.J. 2016. Treatment of pre-treated textile wastewater using moving bed bio-film reactor. *Procedia Technology* 24, pp. 248–255.

Franciscon, E. et al. 2015. Potential of a bacterial consortium to degrade azo dye Disperse Red 1 in a pilot scale anaerobic–aerobic reactor. *Process Biochemistry* 50, pp. 816–825.

Fu, L., Bai, Y.N., Lu, Y.Z., Ding, J., Zhou, D. and Zeng, R.J. 2019. Degradation of organic pollutants by anaerobic methane-oxidizing microorganisms using methyl orange as example. *Journal of Hazardous Materials* 364(9), pp. 264–271.

Fuller, S.J., Mcmillan, D.G.G., Renz, M.B., Schmidt, M., Burke, I.T. and Stewart, D.I. 2014. Extracellular electron transport-mediated fe(iii) reduction by a community of alkaliphilic bacteria that use flavins as electron shuttles. *Applied and Environmental Microbiology* 80(1), pp. 128–137.

Ganesh, R., Boardman, G.D. and Michelesn, D. 1994. Fate of azo dye s in sludge. *Water Research* 28(6), pp. 1367–1376.

García-martínez, Y., Bengoa, C., Stüber, F., Fortuny, A., Font, J. and Fabregat, A. 2015. Biodegradation of acid orange 7 in an anaerobic–aerobic sequential treatment system. *Chemical Engineering and Processing* 94, pp. 99–104.

Ge, H., Batstone, D.J. and Keller, J. 2013. Operating aerobic wastewater treatment at very short sludge ages enables treatment and energy recovery through anaerobic sludge digestion. *Water Research* 47(17), pp. 6546–6557.

Georgiou, D., Metallinou, C., Aivasidis, A., Voudrias, E. and Gimouhopoulos, K. 2004. Decolorization of azo-reactive dyes and cotton-textile wastewater using anaerobic digestion and acetate-consuming bacteria. *Biochemical Engineering Journal* 19, pp. 75–79.

Gerardi, M.H. 2003. *Nitrification and denitrification in the activated sludge process.*

John Wiley & Sons.

Ghaedi, M., Hajati, S., Zaree, M., Shajaripour, Y., Asfaram, A. and Purkait, M.K. 2015. Removal of methyl orange by multiwall carbon nanotube accelerated by ultrasound devise: Optimized experimental design. *Advanced Powder Technology* 26(4), pp. 1087–1093.

Ghaly, A.E., Ananthashankar, R., Alhattab, M. and Ramakrishnan, V. V 2014. Production, characterization and treatment of textile tffluents: A critical review. *Chemical Engineering and Process Technology* 5(1), pp. 1–19.

Ghasemi, E., Ziyadi, H., Moein, A. and Sillanpää, M. 2015. Iron oxide nanofibers : A new magnetic catalyst for azo dyes degradation in aqueous solution. *Chemical Engineering Journal* 264, pp. 146–151.

Gibson, D.T. 1978. Microbial Transformations of Aromatic Pollutants. In: *Aquatic Pollutants*. Elsevier, pp. 187–204.

Gibson, D.T. 1984. *Microbial degradation of organic compounds.* Marcel Dekker Inc.

Gijzen, H.J. 2002. Anaerobic digestion for sustainable development: a natural approach. *Water Science and Technology* 45(10), pp. 321–328.

Gingell, R. and Walker, R. 1971. Mechanisms Of azo reduction by Streptococcus Faecalis Ii. The role of soluble flavins. *Xenobiotica* 1(3), pp. 231–239.

Gorby, Y.A., Svetlana, Y., S., M.J., Rosso, K.M., Moyles, D. and Alice, D. 2006. Electrically conductive bacterial nanowires produced by Shewanella oneidensis strain MR-1. In: *Proceedings of the National Academy of Sciences.*, pp. 11358–11363.

Gorby, Y.A. and Lovley, D.R. 1991. Electron transport in the dissimilatory iron reducer, GS-15. *Applied and Enviromental Microbiology* 57(3), pp. 867–870.

Govindaswami, M., Schmidt, T.M., White, D.C. and Loper, J.C. 1993. Phylogenetic analysis of a bacterial aerobic degrader of azo dyes. *Journal of Biotechnology* 175(18), pp. 6062–6066.

Grbic-Galic, D. and Vogel, T.M. 1987. Transformation of toluene and benzene by

mixed methanogenic cultures. *Applied and Enviromental Microbiology* 53(2), pp. 254–260.

Groenestijn, J. Van, MMA, B., MH, D. and AJB, Z. 1989. Polyphosphate-degrading enzymes in Acinetobacter activated sludge. *Applied and Enviromental Microbiology* 55(1), pp. 219–223.

Guo, C.H., Stabnikov, V. and Ivanov, V. 2010. The removal of nitrogen and phosphorus from reject water of municipal wastewater treatment plant using ferric and nitrate bioreductions. *Bioresource Technology* 101(11), pp. 3992–3999. Available at: http://dx.doi.org/10.1016/j.biortech.2010.01.039.

Guo, J. et al. 2007. Biocalalyst effects of immobilized anthraquinone on the anaerobic reduction of azo dyes by the salt-tolerant bacteria. *Water Research* 41(2), pp. 426–432.

Haghseresht, F. and Lu, G.Q. 1998. Adsorption characteristics of phenolic compounds onto coal-reject-derived adsorbents. *Energy and Fuels* 12(6), pp. 1100–1107.

Hallin, S. et al. 2005. Community survey of ammonia-oxidizing bacteria in full-scale activated sludge processes with different solids retention time. *Journal of Applied Microbiology* 99, pp. 629–640.

Hamed, T.A., Bayraktar, E., Mehmetoğlu, T. and Mehmetoğlu, Ü. 2003. Substrate interactions during the biodegradation of benzene, toluene and phenol mixtures. *Process Biochemistry* 39(1), pp. 27–35.

Haque, E., Jun, J.W. and Jhung, S.H. 2011. Adsorptive removal of methyl orange and methylene blue from aqueous solution with a metal-organic framework material, iron terephthalate (MOF-235). *Journal of Hazardous Materials* 185(1), pp. 507–511.

Harayama, S. and Timmis, K.N. 1992. Aerobic biodegradation of aromatic hydrocarbons. Metal ions in biological systems: volume 28. In: Sigel, H., and Sigel, A. eds. *Degradation of environmental pollutants by microorganisms and their metalloenzymes*. Volume 28. New Yourk. Basel. Hong Kong: Marcel Dekker INC, pp. 99–156.

Harder, E.C. 1919. *Iron-depositing bacteria and their geological relations*. US

Government Printing Office.

Hartley, K.. and Sickerdick, L. 1994. Performance of Australian BNR plants. In: *Second Australian conference on biological nutrient removal from wastewater*. Albury, Victoria, pp. 65–72.

Hayes, L.A., Phillips, E.J.P. and Coates, J.D. 1998. Humic substances as a mediator for microbially catalyzed metal reduction. *Acta Hydrochim. Hydrobiol* 26, pp. 152–157.

He, F., Hu, W. and Li, Y. 2004. Biodegradation mechanisms and kinetics of azo dye 4BS by a microbial consortium. *Chemosphere* 57(4), pp. 293–301.

He, K., Yin, Q., Liu, A., Echigo, S., Itoh, S. and Wu, G. 2017. Enhanced anaerobic degradation of amide pharmaceuticals by dosing ferroferric oxide or anthraquinone-2 , 6-disulfonate. *Journal of Water Process Engineering* 18(6), pp. 192–197.

Heidelberg, J.F. et al. 2002. Genome sequence of the dissimilatory metal ion–reducing bacterium Shewanella oneidensis. *Nature BIotechnology* 20(10), pp. 1118–1123.

Hem, J.D. and Cropper, W.H. 1962. *Chemistry of Iron in Natural Water*. USGS Water Supply Papers, (1459).

Henze, M., Harremoes, P., Jansen, J. la C. and Arvin, E. 2002. *Wastewater Treatment: Biological and Chemical Processes*. Third. Newyork: Springer.

Hernández Leal, L. et al. 2007. Characterisation and biological treatment of greywater. *Water Science and Technology* 56(5), pp. 193–200.

Hideo, E. and Kiang, H. 2019. Geochemical conceptual model of BTEX biodegradation in an iron-rich aquifer. *Applied Geochemistry* 100, pp. 293–304.

Holmes, D.E., Risso, C., Smith, J.A. and Lovley, D.R. 2011. Anaerobic oxidation of benzene by the ahyperthermophilic Archaeon Ferroglobus placidus. *Applied and Environmental Microbiology* 77(17), pp. 5926–5933.

Holmes, D.E. et al. 2017. Metatranscriptomic evidence for direct interspecies electron transfer between Geobacter and Methanothrix species in methanogenic rice paddy

soils. *Applied and Enviromental Microbiology* 83(9), pp. 1–11.

Hsueh, C.-C., Chen, B.-Y. and Yen, C.-Y. 2009. Understanding effects of chemical structure on azo dye decolorization characteristics by Aeromonas hydrophila. *Journal of Hazardous Materials* 167(1–3), pp. 995–1001.

Hsueh, C.C. and Chen, B.Y. 2007. Comparative study on reaction selectivity of azo dye decolorization by Pseudomonas luteola. *Journal of Hazardous Materials* 141(3), pp. 842–849.

Hu, T.L. 2001. Kinetics of azoreductase and assessment of toxicity of metabolic products from azo dyes by Pseudomonas luteola. *Water Science and Technology* 43(2), pp. 261–269.

Hu, Y., He, F., Ma, L., Zhang, Y. and Wu, Z. 2016. Microbial nitrogen removal pathways in integrated vertical-flow constructed wetland systems. *Bioresource Technology* 207, pp. 339–345.

Hunger, K. 2009. *Industrial Dyes chemistry, properties, applications*. Germany: Wiley-VCH.

Hutchins, S.R. 1991. Biodegradation of monoaromatic hydrocarbons by aquifer microorganisms using oxygen , nitrate, or nitrous oxide as the terminal electron acceptor. *Applied and Enviromental Microbiology* 57(8), pp. 2403–2407.

Igor, P., Firmino, M., Erick, M., Silva, R., Cervantes, F.J. and André, B. 2010. Colour removal of dyes from synthetic and real textile wastewaters in one- and two-stage anaerobic systems. *Bioresource Technology* 101(20), pp. 7773–7779.

Ionescu, D. et al. 2015. Biotic and abiotic oxidation and reduction of iron at circumneutral pH are inseparable processes under natural conditions Biotic and abiotic oxidation and reduction of iron at circumneutral pH are inseparable processes under natural conditions. *Geomicrobiology* 32, pp. 221–230.

Irwin, R.J., Mouwrik, M. Van, Stevens, L., Basham, M.D. and Wendy, S. 1997. Environmental Contaminants Encyclopedia Naphthalene Entry. *National Park Service* , pp. 1–80.

Isaka, K., Sumino, T. and Tsuneda, S. 2007. High nitrogen removal performance at moderately low temperature utilizing anaerobic ammonium oxidation reactions. *Journal of Bioscience and Bioengineering* 103(5), pp. 486–490.

Işik, M. and Sponza, D.T. 2005. Effects of alkalinity and co-substrate on the performance of an upflow anaerobic sludge blanket (UASB) reactor through decolorization of Congo Red azo dye. *Bioresource Technology* 96(5), pp. 633–643.

Isık, M. and Sponza, D.T. 2008. Anaerobic/ aerobic treatment of a simulated textile wastewater Mustafa Is. *Separation and Purification Technology* 60, pp. 64–72.

Ivanov, V. 2010. Microbiology of Environmental Engineering Systems. In: *In Environmental Biotechnology*. Humana Press, Totowa, NJ., pp. 19–79.

Ivanov, V., Stabnikov, V., Guo, C.H. and Stabnikova, O. 2014. Wastewater engineering applications of BioIronTech process based on the biogeochemical cycle of iron bioreduction and (bio) oxidation. *AIMS Environmental Science* 1(2), pp. 53–66.

Iwasaki, H. and Matsubara, T. 1972. A nitrite reductase from Achromobacter Cycloclastes. *The Journal of Biochemistry* 71(4), pp. 645–652.

Jayapal, M. et al. 2018. Sequential anaerobic-aerobic treatment using plant microbe integrated system for degradation of azo dyes and their aromatic amines by-products. *Journal of Hazardous Materials* 354, pp. 231–243.

Jern, N.W. 2006. *Industrial Wastewater Treatment*. Imperial College Press 57 Shelton Street Covent Garden London.

Jetten, M.S., Wagner, M, Fuerst, J., van Loosdrecht, M., Kuenen, G. and Strous, M. 2001. Microbiology and application of the anaerobic ammonium oxidation ('anammox') process. *Current Opinion in Biotechnology* 12(3), pp. 283–288.

Jetten, M.S.M., Strous, M., Pas-schoonen, K.T., S.J., Udo, van D. and G.J.M., van de Graaf, A.. 1999. The anaerobic oxidation of ammonium. *FEMS Microbiology Reviews* 22, pp. 421–437.

Jin, D., Kong, X., Li, Y., Bai, Z., Zhuang, G. and Zhuang, X. 2015. Biodegradation of

di-n-Butyl Phthalate by Achromobacter sp. isolated from rural domestic wastewater. *International Journal of Environmental Research and Public Health* 12, pp. 13510–13522.

Jin, H.M., Choi, E.J. and Jeon, C.O. 2013. Isolation of a BTEX-degrading bacterium, janibacter sp. sb2, from a sea-tidal flat and optimization of biodegradation conditions. *Bioresource Technology* 145, pp. 57–64.

Jin, R.C. and Zheng, P. 2009. Kinetics of nitrogen removal in high rate anammox upflow filter. *Journal of Hazardous Materials* 170(2–3), pp. 652–656.

Jin, X.C., Liu, G.Q., Xu, Z.H. and Tao, W.Y. 2007. Decolorization of a dye industry effluent by Aspergillus fumigatus XC6. *Applied Microbiology and Biotechnology* 74(1), pp. 239–243.

Jo, M.S., Rene, E.R., Kim, S.H. and Park, H.S. 2008. An analysis of synergistic and antagonistic behavior during BTEX removal in batch system using response surface methodology. *Journal of Hazardous Materials* 152(3), pp. 1276–1284.

Joe, M.H., Lim, S.Y., Kim, D.H. and Lee, I.S. 2008. Decolorization of reactive dyes by Clostridium bifermentans SL186 isolated from contaminated soil. *World Journal of Microbiology and Biotechnology* 24(10), pp. 2221–2226.

Johnson, D.B. and McGinness, S. 1991. Ferric Iron Reduction by Acidophilic Heterotrophic Bacteria. *Applied and Enviromental Microbiology* 57(1), pp. 207–211.

Jonstrup, M., Kumar, N., Murto, M. and Mattiasson, B. 2011. Sequential anaerobic–aerobic treatment of azo dyes: Decolourisation and amine degradability. *Desalination* 280(1–3), pp. 339–346.

Jørgensen, C.A., Jensen, H.S. and Egemose, S. 2017. Phosphate adsorption to iron sludge from waterworks, ochre precipitation basins and commercial ferrihydrite at ambient freshwater phosphate concentrations. *Environmental Technology* 38(17), pp. 2185–2192.

Joshi, T., Iyengar, L., Singh, K. and Garg, S. 2008. Isolation, identification and application of novel bacterial consortium TJ-1 for the decolourization of structurally

different azo dyes. *Bioresource Technology* 99, pp. 7115–7121.

Juni, E. 1972. Interspecies transformation of Acinetobacter: genetic evidence for a ubiquitous genus. *Journal of Bacteriology* 112(2), pp. 917–931.

Kadlec, R.H. and Wallace, S.D. 2009. *Treatment Wetlands, Second Edition*. CRC Press.

Kalathil, S., Lee, J. and Cho, M.H. 2011. Granular activated carbon based microbial fuel cell for simultaneous decolorization of real dye wastewater and electricity generation. *New Biotechnology* 29(1), pp. 32–37.

Kalathil, S., Lee, J. and Cho, M.H. 2012. Efficient decolorization of real dye wastewater and bioelectricity generation using a novel single chamber biocathode-microbial fuel cell. *Bioresource Technology* 119, pp. 22–27.

Kalyani, D.C., Telke, A.A., Govindwar, S.P. and Jadhav, J.P. 2009. Biodegradation and Detoxification of Reactive Textile Dye by Isolated by Pseudomonas sp. SUK1. *Water Environment Research* 81(3), pp. 298–307.

Kapdan, I.K. and Alparslan, S. 2005. Application of anaerobic-aerobic sequential treatment system to real textile wastewater for color and COD removal. *Enzyme and Microbial Technology* 36(2–3), pp. 273–279.

Kappler, A. and Brune, A. 2002. Dynamics of redox potential and changes in redox state of iron and humic acids during gut passage in soil-feeding termites (Cubitermes spp.). *Soil Biology & Biochemistry* 34, pp. 221–227.

Kargi, F. and Dincer, A.R. 1996. Effect of salt concentration on biological treatment of saline wastewater by fed-batch operation. *Enzyme and Microbial Technology* 19(11), pp. 529–537.

Karl Terzaghi, Peck, R.B. and Mesri, G. 1996. *Methods of test for soils for civil engineering purposes—Part 2: classification tests*. John Wiley & Sons.

Kartal, B. et al. 2007. Candidatus 'Anammoxoglobus propionicus' a new propionate oxidizing species of anaerobic ammonium oxidizing bacteria. *Systematic and Applied Microbiology* 30(1), pp. 39–49.

Keck, A., Klein, J., Kudlich, M., Stolz, A., Knackmuss, H. and Mattes, R. 1997. Reduction of azo dyes by redox mediators originating in the Naphthalenesulfonic acid degradation pathway of Sphingomonas sp. strain BN6. *Applied and Environmental Microbiology* 63(9), pp. 3684–3690.

Keharia, B.K.H. 2012. Reduction of hexavalent chromium by Ochrobactrum intermedium BCR400 isolated from a chromium-contaminated soil. *3 Biotech* 2, pp. 79–87.

Kelly, W.R., Hornberger, G.M., Herman, J.S. and Mills, A.L. 1996. Kinetics of BTX biodegradation and mineralization in batch and column systems. *Journal of Contaminant Hydrology* 23(1–2), pp. 113–132.

Khalid, A., Arshad, M. and Crowley, D.E. 2008. Decolorization of azo dyes by Shewanella sp. under saline conditions. *Appl Microbiol Biotechnol* 79, pp. 1053–1059.

Khan, K.A. and Srivastava, S. 2014. Decolorization and degradation of textile dyes by bacterial Isolates. *Res. Environ. Life Sci.* 7(4), pp. 299–304.

Khan, M.D., Abdulateif, H., Ismail, I.M. and Sabir, S. 2015. Bioelectricity generation and bioremediation of an azo-dye in a microbial fuel cell coupled activated sludge process. *PLOS ONE* , pp. 1–18.

Khan, R., Fulekar, P.B.M.H., Bhawana, P. and Fulekar, M.H. 2013. Microbial decolorization and degradation of synthetic dyes: A review. *Reviews in Environmental Science and Biotechnology* 12(1), pp. 75–97.

Khan, R., Khan, Z., Nikhil, B., Jyoti, D., Datta, M. and To 2014a. Azo dye decolorization under microaerophilic Azo Dye Decolorization under microaerophilic conditions by a bacterial mixture isolated from anthropogenic dye-contaminated soil. *Bioremediation Journal* 18(8), pp. 147–157.

Khan, Z., Jain, K., Soni, A. and Madamwar, D. 2014b. Microaerophilic degradation of sulphonated azo dye e Reactive Red 195 by bacterial consortium AR1 through co-metabolism. *International Biodeterioration & Biodegradation* 94, pp. 167–175.

Khehra, M.S. et al. 2005a. Comparative studies on potential of consortium and

constituent pure bacterial isolates to decolorize azo dyes. *Water Research* 39(20), pp. 5135–5141.

Khehra, M.S., Saini, H.S., Sharma, D.K., Chadha, B.S. and Chimni, S.S. 2005b. Decolorization of various azo dyes by bacterial consortium. *Dyes and Pigments* 67(1), pp. 55–61.

Khelifi, E., Bouallagui, H., Touhami, Y., Godon, J. and Hamdi, M. 2009. Bacterial monitoring by molecular tools of a continuous stirred tank reactor treating textile wastewater. *Bioresource Technology* 100(2), pp. 629–633.

Kiernicka, J., Seignez, C. and Peringer, P. 1999. Escherichia hermanii—a new bacterial strain for chlorobenzene degradation. *Letters in AppliedMicrobiology* (28), pp. 27–30.

Kiliç, N.K., Nielsen, J.L., Yüce, M. and Dönmez, G. 2007. Characterization of a simple bacterial consortium for effective treatment of wastewaters with reactive dyes and Cr(VI). *Chemosphere* 67(4), pp. 826–831.

Kim, G.T. et al. 2005. Dissimilatory Fe (III) reduction by an electrochemically active lactic acid bacterium phylogenetically related to Enterococcus gallinarum isolated from submerged soil. *Journal of Applied Microbiology* (99), pp. 978–987.

Knappi, K.C.A.B.-C.J.S., Z. Zhang, N.C.C.G., Hetheridge, M.J. and Evans, M.R. 2000. Decolorization of an azo dye by unacclimated activated sludge under anaerobic conditons. *Water Research* 34(18), pp. 4410–4418.

Koch, M.S. and Mendelssohn, I.A. 1989. Sulphide as a soil phytotoxin: differential responses in two marsh species. *The Journal of Ecology* , pp. 565–578.

Kong, Q., Hao, H., Shu, L., Fu, R., Jiang, C. and Miao, M. 2014. Enhancement of aerobic granulation by zero-valent iron in sequencing batch airlift reactor. *Journal of Hazardous Materials* 279, pp. 511–517.

Kong, Y., Nielsen, J.L. and Nielsen, P.H. 2005. Identity and ecophysiology of uncultured actinobacterial polyphosphate-accumulating organisms in full-scale enhanced biological phosphorus removal plants. *Applied and Environmental*

*Microbiology* 71(7), pp. 4076–4085.

Kosolapov, D.B. et al. 2004. Microbial processes of heavy metal removal from carbon-deficient effluents in constructed wetlands. *Engineering in Life Sciences* 4(5), pp. 403–411.

Kozich, J.J., Westcott, S.L., Baxter, N.T., Highlander, S.K. and Schloss, P.D. 2013. Development of a dual-index sequencing strategy and curation pipeline for analyzing amplicon sequence data on the miseq illumina sequencing platform. *Applied and Environmental Microbiology* 79(17), pp. 5112–5120.

Krumholz, L.E.E.R., Harris, S.H., Tay, S.T. and Suflita, J.M. 1999. Characterization of two subsurface H2-utilizing bacteria, Desulfomicrobium hypogeium sp. nov. and Acetobacterium psammolithicum sp. nov., and their ecological roles. *Applied and Enviromental Microbiology* 65(6), pp. 2300–2306.

Ku¨sel, K. and Dorsch, T. 2000. Effect of supplemental electron donors on the microbial reduction of Fe(III), sulfate, and CO2 in coal mining–impacted freshwater lake sediments. *Microbial Ecology* 40, pp. 238–249.

Kuai, L., De Vreese, I., Vandevivere, P. and Verstraete, W. 1998. Gac-amended uasb reactor for the stable treatment of toxic textile wastewater. *Environmental Technology* 19(11), pp. 1111–1117.

Kudlich, M., Bishop, P.L., Knackmuss, H.J. and Stolz, A. 1996. Simultaneous anaerobic and aerobic degradation of the sulfonated azo dye Mordant Yellow 3 by immobilized cells from a naphthalenesulfonate-degrading mixed culture. *Applied Microbiology and Biotechnology* 46(5–6), pp. 597–603.

Kudlich, M., Keck, A., Klein, J. and Stolz, A. 1997. Localization of the enzyme system involved in anaerobic reduction of azo dyes by Sphingomonas sp. Strain BN6 and effect of artificial redox mediators on the rate of azo dye reduction. *Applied and Environmental Microbiology* 63(9), pp. 3691–3694.

Kulla, H.G., Franziska, K., Ulrich, M., Barbara, L. and Thomas, L. 1983. Interference of aromatic sulfo groups in the microbial degradation of the azo dyes Orange I and Orange II. *Arch Microbiol* 135, pp. 1–7.

Kumar, K. et al. 2006. Decolorisation, biodegradation and detoxification of benzidine based azo dye. *Bioresource Technology* 97(3), pp. 407–413. doi: 10.1016/j.biortech.2005.03.031.

Kumar, K., Dastidar, M.G. and Sreekrishnan, T.R. 2009. Effect of process parameters on aerobic decolourization of reactive azo dye using mixed culture. *World Academy of Science, Engineering and Technology* 34, pp. 962–965.

Kunapuli, U., Griebler, C., Beller, H.R. and Meckenstock, R.U. 2008. Identification of intermediates formed during anaerobic benzene degradation by an iron-reducing enrichment culture. *Environmental Microbiology* 10, pp. 1703–1712. doi: 10.1111/j.1462-2920.2008.01588.x.

Kuschk, P., Wießner, A., Kappelmeyer, U., Weißbrodt, E., Kästner, M. and Stottmeister, U. 2003. Annual cycle of nitrogen removal by a pilot-scale subsurface horizontal flow in a constructed wetland under moderate climate. *Water Research* 37(17), pp. 4236–4242.

Küsel, K., Roth, U. and Drake, H.L. 2002. Microbial reduction of Fe (III) in the presence of oxygen under low pH conditions. *Environmental Microbiology* 4, pp. 414–421.

Kwon, K., Jo, W., Lim, H. and Jeong, W. 2007. Characterization of emissions composition for selected household products available in Korea. *Journal of Hazardous Materials* 148, pp. 192–198. doi: 10.1016/j.jhazmat.2007.02.025.

Lade, H., Govindwar, S. and Paul, D. 2015. Mineralization and detoxification of the carcinogenic azo dye Congo red and real textile effluent by a polyurethane foam immobilized microbial consortium in an upflow column bioreactor. *International Journal of Environmental Research and Public Health* 12(6), pp. 6894–6918. doi: 10.3390/ijerph120606894.

Lee, Y.H., Matthews, R.D. and Pavlostathis, S.G. 2006. Biological decolorization of reactive anthraquinone and phthalocyanine dyes under various oxidation–reduction conditions. *Water environment research* 78(2), pp. 156–169.

León, K.B. De et al. 2015. Complete genome sequence of Pelosinus fermentans

JBW45, a member of a remarkably competitive group of Negativicutes in the Firmicutes phylum. *Genome Announcements* 3(5), pp. 3–4.

Li, H., Xiao, D.L., He, H., Lin, R. and Zuo, P.L. 2013. Adsorption behavior and adsorption mechanism of Cu(II) ions on amino-functionalized magnetic nanoparticles. *Transactions of Nonferrous Metals Society of China (English Edition)* 23(9), pp. 2657–2665.

Li, J. and Bishop, P.L. 2002. In situ identification of azo dye inhibition effects on nitrifying biofilms using microelectrodes. *Water Science and Technology* 46(1–2), pp. 207–214.

Li, S., Cao, Y., Bi, C. and Zhang, Y. 2017a. Promoting electron transfer to enhance anaerobic treatment of azo dye wastewater with adding Fe(OH)3. *Bioresource Technology* 245, pp. 138–144.

Li, W., Liu, N., Cai, L., Jiang, J. and Chen, J. 2011. Reduction of Fe (III) chelated with citrate in an NO x scrubber solution by Enterococcus sp. FR-3. *Bioresource Technology* 102(3), pp. 3049–3054.

Li, X., Zhang, W., Liu, T., Chen, L., Chen, P. and Li, F. 2016. Changes in the composition and diversity of microbial communities during anaerobic nitrate reduction and Fe (II) oxidation at circumneutral pH in paddy soil. *Soil Biology and Biochemistry* 94, pp. 70–79. Available at: http://dx.doi.org/10.1016/j.soilbio.2015.11.013.

Li, X. et al. 2017b. Simultaneous Fe (III) reduction and ammonia oxidation process in Anammox sludge. *Journal of Environmental Sciences* 64(Iii), pp. 42–50.

Li, X. et al. 2018. A novel method of simultaneous NH4+ and NO3− removal using Fe cycling as a catalyst: Feammox coupled with NAFO. *Science of the Total Environment* 631–632(1), pp. 153–157.

Li, Y., Zhang, Y., Quan, X., Zhang, J., Chen, S. and Afzal, S. 2014. Enhanced anaerobic fermentation with azo dye as electron acceptor: Simultaneous acceleration of organics decomposition and azo decolorization. *Jornal of Environmental Science* 26(10), pp. 1970–1976.

Li, Z., Zhang, X., Lin, J., Han, S. and Lei, L. 2010. Azo dye treatment with simultaneous electricity production in an anaerobic-aerobic sequential reactor and microbial fuel cell coupled system. *Bioresource Technology* 101(12), pp. 4440–4445.

Lier, J.B. van, Mahmoud, N. and Zeeman, G. 2008. Anaerobic Wastewater Treatment. In: *Online course on Bbological wastewater treatment: principles, modeling and design*. IWA publishing., pp. 401–440.

Lin, C.C.W.C. et al. 2012. Novel oxygen-releasing immobilized cell beads for bioremediation of BTEX-contaminated water. *Bioresource Technology* 124, pp. 45–51.

Littlejohns, J. V. and Daugulis, A.J. 2008. Kinetics and interactions of BTEX compounds during degradation by a bacterial consortium. *Process Biochemistry* 43(10), pp. 1068–1076.

Liu, J.-H., Maity, J.P., Jean, J.-S., Chen, C.-Y., Ho, C.-C.C. and Sin-Yi 2010. Biodegradation of benzene by pure and mixed cultures of Bacillus spp . *World J Microbiol Biotechnol (2010)* , pp. 1557–1567. doi: 10.1007/s11274-010-0331-9.

Liu, J., Xiong, J., Tian, C., Gao, B., Wang, L. and Jia, X. 2018. The degradation of methyl orange and membrane fouling behavior in anaerobic baffled membrane bioreactor. *Chemical Engineering Journal* 338, pp. 719–725.

Liu, T. et al. 2017a. Comparative study of the photocatalytic performance for the degradation of different dyes by ZnIn2S4: adsorption, active species, and pathways. *RSC Adv.* 7, pp. 12292–12300.

Liu, W. et al. 2016. Methylene blue enhances the anaerobic decolorization and detoxication of azo dye by Shewanella onediensis MR-1. *Biochemical Engineering Journal* 110, pp. 115–124.

Liu, Y., Zhang, Y., Quan, X., Chen, S. and Zhao, H. 2011a. Applying an electric field in a built-in zero valent iron-Anaerobic reactor for enhancement of sludge granulation. *Water Research* 45(3), pp. 1258–1266.

Liu, Y., Zhang, Y., Zhao, Z., Li, Y., Quan, X. and Chen, S. 2012. Enhanced azo dye

wastewater treatment in a two-stage anaerobic system with Fe0 dosing. *Bioresource Technology* 121, pp. 148–153.

Liu, Y.H., Ye, M., Lu, Y., Zhang, X. and Li, G. 2011b. Improving the decolorization for textile dyes of a metagenome-derived alkaline laccase by directed evolution. *Appl Microbiol Biotechnol* 91, pp. 667–675. doi: 10.1007/s00253-011-3292-5.

Liu, Y.N. et al. 2017b. Exclusive extracellular bioreduction of Methyl Orange by azo reductase-free Geobacter sulfurreducens. *Environmental Science and Technology* 51(15), pp. 8616–8623. doi: 10.1021/acs.est.7b02122.

Long, A., Heitman, J., Tobias, C., Philips, R. and Song, B. 2013. Co-Occurring Anammox, Denitrification, and Codenitrification in Agricultural Soils. *American society for microbilogy* 79(1), pp. 168–176. doi: 10.1128/AEM.02520-12.

Lötter, L.H. 1985. The role of bacterial phosphate metabolism in enhanced phosphorus removal from the activated sludge process. *Water Science and Technology* 17(11–12), pp. 127–138.

Lotti, T. et al. 2015. Pilot-scale evaluation of anammox-based mainstream nitrogen removal from municipal wastewater. *Environmental Technology ISSN:* 3330

Lovley, D.R. 1987. Organic matter mineralization with the reduction of Ferric Iron: A review. *Geomicrobiol* 5(3), pp. 375–399.

Lovley, D.R., Baedecker, M.J., Lonergan, D.J., Cozzarelli, I.M., Phillips, E.J.P. and Siegelt, D.I. 1989. Oxidation of aromatic contaminants coupled to microbial iron reduction. *Nature* 339(5), pp. 297–300.

Lovley, D.R., Chapelle, F.H., Phillips, E.J.P. and Carolina, N. 1990. Fe (lll)-reducing bacteria in deeply buried sediments of the Atlantic Coastal Plain. *Geology* 18(10), pp. 954–957.

Lovley, D.R. 1993. Dissimilatory metal reduciton. *Annu. Rev. Microbiol* 47, pp. 263–90.

Lovley, D.R. et al. 1993. Geobacter metallireducens gen. nov. sp. nov., a microorganism capable of coupling the complete oxidation of organic compounds to

the reduction of iron and other metals. *Arch Microbio* 159, pp. 336–344.

Lovley, D.R., Woodward, J.C. and Chapellet, B.F.H. 1994. Stimulated anoxic biodegradation of aromatic hydrocarbons using Fe (III) ligands. *Nature* 370(July), pp. 128–131.

Lovley, D.R. et al. 1996. Humic substances as electron acceptors for microbial respiration. *Nature* 382(8), pp. 445–448.

Lovley, D.R. 1997. Microbial Fe (III) reduction in subsurface environments. *Microbiology Reviews* 20, pp. 305–313.

Lovley, D.R., Holmes, D.E. and Nevin, K.P. 2002. Advances in Microbial Physiology. In: *Advances in Microbial Physiology*. Elsevier

Lovley, D.R. 2011a. Environmental Science bioremediation of energy-related contamination. *Energy & Environmental Science* 4, pp. 4896–4906. doi: 10.1039/c1ee02229f.

Lovley, D.R. 2011b. Live wires: Direct extracellular electron exchange for bioenergy and the bioremediation of energy-related contamination. *Energy and Environmental Science* 4(12), pp. 4896–4906. doi: 10.1039/c1ee02229f.

Lovley, D.R. and Lonergan, D.J. 1990. Anaerobic oxidation of toluene, phenol, and p-cresol by the dissimilatory iron-reducing organism, GS-15. *Applied and Environmental Microbiology* 56(6), pp. 1858–1864. doi: 10.1128/aem.72.5.3236-3244.2006.

Lovley, R.D. and Philips, J.P.E. 1988. Novel mode of microbial energy metabolism: Organic carbon oxidation coupled to dissimilatory reduction of iron or manganese. *Applied and Environmental Microbiology* 54(6), pp. 1472–1480.

Lundgren, D.G. 1980. Ore leaching by bacteria. *Annual Review of Microbiology* 34, pp. 263–283.

Luu, Y. and Ramsay, J.A. 2003. Review : microbial mechanisms of accessing insoluble Fe(III) as an energy source. *World Journal of Microbiology & Biotechnology* 19, pp. 215–225.

Ma, B. et al. 2016. Biological nitrogen removal from sewage via anammox : Recent advances. *Bioresource Technology* 200, pp. 981–990.

Magrí, A., Vanotti, M.B. and Szögi, A.A. 2012. Anammox sludge immobilized in polyvinyl alcohol (PVA) cryogel carriers. *Bioresource Technology* 114, pp. 231–240. doi: 10.1016/j.biortech.2012.03.077.

Malovanyy, A., Yang, J., Trela, J. and Plaza, E. 2015. Combination of upflow anaerobic sludge blanket (UASB) reactor and partial nitritation/anammox moving bed biofilm reactor (MBBR) for municipal wastewater treatment. *Bioresource Technology* 180, pp. 144–153.

Maltais-Landry, G., Maranger, R., Brisson, J. and Chazarenc, F. 2009. Nitrogen transformations and retention in planted and artificially aerated constructed wetlands. *Water Research* 43(2), pp. 535–545.

Manenti, D.R. et al. 2014. Assessment of a multistage system based on electrocoagulation, solar photo-Fenton and biological oxidation processes for real textile wastewater treatment. *Chemical Engineering Journal* 252, pp. 120–130. Available at: http://dx.doi.org/10.1016/j.cej.2014.04.096.

Manu, B. and Chaudhari, S. 2002a. Anaerobic decolorisation of simulated textile wastewater containing azo dyes. *Bioresource Technology* 82(3), pp. 225–231.

Manu, B. and Chaudhari, S. 2002b. Anaerobic decolorization of simulated textile wastewater containing azo dyes. *Bioresource Technology* 82, pp. 225–231.

Manu, B. and Chaudhari, S. 2003. Decolorization of indigo and azo dyes in semicontinuous reactors with long hydraulic retention time. *Process Biochemistry* 38

Margot, J., Lochmatter, S., Barry, D.A. and Holliger, C. 2016. Role of ammonia-oxidizing bacteria in micropollutant removal from wastewater with aerobic granular sludge. *Water Sci. Technol.* 73, pp. 564–575.

Marsili, E., Baron, D.B., Shikhare, I.D., Coursolle, D., Gralnick, J.A. and Bond, D.R. 2008. Shewanella secretes flavins that mediate extracellular electron transfer. *Proceedings of the National Academy of Sciences* 105(10), pp. 3968–3973.

Massalha, N., Basheer, S. and Sabbah, I. 2007. Effect of adsorption and bead size of immobilized biomass on the rate of biodegradation of phenol at high concentration levels. *Ind. Eng. Chem. Res* 46, pp. 6820–6824. doi: 10.1021/ie070057v.

Mazzeo, D.E.C., Levy, C.E., de Angelis, D. de F. and Marin-Morales, M.A. 2010. BTEX biodegradation by bacteria from effluents of petroleum refinery. *Science of the Total Environment* 408(20), pp. 4334–4340. doi: 10.1016/j.scitotenv.2010.07.004.

Mccarty, D.K., Moore, J.N. and Marcus, W.A. 1998. Mineralogy and trace element association in an acid mine drainage iron oxide precipitate ; comparison of selective extractions. *Applied Geochemistry* 13(97), pp. 165–176.

McCarty, P.L. 1971. Energetics and bacterial growth. *Organic compounds in aquatic environments* 1, pp. 157–172.

Meetani, M. and Rauf, M.A. 2013. Application of LC-MS to the analysis of advanced oxidation process (AOP) degradation of dye products and reaction mechanisms. *Trends in Analytical Chemistry* 49(9), pp. 31–44.

Milch, A., Springer, J., Braunsehweig, T.I., Entf, S. and Versuche, K. 1936. Nachweis yon durch S~iuerung entf~irbten kiinstlichen Eigelbiarbstoffen in Milchspeiseeis. *Biochcm.* 226(1927), pp. 30–32.

Min, W., Kangbi, Q., Junmei, W. and Zhongzhong, D. 2011. Decolorizing activity of Malachite Green and Its mechanisms involved in dye biodegradation by Achromobacter xylosoxidans MG1. *Journal of Mlecular Microbiology and Biotechnology* 20, pp. 220–227. doi: 10.1159/000330669.

Mino T, Liu WT, K.F.& M.T. 1995. Modelling glycogen storage and denitrification capability of microorganisms in enhanced biological phospate removal process. *Wat. Sci. Tech* 31(2), pp. 25–34.

Mitra, S. and Roy, P. 2011. BTEX : A serious ground-water contaminant. *Research Journal of Environmental Sciences* 5(5), pp. 394–398.

Miura, Y., Hiraiwa, M.N., Ito, T., Itonaga, T., Watanabe, Y. and Okabe, S. 2007. Bacterial community structures in MBRs treating municipal wastewater: Relationship

between community stability and reactor performance. *Water Research* 41(3), pp. 627–637. doi: 10.1016/j.watres.2006.11.005.

Moe, W.M. et al. 2012. Pelosinus defluvii sp. nov., isolated from chlorinated solvent-contaminated groundwater, emended description of the genus Pelosinus and transfer of Sporotalea propionica to Pelosinus. *International Journal of Systematic and Evolutionary Microbiology* (62), pp. 1369–1376. doi: 10.1099/ijs.0.033753-0.

Moosvi, S., Kher, X. and Madamwar, D. 2007. Isolation, characterization and decolorization of textile dyes by a mixed bacterial consortium JW-2. *Dyes and Pigments* 74, pp. 723–729.

Morales-Ibarria, W.R.V.-M.M.G., Velázquez, E.K., Ramírez-Saad, H. and Razo-Flores, E. 2008. Benzene biodegradation under anaerobic conditions coupled with metal oxides reduction. *Water Air Soil Pollut* 192, pp. 165–172.

Morlett-chávez, J.A. et al. 2010. Kinetics of BTEX biodegradation by a microbial consortium acclimatized to unleaded gasoline and bacterial strains isolated from it. *International Biodeterioration and Biodegradation* 64(7), pp. 581–587.

Mouchet, P. 1992. From conventional to biological removal of iron and manganese in France. *Journal American Water Works Association* 84(4), pp. 158–167.

Müller, J.B. et al. 2017. Combined iron and sulfate reduction biostimulation as a novel approach to enhance BTEX and PAH source-zone biodegradation in biodiesel blend-contaminated groundwater. *Journal of Hazardous Materials* 326, pp. 229–236.

Munch, J.C. and Ottow, J.C.G. 1980. Preferential reduction of amorphous to crystalline iron oxides by bacterial activity. *Soil Science* 129(1), pp. 15–21.

Murali, V., Ong, S., Ho, L. and Wong, Y. 2013a. Decolorization of methyl orange using upflow anaerobic sludge blanket (UASB) reactor—An investigation of co-substrate and dye degradation kinetics. *Desalination and Water Treatment* 3994(2016)

Murali, V., Ong, S., Ho, L. and Wong, Y. 2013b. Evaluation of integrated anaerobic–aerobic biofilm reactor for degradation of azo dye methyl orange. *Bioresource Technology* 143, pp. 104–111.

Myers, C.R. and Myers, J.M. 1992. Localization of cytochromes to the outer membrane of anaerobically grown Shewanella putrefaciens MR-1. *Jornal of Bacteriology* 174(11), pp. 3429–3438.

Nakajima, K., Hirota, K., Nodasaka, Y. and Yumoto, I. 2005. Alkalibacterium iburiense sp. nov., an obligate alkaliphile that reduces an indigo dye. *International Journal of Systematic and Evolutionary Microbiology* 55, pp. 1525–1530. doi: 10.1099/ijs.0.63487-0.

Nakhla, G. 2003. Biokinetic modeling of in situ bioremediation of BTX compounds — impact of process variables and scaleup implications. *Water Research* 37, pp. 1296–1307.

Nales, M., Butler, B.J., Edwards, E.A., Nales, M., Butler, B.J. and Edwards, E.A. 2010. Anaerobic Benzene Biodegradation : A Microcosm Survey Anaerobic Benzene Biodegradation : A Microcosm Survey. *Bioremediation Journal* 9868. doi: 10.1080/10889869891214268.

Namasivayam, C. and Arasi, D.J.S.E. 1997. Removal of Congo Red from wastewater by Red adsorption onto waste red mud. *Chemosphere* 34(2), pp. 401–417.

Namasivayam, C. and Sumithra, S. 2005. Removal of direct red 12B and methylene blue from water by adsorption onto Fe (III)/ Cr (III) hydroxide, an industrial solid waste. *Journal of Environmental Management* 74, pp. 207–215.

Nasuha, N., Hameed, B.H. and Din, A.T.M. 2010. Rejected tea as a potential low-cost adsorbent for the removal of methylene blue. *Journal of Hazardous Materials* 175(1–3), pp. 126–132.

Nealson, K.H. 1982. Microbiological oxidation and reduction of iron. In: *Mineral Deposits and the Evolution of the Biosphere*. Springer, pp. 51–65.

Nevin, K.P. and Lovley, D.R. 2000. Lack of production of electron-shuttling compounds or solubilization of Fe (III) during reduction of insoluble Fe (III) oxide by Geobacter metallireducens. *Applied and Enviromental Microbiology* 66(5), pp. 2248–2251.

Nevin, K.P. and Lovley, D.R. 2002a. Mechanisms for accessing insoluble Fe (III) oxide during dissimilatory Fe (III) reduction by Geothrix fermentans. *Applied and Enviromental Microbiology* 68(5), pp. 2294–2299. doi: 10.1128/AEM.68.5.2294.

Nevin, K.P. and Lovley, D.R. 2002b. Mechanisms for Fe (III) oxide reduction in sedimentary environments mechanisms for Fe (III) oxide reduction in sedimentary environments. *Geomicrobiology Journal* 0451(Iii)

Newman, D.K. and Kolter, R. 2000. A role for excreted quinones in extracellular electron transfer. *Nature* 405(5), pp. 13–16.

Ng, S., Chen, T., Lin, R., Zhang, X., Ni, C. and Sun, D. 2014. Decolorization of textile azo dye and Congo red by an isolated strain of the dissimilatory manganese-reducing bacterium Shewanella xiamenensis BC01. *Applied Microbiology and Biotechnology* 98(5), pp. 2297–2308. doi: 10.1007/s00253-013-5151-z.

Nicholls, H.A. and Osborn, D.W. 1979. Bacterial stress: Prerequisite for biological removal of phosphorus. *Journal of the Water Pollution Control Federation* 51(3), pp. 557–569.

Nilsson, I., Möller, A., Mattiasson, B., Rubindamayugi, M.S.T. and Welander, U. 2006. Decolorization of synthetic and real textile wastewater by the use of white-rot fungi. *Enzyme and Microbial Technology* 38(1–2), pp. 94–100. doi: 10.1016/j.enzmictec.2005.04.020.

Northwest, P., Rosso, M.K., Zachara, M.J., Fredrickson, K.J., Yuri, A.G. and Smith, C.S. 2003. Nonlocal bacterial electron transfer to hematite surfaces. *Geochimica et Cosmochimica Acta* 67(5), pp. 1081–1087.

O'Neill, C. et al. 2000a. Azo-dye degradation in an anaerobic-aerobic treatment system operating on simulated textile effluent. *Applied microbiology and biotechnology* 53(2), pp. 249–254. doi: 10.1007/s002530050016.

O'Neill, C.O., Hawkes, F.R., Hawkes, D.L., Esteves, S. and Wilcox, S.J. 2000b. Anaerobic-aerobic biotreatment of simulated textile effluent containing varied ratios of starch and azo dye. *Water Research* 34(8), pp. 2355–2361.

Ogugbue, C.J., Sawidis, T. and Oranusi, N.A. 2012. Bioremoval of chemically different synthetic dyes by Aeromonas hydrophila in simulated wastewater containing dyeing auxiliaries. *Ann Microbiol* 62, pp. 1141–1153. doi: 10.1007/s13213-011-0354-y.

Oh, Y. and Bartha, R. 1997. Construction of a bacterial consortium for the bio ® ltration of benzene , toluene and xylene emissions. *World Journal of Microbiology & Biotechnology* 13, pp. 627–632.

Ong, S.A., Uchiyama, K., Inadama, D., Ishida, Y. and Yamagiwa, K. 2010a. Performance evaluation of laboratory scale up-flow constructed wetlands with different designs and emergent plants. *Bioresource Technology* 101(19), pp. 7239–7244. Available at: http://dx.doi.org/10.1016/j.biortech.2010.04.032.

Ong, S.A., Uchiyama, K., Inadama, D., Ishida, Y. and Yamagiwa, K. 2010b. Treatment of azo dye Acid Orange 7 containing wastewater using up-flow constructed wetland with and without supplementary aeration. *Bioresource Technology* 101(23), pp. 9049–9057.

Oon, Y.L. et al. 2018. Up-flow constructed wetland-microbial fuel cell for azo dye, saline, nitrate remediation and bioelectricity generation: From waste to energy approach. *Bioresource Technology* 266(4), pp. 97–108.

Otiteley, C.J., Davison, W. and Edmumunds, W.M. 1997. Chemical catalysis of nitrate reduction by iron (II). *Geochimica et Cosmochimica Acta* 61(9), pp. 1819–1828.

Ozer, A. and Turabik, M. 2006. Biosorption of Acid Blue 290 (AB 290) and Acid Blue 324 (AB 324) dyes on Spirogyra rhizopus. *Journal of Hazardous Materials* 135, pp. 355–364. doi: 10.1016/j.jhazmat.2005.11.080.

Painter, H.A. and Loveless, J.E. 1983. Effect of temperature and pH value on the growth-rate constants of nitrifying bacteria in the activated-sludge process. *Water Research* 17(3), pp. 237–248. doi: 10.1016/0043-1354(83)90176-8.

Pandey, A., Singh, P. and Leela Iyengar 2007a. Bacterial decolorization and degradation of azo dyes. *International Biodeterioration & Biodegradation* 59, pp. 73–84.

Pandey, A. et al. 2007b. Review Bacterial decolorization and degradation of azo dyes. *International Biodeterioration and Biodegradation* 59(2), pp. 73–84.

Pandey, S., Saha, P., Barai, P.K. and Maiti, T.K. 2010. Characterization of a Cd 2+ - resistant strain of Ochrobactrum sp. isolated from slag disposal site of an iron and steel factory. *Curr Microbiol* 61, pp. 106–111. doi: 10.1007/s00284-010-9583-8.

Paper, O., Seesuriyachan, P., Kuntiya, A., Sasaki, K. and Techapun, C. 2009. Comparative study on methyl orange removal by growing cells and washed cell suspensions of Lactobacillus casei TISTR 1500. *World Journal of Microbiology and Biotechnology* 25(6), pp. 973–979.

Paredes, D., Kuschk, P., Mbwette, T.S.A., Stange, F., Müller, R.A. and Köser, H. 2007. New aspects of microbial nitrogen transformations in the context of wastewater treatment-a review. *Engineering in Life Sciences* 7(1), pp. 13–25.

Park, H.S. et al. 2001. A novel electrochemically active and Fe ( III )-reducing bacterium phylogenetically related to Clostridium butyricum isolated from a microbial fuel cell. *Anaerobe* 7, pp. 297–306. doi: 10.1006/anae.2001.0399.

Parshetti, G.K., Telke, A.A., Kalyani, D.C. and Govindwar, S.P. 2010. Decolorization and detoxification of sulfonated azo dye methyl orange by Kocuria rosea MTCC 1532. *Journal of Hazardous Materials* 176(1–3), pp. 503–509.

Pasti-Grigsby, M.B., Paszczynski, A., Goszczynski, S., Crawford, D.L. and Crawford, R.L. 1992. Influence of aromatic substitution patterns on azo dye degradability by Streptomyces spp. and Phanerochaete chrysosporium. *Applied and Environmental Microbiology* 58(11), pp. 3605–3613.

Patel, S.P.U.D. 2015. Destruction of azo dyes by anaerobic – aerobic sequential biological treatment : a review. (2), pp. 405–420. doi: 10.1007/s13762-014-0499-x.

Patel, U.D., Ruparelia, J. and Patel, M. 2018. Biodegradation of a real dye wastewater containing high concentration of total dissolved inorganic salts (TDIS) in a lab-scale activated sludge unit. *Journal of The Institution of Engineers* 99(1), pp. 11–16.

Pearce, C.I., Lloyd, J.R. and Guthrie, J.T. 2003. The removal of colour from textile

wastewater using whole bacterial cells: A review. *Dyes and Pigments* 58(3), pp. 179–196. doi: 10.1016/S0143-7208(03)00064-0.

Perei, K., Rákhely, G., Kiss, I., PolyáK, B. and K, L.K. 2001. Biodegradation of sulfanilic acid by Pseudomonas paucimobilis. *Appl Microbiol Biotechnol* 55, pp. 101–107.

Pereira, L., Pereira, R., Pereira, M.F.R., Zee, F.P. Van Der, Cervantes, F.J. and Alves, M.M. 2010. Thermal modification of activated carbon surface chemistry improves its capacity as redox mediator for azo dye reduction. *Journal of Hazardous Materials* 183(1–3), pp. 931–939. Available at: http://dx.doi.org/10.1016/j.jhazmat.2010.08.005.

Phugare, S.S., Kalyani, D.C., Surwase, S.N. and Jadhav, J.P. 2011. Ecofriendly degradation, decolorization and detoxification of textile effluent by a developed bacterial consortium. *Ecotoxicology and Environmental Safety* 74(5), pp. 1288–1296. Available at: http://dx.doi.org/10.1016/j.ecoenv.2011.03.003.

Pikuta, E. V et al. 2006. Trichococcus patagoniensis sp. nov., a facultative anaerobe that grows at -5 C, isolated from penguin guano in Chilean Patagonia. *International Journal of Systematic and Evolutionary Microbiology* 56, pp. 2055–2062. doi: 10.1099/ijs.0.64225-0.

Pinheiro, H.M., Touraud, E. and Thomas, O. 2004. Aromatic amines from azo dye reduction: Status review with emphasis on direct UV spectrophotometric detection in textile industry wastewaters. *Dyes and Pigments* 61(2), pp. 121–139. doi: 10.1016/j.dyepig.2003.10.009.

Plumb, J.J., Bell, J. and Stuckey, D.C. 2001. Microbial populations associated with treatment of an industrial dye effluent in an anaerobic baffled reactor. *Applied and Environmental Microbiology* 67(7), pp. 3226–3235. doi: 10.1128/AEM.67.7.3226.

Poonam, N., Banat, I.M., Singh, D. and Marchanv, R. 1996. Microbial process for the decolorization of textile effluent containing azo, Diazo and reactive dyes. *Process Biochemistry* 31(5), pp. 435–442.

Popli, S. and Patel, U.D. 2015. Destruction of azo dyes by anaerobic–aerobic sequential biological treatment: a review. *International Journal of Environmental*

*Science and Technology* 12(1), pp. 405–420. doi: 10.1007/s13762-014-0499-x.

Potter, T.L. and Simmons, K.E. 1998. *Composition of petroleum mixtures*. Amherst Scientific Publishers Massachusetts.

Prade, R.A. and Penninckx, M.J. 2002. Dissimilatory Fe (III) and Mn (IV) reduction. In: *Advances in microbial physiology*. Elsevier

Prato-garcia, D., Cervantes, F.J. and Buitrón, G. 2013. Azo dye decolorization assisted by chemical and biogenic sulfide. *Journal of Hazardous Materials* 250–251, pp. 462–468. Available at: http://dx.doi.org/10.1016/j.jhazmat.2013.02.025.

Prosser, J.I. 1990. Autotrophic nitrification in bacteria. In: *Advances in microbial physiology*. Elsevier, pp. 125–181.

Providenti, M.A., Lee, H. and Trevors, J.T. 1993. Selected factors limiting the microbial degradation of recalcitrant compounds. *Journal of Industrial Microbiology* 12, pp. 379–395.

Punj, S. and John, G.H. 2009. Purification and identification of an FMN-dependent NAD (P) H azoreductase from Enterococcus faecalis. *Current Issues in Molecular Biology* 11(2), pp. 59–66.

Punzi, M. et al. 2015. Combined anaerobic-ozonation process for treatment of textile wastewater: Removal of acute toxicity and mutagenicity. *Journal of Hazardous Materials* 292, pp. 52–60.

Rabaey, K. and Boon, N. 2005. Microbial phenazine production enhances electron transfer in biofuel cells. *Environ. Sci. Technol* 39, pp. 3401–3408.

Rafii, F., Franklin, W. and Cerniglia, C.E. 1990. Azoreductase activity of anaerobic bacteria isolated from human intestinal microflora. *Appl Environ Microbiol* 56(7), pp. 2146–2151.

Ramachandran, P., Sundharam, R., Palaniyappan, J. and Munusamy, A.P. 2013. Potential process implicated in bioremediation of textile effluents: A review. *Advances in Applied Science Research* 4(1), pp. 131–145.

Rasool, K., Mahmoud, K.A. and Lee, D.S. 2015. Influence of co-substrate on textile wastewater treatment and microbial community changes in the anaerobic biological sulfate reduction process. *Journal of Hazardous Materials* 299, pp. 453–461. Available at: http://dx.doi.org/10.1016/j.jhazmat.2015.07.044.

Rasool, K., Shahzad, A. and Lee, D.S. 2016. Exploring the potential of anaerobic sulfate reduction process in treating sulfonated diazo dye: Microbial community analysis using bar-coded pyrosequencing. *Journal of Hazardous Materials* 318, pp. 641–649. doi: 10.1016/j.jhazmat.2016.07.052.

Rau, J., Knackmuss, H.-J. and Stolz, A. 2002. Effects of different quinoid redox Mediators on the anaerobic reduction of azo dyes by bacteria. *Environ. Sci. Technol* , pp. 1497–1504.

Reguera, G., Mccarthy, K.D., Mehta, T., Nicoll, J.S., Tuominen, M.T. and Lovley, D.R. 2005. Extracellular electron transfer via microbial nanowires. *Nature* 435(6), pp. 1098–1101. doi: 10.1038/nature03661.

Reusser, D.E. and Istok, J.D. 2002. In situ transformation of deuterated toluene and xylene to benzylsuccinic acid analogues in BTEX-contaminated aquifers. *Environ. Sci. Technol* 36(19), pp. 4127–4134. doi: 10.1021/es0257366.

Reviews, M. 1991. Dissimilatory Fe (III) and Mn ( IV) Reduction. M, D. et al. eds. *Reviews, Microbiological* 55(6), pp. 259–287.

Roberts, M. 2018. *In-Situ Microbial Dissolution of Iron Mineral-Bearing Wastes for Metal Recovery*. Cardiff University.

Robertson, W.J., Bowman, J.P., Franzmann, P.D. and Mee, B.J. 2001. Desulfosporosinus meridiei sp. nov., a spore- forming sulfate-reducing bacterium isolated from gasolene-contaminated groundwater. *International Journal of Systematic and Evolutionary Microbiology* 51, pp. 133–140.

Robinson, T., Mcmullan, G., Marchant, R. and Nigam, P. 2001. Remediation of dyes in textile ffluent: A critical review on current treatment technologies with a proposed alternative. *Bioresource Technology* 77, pp. 247–255.

Robledo-Ortíz, J., … D.R.-A.-I. and 2011, U. 2011. Benzene, toluene, and o-xylene degradation by free and immobilized P. putida F1 of postconsumer agave-fiber/polymer foamed composites. *International biodeterioration & and iodegradation* 65(3), pp. 539–546.

Rooney-varga, J.N., Anderson, R.T., Fraga, J.L. and Lovley, D.R. 1999. Microbial communities associated with anaerobic benzene degradation in a petroleum-contaminated aquifer. *Applied and Environmental Microbiology* 65(7), pp. 3056–3063.

Rosenberg, E., DeLong, E.F., Stackebrandt, E., Lory, S. and Thompson, F. 2013. The prokaryotes, prokaryotic physiology and biochemistry. In: *The Prokaryotes*. Available at: http://www.springer.com/us/book/9783642301933.

Rosenkranz, F., Cabrol, L., Carballa, M., Cruz, L., Chamy, R. and Lema, J.M. 2013. Relationship between phenol degradation efficiency and microbial community structure in an anaerobic SBR. *Water Research* 47(17), pp. 6739–6749. Available at: http://dx.doi.org/10.1016/j.watres.2013.09.004.

Rotaru, A. et al. 2014. Direct interspecies electron transfer between Geobacter metallireducens and Methanosarcina barkeri. *Applied and Environmental Microbiology* 80(15), pp. 4599–4605. doi: 10.1128/AEM.00895-14.

Ruiz-urigüen, M., Shuai, W. and Jaffé, P.R. 2018. Electrode Colonization by the Feammox Bacterium. *Applied and Environmental Microbiology* 84(24), pp. 1–18.

Russ, R., RAU, J. and Stolz, A. 2000. The function of cytoplasmic flavin reductases in the reduction of azo dyes by bacteria. *Applied and Environmental Microbiology* 66(4), pp. 1429–1434.

S. Kalyuzhnyi, V.S. 2000. Biomineralisation of azo dyes and their break-down products in anaerobic–aerobic hybrid and UAS Breactors. *Wat. Sci. Tech* 41(12), pp. 23–30.

Sack, T.M. and Steele, D.H. 1992. A survey of household products for volatile organic compounds. *Atmospheric Environmen* 26(6), pp. 1063–1070.

Sandhya, S., Sarayu, K. and Swaminathan, K. 2008. Determination of kinetic constants of hybrid textile wastewater treatment system. *Bioresource Technology* 99(13), pp. 5793–5797.

Sandhya, S. and Swaminathan, K. 2006. Kinetic analysis of treatment of textile wastewater in hybrid column upflow anaerobic fixed bed reactor. *Chemical Engineering Journal* 122, pp. 87–92. doi: 10.1016/j.cej.2006.04.006.

Santos, A.B. dos, Cervantes, F.J. and Lier, J.B. van 2007. Review paper on current technologies for decolourisation of textile wastewaters: Perspectives for anaerobic biotechnology. *Bioresource Technology* 98(12), pp. 2369–2385.

Dos Santos, A.B., Traverse, J., Cervantes, F.J. and Van Lier, J.B. 2005. Enhancing the electron transfer capacity and subsequent color removal in bioreactors by applying thermophilic anaerobic treatment and redox mediators. *Biotechnology and Bioengineering* 89(1), pp. 42–52.

Santos, S.C.R. and Boaventura, R.A.R. 2016. Adsorption of cationic and anionic azo dyes on sepiolite clay: Equilibrium and kinetic studies in batch mode. *Journal of Environmental Chemical Engineering* 4(2), pp. 1473–1483.

Saratale, G.D., Saratale, R.G., Chang, J.S. and Govindwar, S.P. 2011. Fixed-bed decolorization of Reactive Blue 172 by Proteus vulgaris NCIM-2027 immobilized on Luffa cylindrica sponge. *International Biodeterioration and Biodegradation* 65(3), pp. 494–503.

Sarkar, J. et al. 2016. Biostimulation of indigenous microbial community for bioremediation of petroleum refinery sludge. *Frontiers in Microbiology* 7(9), pp. 1–20.

Sarvajith, M., Reddy, G.K.K. and Nancharaiah, Y. V. 2018. Textile dye biodecolourization and ammonium removal over nitrite in aerobic granular sludge sequencing batch reactors. *Journal of Hazardous Materials* 342, pp. 536–543.

Schröder, A. and Südekum, K.-H. 1999. Glycerol as a by-product of biodiesel production in diets for ruminants. In: *Proceedings of the 10th International Rapeseed Congress.*, pp. 26–29.

Schuppert, B., Sehink, B. and Eberhard-karls-universitfit, L.M.I. Der 1990. Fermentation of methoxyacetate to glycolate and acetate by newly isolated strains of Acetobacterium sp. *Arch Microbiol* 153, pp. 200–204.

Schwertmann, U. and Cornell, R.M. 2000. *Iron oxides in the laboratory*. Second Edi. John Wiley & Sons.

Sedlak, R.I. 1991. *Phosphorus and nitrogen removal from municipal wastewater: principles and practice*. CRC press.

Seeliger, S., Cord-ruwisch, R. and Schink, B. 1998. A Periplasmic and extracellular c-type cytochrome of Geobacter sulfurreducens acts as a ferric iron reductase and as an electron carrier to other acceptors or to partner bacteria. *Jornal of Bacteriology* 180(14), pp. 3686–3691.

Seifi, L., Torabian, A., Kazemian, H., Bidhendi, G.N., Azimi, A.A. and Charkhi, A. 2011. Adsorption of petroleum monoaromatics from aqueous solutions using granulated surface modified natural nanozeolites: Systematic study of equilibrium isotherms. *Water, Air, and Soil Pollution* 217(1–4), pp. 611–625.

Şen, S. and Demirer, G.N. 2003. Anaerobic treatment of real textile wastewater with a fluidized bed reactor. *Water Research* 37(8), pp. 1868–1878.

Shah, M.P., Patel, K.A., Nair, S.S. and Darji, A.M. 2013. Microbial decolourization of methyl orange dye by Pseudomonas spp. *OA Biotechnology* 2(1), p. 10.

Shahwan, T. and Erten, H.N. 2004. Temperature effects in barium sorption on natural kaolinite and chlorite – illite clays. *Journal of Radioanalytical and Nuclear Chemistry* 260(1), pp. 43–48.

Shariati, S.R.P., Bonakdarpour, B., Zare, N. and Ashtiani, F.Z. 2011. The effect of hydraulic retention time on the performance and fouling characteristics of membrane sequencing batch reactors used for the treatment of synthetic petroleum refinery wastewater. *Bioresource Technology* 102(17), pp. 7692–7699. Available at: http://dx.doi.org/10.1016/j.biortech.2011.05.065.

Sharmasarkar, S., Jaynes, W.F. and VANCE, G.F. 2000. BTEX sorption by

Montmorillonite organo-clay: Tmpa, admam, hdtma. *Water, Air, and Soil Pollution* (119), pp. 257–273.

Shelobolina, E.S., Anderson, R.T., Vodynitskii, Y.N., Sivtsov, A. V., Yurctich, R. and Loveley, D.R. 2004. Importance of clay size minerals for Fe(III) respiration in a petroleum-contaminated aquifer. *Geobiology* (2), pp. 67–76.

Shen, D.S., Liu, X.W. and He, Y.H. 2005. Studies on adsorption, desorption and biodegradation of pentachlorophenol by the anaerobic granular sludge in an upflow anaerobic sludge blanket (UASB) reactor. *Journal of Hazardous Materials* 125(1–3), pp. 231–236. doi: 10.1016/j.jhazmat.2005.05.034.

Shen, N., Huo, Y.C., Chen, J.J., Zhang, F., Zheng, H. and Zeng, R.J. 2015. Decolorization by Caldicellulosiruptor saccharolyticus with dissolved hydrogen under extreme thermophilic conditions. *Chemical Engineering Journal* 262, pp. 847–853.

Shih, Y., Tso, C. and Tung, L. 2010. Rapid degradation of methyl orange with nanoscale iron particles. *Jornal of Enviroment Engineer* 20(3), pp. 137–143.

Shim, H. and Yang, S.T. 1999. Biodegradation of benzene, toluene, ethylbenzene, and o-xylene by a coculture of Pseudomonas putida and Pseudomonas fluorescens immobilized in a fibrous-bed bioreactor. *Journal of Biotechnology* 67(2–3), pp. 99–112.

Shim, H. and Yang, S.T. 2002. BTEX removal from contaminated groundwater by a co-culture of Pseudomonas putida and Pseudomonas fluorescens immobilized in a continuous fibrous-bed bioreactor. *Journal of Chemical Technology and Biotechnology* 77(12), pp. 1308–1315. doi: 10.1002/jctb.711.

Shrestha, D., Embree, M., Zengler, K. and Wardman, C. 2014. A new model for electron flow during anaerobic digestion: direct interspecies electron transfer to Methanosaeta for the reduction of carbon dioxide to methane. *Energy Environ. Sci* (7), pp. 408–415. doi: 10.1039/c3ee42189a.

Shrestha, J., Rich, J.J., Ehrenfeld, J.G. and Jaffe, P.R. 2009. Oxidation of ammonium to nitrite under iron-reducing conditions in wetland soils: Laboratory, field demonstrations, and push-pull rate determination. *Soil Science* 174(3), pp. 156–164.

Siddique, T., Penner, T., Klassen, J. and Foght, J.M. 2012. Microbial communities involved in methane production from Hhydrocarbons in oil sands tailings. *Environmental Science and Technology* 46, p. 9802−9810. doi: 10.1021/es302202c.

Silva, M.L.B. Da and Alvarez, P.J.J. 2002. Effects of ethanol versus MTBE on benzene, toluene, ethylbenzene, and xylene natural attenuation in aquifer columns. *Journal of Environmental Engineering* 128(9), pp. 862–867.

Simantiraki, F., Kollias, C.G., Maratos, D., Hahladakis, J. and Gidarakos, E. 2013. Qualitative determination and application of sewage sludge and municipal solid waste compost for BTEX removal from groundwater. *Journal of Environmental Chemical Engineering* 1(1–2), pp. 9–17. Available at: http://dx.doi.org/10.1016/j.jece.2013.02.002.

Singer, P.C. and Little, L.W. 1975. Characterization and treatment of textile dyeing wastewaters. *J. Water Pollut.* 47, p. 10.

Singh, K. and Arora, S. 2011. Removal of synthetic textile dyes from wastewaters: A critical review on present treatment technologies. *Critical Reviews in Environmental Science and Technology* 41(9), pp. 807–878. doi: 10.1080/10643380903218376.

Singh, M., Singh, H. and Kumar, D. 2006. Biodegradation of azo dye C. I. Acid Red 88 by an anoxic aerobic sequential bioreactor. *Dyes and Pigments* 70, pp. 1–7.

Singh, R. and Celin, S.M. 2010. Biodegradation of BTEX (benzene, toluene, ethyl benzene and xylene) compounds by bacterial strain under aerobic conditions. *Journal of Ecobiotechnology* 2(4), pp. 2077–0464. Available at: http://journal-ecobiotechnology.com/.

Sliekers, A.O., Third, K.A., Abma, W., Kuenen, J.G. and Jetten, M.S.M. 2003. CANON and Anammox in a gas-lift reactor. *FEMS Microbiology Letters 218* 218, pp. 339–344. doi: 10.1016/S0378-1097(02)01177-1.

Smalley, J.W., Silver, J., Birss, A.J., Withnall, R. and Titler, P.J. 2003. The haem pigment of the oral anaerobes Prevotella nigrescens and Prevotella intermedia is composed of iron (III) protoporphyrin IX in the monomeric form. *Microbiology* 149, pp. 1711–1718. doi: 10.1099/mic.0.26258-0.

Solís, M. et al. 2012a. Microbial decolouration of azo dyes: A review. *Process Biochemistry* 47(12), pp. 1723–1748.

Solís, M., Solís, A., Pérez, H.I., Manjarrez, N. and Flores, M. 2012b. Microbial decolouration of azo dyes: A review. *Process Biochemistry* 47(12), pp. 1723–1748. Available at: http://dx.doi.org/10.1016/j.procbio.2012.08.014.

Somasiri, W., Li, X.F., Ruan, W.Q. and Jian, C. 2008. Evaluation of the efficacy of upflow anaerobic sludge blanket reactor in removal of colour and reduction of COD in real textile wastewater. *Bioresource Technology* 99(9), pp. 3692–3699. doi: 10.1016/j.biortech.2007.07.024.

Sorokin, D.Y., Marc, Æ.T.P.T.Æ., Muyzer, G. and Polysulfide, S.Á.T.Á. 2008a. Dethiobacter alkaliphilus gen. nov. sp. nov., and Desulfurivibrio alkaliphilus gen. nov. sp. nov.: two novel representatives of reductive sulfur cycle from soda lakes. *Extremophiles* 12, pp. 431–439. doi: 10.1007/s00792-008-0148-8.

Sorokin, I.D. et al. 2008b. Natronobacillus azotifigens gen. nov., sp. nov. , an anaerobic diazotrophic haloalkaliphile from soda-rich habitats. *Extremophiles* 12, pp. 819–827. doi: 10.1007/s00792-008-0188-0.

Sperling, M. von 2007. Wastewater characteristics, treatment and disposal. In: *Biological Wastewaster Treatment series*. London: IWA Publishing, pp. 22–82.

Von Sperling, M. 2007. Activated sludge and aerobic biofilm reactors. In: *Biological Wastewater Treatment Series*. London: IWA Publishing, p. 338. doi: 10.2166/9781780402123.

Von Sperling, M. and Chernicharo, L. 2005. *Biological wastewater treatment in warm climate regions. Volume I*. IWA publishing, London.

Sponza, D.T. 2002. Decolorization and azo dye degradation by anaerobic/ aerobic sequential process. *Enzyme and Microbial Technology* 31, pp. 102–110.

Sponza, D.T. and Uluköy, A. 2005. Treatment of 2,4-dichlorophenol (DCP) in a sequential anaerobic (upflow anaerobic sludge blanket) aerobic (completely stirred tank) reactor system. *Process Biochemistry* 40(11), pp. 3419–3428. doi:

10.1016/j.procbio.2005.01.020.

Spychała, M. and Starzyk, J. 2015. Bacteria in non-woven textile filters for domestic wastewater treatment. *Environmental technology* 36(5–8), pp. 937–945. doi: 10.1080/09593330.2014.969326.

Stein, L.Y., Duc, M.T. La, Grundl, T.J. and Nealson, K.H. 2001. Bacterial and archaeal populations associated with freshwater ferromanganous micronodules and sediments. *Environmental Microbiology* 3, pp. 10–18.

Stolz, A. 2001. Basic and applied aspects in the microbial degradation of azo dyes. *Appl Microbiol Biotechnol* 56, pp. 69–80.

Strous, M., Heijnen, J.J., Kuenen, J.G. and Jetten, M.S.. 1998. The sequencing batch reactor as a powerful tool for the study of slowly growing anaerobic ammonium-oxidizing microorganisms. *Appl Microbiol Biotechnol* 50, pp. 589–596.

Suarez, S., Lema, J.M. and Omil, F. 2010. Removal of pharmaceutical and personal care products (PPCPs) under nitrifying and denitrifying conditions. *Water Research* 44(10), pp. 3214–3224. Available at: http://dx.doi.org/10.1016/j.watres.2010.02.040.

Sylvia, D.M., Fuhrmann, J.J., Hartel, P.G., Zuberer, D. a, Darmstadt, T.U. and Hall, P. 2005. *Principles and applications of soil microbiology*. Prentice Hall Upper Saddle River New Jersey.

Takahata, Y.O.H., Hoaki, T. and Watanabe, K. 2007. Degradative capacities and bioaugmentation potential of an anaerobic benzene-degrading Bacterium strain DN11. *Environ. Sci. Technol.* 41(17), pp. 6222–6227.

Talarposhti, A.M., Donnelly, T. and Anderson, G.K. 2001. Colour removal from a simulated dye wastewater using a two-phase anaerobic packed bed reactor. *Water Research* 35(2), pp. 425–432. doi: 10.1016/S0043-1354(00)00280-3.

Tang, C., Zheng, P., Chai, L. and Min, X. 2013. International biodeterioration and biodegradation characterization and quanti fi cation of anammox start-up in UASB reactors seeded with conventional activated sludge. *International Biodeterioration and Biodegradation* 82, pp. 141–148.

Tang, C.J. et al. 2017. Removal of nitrogen from wastewaters by anaerobic ammonium oxidation (ANAMMOX) using granules in upflow reactors. *Environmental Chemistry Letters* 15(2), pp. 311–328.

Tanner, C.C. and Kadlec, R.H. 2003. Oxygen flux implications of observed nitrogen removal rates in subsurface-flow treatment wetlands. *Water Science and Technology* 48(5), pp. 191–198.

Tauber, M.M., Gübitz, G.M. and Rehorek, A. 2008. Degradation of azo dyes by oxidative processes-Laccase and ultrasound treatment. *Bioresource Technology* 99(10), pp. 4213–4220.

Tay, T.L., Ivanov, V., Stabnikova, O., Wang, J., Examiner, P. and Prince, F. 2008. *Composition and methods for the treatment of wastewater and other waste* US 7,393,452 B2 [Patent].

Tchobanoglous, G., Burton, F.L. and Stensel, H.D. 2003. Wastewater engineering: treatment, disposal, and reuse. *American Water Works Association. Journal* 5, p. 201.

Tegli, S., Cerboneschi, M., Corsi, M., Bonnanni, M. and Bianchini, R. 2014. Water recycle as a must: decolorization of textile wastewaters by plant-associated fungi. *Journal of basic microbiology* 54, pp. 120–132.

Telke, A.A., Kalyani, D.C., Dawkar, V. V. and Govindwar, S.P. 2009. Influence of organic and inorganic compounds on oxidoreductive decolorization of sulfonated azo dye C.I. Reactive Orange 16. *Journal of Hazardous Materials* 172(1), pp. 298–309.

Texier, A. and Zepeda, A. 2012. Simultaneous elimination of carbon and nitrogen compounds of petrochemical effluents by nitrification and denitrification. *Petrochemicals* 28(5), pp. 101–134.

Thamdrup, B. 2000. Bacterial Manganese and Iron Reduction in Aquatic Sediments. *Advances in Microbial Ecology* (1), pp. 41–84.

Thao, T.P., Kao, H.C., Juang, R.S. and Lan, J.C.W. 2013. Kinetic characteristics of biodegradation of methyl orange by Pseudomonas putida mt2 in suspended and immobilized cell systems. *Journal of the Taiwan Institute of Chemical Engineers*

44(5), pp. 780–785.

Thuar, R.K., Jungerman, K. and Decker, K. 1977. Energy conservation in chemotrophic anaerobic bacteria. *Bacteriological Reviews* 41(1), pp. 100–180.

Tindall, B.J. 2005. Petrimonas sulfuriphila gen. nov., sp. nov., a mesophilic fermentative bacterium isolated from a biodegraded oil reservoir. *International Journal of Systematic and Evolutionary Microbiology (2005),* (55), pp. 1113–1121.

Togo, C.A., Clifford, C., Mutambanengwe, Z. and Whiteley, C.G. 2008. Decolourisation and degradation of textile dyes using a sulphate reducing bacteria (SRB) – biodigester microflora co-culture. *African Journal of Biotechnology* 7(2), pp. 114–121.

Tomei, M.C., Soria Pascual, J. and Mosca Angelucci, D. 2016a. Analysing performance of real textile wastewater bio-decolourization under different reaction environments. *Journal of Cleaner Production* 129, pp. 468–477.

Tomei, M.C., Mosca Angelucci, D. and Daugulis, A.J. 2016b. Sequential anaerobic-aerobic decolourization of a real textile wastewater in a two-phase partitioning bioreactor. *Science of the Total Environment* 573, pp. 585–593.

Tony, B.D., Goyal, D. and Khanna, S. 2009. Decolorization of textile azo dyes by aerobic bacterial consortium. *International Biodeterioration and Biodegradation* 63(4), pp. 462–469. Available at: http://dx.doi.org/10.1016/j.ibiod.2009.01.003.

Torrent, J., Schwertmann, U. and Barrón, V. 1992. Fast and slow phosphate sorption by goethite-rich natural materials. *Clays and Clay Minerals* 40(1), pp. 14–21. doi: 10.1346/CCMN.1992.0400103.

Torrijos, V., Gonzalo, O.G., Ruiz, I. and Soto, M. 2016. Effect of by-pass and ef fl uent recirculation on nitrogen removal in hybrid constructed wetlands for domestic and industrial wastewater treatment. *Water Research* 103, pp. 92–100. Available at: http://dx.doi.org/10.1016/j.watres.2016.07.028.

USEPA 2011. *Water quality assessment and total maximum daily loads information.* Environmental Protection Agency.

Vadivelan, V. and Vasanth Kumar, K. 2005. Equilibrium, kinetics, mechanism, and process design for the sorption of methylene blue onto rice husk. *Journal of Colloid and Interface Science* 286(1), pp. 90–100.

Valladares Linares, R., Li, Z., Abu-Ghdaib, M., Wei, C.H., Amy, G. and Vrouwenvelder, J.S. 2013. Water harvesting from municipal wastewater via osmotic gradient: An evaluation of process performance. *Journal of Membrane Science* 447, pp. 50–56. Available at: http://dx.doi.org/10.1016/j.memsci.2013.07.018.

Venosa, A.D. and Zhu, X. 2003. Biodegradation of crude oil contaminating marine shorelines and freshwater wetlands. *Spill Science and Technology Bulletin* 8(2), pp. 163–178. doi: 10.1016/S1353-2561(03)00019-7.

Viggi, C.C., Fazi, S. and Franzetti, A. 2018. Anaerobic electrogenic oxidation of toluene in a continuous-flow bioelectrochemical reactor: process performance, microbial community analysis, and biodegradation pathways. *Environmental Science Water Research & Technology* 4, pp. 2136–2145. doi: 10.1039/c8ew00666k.

Vimonses, V., Jin, B. and Chow, C.W.K. 2010. Insight into removal kinetic and mechanisms of anionic dye by calcined clay materials and lime. *Journal of Hazardous Materials* 177(1–3), pp. 420–427.

Volesky, B. and Holan, Z.R. 1995. Biosorption of Heavy Metals. *Biotechnol. Prog* 11, pp. 235–250.

Vymazal, J. 2007. Removal of nutrients in various types of constructed wetlands. *Science of the Total Environment* 380(1–3), pp. 48–65. doi: 10.1016/j.scitotenv.2006.09.014.

Vymazal, J. 2013. The use of hybrid constructed wetlands for wastewater treatment with special attention to nitrogen removal : A review of a recent development. *Water Research* 47(14), pp. 4795–4811. doi: 10.1016/j.watres.2013.05.029.

Wang, H., Zheng, X.W., Su, J.Q., Tian, Y., Xiong, X.J. and Zheng, T.L. 2009. Biological decolorization of the reactive dyes Reactive Black 5 by a novel isolated bacterial strain Enterobacter sp. EC3. *Journal of Hazardous Materials* 171(1–3), pp. 654–659.

Wang, L., LI, C. and Jiang, H. 2014. Degradation and decolorization characteristics of ozy dye methyl orange by Strain Citrobacter sp. LW-3. *Acta Scientiae Circumstantiae* 34(9), pp. 2213–2218.

Wang, M., Zhang, D.Q., Dong, J.W. and Tan, S.K. 2017. Constructed wetlands for wastewater treatment in cold climate- A review. *Journal of Environmental Sciences* 57, pp. 293–311.

Wang, X., Wang, S., Xue, T., Li, B. and Dai, X. 2015. Treating low carbon / nitrogen (C/N) wastewater in simultaneous nitrification-endogenous denitrification and phosphorous removal (SNDPR) systems by strengthening anaerobic intracellular carbon storage. *Water Research* 77, pp. 191–200.

Wang, Z., Xue, M., Huang, K. and Liu, Z. 2010. Textile Dyeing Wastewater Treatment. *Advances in Treating Textile Effluent* 5, pp. 91–116.

Wang, Z., Yin, Q., Gu, M., He, K. and Wu, G. 2018. Enhanced azo dye Reactive Red 2 degradation in anaerobic reactors by dosing conductive material of ferroferric oxide. *Journal of Hazardous Materials* 357(1), pp. 226–234. doi: 10.1016/j.jhazmat.2018.06.005.

Wang, Z.W., Liang, J.S. and Liang, Y. 2013. Decolorization of Reactive Black 5 by a newly isolated bacterium Bacillus sp. YZU1. *International Biodeterioration and Biodegradation* 76, pp. 41–48. doi: 10.1016/j.ibiod.2012.06.023.

Watanabe, K., Manefield, M., Lee, M. and Kouzuma, A. 2009. Electron shuttles in biotechnology. *Current Opinion in Biotechnology* 20, pp. 633–641. doi: 10.1016/j.copbio.2009.09.006.

Weber, K.A., Achenbach, L.A., Coates, J.D., Weber, K.A., Achenbach, L.A. and Coates, J.D. 2006. Microorganisms pumping iron: Anaerobic microbial iron oxidation and reduction. *Nature Reviews Microbiology* 4, pp. 752–764. doi: 10.1038/nrmicro1490.

Webster, G., Newberry, C.J., Fry, J.C. and Weightman, A.J. 2003. Assessment of bacterial community structure in the deep sub-seafloor biosphere by 16S rDNA-based techniques: A cautionary tale. *Journal of Microbiological Methods* 55(1), pp. 155–

164. doi: 10.1016/S0167-7012(03)00140-4.

Weelink, S.A.B., van Eekert, M.H.A. and Stams, A.J.M. 2010. Degradation of BTEX by anaerobic bacteria: Physiology and application. *Reviews in Environmental Science and Biotechnology* 9(4), pp. 359–385.

Wei, M., Yu, Z. and Zhang, H. 2015. Molecular characterization of microbial communities in bioaerosols of a coal mine by 454 pyrosequencing andreal-time PCR. *Jurnal of Environmental sScience* 30, pp. 241–251. doi: 10.1016/j.jes.2014.07.035.

Weng, C.H. and Pan, Y.F. 2006. Adsorption characteristics of methylene blue from aqueous solution by sludge ash. *Colloids and Surfaces A: Physicochemical and Engineering Aspects* 274(1–3), pp. 154–162. doi: 10.1016/j.colsurfa.2005.08.044.

White, G.F., Shi, Z., Shi, L., Wang, Z., Dohnalkova, A.C. and Marshall, M.J. 2013. Rapid electron exchange between surface-exposed bacterial cytochromes and Fe (III) minerals. In: *Proceedings of the National Academy of Sciences*., pp. 6346–6351. doi: 10.1073/pnas.1220074110.

Wiesmann, U. 1994. Biological nitrogen removal from wastewater. In: *Biotechnics/wastewater*. Springer, pp. 113–154.

Wijetunga, S., Li, X.F. and Jian, C. 2010. Effect of organic load on decolourization of textile wastewater containing acid dyes in upflow anaerobic sludge blanket reactor. *Journal of Hazardous Materials* 177(1–3), pp. 792–798. Available at: http://dx.doi.org/10.1016/j.jhazmat.2009.12.103.

Wijsman, J.W.M., Middelburg, J.J. and Heip, C.H.R. 2001. Reactive iron in Black Sea Sediments: implications for iron cycling. *Marine Geology* 172, pp. 167–180.

Willmott, N.J. 1997. *The use of bacteria-polymer composites for the removal of colour from reactive dye effluents*. University of Leeds.

Winkler, M.H., Le, Q.H. and Volcke, E.I.P. 2015. Influence of partial denitrification and mixotrophic growth of NOB on microbial distribution in aerobic granular sludge. *Environmental Science and Technology* 49, p. 11003−11010.

Wolicka, D. and Borkowski, A. 2012. Microorganisms and crude oil. In: Romero-

Zerón, L. ed. *Introduction to enhanced oil recovery (EOR) processes and bioremediation of oil-contaminated sites*. Croatia: Intech, Rijeka, pp. 113–142.

Xiao, H., Peng, H. and Yang, P. 2011. Performance of a new-type integrated biofilm reactor in treating high concentration organic wastewater. *Procedia Environmental Sciences* 11, pp. 674–679.

Xin, B.P., Wu, C.H., Wu, C.H. and Lin, C.W. 2013. Bioaugmented remediation of high concentration BTEX-contaminated groundwater by permeable reactive barrier with immobilized bead. *Journal of Hazardous Materials* 244–245, pp. 765–772. doi: 10.1016/j.jhazmat.2012.11.007.

Xu, B., Chen, B., Hsueh, C., Qin, L. and Chang, C. 2014. Deciphering characteristics of bicyclic aromatics–mediators for reductive decolorization and bioelectricity generation. *Bioresourcr Technology* 163, pp. 280–286.

Xu, M., Guo, J. and Kong, X. 2007. Fe (III)-enhanced Azo Reduction by Shewanella decolorationis S12. *Appl Microbiol Biotechnol* (74), pp. 1342–1349.

Yadav, A.K., Jena, S., Acharya, B.C. and Mishra, B.K. 2012. Removal of azo dye in innovative constructed wetlands: Influence of iron scrap and sulfate reducing bacterial enrichment. *Ecological Engineering* 49, pp. 53–58.

Yang, Q., Zhang, W., Zhang, H., Li, Y. and Li, C. 2011. Wastewater treatment by alkali bacteria and dynamics of microbial communities in two bioreactors. *Bioresource Technology* 102(4), pp. 3790–3798.

Yang, W.H., Weber, K.A., Silver, W.L., A.Weber, K. and Silver, W.L. 2012. Nitrogen loss from soil through anaerobic ammonium oxidation coupled to iron reduction. *Nature Geoscience* 5(8), pp. 538–541.

Yang, Y., Peng, H., Niu, J., Zhao, Z. and Zhang, Y. 2019. Promoting nitrogen removal during Fe (III) reduction coupled to anaerobic ammonium oxidation (Feammox) by adding. *Environmental Pollution* 247, pp. 973–979.

Yao, Y. et al. 2011a. Equilibrium and kinetic studies of methyl orange adsorption on multiwalled carbon nanotubes. *Chemical Engineering Journal* 170(1), pp. 82–89.

Available at: http://dx.doi.org/10.1016/j.cej.2011.03.031.

Yao, Y., He, B., Xu, F. and Chen, X. 2011b. Equilibrium and kinetic studies of methyl orange adsorption on multiwalled carbon nanotubes. *Chemical Engineering Journal* 170(1), pp. 82–89. Available at: http://dx.doi.org/10.1016/j.cej.2011.03.031.

Yemashova, N.A., Kotova, I.B., Netrusov, A.I. and Kalyuzhnyi, S. V 2009. Special traits of Decomposition of azo dyes by anaerobic microbial communities. *Applied Biochemistry and Microbiology* 45(2), pp. 176–181.

Yoo, E.S., Libra, J. and Adrian, L. 2001. Mechanism of decolorization of azo dyes in anaerobic mixed culture. *J. Environ. Eng* 127(9), pp. 844–849.

You, X., Guaya, D., Farran, A. and Luis, J. 2015. Phosphate removal from aqueous solution using a hybrid impregnated polymeric sorbent containing hydrated ferric oxide ( HFO ). *J Chem Technol BiotechnoL* (December 2014). doi: 10.1002/jctb.4629.

Yu, J., Wang, X. and Yue, P.L. 2001. Optimal decolorization and kinetic modeling of synthetic dyes by pseudomonas strains. *Water Research* 35(15), pp. 3579–3586. doi: 10.1016/S0043-1354(01)00100-2.

Yu, L., Li, W.W., Lam, M.H.W. and Yu, H.Q. 2011. Adsorption and decolorization kinetics of methyl orange by anaerobic sludge. *Applied Microbiology and Biotechnology* 90(3), pp. 1119–1127.

Yu, L., Li, W. and Lam, M.H. 2012. Isolation and characterization of a Klebsiella oxytoca strain for simultaneous azo-dye anaerobic reduction and bio-hydrogen production. *Appl Microbiol BiotechnoL* 95, pp. 255–262. doi: 10.1007/s00253-011-3688-2.

Yu, L. et al. 2015. Microbial community structure associated with treatment of azo dye in a start-up anaerobic sequenced batch reactor. *Journal of the Taiwan Institute of Chemical Engineers* 54, pp. 118–124.

Yu, L., Wang, S., Tang, Q., Cao, M., Li, J. and Yuan, K. 2016. Enhanced reduction of Fe(III) oxides and methyl orange by Klebsiella oxytoca in presence of anthraquinone-2-disulfonate. *Applied Microbiology and Biotechnology* , pp. 4617–4625. Available

at: http://dx.doi.org/10.1007/s00253-016-7281-6.

Yu, X. and Amrhein, C. 2006. Perchlorate reduction by uutotrophic bacteria in the presence of zero-valent iron. *Environ. Sci. Technol* 40(4), pp. 1328–1334.

Zaan, B.M. Van Der et al. 2012. Anaerobic benzene degradation under denitrifying conditions : Peptococcaceae as dominant benzene degraders and evidence for a syntrophic process. *Environmental Microbiology* 14(5), pp. 1171–1181. doi: 10.1111/j.1462-2920.2012.02697.x.

van der Zee, F.P. et al. 2001. Azo dye decolourisation by anaerobic granular sludge. *Chemosphere* 44(5), pp. 1169–76. Available at: http://www.ncbi.nlm.nih.gov/pubmed/11513405.

Van der Zee, F.P. and Cervantes, F.J. 2009. Impact and application of electron shuttles on the redox (bio)transformation of contaminants: A review. *Biotechnology Advances* 27(3), pp. 256–277. Available at: http://dx.doi.org/10.1016/j.biotechadv.2009.01.004.

Van Der Zee, F.P. and Villaverde, S. 2005a. Combined anaerobic-aerobic treatment of azo dye -A short review of bioreactor studies. *Water Research* 39(8), pp. 1425–1440. doi: 10.1016/j.watres.2005.03.007.

Van Der Zee, F.P. and Villaverde, S. 2005b. Combined anaerobic-aerobic treatment of azo dyes- a short review of bioreactor studies. *Water Research* 39, pp. 1425–1440.

Zeikus, J.G., Jain, M.K. and Elankovan, P. 1999. Biotechnology of succinic acid production and markets for derived industrial products. *Appl Microbiol Biotechnol* 51, pp. 545–552.

Zeng, Q., Hao, T., Mackey, H.R., Wei, L., Guo, G. and Chen, G. 2017. Alkaline textile wastewater biotreatment: A sulfate-reducing granular sludge based lab-scale study. *Journal of Hazardous Materials* 332, pp. 104–111. Available at: http://dx.doi.org/10.1016/j.jhazmat.2017.03.005.

Zepeda, A., Texier, A.C., Razo-Flores, E. and Gomez, J. 2006. Kinetic and metabolic study of benzene, toluene and m-xylene in nitrifying batch cultures. *Water Research* 40(8), pp. 1643–1649.

Zhang, H.L.R. and Tang, L. 2014. In vivo and in vitro decolorization of synthetic dyes by laccase from solid state fermentation with Trametes sp. SYBC-L4. *Bioprocess and Biosystems Engineering* 37, pp. 2597–2605.

Zhang, J. et al. 2012a. An anaerobic reactor packed with a pair of Fe-graphite plate electrodes for bioaugmentation of azo dye wastewater treatment. *Biochemical Engineering Journal* 63, pp. 31–37.

Zhang, J., Zhang, Y., Quan, X., Chen, S. and Afzal, S. 2013a. Enhanced anaerobic digestion of organic contaminants containing diverse microbial population by combined microbial electrolysis cell (MEC) and anaerobic reactor under Fe(III) reducing conditions. *Bioresource Technology* 136, pp. 273–280.

Zhang, L., Zhang, C., Cheng, Z., Yao, Y. and Chen, J. 2013b. Biodegradation of benzene, toluene, ethylbenzene, and o-xylene by the bacterium Mycobacterium cosmeticum byf-4. *Chemosphere* 90(4), pp. 1340–1347.

Zhang, T., Tremblay, P., Chaurasia, A.K., Smith, J.A., Bain, T.S. and Lovley, D.R. 2013c. Anaerobic benzene oxidation via phenol in Geobacter Metallireducens. *Applied and Environmental Microbiology* 79(24), pp. 7800–7806. doi: 10.1128/AEM.03134-13.

Zhang, Y., Jing, Y., Zhang, J., Sun, L. and Quan, X. 2011. Performance of a ZVI-UASB reactor for azo dye wastewater treatment. *Journal of Chemical Technology and Biotechnology* 86(2), pp. 199–204.

Zhang, Y., Liu, Y., Jing, Y., Zhao, Z. and Quan, X. 2012b. Steady performance of a zero valent iron packed anaerobic reactor for azo dye wastewater treatment under variable influent quality. *Journal of Environmental Sciences* 24(4), pp. 720–727.

Zhang, Y. and Pan, B. 2014. Modeling batch and column phosphate removal by hydrated ferric oxide-based nanocomposite using response surface methodology and artificial neural network. *Chemical Engineering Journal* 249, pp. 111–120. Available at: http://dx.doi.org/10.1016/j.cej.2014.03.073.

Zhao, J., Feng, L., Yang, G., Dai, J. and Mu, J. 2017a. Development of simultaneous nitrification-denitrification (SND) in biofilm reactors with partially coupled a novel

biodegradable carrier for nitrogen-rich water purification. *Bioresource Technology* 243, pp. 800–809.

Zhao, Z., Li, Y., Quan, X. and Zhang, Y. 2017b. Towards engineering application: Potential mechanism for enhancing anaerobic digestion of complex organic waste with different types of conductive materials. *Water Research* 115, pp. 266–277.

Zhilina, T.N., Zavarzina, D.G., Kolganova, T. V, Lysenko, A.M. and Tourova, T.P. 2009. Alkaliphilus peptidofermentans sp. nov., a new Alkaliphilic bacterial soda lake isolate capable of peptide fermentation and Fe(III) reduction. *Microbiology* 78(4), pp. 496–505.

Zhou, G.W. et al. 2016a. Electron shuttles enhance anaerobic ammonium oxidation coupled to iron(III) reduction. *Environmental Science and Technology* 50(17), pp. 9298–9307. doi: 10.1021/acs.est.6b02077.

Zhou, G.W. et al. 2016b. Electron shuttles enhance anaerobic ammonium oxidation coupled to iron(III) reduction. *Environmental Science and Technology* 50(17), pp. 9298–9307. doi: 10.1021/acs.est.6b02077.

Zhu, G., Peng, Y., Li, B., Guo, J., Yang, Q. and Wang, S. 2008. Biological removal of nitrogen from wastewater. In: *Reviews of environmental contamination and toxicology*. Springer New York, pp. 159–195.

Zhu, H. et al. 2012. Effective photocatalytic decolorization of methyl orange utilizing TiO2/ZnO/chitosan nanocomposite films under simulated solar irradiation. *Desalination* 286, pp. 41–48.

Zhu, H.Y., Jiang, R. and Xiao, L. 2010. Adsorption of an anionic azo dye by chitosan/kaolin/γ-Fe2O3 composites. *Applied Clay Science* 48(3), pp. 522–526.

Zhu, Y., Xu, J., Cao, X., Cheng, Y. and Zhu, T. 2018a. Characterization of functional microbial communities involved in diazo dyes decolorization and mineralization stages. *International Biodeterioration and Biodegradation* 132, pp. 166–177.

Zhu, Y., Cao, X., Cheng, Y. and Zhu, T. 2018b. Performances and structures of functional microbial communities in the mono azo dye decolorization and

mineralization stages. *Chemosphere* 210, pp. 1051–1060.

Zimmermann, T., Kulla, H.G. and Leisinger, T. 1982. Properties of purified Orange I1 Azoreductase, the enzyme initiating azo dye degradation by Pseudumunas KF46. *European Journal of Biochemistry* 203, pp. 197–203.

# Appendix 1: The dyes and chemicals used by Blackburn Yarn Dyers Ltd

| Product | Dye / Chemical | Type |
|---|---|---|
| Astrazon Blue FGRL 200% | Dye | Basic |
| Best Acid Blue SWP | Dye | Acid |
| Best Acid Golden Yellow SWP | Dye | Acid |
| Best Acid Red SWP | Dye | Acid |
| Dianix Black XF2 | Dye | Disperse |
| Dianix Blue E-R 150% | Dye | Disperse |
| Dianix Luminous Pink 5B | Dye | Disperse |
| Dianix Luminous Yellow 10G | Dye | Disperse |
| Dianix Navy S-2G | Dye | Disperse |
| Dianix Red CBN-SF | Dye | Disperse |
| Dianix Red S-2B | Dye | Disperse |
| Dianix Red S-G | Dye | Disperse |
| Dianix Rubine S-2G | Dye | Disperse |
| Dianix Yellow Brown S-ER | Dye | Disperse |
| Dianix Yellow Brown XF | Dye | Disperse |
| Dianix Yellow C-5G | Dye | Disperse |
| Dianix Yellow S-6G | Dye | Disperse |
| Duractive Blue H-RN | Dye | Reactive |
| Duractive Yellow S-RN | Dye | Reactive |
| Durantine Brill Blue BL 150% | Dye | Direct |
| Durantine Scarlet 2GS | Dye | Direct |
| Evron Red C-2BL | Dye | Acid |
| Indanthren Blue C-BC Plus | Dye | Vat |
| Indanthren Blue CLF Colloisol | Dye | Vat |
| Indanthren Blue RS Colloisol | Dye | Vat |
| Indanthren Bordeaux RR | Dye | Vat |
| Indanthren Brilliant Blue RCL Colloisol | Dye | Vat |
| Indanthren Brilliant Orange GR Collosiol | Dye | Vat |
| Indanthren Brilliant Violet 3B Coll | Dye | Vat |
| Indanthren Brown BR Colloisol | Dye | Vat |
| Indanthren Brown RN Colloisol | Dye | Vat |
| Indanthren Direct Black 5589 Coll | Dye | Vat |
| Indanthren Grey 5607 Collosion | Dye | Vat |
| Indanthren Olive Green B | Dye | Vat |
| Indanthren Olive MW Coll | Dye | Vat |
| Indanthren Olive R | Dye | Vat |
| Indanthren Orange 3G | Dye | Vat |
| Indanthren Red FBB Coll | Dye | Vat |
| Indanthren Yellow 5GF | Dye | Vat |
| Indanthren Yellow F3GC | Dye | Vat |

| | | |
|---|---|---|
| Indigo Coat | Dye | Vat |
| Intracron Black V-CKN 150 | Dye | Reactive |
| Intracron Blue E-GN 125 | Dye | Reactive |
| Intracron Brilliant Orange V-3R | Dye | Reactive |
| Intracron Golden Yellow V-RN | Dye | Reactive |
| Intracron Red V-RB 160 | Dye | Reactive |
| Intralite Fast Red 6B 200 | Dye | Direct |
| Intralite Fast Violet 5B 250 | Dye | Direct |
| Isolan Black 2S-LD | Dye | Acid |
| Itoacid Milling Green 5GW | Dye | Acid |
| Itoacid Milling Navy R 182% | Dye | Acid |
| Itoacid Milling Red CB | Dye | Acid |
| Itoacid Milling Violet FBL | Dye | Acid |
| Itoacid Milling Yellow 4GL | Dye | Acid |
| Itodirect Blue FGL | Dye | Direct |
| Itofix Bordeaux VMHLF | Dye | Reactive |
| Itofix Brilliant Violet VSB special | Dye | Reactive |
| Itofix Navy CTR | Dye | Reactive |
| Itofix Navy VM3GF conc | Dye | Reactive |
| Itofix Navy VMBF | Dye | Reactive |
| Itofix Red CT3B | Dye | Reactive |
| Itofix Red VM3BS 150% | Dye | Reactive |
| Itofix Yellow CT-4R | Dye | Reactive |
| Itofix Yellow CTSNR | Dye | Reactive |
| Itofix Yellow VMRL 150% | Dye | Reactive |
| Itolevelling Blue R 200% | Dye | Acid |
| Itolevelling Red FRLL 200% | Dye | Acid |
| Itolevelling Red K2BLL | Dye | Acid |
| Itolevelling Rhodamine B 400% | Dye | Acid |
| Itolevelling Yellow 8GX | Dye | Acid |
| Itolevelling Yellow NFG | Dye | Acid |
| Itosperse Bordeaux 2R 160% | Dye | Disperse |
| Itosperse Rubine C-BL 150% | Dye | Disperse |
| Itosperse Turq Blue CGLF 200% | Dye | Disperse |
| Itovat Black 1188 | Dye | Vat |
| Jerdirect Brown RL | Dye | Direct |
| Jerdirect Orange AGA 150% | Dye | Direct |
| Jerdirect Rubine BD | Dye | Direct |
| Levafix Amber CA-N | Dye | Reactive |
| Levafix Blue CA | Dye | Reactive |
| Levafix Brilliant Blue E-FFN | Dye | Reactive |
| Levafix Brilliant Red CA | Dye | Reactive |
| Levafix Brilliant Yellow CA | Dye | Reactive |
| Levafix Fast Red CA | Dye | Reactive |
| Levafix Olive CA 100 | Dye | Reactive |
| Maxilon Black FBL | Dye | Basic |
| Maxilon Golden Yellow GL Liq. 200% | Dye | Basic |

| Product | Dye / Chemical | Type |
|---|---|---|
| Maxilon Red SL 200% | Dye | Basic |
| Novacron Orange BR | Dye | Reactive |
| Novacron Red EC-2BL | Dye | Reactive |
| Novacron Red FN-R | Dye | Reactive |
| Novacron Red LS-BN | Dye | Reactive |
| Novacron Super Black R | Dye | Reactive |
| Novacron Yellow EC-2R | Dye | Reactive |
| Novasol Golden Yellow RK MD | Dye | Vat |
| Novasol Green BF | Dye | Vat |
| Novasol Red 6B | Dye | Vat |
| Nylanthrene Blue C-GLF 200 | Dye | Acid |
| Nylanthrene Rubine C5BL 200 | Dye | Acid |
| Procion Blue H-ERD | Dye | Reactive |
| Procion Flavine H-EXL | Dye | Reactive |
| Procion Turquoise H-EXL | Dye | Reactive |
| Remazol Br. Blue R spec. | Dye | Reactive |
| Remazol Brilliant Violet 5R | Dye | Reactive |
| Remazol Deep Red RGB | Dye | Reactive |
| Remazol Golden Yellow RGB | Dye | Reactive |
| Remazol Grey SAM | Dye | Reactive |
| Remazol Midnight Black RGB 01 | Dye | Reactive |
| Remazol Terra Cotta SAM | Dye | Reactive |
| Remazol Turquoise Blue G 133% | Dye | Reactive |
| Remazol Ultra Carmine RGB | Dye | Reactive |
| Remazol Ultra Navy Blue RGB | Dye | Reactive |
| Remazol Ultra Red RGB | Dye | Reactive |
| Sirius Grey K-CGL | Dye | Direct |
| Solophenyl Yellow ARLE 154% | Dye | Direct |
| Telon Red M-3B 80% | Dye | Acid |
| Telon Rubine A5B 01 | Dye | Acid |
| Telon Turquoise M-5G 85% | Dye | Acid |
| Telon Yellow ARB | Dye | Acid |
| **Product** | **Dye / Chemical** | **Type** |
| Acetic Acid | Chemical | Dyeing Agent |
| Albafix R | Chemical | Fixing Agent |
| Albatex OR | Chemical | Levelling Agent |
| Albigen A | Chemical | Levelling Agent |
| Ammonia | Chemical | Stripping Agent |
| Assist PNP | Chemical | Protecting Agent |
| Buffer BDP | Chemical | PH Regulator |
| Buffer NAT NEW | Chemical | PH Regulator |
| Catalase BF | Chemical | Reducing Agent |
| Caustic Soda | Chemical | Dyeing Agent |
| Common Salt | Chemical | Dyeing Agent |
| Contavan DSA | Chemical | Protecting Agent |
| Eganal PS | Chemical | Levelling Agent |

| Felosan LPJ | Chemical | Wetting Agent |
|---|---|---|
| Formic Acid | Chemical | Stripping Agent |
| Heptol EMG | Chemical | Sequestrant |
| Hydrocol WOM | Chemical | Fixing Agent |
| Hydrogen Peroxide | Chemical | Oxidising Agent |
| Hydrosulfite EN | Chemical | Reducing Agent |
| Jernol PEC | Chemical | Levelling Agent |
| Kollasol BWA | Chemical | Wetting Agent |
| Kollasol LOK | Chemical | Wetting Agent |
| Lufibrol Chelant TB | Chemical | Sequestrant |
| Meropan VD New | Chemical | Sequestrant |
| Mystox SR | Chemical | Fungicide |
| Nicca Sunsolt LM7 | Chemical | Stripping Agent |
| Nylofixan P liq | Chemical | Fixing Agent |
| Optifix TPS | Chemical | Fixing Agent |
| Oxalic Acid | Chemical | Stripping Agent |
| Perigen KPS | Chemical | Levelling Agent |
| Quest K150A | Chemical | PH Regulator |
| Ruco-Flow EP1000 | Chemical | PH Regulator |
| Rucogal ACD | Chemical | PH Regulator |
| Rucogal PAN | Chemical | Levelling Agent |
| Rucogal PAX | Chemical | Levelling Agent |
| Rucogal SUR | Chemical | Levelling Agent |
| Rucogen REG | Chemical | Scouring Agent |
| Rucorit GOX | Chemical | Oxidising Agent |
| Ruco-Tex NKS 150 | Chemical | Dispersing Agent |
| Rugwash | Chemical | Scouring Agent |
| Sarabid DLO | Chemical | Scouring Agent |
| Sera Con M-LU | Chemical | Oxidising Agent |
| Sera Con N-VS | Chemical | PH Regulator |
| Sera Con P-NR | Chemical | Oxidising Agent |
| Sera Fast C-RD | Chemical | Scouring Agent |
| Sera Quest M-USP | Chemical | Sequestrant |
| Sera Wash C-NEC | Chemical | Scouring Agent |
| Sera Wet C-NR | Chemical | Wetting Agent |
| Setacrystal BC 150% | Chemical | Dispersing Agent |
| Sirrix SB Liq | Chemical | Protecting Agent |
| Soap Flakes | Chemical | Scouring Agent |
| Sodium Acetate | Chemical | PH Regulator |
| Sodium Carbonate | Chemical | PH Regulator |
| Sodium Hypochlorite | Chemical | Bleaching Agent |
| Sodium Perborate | Chemical | Oxidising Agent |
| Sodium Sulphate | Chemical | Dyeing Agent |
| Subitol SAN neu | Chemical | Wetting Agent |

# Appendix 2: Removal rates calculations

Phase one calculation:

MO Removal rate $(g/m^3/day) = q(C_o - C_t)/V$

Where q is the flow rate 0.1 l/day, $C_o$ is the initial MO concentration, and $C_t$ is the MO concentration at time t, convert MO from mg to g by dividing it by 1000. V is the volume of 128 g wet sludge in each column which is equal to 107cm$^3$ using Table 3-2. Convert the sludge volume from cm$^3$ to m$^3$ by divided it by1000000.

Phase two calculation:

MO removal rate $(g/m^3/day) = q(C_o - C_t)/V$

Where q is the flow rate of 0.3 l/day. $C_o$ is the initial MO concentration, and $C_t$ is the MO concentration at time t, convert MO from mg to g by dividing it by 1000. V is the volume of 28 g wet sludge in each column which is equal to 22.22 cm$^3$ using Table 3-2. Convert the sludge volume from cm$^3$ to m$^3$ by divided it by1000000.

TC removal rate $(g/m^3/day) = q(C_o - C_t)/V$

Where q is the flow rate of 0.3 l/day. $C_o$ is the initial TC concentration, and $C_t$ is the TC concentration at time t, convert TC from mg to g by dividing it by 1000. V is the volume of 28 g wet sludge in each column which is equal to 22.22 cm$^3$ using Table 3-2. Convert the sludge volume from cm$^3$ to m$^3$ by divided it by1000000.

TN removal rate $(g/m^3/day) = q(C_o - C_t)/V$

Where q is the flow rate of 0.3 l/day. $C_o$ is the initial TN concentration, and $C_t$ is the TN concentration at time t, convert TN from mg to g by dividing it by 1000. V is the volume of 28 g wet sludge in each column which is equal to 22.22 cm$^3$ using Table 3-2. Convert the sludge volume from cm$^3$ to m$^3$ by divided it by1000000.

TN removal rate $(g/m^2/day) = q(C_o - C_t)/Area$

Where q is the flow rate of 0.3 l/day. $C_o$ is the initial TN concentration, and $C_t$ is the TN concentration at time t, convert TN from mg to g by dividing it by 1000. The area

is the cross-sectional area of the column used was 5.31 cm$^2$ based on the radios of the column used and to convert it to m$^2$ it needs to be divided by 10000.

TN removal rate (g/kg/day) $= q(C_o - C_t)/$ weight

Where q is the flow rate of 0.3 l/day. $C_o$ is the initial TN concentration, and $C_t$ is the TN concentration at time t, convert TN from mg to g by dividing it by 1000. Weight is the amount of wet sludge used in each column which was 28 g, and it can be converted to kg by dividing it by 1000.

Phase three and municipal wastewater calculation:

TC removal rate (g/m$^3$/day) $= q(C_o - C_t)/V$

Where q is the flow rate of 0.1 l/day. $C_o$ is the initial TC concentration, and $C_t$ is the TC concentration at time t, convert TC from mg to g by dividing it by 1000. V is the volume of 28 g wet sludge in each column (MWT, MX and WT) which is equal to 22.22 cm$^3$ MWT, 23.80 cm$^3$ WT and 27.02 cm$^3$ MX using Table 3-2. Convert the sludge volume from cm$^3$ to m$^3$ by divided it by1000000.

TN removal rate (g/m$^3$/day) $= q(C_o - C_t)/V$

Where q is the flow rate of 0.1 l/day. $C_o$ is the initial TN concentration, and $C_t$ is the TN concentration at time t, convert TC from mg to g by dividing it by 1000. V is the volume of 28 g wet sludge in each column (MWT, MX and WT) which is equal to 22.22 cm$^3$ MWT, 23.80 cm$^3$ WT and 27.02 cm$^3$ MX using Table 3-2. Convert the sludge volume from cm$^3$ to m$^3$ by divided it by1000000.

TN removal rate (g/m$^2$/day) $= q(C_o - C_t)/$Area

Where q is the flow rate of 0.1 l/day. $C_o$ is the initial TN concentration, and $C_t$ is the TN concentration at time t, convert TN from mg to g by dividing it by 1000. The area is the cross-sectional area of the column used which was 5.31 cm$^2$ based on the radios of the column used and to convert it to m$^2$ it needs to be divided by 10000.

TN removal rate (g/kg/day) $= q(C_o - C_t)/$ weight

Where q is the flow rate of 0.1 l/day. $C_o$ is the initial TN concentration, and $C_t$ is the TN concentration at time t, convert TN from mg to g by dividing it by 1000. Weight is the amount of wet sludge used in each column which was 28 g, and it can be converted to kg by dividing it by 1000.